

# **Energy Management and Controlling of Microgrid Using Improved and Enhanced Model Predictive Control**



**Muhammed Cavus**

**Supervisors:** Prof. Damian Giaouris

Dr. Adib Allahham

Dr. Kabita Adhikari

Electrical Engineering

Newcastle University

This dissertation is submitted for the degree of

*Doctor of Philosophy*



## Abstract

The widespread adoption of renewable energy sources (RESs) has occurred in an attempt to stop the progression of global warming. This growing adaptation has resulted in a significant shift in the topologies of traditional power networks, and as a result, the concept of a microgrid (MG) has emerged. MGs represent a paradigm shift from remote central power plants to more localized distributed generation and are a growing sector of the energy industry. Controlling MGs is difficult due to their complexity and diverse properties each asset in the MG has. Various solutions have been proposed to address the difficult problem of MG management. Some of these methods are considered optimal for managing MG assets. Other works are based on a systems-based methodology and address the scalability and simplicity of synthesizing an energy management system (EMS) for an MG. MPC is a sophisticated method used to control power systems while satisfying multiple constraints to achieve an optimal solution based on various criteria. MPC is an effective technique with several advantages; however, its implementation is frequently challenging and requires significant computing power. On the other hand, control strategies based on  $\varepsilon$ -variables can simplify the control structure, allowing for greater scalability and even resilience. These control strategies are methods that can be utilized to model MG control strategies. The main target of this thesis is to present a hybrid method that can simplify the implementation of MPC using  $\varepsilon$ -variables and make it more effective for complex energy systems. Our findings indicate that combining MPC with  $\varepsilon$ -variables can significantly simplify the control structure, thereby allowing the implementation of more complex control strategies. Then, these more complex control strategies can be utilized to provide additional advantages to the energy system, such as scalability and robustness.

Although practical methods for modelling control strategies in MGs,  $\varepsilon$ -variables-based logical control strategies, can make the control structure more scalable, this approach is not optimal. S-MPC is an advanced method for controlling power systems while satisfying multiple constraints to achieve an optimal solution based on multiple criteria. Nevertheless, its implementation is complicated. Another target of the thesis proposes a novel systems approach known as the extended optimal  $\varepsilon$ -variable method, which was created by combining the  $\varepsilon$ -variable based control method with the S-MPC method in order to address these issues. This novel method has improved the adaptability and scalability of an MG's control structure and significantly enhanced the MG's energy management optimization. Our findings indicate that the extended optimal  $\varepsilon$ -variable method: (i) reduces the operational cost of MG by nearly 35%; (ii) reduces the usage of the battery energy storage system (BESS) by 42%; and (iii) increases the practicability of PV usage by 28%. By translating the results of S-MPC to the  $\varepsilon$ -variable method, our novel extended

---

optimal  $\varepsilon$ -variable technique also significantly improves the adaptability and scalability of the control structure of the MG.

Regarding flexible hybrid MGs with plug-and-play (PnP) assets, these are difficult to control because of their complexity and asset characteristics. As mentioned previously,  $\varepsilon$ -variables-based logic control strategies are one method for addressing these challenges. The resulting controller is not, however, optimal. MPC employs a mathematical model of the system to predict its behaviour and determine the best control action. Nevertheless, MPC cannot design and control multiple models, so it cannot control flexible hybrid MGs. S-MPC, on the other hand, uses multiple models to represent system operating modes or scenarios. S-MPC selects a model and control strategy based on the system's state and performance objectives, enabling it to manage systems with mode-dependent dynamics. However, the development and validation of the design and management of multiple models of the MGs are challenging. Additionally, S-MPC is more challenging to implement due to its multiple steps. Therefore, the last target of this thesis proposes a novel hybrid framework/method based on  $\varepsilon$ -variables and conventional MPC to generate and validate the S-MPC automatically. To solve the S-MPC optimization problem in a compact form, a quadratic programming (QP) approach that minimizes or maximizes the objective functions under the constraints of bounds, linear equality, and inequality is then considered. This novel strategy significantly improves the energy management optimization of a flexible hybrid MG and reduces computational complexity. The suggested control method is as follows: (i) reduce imported energy from the grid by approximately 46.7% and (ii) increase exported energy to the grid by approximately 50.8%. By translating the decisions of S-MPC into  $\varepsilon$ -variables, S-MPC implementation is simplified.

# Publications

## Conference Papers (Chapter 3)

1. Cavus Muhammed, Adib Allahham, Kabita Adhikari, Mansoureh Zangiabadia, and Damian Giaouris. "Control of microgrids using an enhanced Model Predictive Controller." PEMD. (2022): 660-665.
2. Cavus Muhammed, Adib Allahham, Kabita Adhikari, Mansoureh Zangiabadia, and Damian Giaouris. "Energy Management of Microgrids using a Flexible Hybrid Predictive Controller." 2nd World Energy Conference And 7th UK Energy Storage Conference. (2022).

## Journal Papers (Chapter 1, 4 and 5)

1. Pamulapati Trinadh, Muhammed Cavus, Ishioma Odigwe, Adib Allahham, Sara Walker, and Damian Giaouris. "A Review of Microgrid Energy Management Strategies from the Energy Trilemma Perspective." Energies 16, no. 1 (2022): 289. (Chapter 1).
2. Cavus Muhammed, Adib Allahham, Kabita Adhikari, Mansoureh Zangiabadi, and Damian Giaouris. "Energy Management of Grid-Connected Microgrids Using an Optimal Systems Approach." IEEE Access 11 (2023): 9907-9919. (Chapter 4).
3. Cavus, Muhammed, Adib Allahham, Kabita Adhikari, and Damian Giaouris. "A hybrid method based on logic predictive controller for flexible hybrid microgrid with plug-and-play capabilities." Applied Energy 359 (2024): 122752. (Chapter 5).



## **Declaration**

I hereby declare that except where specific reference is made to the work of others, the contents of this dissertation are original and have not been submitted in whole or in part for consideration for any other degree or qualification in this, or any other university. This dissertation is my own work and contains nothing which is the outcome of work done in collaboration with others, except as specified in the text and Acknowledgements. This dissertation contains fewer than 80,000 words including appendices, bibliography, footnotes, tables and equations and has fewer than 150 figures.

Muhammed Cavus  
June 2024



## **Acknowledgements**

I am grateful to everyone who has helped me finish this thesis. Their advice, support, and unfailing faith in my abilities have all shaped my work.

First and foremost, I want to thank my primary supervisor, Damian Giaouris, for their essential direction, insightful input, and continual support. Their knowledge and passion have been crucial in influencing the course of this research. I'd also like to thank my co-supervisor, Adib Allahham, for their intelligent recommendations, thought-provoking discussions, and encouragement, which considerably improved this thesis.

I am grateful to my family, especially my wife, for their unending love, support, and patience. Their encouragement through times of self-doubt and unshakable belief in me have been my motivators.

I'd like to thank my friends and co-workers for their insightful comments and stimulating debates, which improved the overall quality of this work.

Finally, I'd like to thank the academic resources, the Turkish Ministry of National Education, and the institutions that provided the tools and materials for my research.

Please accept my heartfelt gratitude to everyone who had a role, no matter how great or small, in completing this thesis. This achievement would not have been achieved without each and every one of you.



## Table of Contents

Publications . . . . .	v
<b>List of Figures</b>	<b>xv</b>
<b>List of Tables</b>	<b>xvii</b>
<b>Nomenclature</b>	<b>xix</b>
<b>1 Introduction</b>	<b>1</b>
1.1 Background . . . . .	1
1.2 Overview . . . . .	3
1.3 About MGs . . . . .	4
1.3.1 MG Architecture and Elements . . . . .	5
1.4 Control Scheme of MGs . . . . .	7
1.4.1 Primary Control Level . . . . .	7
1.4.2 Secondary Control Level . . . . .	7
1.4.3 Tertiary Control Level . . . . .	9
1.5 Control Architectures . . . . .	9
1.5.1 Centralized Control . . . . .	10
1.5.2 Decentralized Control . . . . .	10
1.5.3 Hierarchical Control . . . . .	11
<b>2 Literature Review</b>	<b>13</b>
2.1 Control Strategies for MGs . . . . .	13
2.1.1 Objective Functions and Constraints . . . . .	14
2.1.2 Optimization and Control Methods . . . . .	14
2.1.3 Classical Approaches . . . . .	14
2.1.4 Heuristic and Meta-heuristic Methods . . . . .	15
2.1.5 Artificial Intelligent Methods . . . . .	16
2.2 Objectives of Thesis . . . . .	23
2.3 Thesis Contributions . . . . .	24
2.4 Thesis Organization . . . . .	24
<b>3 Control of Microgrids using an Enhanced MPC</b>	<b>27</b>
3.1 Overview . . . . .	27

## Table of Contents

---

3.2	Introduction . . . . .	28
3.3	Motivation for the Proposed Method . . . . .	30
3.4	Structure of the PV-Battery-Grid system (PBG) . . . . .	30
3.5	General Information for the Implementation of MPC . . . . .	31
3.5.1	Defining a State-space Plant Model . . . . .	34
3.5.2	Predictive Control within One Optimization Window . . . . .	35
3.5.3	Optimization . . . . .	37
3.5.4	Receding Horizon Control ( <b>Point 9</b> ) . . . . .	39
3.5.5	Formulation of Constrained Control Problems . . . . .	40
3.5.6	Constraints in Multi-input and Multi-output Plants . . . . .	41
3.5.7	Numerical Solutions Using QP . . . . .	46
3.5.8	Predictive Control of MIMO Systems . . . . .	47
3.6	The modelling of PBG using the MPC . . . . .	48
3.6.1	The constraints of the components of PBG ( <b>Point 5</b> ) . . . . .	49
3.6.2	Objective Functions of PBG ( <b>Point 6</b> ) . . . . .	50
3.6.3	Reference Matrix for the PBG . . . . .	50
3.6.4	The calculation of receding horizon control: . . . . .	50
3.7	The Implementation of $\varepsilon$ -variables for the PBG . . . . .	51
3.8	The Implementation of hybrid MPC- $\varepsilon$ -variables technique ( <b>Point 23-24</b> ) . . . . .	54
3.9	The comparison of $\varepsilon$ -variables and if/else statement . . . . .	58
3.10	Results and Discussions . . . . .	58
3.10.1	Simulation results of hybrid MPC- $\varepsilon$ -variables technique . . . . .	58
3.11	Conclusion . . . . .	66
<b>4</b>	<b>Energy Management of Grid-Connected Microgrids using an Optimal Systems Approach</b>	<b>69</b>
4.1	Overview . . . . .	69
4.2	Introduction . . . . .	70
4.3	General Information for the Implementation of S-MPC with Finite-horizon LQR in Compact Formulation . . . . .	74
4.4	Methodology of building optimal systems-based EMS of a MG . . . . .	79
4.5	The building optimal system based EMS . . . . .	80
4.5.1	A. Step 1: Building the EMS using $\varepsilon$ -variables . . . . .	80
4.5.2	B. Step 2: Systematic Generation of the Extended Optimal Control Problem Using S-MPC Formulation . . . . .	82
4.5.3	C. Step 3: Translating the Optimal Control Decisions of S-MPC to $\varepsilon$ -variables . . . . .	87
4.5.4	Summary of the Building the Extended Optimal $\varepsilon$ -variables Method . . . . .	87
4.6	Results and Discussions . . . . .	90
4.6.1	Simulation Results of the Extended Optimal $\varepsilon$ -variables Method . . . . .	90

4.6.2	The Illustrating the Adaptability and Scalability of the Extended Optimal $\epsilon$ -variables Method . . . . .	92
4.7	Conclusion . . . . .	97
<b>5</b>	<b>A Hybrid Method Based on Logic Predictive Controller for Flexible Hybrid Microgrid with Plug-and-Play Capabilities</b>	<b>99</b>
5.1	Overview . . . . .	99
5.2	Introduction . . . . .	99
5.2.1	Literature Review . . . . .	100
5.2.2	Contributions and research questions . . . . .	101
5.2.3	Organization of this chapter . . . . .	102
5.3	Hybrid method based to control flexible MG with PnP capabilities . . . . .	102
5.4	The Proposed Optimal Systems-Based EMS . . . . .	103
5.4.1	Step 1: Defining the operational modes and switching conditions (the logical control system approach) . . . . .	104
5.4.2	Step 2: Generating the optimal controller for each operational mode . . . . .	110
5.4.3	Step 3: Implementing the optimal decisions using the logic control . . . . .	116
5.5	Use Cases: Simulation results and discussions . . . . .	119
5.5.1	Use Case 1: Control of the flexible hybrid MG using logic control . . . . .	120
5.5.2	Use Case 2: Controlling the flexible hybrid MG using S-MPC . . . . .	122
5.5.3	Use Case 3: Incorporating plug-and-play EV fleet . . . . .	124
5.5.4	Use Case 4: Islanded MG . . . . .	127
5.6	Conclusions . . . . .	128
<b>6</b>	<b>Conclusions</b>	<b>131</b>
6.0.1	Future Works . . . . .	133
<b>Appendix A Appendix</b>		<b>137</b>
A.1	Microgrid Configuration Details for Chapter 3 . . . . .	137
<b>Appendix B</b>		<b>139</b>
B.1	System Parameter Details for Chapter 4 . . . . .	139
<b>Appendix C</b>		<b>141</b>
C.1	Parameters for the Real System for Chapter 5 (Ipsakis et al. (2009)) . . . . .	141
<b>References</b>		<b>143</b>



## List of Figures

1.1	Representing of hybrid energy system using graph method. . . . .	3
1.2	MG components, type, mode of operation, control, and optimization methods .	5
1.3	Different levels of control in hierarchical architecture . . . . .	6
1.4	Hierarchical control structure. . . . .	11
2.1	Objective functions constraints and optimization methods for optimum operation of MG systems. . . . .	13
2.2	Control approaches for EMSs. . . . .	15
2.3	Constituents of MPC for achieving objectives in MGs-EMS . . . . .	22
3.1	The illustration of directed graph . . . . .	29
3.2	Structure of the PBG system . . . . .	31
3.3	The schematic of MPC . . . . .	32
3.4	The basic idea for MPC (Seborg et al. (2016)) . . . . .	32
3.5	A graph shown in state space; points addressed in the text are indicated by numbers.	52
3.6	The flow-chart of the proposed method (MPC- $\epsilon$ -variables) . . . . .	55
3.7	The detailed flow chart of the hybrid MPC- $\epsilon$ -variables technique. . . . .	56
3.8	The illustration of the if/else statement . . . . .	59
3.9	Hourly PV and load demand (120 hours) for the building in the UK during the autumn season. . . . .	60
3.10	The results of power flows using (a) the MPC, (b) the MPC- $\epsilon$ -variables, and (c) the MPC- $\epsilon$ -variables when $SOAcc(1) = 0.55$ during the autumn. . . . .	61
3.11	The results of power flows and $SOC$ of the battery using the MPC- $\epsilon$ -variables .	62
3.12	Hourly PV and load demand (120 hours) for the building in the UK during summer.	63
3.13	The results of power flows using (a) the MPC, (b) the MPC- $\epsilon$ -variables, and (c) the MPC- $\epsilon$ -variables when $SOAcc(1) = 0.55$ during the summer. . . . .	64
3.14	The results of power flows and $SOC$ of the battery using the MPC- $\epsilon$ -variables during summer. . . . .	65
3.15	The results of power flows and $SOC$ of the battery using the MPC - $\epsilon$ -variables	66
4.1	The flowchart of the implementation of MPC in a compact form . . . . .	78
4.2	Flow chart of the optimal system based on EMS. . . . .	79
4.3	Conceptual microgrid structure proposed in this work. . . . .	80
4.4	Flow chart for the standard $\epsilon$ -variables . . . . .	81

4.5	The flowchart of building the extended optimal $\varepsilon$ -variables technique for the MG is shown in Figure 4.2. . . . .	88
4.6	(a) Power flows and (b) SOAcc of the accumulators for four days (96 hours) using the standard $\varepsilon$ -variables method. . . . .	90
4.7	(a) Power flows and (b) SOAcc of the accumulators for four days (96 hours) using the extended optimal $\varepsilon$ -variables method. . . . .	91
4.8	Power flows for one year (8760 hours) using the standard $\varepsilon$ -variables method and the extended optimal $\varepsilon$ -variables method. . . . .	92
4.9	The translating of results of S-MPC to the $\varepsilon$ -variables method for (a) power flows and (b) SOAcc of the accumulator. . . . .	93
4.10	The illustration of the scalability of the extended optimal $\varepsilon$ -variables method when adding the diesel generator . . . . .	94
4.11	The hysteresis zone for the extended optimal $\varepsilon$ -variables technique in the MG . . . . .	94
4.12	The results of power flows and $SOAcc^{BAT}$ when changing $stp_{DG \rightarrow LD}^{SOAcc^{BAT}}$ . . . . .	95
4.13	The results of power flows and $SOAcc^{BAT}$ when changing $str_{BAT \rightarrow LD}^{SOAcc^{BAT}}$ . . . . .	96
4.14	The results of the state of charge of the battery using (a) $\varepsilon$ -variables and (b) extended optimal $\varepsilon$ -variables . . . . .	96
5.1	Flow chart of the algorithm generating S-MPC from the MPC automatically. . . . .	103
5.2	A brief flow chart of our proposed method. . . . .	104
5.3	Hybrid MG Structure. . . . .	105
5.4	The illustration of the different operational modes, the switching conditions, and the state variables in each mode using the automata/graph method. . . . .	106
5.5	A graph shown in state space (in the first step) for the hybrid control method; numbers indicate points addressed in the text. . . . .	107
5.6	The flow chart of the $\varepsilon$ -variables . . . . .	109
5.7	A graph is shown in the second step for the hybrid control method; points addressed in the text are indicated by numbers. . . . .	110
5.8	A graph shown in the third step for the hybrid control method; points addressed in the text are indicated by numbers. . . . .	117
5.9	Flow-chart of the proposed hybrid optimal method for the flexible hybrid MG. . . . .	118
5.10	The results of working of logical controller based-EMS . . . . .	121
5.11	The results of power flows using standard $\varepsilon$ -variables . . . . .	122
5.12	The results of power flows using the S-MPC method . . . . .	123
5.13	The results for the standard $\varepsilon$ -variables and optimal $\varepsilon$ -variables for one year. . . . .	123
5.14	Incorporating plug-and-play EV fleet using the logical controller and MPC controller based-EMS . . . . .	125
5.15	The illustration of the SOAcc of the battery is the hybrid control method. . . . .	126
5.16	The results of power flows (adding the EV fleet and removing the utility grid). . . . .	126
5.17	The results of power flow when the MG is in grid-connected mode and islanded mode . . . . .	127

## List of Tables

2.1	MPC control approach with main contributions in review articles. . . . .	19
2.2	MPC control approach with objectives and key findings. . . . .	20
4.1	The Comparison of Optimization Methods . . . . .	72
4.2	Values of System Parameters . . . . .	90
4.3	Numerical comparisons of $\varepsilon$ -variables method and extended optimal $\varepsilon$ -variables method . . . . .	92
5.1	Parameters for the real system (Ipsakis et al. (2009)). . . . .	120



## Nomenclature

### Greek Symbols

- $\eta_{ch}^l$  Charging efficiency of accumulator  $l$
- $\eta_{dis}^l$  Discharging efficiency of accumulator  $l$
- $\varepsilon_i$  State of converter  $i$
- $\varepsilon_i^{Avl}$  Boolean variable that determines the availability of using converter  $i$
- $\varepsilon_i^{Gen}$  Generic condition for converter  $i$
- $\varepsilon_i^{Req}$  Boolean variable that determines the requirement of using converter  $i$
- $\varepsilon_{a \rightarrow b}(k)$  Binary variable that describes the state of connection between nodes a and b
- $\mu, \gamma, \bar{\mu}, \bar{\gamma}$  Constraints in compact form
- $\phi$  Evolution Operator
- $\Delta t$  Time interval, 1h

### Acronyms / Abbreviations

- $CO_2$  Carbon-dioxide
- $H_2$  Hydrogen
- $H_2O$  Water
- $RS^{Acc}$  Set of accumulators
- $RS^{Con}$  Set of converters
- $SOAcc^l$  State of accumulator  $l$
- $SOAcc^l(1)$  Initial value of state of the accumulator  $l$
- $SOAcc_{max}^l$  Maximum value state of accumulator  $l$
- $SOAcc_{min}^l$  Minimum value state of accumulator  $l$
- AB Active Building

## Nomenclature

---

$A, B$	Coefficients for the plant model of the S-MPC
ABC	Artificial Bee Colony
ACO	Ant Colony Optimization
AI	Artificial Intelligence
$BAT$	Battery
BESS	Battery Energy Storage System
BIM	Building-Integrated Microgrid
$C(k)$	Control weight matrices
$C_l$	Capacities of accumulator $l$ , [kWh]
CC	Central Controller
$n_c$	The number of cells for the EL
$n_{cFC}$	The number of cells for the FC
$C_{EV_{1,2,3}}^{max}(k)$	Maximum battery capacities for $EV_1$ , $EV_2$ and $EV_3$
CHP	Combined Heat and Power
CS	Cuckoo Search
DR	Demand Response
DER	Distributed Energy Resource
DR-MPC	Distributed Robust MPC
DSM	Demand Side Management
$EL$	Electrolyzer
$n_{H_2}$	The generation rate of $H_2$ in the EL
$n_e$	The number of electrons
EMS	Energy Management System
ESS	Energy Storage System
EV	Electric Vehicle
$F_{a \rightarrow b}^j(k)$	Flow of $j$ from node $a$ to node $b$
$FC$	Fuel cell

FLC	Fuzzy Logic Controller
<i>Flow</i>	Set of flows
FQB	Frequency-Reactive Power Boost
<i>FT</i>	Fuel Tank
GA	Genetic Algorithm
GHG	Greenhouses-gas
GPC	Generalized Predictive Controller
<i>GR</i>	Grid
GT	Game Theory
GWO	Grey-Wolf Optimizer
HC	Hysteresis Controller
HRES	Hybrid Renewable Energy System
HVAC	Heating, Ventilation, and Air Conditioning
IoT	Internet of Things
<i>k</i>	Discrete-time instant
KNN	k-Nearest Neighbour
<i>L</i>	Logical Operator, [AND/OR]
LC	Local Controller
<i>LD</i>	Load
LP	Linear Programming
LQI	Linear Quadratic Integrator
LQR	Linear Quadratic Regulator
LSTM	Long Short-Term Memory
MAS	Multi-Agent System
MCF	Multi-Commodity Flow
MFC	Multi-Flow Control
MG	Microgrid

## Nomenclature

---

MILP	Mixed-Integer Linear Programming
MIQP	Mixed-Integer Quadratic Programming
MLD	Mixed Logic Dynamic
ML	Machine Learning
MPC	Model Predictive Control
MS	Master-Slave
MTLBO	Modified Teaching-Learning-Based Optimization
$N_c$	Control horizon, 24h
$n_F$	Faraday's constant
NLP	Non-linear Programming
NN	Neural Network
$N_p$	Prediction horizon, 24h
$P_i^j$	Power of j from node a to node b
PBG	Photovoltaic-Battery-Grid
PCM	Active/Reactive Power Mode
PD	Primal-Dual
$P_m^{max}$	Maximum values of power flows, 5 kW
$P_{net}(k)$	Differences between energy generation and consumption
PnP	Plug-and-Play
PPA	Power Pinch Analysis
PSO	Particle Swarm Optimization
PV	Photovoltaic
$Q(k)$	State weight matrices
$Q_f(k)$	Final weight matrices
QP	Quadratic Programming
R-MPC	Robust MPC
$R(k)$	Reference matrices

RBC	Rule-Based Control
RES	Renewable Energy Source
RL	Reinforcement Learning
S-MPC	Switched Model Predictive Control
$S$	State space
SCF	Single-Commodity Flow
SFC	Single-Flow Control
$str_{a \rightarrow b}^{SOAcc^l}$	Starting value of hysteresis zone of accumulator $i$ for the connection a to b
$U(k)$	Predictive control vector
$u(k)$	Control (input) variables for the MG
UK	United Kingdom
V2B	Vehicle-to-Building
VCM	Voltage Control Mode
VDP	Voltage-Active Power Droop
VSI	Voltage Source Inverter
$w$	Weighting factor
$n_{H_2O}$	The generation rate of $H_2O$ in the FC
WT	Wind Turbine
$x(k)$	State vector for the MG
$y(k)$	Output vector for the MG



## Chapter 1. Introduction

The impact of energy generation through conventional fossil fuels on satisfying the increase in electricity load demand, emissions, and socio-economical, environmental, and climate changes are raising the alarm to look for alternative low-carbon, sustainable RESs, storage systems, and networks (Kerr (2022)). The Net Zero goals of countries around the world, especially the UK (target to decarbonize all sectors by 2050, and 100% zero-carbon generation by 2035), show significant green movement towards carbon neutrality by encouraging production and utilization of power from RESs (Rutter and Sasse (2022)). An increase in the adaptation of RESs has led to a significant change in the topologies of traditional power networks, and now we have the concept of a MG (Cavus et al. (2022a,b)).

### 1.1. Background

MGs, a new concept in power networks, have emerged as a result of the growing use of RESs. MGs are small, self-sufficient electricity distribution systems that can function independently or in tandem with the main power grid. Typically, they comprise distributed RESs, energy storage systems (ESSs), and loads. MGs offer a more localized, efficient, and sustainable method of producing and distributing electricity, and they can provide greater energy security and dependability than conventional grid systems (Ocanha et al. (2020); Tobajas et al. (2022); Zhang et al. (2022)).

However, MG power system control can be difficult due to the MG's complexity and the varying properties of each asset. Several authors (Aaslid et al. (2022); Alipour et al. (2022); Wang et al. (2022b); Zhu et al. (2021)) have used stochastic dynamic programming and optimisation techniques. The operation of renewable energy systems has been optimised using the Cuckoo Search (CS) algorithm and the GOA to minimise total distribution network losses (Suresh and Edward (2020)). Distributed proximal primal-dual (PD) was utilised by Wang et al. (2022a) to optimise a distributed energy management problem for responsive loads and distributed generators with transmission losses. A PD-based distributed algorithm with dynamic weights is developed to achieve optimal energy management while maintaining tolerable operational costs and GHG emissions. Furthermore, the proposed technique has lower computational complexity than distributed optimisation algorithms reported by Liu and Yang (2022). The teaching learning-based optimisation (TLBO) technique was utilised to solve a multi-objective optimisation issue, lowering costs and increasing MG reliability. The results showed that charging and discharging ESSs could minimise MG costs while boosting system performance and reliability (Rahmani et al. (2023)). Zhang et al. (2016) presents simulation results that demonstrate the efficiency of

the master-slave (MS) peer-to-peer integration MG control method based on communication in achieving stable operation of the MG in grid-connected and islanded states, as well as smooth switching between these two modes. Advanced control strategies, such as MPC, have been developed to address these challenges. MPC is a mathematical control method that predicts a system's behaviour and determines the optimal control action using a model of the system. However, MPC implementation in MGs can be computationally intensive and complicated (Hu et al. (2021); Ulutas et al. (2020); Vazifeh et al. (2019); Villalón et al. (2020)).

As an alternative,  $\varepsilon$ -variables-based control strategies have been proposed as a method to simplify the control structure of MGs, allowing for greater scalability and resilience.  $\varepsilon$ -variables are a type of logic variable that can be used to model control strategies effectively and practically. However, the logical controller is not always the most efficient (Giaouris et al. (2018, 2013)). According to graph theory, a hybrid energy system can be defined as a set of power sources, including RESs, as well as loads, storage equipment, and other devices that enable the transfer of energy and/or matter. Using a directed graph to depict a MG is a widely recognised method, as evidenced by the work of Giaouris et al. (2018). This methodology has been demonstrated to significantly streamline the examination, investigation, and formulation and, ultimately, the optimal functioning of hybrid energy systems. In this context, each individual device is symbolised by a node, while the connection between the devices is denoted by an arrow or an edge, which signifies the transfer of energy or matter between two nodes. The main idea behind the  $\varepsilon$ -variable method is that every asset is symbolized by a node, and every flow of matter/energy is symbolized by an edge in the complicated MG system, as demonstrated in Figure 1.1. This power system's analysis, management, and operation can be simplified using this theory and the aforementioned evolution operators. This method states that any hybrid power system consists of three key factors: converters, accumulators, and flows. The converters are used to convert the energy/matter to matter/energy, the accumulators accumulate energy/matter, and the flows symbolize the flow of energy/matter. Lastly, the control statements are the evolution operators based on the logical operators, illustrating the different types of EMSs exploited by the multi-vector system (Giaouris et al. (2018)).

Furthermore, the emerging concept of flexible hybrid MGs with PnP assets has even greater control challenges. These MGs consist of various assets that can be added or removed as needed, resulting in a more complex and dynamic energy system. This requires sophisticated control strategies that can accommodate mode-dependent dynamics and multiple system models.

This thesis proposes different kinds of novel hybrid control methods. One of them combines  $\varepsilon$ -variables with traditional MPC in order to simplify the implementation of MPC and make it more effective for complex energy systems, such as flexible hybrid MGs. Another method is called extended optimal  $\varepsilon$ -variables in order to produce an optimal  $\varepsilon$ -variables. Also, a novel hybrid framework/method based on  $\varepsilon$ -variables and traditional MPC to generate and validate the S-MPC automatically has been generated that has the ability to permit more complex EMSs to be adopted readily.

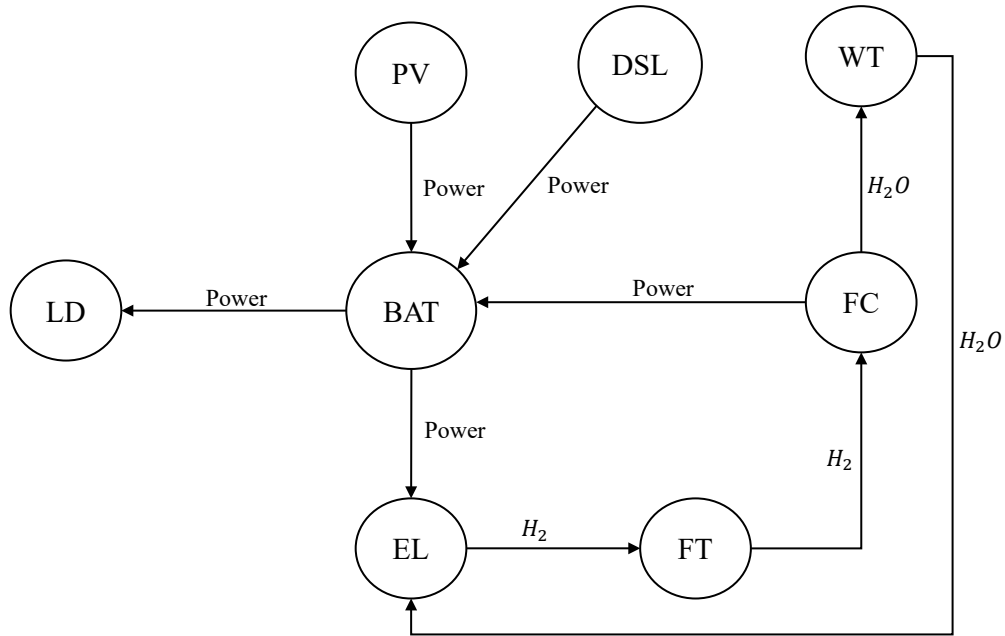


**Figure 1.1** Representing of hybrid energy system using graph method.

## 1.2. Overview

MGs have emerged as a new concept in power networks as a result of the expanding use of RESs. MGs are smaller power systems that can operate autonomously or in conjunction with the main grid. They provide numerous advantages, including enhanced dependability, decreased greenhouse gas (GHG) emissions, and enhanced energy efficiency. However, MG power system control is difficult due to its complexity and the unique characteristics of each system asset.

MPC, S-MPC and  $\varepsilon$ -variables are improved in this thesis. MPC predicts the system's behaviour and determines the optimal control action using a mathematical model of the system. However, implementing MPC in MGs can be computationally intensive and complicated.  $\varepsilon$ -variables-based control strategies have been proposed as an alternative method to simplify the control structure of MGs, allowing for greater scalability and resilience.

Despite their advantages, neither MPC nor  $\varepsilon$ -variables-based control strategies are sufficient to handle the complexity of flexible hybrid MGs with PnP assets on their own. Flexible hybrid MGs have assets that can be connected or disconnected, and their characteristics can change quickly, making them challenging to control.

This thesis proposes one of the novel hybrid methods that combine MPC with  $\varepsilon$ -variables to simplify the implementation of MPC and increase its efficacy for complex energy systems. The proposed method automatically generates and verifies Switched Model Predictive Control (S-MPC) by translating S-MPC decisions into  $\varepsilon$ -variables. S-MPC employs multiple models to represent system operating modes or scenarios. It selects a model and control strategy based on system state and performance objectives, enabling it to manage systems with mode-dependent dynamics.

The other hybrid method proposed significantly simplifies the control structure, enabling the use of more complex control strategies to provide additional benefits to the energy system, such

as scalability and robustness. On a flexible hybrid MG, the method is validated, demonstrating its efficacy by decreasing imported energy from the grid by nearly 46.7% and increasing exported energy to the grid by nearly 50.8%. By combining the strengths of MPC and  $\epsilon$ -variables-based control strategies, this dissertation contributes to the field of MG control by proposing a method that can facilitate the implementation of advanced control strategies for renewable energy systems.

### 1.3. About MGs

MG is a system component that includes RESs, ESSs, heating and cooling systems, and local loads such as active buildings (ABs) that can function as consumers/prosumers, among other things. In a controlled and coordinated way, MGs can operate in both grid-connected and/or islanded modes. The advantages of MGs are twofold. The MGs enable improved control and intra/interoperability of the various components at the local level. MGs improve power system dependability and give techno-socioeconomic benefits to both end users and energy system operators (Thirunavukkarasu et al. (2022)). Control and energy management of MGs is a critical problem due to their various properties, control capacities, and modes of operation. The nature of MGs varies depending on the application in terms of type (AC, DC, and hybrid), mode of operation (grid or islanded), and control architecture (centralized, decentralized, distributed, and hierarchical). Figure 1.2 depicts an overview diagram of MGs' type, mode, control, and optimization methods.

MGs have numerous benefits, including GHG reduction, reactive power support to raise voltage profile, decentralization of energy supply, and demand response (DR) (Zia et al. (2018)). Previous studies have investigated the use of MGs because of their expanding popularity. Hirsch et al. (2018), for example, examined some of the elements contributing to adopting an MG in a power system and its contributions to energy security, economics, and clean energy generation. Cagnano et al. (2020) examined MG functionalities, device combinations, and control topologies. Dawoud et al. (2018) offered a set of requirements and instructions that can assist in addressing the issues encountered in real-world MG applications. Many optimization strategies and tools for increasing MG use were proposed by Meng et al. (2016) and Zia et al. (2018) examined the implementation of EMS concepts and solutions in MGs.

An EMS maintains an MG's efficiency and economic activity based on the output power generated by distributed energy resources (DERs), device state, predicted load and weather, and electricity and fuel costs. An EMS can correlate and control the output power of DERs, ESSs, and energy exchanges. As a result, an EMS can be utilized to achieve a single or several goals, such as lowering daily operational expenses, performing real-time and reactive power monitoring, reducing losses, and balancing energy in transmission lines. In this instance, an EMS is necessary for MGs to work efficiently, reliably, and meet power balance in the short and long term (Koussa and Koussa (2015)).

The control of MG is crucial in addressing the issues posed by integrating DER units such as photovoltaic (PV) systems, wind turbines (WTs), microturbines that utilize the combined heat

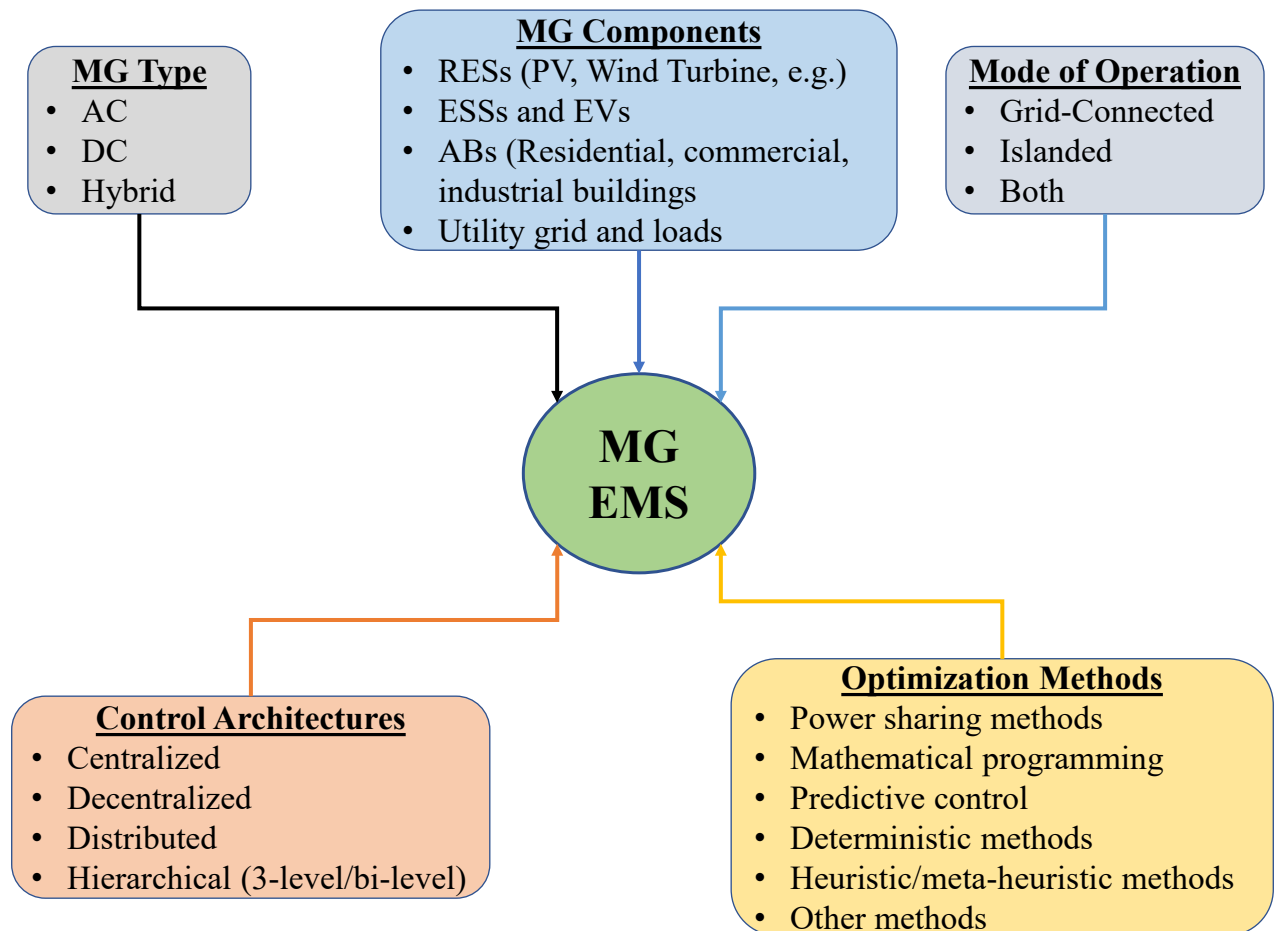


**Figure 1.2** MG components, type, mode of operation, control, and optimization methods

and power (CHP) system, and fuel cells and batteries in power systems. However, due to the unpredictable behaviour of such integration and the intermittent nature of RESs, integrating RESs into the main grid is impractical. As a result, the power system's reliability index decreases during the intermittent dispatching of RESs. The electricity system's resilience can be increased by implementing an adequate protection strategy, increasing redundancy, building isolation systems, and implementing conventional DERs. In this regard, the required norms and regulations should be established as standards for linking DERs to regular electric power systems (Zahraoui et al. (2021)).

### 1.3.1. MG Architecture and Elements

An efficient MG EMS depends on control architecture and optimization algorithms capable of managing their assets. MG control architectures include centralized, decentralized, distributed, and hierarchical control methods. Decentralized and distributed control systems have various advantages over centralized control methods, including increased flexibility, dependability, resilience, and the capacity to avoid whole-system failure (Espina et al. (2020)). Chamorro et al. (2020); Karavas et al. (2017); Mohseni and Moghaddas-Tafreshi (2018); Yazdani and Mehrizi-Sani (2014) describe the evolution of MG control and research topics addressed using

decentralized, distributed, hierarchical control structures. The control architecture chosen is determined by the type of MG, mode of operation, and user or operator needs.

Anvari-Moghaddam et al. (2017); Bogaraj and Kanakaraj (2016); Boudoudouh and Maâroufi (2018) give an overview of cooperative control frameworks with centralized, decentralized, distributed, and hierarchical designs, as well as their operations for DC MGs. Hierarchical techniques using artificial intelligence (AI), multi-agent system (MAS), and meta-heuristics algorithms are preferred over alternative control schemes for DC MGs (Nunna and Doolla (2013)). Dou and Liu (2013) addressed a review and comparison of distributed control systems for AC MGs, as well as the impact of communication failure on them. Belgana et al. (2014) provides a study of centralized and decentralized MG control from the standpoint of reliability. For the purpose of frequency regulation and economic dispatch in the islanded mode for AC MGs, a distributed hierarchical control system is designed in a coordinated manner (Urias et al. (2014)). For islanded MGs, consensus-based adaptive control in a distributed manner, taking uncertainty and disturbances into consideration, was established in Kuznetsova et al. (2014). The overview of hierarchical approaches for both AC and DC types of MGs may be found in Garcia Vera et al. (2019). For AC, DC, and hybrid MG systems, hierarchical control techniques are reviewed in Lin et al. (2018) and Ali et al. (2021). Achieving the primary, secondary, and tertiary levels of control in MGs increases operating efficiency and provides flexibility because of the variances in time scales. Local voltage control is often handled at the primary level in a hierarchical control system, followed by frequency regulation and voltage restoration at the secondary level and energy management at the tertiary level, as shown in Figure 1.3.

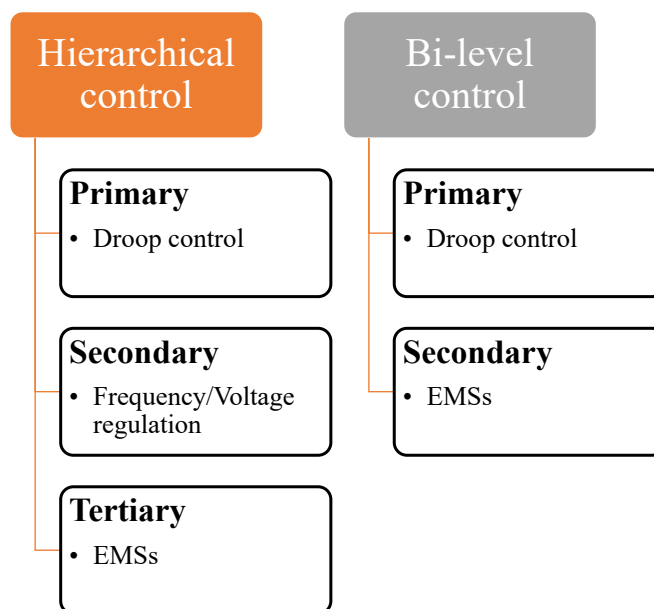


**Figure 1.3** Different levels of control in hierarchical architecture

## 1.4. Control Scheme of MGs

### 1.4.1. Primary Control Level

Primary control, also known as field control or the first level, depends entirely on the system's variables and local measurements (e.g., voltage and frequency). At this level, communication mechanisms are not required for the various elements and other categories of droop controls. This level ensures DERs' dependability, effective power-sharing, improved performance, and PnP capability. Active/reactive power mode (PCM) or voltage control mode (VCM) implementation in DERs allows users to control active and reactive power output and coordinate power-sharing across DERs as handled by voltage source inverter (VSI) controllers. In an MG, the PCM and VCM operate in grid-connected and island modes, respectively. The droop is used to modify the VSI's output power-sharing. The droop characteristics should be used to alter the active/reactive power or voltage and frequency to adjust the output power-sharing from the VSI (Borazjani et al. (2014)).

Droop control is an autonomous method for managing an MG's power dispatch frequency and amplitude. Droop is a common power-sharing mechanism that has primarily been used in MGs. Given the uncertainty of line impedances and the power produced from RESs, this strategy promotes power-sharing among DER inverters, resulting in an imbalanced power system. The conventional droop control seeks to establish a constant droop gain. An appropriate gain in droop control influences MG stability, voltage regulation, and power-sharing management (Mohammadi and Ajaei (2019)).

Several strategies for improving droop gain accuracy have been presented. For example, Datta et al. (2020) used the droop control strategy to adjust a multi-gain to manage power-sharing in a wind farm. Joung et al. (2018) investigated the droop gain in classical droop control for decoupling the frequency and voltage control of DERs, which can maintain grid frequency and voltage constants. Although conventional droop control is simple to build and apply, it has certain problems when used in MGs, including voltage reduction due to current equality, the inability to manage non-linear loads, and the entrenched trade-off between voltage and power-sharing (Kumar and Pathak (2020)). To remedy these issues, non-traditional droop control has been adopted. Various approaches, such as load sharing (Azizi et al. (2019)), voltage-active power droop (VPD) and frequency-reactive power boost (FQB) (Sao and Lehn (2008)), virtual output impedance (Razi et al. (2019)), and adaptive voltage droop (Wang et al. (2018)), have also been used to improve droop management in MGs.

### 1.4.2. Secondary Control Level

The secondary control level of MGs tries to rectify flaws in the primary control level, such as voltage deviations. This level, also known as the EMS level, improves power quality, restores the power system, ensures economical operations, and reduces frequency and voltage deviations and fluctuations induced by primary level droop control (Sahoo et al. (2017)). In MGs, the secondary control level is regarded as complex. Given the fluctuations in employment and the

power dispatched from DERs, the command and update between the loads and DERs must be in high communication and speed to ensure MG power generation. The goals and objectives of EMSs in MGs are presented in the subsections below. The subsections that follow describe the goals and objectives of EMSs in MGs.

**Minimize the Cost:** Luna et al. (2016) investigated an EMS in an MG that is integrated with a grid-connected BESS and uses mixed-integer linear programming (MILP) to reduce running costs and increase self-consumption. Jabarnejad (2020) created a MILP strategy to assure optimal power flow while lowering energy generation costs and GHG emissions. Sarabi et al. (2016) recommended utilizing linear programming (LP) to reduce the annual energy bill of railway station parking by adopting plug-in electric vehicles (EVs). Riffonneau et al. (2011) developed an effective power management technique for connected grids, PVs, and BESSs using dynamic programming. The suggested regulation maximizes economic gains while minimizing BESS degradation. Dong et al. (2019) presented an MG based on CHP and RES while considering the economy, environment, and flexibility to reduce operating expenses and  $CO_2$  emissions. Sultana et al. (2016) created an EMS controller that decreases voltage drop and extends the life of lithium-ion batteries. Chiang et al. (2017) developed an EMS controller to limit voltage loss to extend lithium-ion batteries' life. Ju et al. (2016) used mathematical optimization to anticipate day-ahead output to prevent shortages in various DERs. Zhao et al. (2020) devised an optimization technique for MGs that employs day-ahead market operations to reduce DR costs. Zahraoui et al. (2021) developed a risk-based technique for improving the overall transient stability of power systems by using LP to reduce shedding costs. Giraldo et al. (2018) provided a comprehensive MG framework that can operate in both grid-connected and isolated modes and solves the objective function using the convex mixed-integer technique.

EMS difficulties in MGs have also been solved using various meta-heuristic optimization techniques. Elsieid et al. (2016) developed an advanced real-time EMS employing the genetic algorithm (GA) to limit energy costs and carbon emissions concurrently while maximizing power penetrating from REs. Particle swarm optimization (PSO) was used by Grisales-Noreña et al. (2020) to lower the cost of electricity obtained from utility networks. Marzband et al. (2015) employed an artificial bee colony (ABC) to optimize production costs and boost RESs penetration in MGs. Roy et al. (2019) investigated an EMS in an MG utilizing an ant-lion optimizer, which parameterizes the uncertainty in solar and wind energy generation. This optimizer meets the load demand at the lowest possible cost while considering the constraints.

Other articles have employed hybrid or modified optimization approaches, such as a hybrid of the bacterial foraging optimization algorithm and GA, to minimize power costs and reduce peak-to-average ratio (Javaid et al. (2017)). The hybrid ABC-PSO analyzes the techno-economic MG and reduces the total cost (Singh et al. (2020)).

**Power Quality:** The intermittent and unstable nature of RESs can cause oscillations in power quality and stability Luo et al. (2016). By monitoring the control equipment utilizing control theories and optimization approaches, the EMS can increase power quality and stability in the power system (Mousazadeh Mousavi et al. (2018)). Several control mechanisms and procedures

in EMSs for increasing power quality have been proposed in the literature. Mei et al. (2017), for example, presented the moth-flame optimization technique to decrease voltage deviation and overall system transmission loss and increase power stability through reactive compensator sizing. To actualize power flow in DERs and supply the outage area, Wang et al. (2020) created a service model for an imbalanced three-phase active process distributed utilizing a multi-terminal soft open point system. The concept was stated as a set of goals that included maximizing the restored load while reducing voltage imbalance and power loss. Mousazadeh Mousavi et al. (2018) suggested a unique control that uses the PV and battery energy storage interfacing inverter to increase power quality while considering many constraints, such as battery service life and charging/discharging status. Sahoo et al. (2021) proposed a novel centralized energy management strategy for managing voltage flow and inverter flexibility in a solar-battery hybrid MG. Aljohani et al. (2020) used the vector-decouple technique to maintain stability and manage the hybrid MG. They devised a controller that assesses efficiency and robustness while improving voltage output and frequency quality. Nasr et al. (2020) suggested a multi-objective function that involves minimizing an MG's voltage deviation to maintain voltage balance and satisfy the contingency constraint. Zhang and Li (2020) used multi-objective optimization approaches to solve a multi-objective function optimal reactive power dispatch problem and suggested a model that minimizes active power loss and voltage variations. Leonori et al. (2016) created an optimal power flow plan for a grid-connected to a BESS, used the BESS to increase power stability, and managed power in real-time with a fuzzy EMS controller.

### ***1.4.3. Tertiary Control Level***

The tertiary control level, as the top-level control, maintains the optimality of the operation, specifically the efficiency and cost between the MG and the primary grid, and vice versa. Because of the complexity of the computation and forecast model of economic and meteorological data, this level typically has a slow dynamic response to define the ideal active and reactive power references of each distributed generator (Yamashita et al. (2020b)). The prediction model aids in weather classification, network optimization, and uncertainty quantification. At this level, various methods such as ML (Chaouachi et al. (2012)), long short-term memory (LSTM) (Qing and Niu (2018)), k-nearest neighbours (kNN) (Pedro and Coimbra (2015)), generalized regression neural network (NN) (Ramsami and Oree (2015)), NN ensemble (Raza et al. (2018)), and deep recurrent NNs (Alzahrani et al. (2017)) are used to formulate the forecasting and prediction model. Although the secondary level is concerned with power quality and DER sharing, the tertiary level is concerned with economic aspects, energy market involvement, and power-sharing trends.

## **1.5. Control Architectures**

Distributed and hybrid RES generators (e.g., PV panels and WTs) are used in hybrid energetic systems or MG systems to produce clean energy (e.g., solar, wind). In contrast, ESSs are installed

to compensate for the fluctuation between RESs generation and load consumption. Depending on the desired and established objectives, these hybrid systems can function in either grid-connected or standalone modes. Since the penetration of these distributed generators is increasing, new EMSs are needed to ensure seamless integration into the existing electrical network.

As a result, implementing an energy management approach should improve the dynamic response of DERs under varying operating conditions and maximise the use of RES power generation while ensuring system stability when one or more sources are connected or disconnected from the system. These control systems can be divided into three categories: centralized, decentralized, and hierarchical control. The rest of this section discusses these control strategies.

### ***1.5.1. Centralized Control***

To handle many system elements, centralized control approaches employ a single central controller (CC) comprising a high-performance processing unit and a secure communication architecture (e.g., RESs, storage systems). Each entity employs a local controller (LC) to communicate and interact with the CC. Furthermore, the CC can monitor, gather, and analyze real-time data using cutting-edge communication and computing technologies (e.g., the Internet of Things (IoT), Big-Data). This lets all entities work with the central energy management controller while providing a flexible MG operation in grid-connected and standalone mode. The CC gathers data such as RES energy output, energy consumption patterns, energy prices from market operators, and meteorological conditions before executing the most optimal and efficient system control.

Many research studies have created and implemented centralized energy management techniques. For instance, the authors of Tsikalakis and Hatziaargyriou (2011) presented a centralized controller in order to maximize the operation of MG by optimizing the production of dispersed RESs generators while creating back-and-forth energy transfer with the main utility grid. The proposed solution's efficiency on the MG system was studied by analyzing a typical case network operating under various market policies and spot market pricing. Moreover, the authors of [19] created a centralized EMS for a standalone MG system based on the model predictive control approach to reduce computational demands. In fact, nonlinear programming (NLP) and MILP techniques were used to solve the problem iteratively (Warnier et al. (2017)).

### ***1.5.2. Decentralized Control***

Unlike centralized techniques, each entity in decentralized control is regarded as autonomous by employing an LC. This signifies that a leader controls various groupings of entities. The phrases 'decentralized' and 'distributed controls' are frequently used interchangeably in the literature Kermani et al. (2020); Yamashita et al. (2020b). Distributed control can be considered a decentralized control in which LCs elect the leader entity based on local measurements such as frequency and voltage levels. They may also share information with their neighbours. For distributed control, LCs not only use local measurements, but they can also communicate and receive information from other LCs (Pourbabak et al. (2019)). With decentralized control

systems, limited local connections are necessary, and the control choices are made based only on local measurements.

### 1.5.3. Hierarchical Control

Figure 1.4 shows that a compromise between fully centralized and decentralized control structures is reached by providing hierarchical control structures (Molzahn et al. (2017); Van et al. (2020)) based on three control levels: primary, secondary, and tertiary.

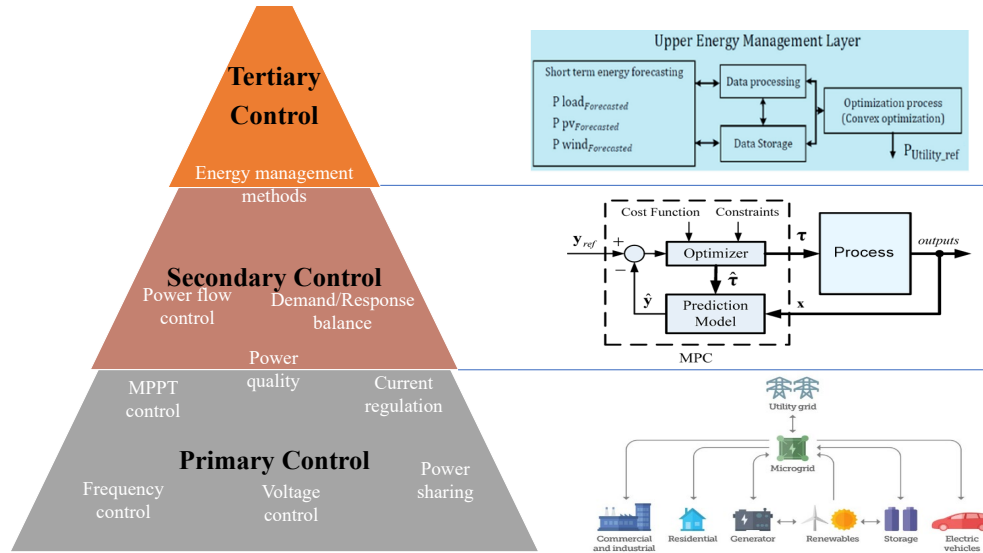


**Figure 1.4** Hierarchical control structure.

The primary control level stabilizes the voltage and frequency generated by each source in order to stay within the standards' limitations (Elmouatamid et al. (2020, 2021); Gaiceanu et al. (2020)). Furthermore, the principal control level recognizes the operating mode of MG systems, allowing them to function in grid-connected and standalone modes (Prabaharan et al. (2018)). After the system's load variation, the secondary control level's MG voltage and frequency are restored. The goal is to maintain and improve power quality within the specified standards, allowing synchronization between MG systems and the main electrical network (González-Romera et al. (2020)).

The key objectives of tertiary control are the power flow control in the grid-connected mode, ensuring the optimal operation in both modes, such as capacitance and inductance (Guerrero et al. (2012)). Figure 1.4 depicts the structures of the hierarchical control levels.

In summary, there are many advantages of MG usage: (i) it can operate as islanded systems under power grid outage situations; (ii) it can balance energy production and energy consumption; (iii) its generation resources can be scheduled and dispatched properly; (iv) it can accomplish high reliability and resiliency; (v) it can sustain the reliability development, reduction in the running cost, and market contribution; (vi) it can reduce the power losses among distributed energy sources; (vii) it can enhance the network congestion. However, there have been several issues recently with the MG control. These are (i) scalability when the MG structure is getting

more complicated, (ii) adaptability or flexibility when the MG structure is changed or modified (for instance, removing a utility grid and adding a diesel generator), (iii) complexity of the control method on the MG control, such as the implementation of MPC and S-MPC and (iv) optimal control among power flows on the MG components.

The next chapter will explain different kinds of control methods for MGs and compare control strategies. Also, this chapter will prove that MPC is an advanced and efficient method compared to other control strategies.

## Chapter 2. Literature Review

### 2.1. Control Strategies for MGs

Utilizing several energy sources in MG systems necessitates employing effective control strategies/approaches for controlling energy flow. This necessitates the creation and deployment of EMSs. In fact, as shown in Figure 2.1, optimization strategies for DR, demand-side management (DSM), and power quality control are required to meet various EMS objectives while satisfying multiple restrictions, such as energy price reduction and occupant comfort maximization.

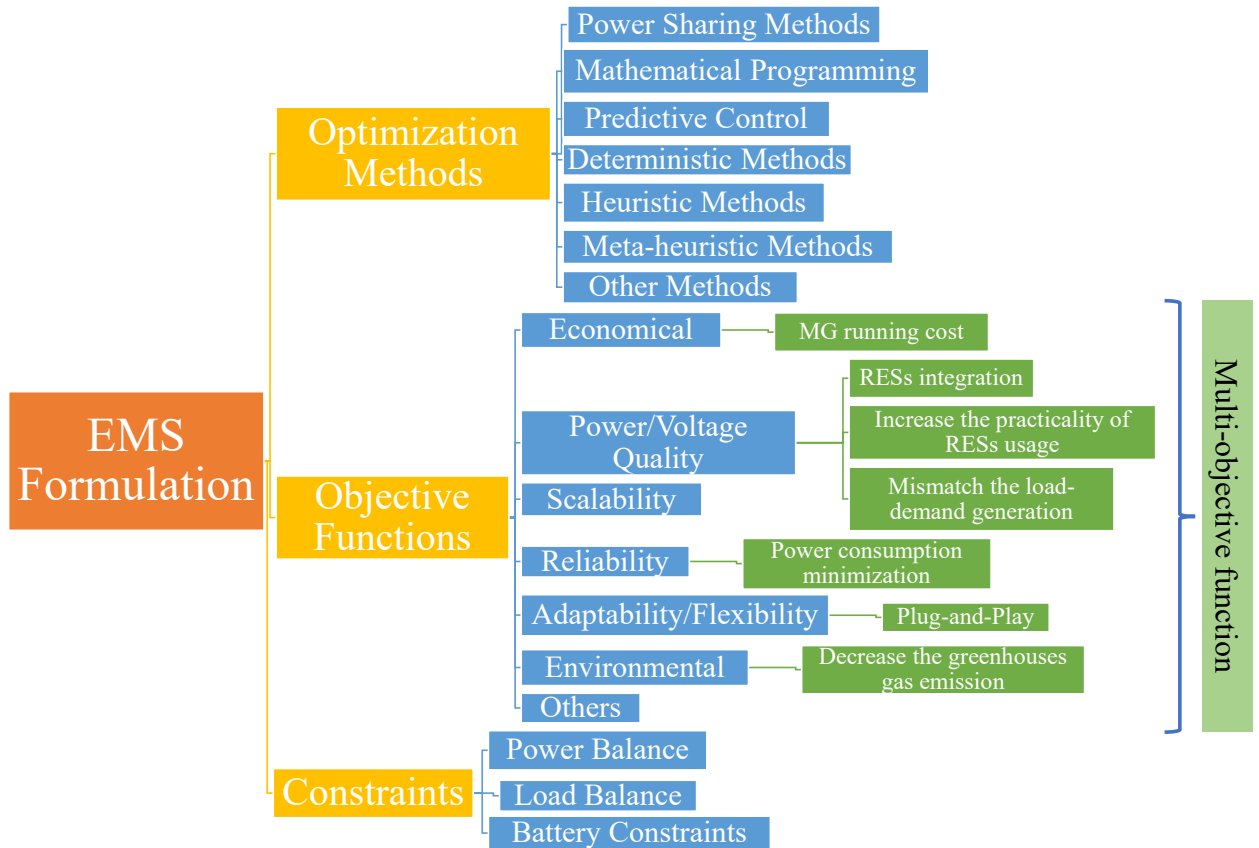


**Figure 2.1** Objective functions constraints and optimization methods for optimum operation of MG systems.

As shown in Figure 2.1, several approaches have been presented that use various goal functions and restrictions in conjunction with optimization methods for efficient energy management.

### **2.1.1. Objective Functions and Constraints**

Implementing EM control techniques specifies the primary aim functions, which may be connected to operation cost, pollution, dependability, and power quality (Cannata et al. (2019); Hannan et al. (2020); Jiménez-Fernández et al. (2018); Li et al. (2017)). For example, the primary goal of employing economic objective functions is to reduce the cost of power. For cost reduction in MGs, many formulations have been investigated. For example, the authors of Liu et al. (2014) developed an EM technique for reducing electricity costs in a residential MG composed of many houses with DERs. This EM method took into account predefined purchasing/selling decisions for each time slot to save power costs and scheduling decisions for the shifted loads. Researchers defined cost minimization as a dynamic economic load dispatch problem. A meta-heuristic algorithm was presented and compared to various methods such as differential evolution, GAs, and PSO (Kamboj et al. (2016)). The authors of Haidar et al. (2020) developed an ideal technique by comparing the performance of various hybrid MG systems. A mathematical approach was investigated for sizing the MG component to meet the lowest cost while increasing load demand under different weather conditions. The obtained findings demonstrated the ideal configuration for MG system components to achieve the lowest energy and net present costs. The authors of Elkazaz et al. (2020) described an EMS that selects the appropriate setting for a central battery storage system based on a defined cost function to minimize an MG's daily running cost while optimizing the deployed RES's self-consumption.

Following the definition of the system's constraints and objective functions, appropriate optimization methods are necessary to ensure the power flow exchange between installed RES/storage and MGs on the one hand and MGs and the utility grid on the other.

### **2.1.2. Optimization and Control Methods**

Many studies on MG control have been conducted based on system topologies, architectures, and operating modes (Ontiveros et al. (2017); Rathor and Saxena (2020); Shayeghi et al. (2019)). For example, optimization and control methods should handle the stochastic nature of the installed RES generators by guaranteeing a reliable supply of power to customers while keeping the storage system, electricity bill, and occupants' comfort at the appropriate operating conditions. Figure 2.2 depicts a proposed taxonomy of the most prevalent MG control approaches utilized in MG operations.

### **2.1.3. Classical Approaches**

Several energy management optimization methods, such as mixed integer linear and NLP, are classical. These approaches can be considered efficient strategies for controlling MG systems following the objectives and constraints outlined. For instance, the authors of Sukumar et al. (2017) developed an MG EMS for power sharing, power trading with the main grid, continuous run, and on/off mixed mode based on the LP optimization method. In this study, the on/off mode was solved using a MILP solution approach, which maximized the operation of the MG

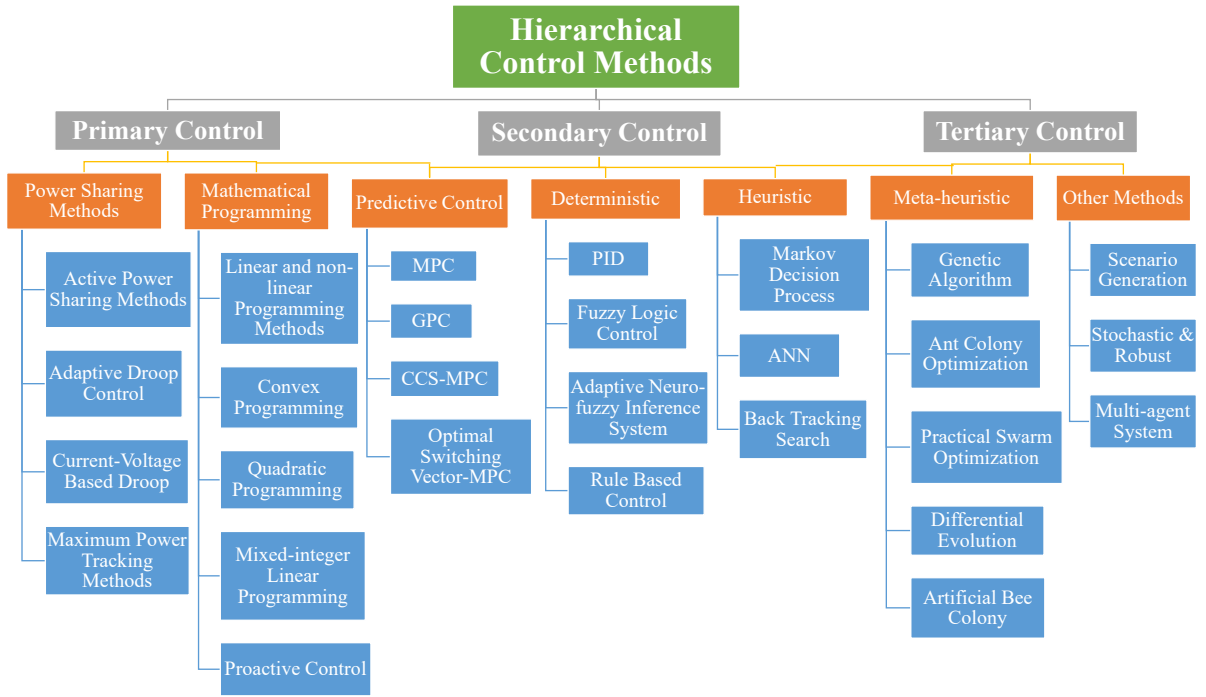


Figure 2.2 Control approaches for EMSs.

concerning the main grid, fuel cell, and ESS operation modes. The authors of Nemati et al. (2018) created a real-coded GA and a MILP-based approach for scheduling MG unit commitment and economic dispatch. The study considered voltage restrictions, equipment loadings, and unit constraints in its formulation. The authors of Shekari et al. (2019) presented another intriguing paper offering a MILP-based solution for regulating electrical and heat needs in a multiple MG scenario. For optimal scheduling of MG, the proposed technique examined various energy converters and storages, distributed energy generators, and electricity/heat storage units, as well as technical and economic linkages between electricity and natural gas systems. The deployed algorithm was created using AC power flow. The deployed model obeyed reactive power and voltage security limitations, allowing the MG system to operate at the lowest possible cost.

2.1.4. Heuristic and Meta-heuristic Methods

Heuristics and evolutionary algorithms are commonly used to solve single and multi-objective optimization issues. The authors of (Papari et al. (2017)) proposed a heuristic strategy for optimizing the operation and energy management of DC MG systems. The investigated problem was formulated as a single-objective optimization problem with the sole goal of cost minimization. By combining the Harmony search algorithm and enhanced differential evolution, the authors of (Khan et al. (2019)) proposed a meta-heuristic-based system. Several knapsacks were employed to ensure power consumption did not exceed a specified threshold value during peak periods. The authors provided an economic model for ESSs and an actual coded-GA model for MG systems working in a grid-connected mode (Chen et al. (2011)). Based on its capital, energy arbitrage revenue, operating cost, and maintenance cost, the created algorithm optimized the present cost of an ESS during its lifespan. The authors of Radosavljević et al. (2016) proposed a GA-based

optimal EMS for a grid-connected MG system that considered the electricity price, power consumption, and unpredictability of RES generation. Compared to the GA and combinatorial PSO, the work demonstrated that the PSO method is more effective in finding the optimal solution of the examined optimization function. The authors of (Marzband et al. (2014)) used the multi-period gravitational search technique to solve a deterministic energy management problem. The authors of Aghajani et al. (2015) solved the EMS problem using a multi-objective PSO approach, which was regarded as a multi-objective problem. The authors of Alavi et al. (2015); Rabiee et al. (2016) used PSO-based techniques to tackle the EMS problem as a single-objective problem. Another paper by the authors of EI-Bidairi et al. (2018) combined an intelligent expert system called fuzzy logic with a meta-heuristic algorithm called Grey-Wolf Optimizer (GWO). The presented methodologies tackled MG systems' economic and environmental optimization concerns by considering RES uncertainties and power demand fluctuations.

Heuristic optimisation approaches generally use exploratory methods to solve optimization problems in a reasonable amount of time. They are, however, unable to guarantee the optimality of the produced outcomes (Khan et al. (2016)). The meta-heuristic approaches are effective and widely utilized methods for control and energy management in the MG system. Many works in the literature have examined the effectiveness of various tactics. In certain works, the meta-heuristic control has been linked with other control systems in order to profit from the performance of both approaches (Grisales-Noreña et al. (2020); Khan et al. (2020)).

### **2.1.5. Artificial Intelligent Methods**

EMS optimization strategies are classified as AI-based, conventional mathematics, meta-heuristic, and others. AI-based methodologies include fuzzy logic, game theory (GT), multi-agent, NN, and reinforcement learning (RL). Conventional ways include dynamic programming, resilient programming, stochastic programming, bi-level programming, and mixed integer programming methods. Meta-heuristic techniques include swarm intelligence, evolution, and heuristic approaches. The authors of Thirunavukkarasu et al. (2022) comprehensively evaluated optimization approaches for tackling many control objectives in MG EMS.

The authors of Motevasel and Seifi (2014) presented an expert system for energy management in MG systems that uses NNs to estimate the power generation of installed RESs. The authors proposed a mathematical model for intelligent load control in a standalone MG system (Solanki et al. (2015)). NNs were employed to model the examined loads, and predictive control was applied to manage the energy based on projected load variation. The authors of Venayagamoorthy et al. (2016) presented an EMS for an MG connected to the utility grid to optimize renewable energy utilization while minimizing carbon emissions. Two NNs were employed to model the proposed EMS using evolutionary adaptive dynamic programming and learning ideas. One NN was utilized for the management approach, while the other was employed to test the optimal system's performance. The authors of Wang et al. (2019) presented a Lagrange-programming NNs technique for effective MG system control and administration, aiming to lower the overall

cost of MG. This work divided the load into controllable, thermal, price-sensitive, and critical loads (Mahmoud et al. (2017); Roslan et al. (2019)).

RL-based approaches have been widely employed in decision-making due to their adaptability to the environment and incorporation of user input into the control logic. Vázquez-Canteli and Nagy (2019) provides a full examination of modelling methodologies and algorithms for DR using RL. Depending on the penalties and rewards generated, RL can work with MASs to produce DRs. In Azuatalam et al. (2020), an effective scheduling and control technique for heating, ventilation, and air conditioning (HVAC) systems was created. As compared to a hand-crafted baseline controller, the results showed that the RL-based controller could reduce energy use by 22% while preserving interior thermal comfort. Furthermore, NNs are used in EMS schemes focusing on the optimal functioning of renewable energy integration (Urias et al. (2014)). Urias et al. (2014) presents an RNN-based EMS and a multi-agent-based weather forecasting technique. The RL approach has also been used to optimize the coordination of several ESSs in a MG while considering a linked topology (Qiu et al. (2015)).

Because of its flexibility for given restrictions, cheap computing time and complexity, and ease of implementation, Ant Colony Optimization (ACO) is one of the more often utilized approaches for energy management in MG systems. The behaviour of real ants inspires this classical method to seek reasonable solutions to a given optimization issue. It is a simple computational agent that turns optimization issues into shortest-path problems on a weighted network. In Rahim et al. (2016), the authors used an ACO approach for energy management in DSM. To acquire a plausible solution for the intended objective function, the authors first built an energy management controller model utilizing multiple knapsack problems and then utilized an ACO technique. The authors aimed to demonstrate that the ACO efficiently reduces electricity bills and minimizes peak-to-average ratio while considering user happiness. The authors of Esmat et al. (2013) created another ACO approach by investigating a combined cost optimization scheme to decrease operational costs and pollution levels while serving the MG's load demand. To test the suggested method's performance, it was compared to two other techniques, Lagrange and Gradient. Other AI-based optimization methods have primarily been employed in the literature for energy management and optimization challenges. The authors of Chenghui et al. (2007) reported PSO for energy management fuzzy controller design in dual-source powered electric cars. A mathematical model of the energy management problem was used to examine the power of energy storage.

### ***Predictive Control Methods***

MPC and generalized predictive controller (GPC) are well-known techniques for predicting future events and forecasting appropriate control actions. In fact, they can feature optimization methods, allowing them to incorporate system limits and disturbances into anticipated control decisions. For instance, the GPC is commonly employed in advanced control applications, such as energy management and building automation systems (Buyak et al. (2017); Rahmani-Andebili and Shen (2017)). Moreover, the authors of Rahmani-Andebili and Shen (2017) proposed an

adaptive and dynamic optimization technique based on the stochastic MPC approach. The proposed energy management technique solved the DER scheduling problem for smart houses with varied energy sources. Its goal was to address the PV power generation's unpredictability and variability. This study was created for large-scale smart dwellings, taking into account their neighbours' collaboration. Another intriguing paper was presented by the authors of Bordons et al. (2019), who proposed an EMS using an MPC, with a basic state-space model utilized for MG system performance modelling. This work regarded the RES power generation and consumption as measurable disturbances parameters for the EMS. As a result, the storage systems and costs were modelled as constraints on the MG system, and the state-space equations were used to solve them. For the economic optimization of an MG laboratory, the authors of Mendes et al. (2016) utilized an algorithm based on the MPC model. The laboratory housed a hybrid hydrogen storage system, a battery bank with a utility grid link, and an EV charging station. A hierarchical control structure was developed along with the MPC approach, which operated at different time frames. The proposed approaches worked on the first level to keep the MG stable and on the second level to control the purchase and sale of power to the utility grid, regulate the usage of energy storages, and maximize the use of RESs. The given findings demonstrated the dependability of the proposed control algorithm for managing the MG system. The authors of Garcia-Torres et al. (2018) developed an optimal energy management strategy for the MG with external agents, such as a battery storage system and fuel cell EVs, based on the MPC controller. A mixed-integer quadratic programming (MIQP) method was used to tackle the MPC issues. The plant was modelled using the Mixed Logic Dynamic (MLD) framework, and the operating and degradation costs were factored into the objective function. The authors of Parisio et al. (2014) created an MPC strategy for optimizing the operation of an MG system. A mixed-integer-linear framework was shown with economic dispatch, energy storage, unit commitment, and grid interaction. The cost was addressed and parameterized in great depth throughout the problem formulation. The experimental findings were presented, demonstrating the effectiveness of the proposed technique of saving money in comparison to existing practice.

The MPC approach outperforms other methods for implementing control and optimization architectures for MGs-EMS. AI-based EMS approaches enable flexibility in addressing MGs-EMS PnP capabilities. The EMS algorithms should be scalable in order to solve increases in dimensionality or non-linearity in the objective formulations. AI approaches such as RL and ML methods and meta-heuristics that can manage such complex goal functions are gaining prominence in recent studies due to increased data availability and the capacity to handle the system's dynamic nature. The computational complexity should be decreased by using efficient solvers and various simulation platforms.

As illustrated in Table 2.1, MPC employs various optimization techniques, such as rolling (receding), finite horizon, convex programming, MILP, and multivariable optimization. 2.1 depicts the elements of MPC-based control techniques for solving different kinds of objectives in MG-EMS, as listed in Table 2.2.

Ref.	Main Contributions
Kamal and Chowdhury (2022)	MPC has emerged as a possible alternative to traditional methodologies for everything from voltage regulation and frequency management to power flow management and economic optimization. MPC possesses the most accurate forecasting model.
Konneh et al. (2022)	The advantages of MPC over several methodologies for modelling uncertainty are demonstrated in this review work for grid-connected and islanded systems. It demonstrated the characteristics, strengths, and drawbacks of numerous MPC modelling methods, as well as some of their adjustments for dealing with uncertainty in MGs.
Babayomi et al. (2022)	MPC allows for the multivariable control of power electronic systems while addressing physical restrictions without needing a cascaded structure. These qualities result in fast control dynamic response and good nonlinear system performance. MPC is more adaptable, with multivariable and intuitive properties for smart grid and MG systems.
Hu et al. (2021)	This paper provided a comprehensive overview of MPC in individual and inter-connected MGs, including control techniques at the converter and grid levels, as well as control strategies applied to three tiers of the hierarchical control architecture. According to this study, MPC is emerging as a feasible alternative to existing methodologies in voltage regulation, frequency control, power flow management, energy management, and economic operation optimization.
Tarragona et al. (2021)	This study summarised the most recent enhancements to tackle computational issues and an assessment of the objective functions utilized in each study, which were primarily concerned with minimizing energy costs, peak power, and $CO_2$ emissions. MPC is the most promising technique for decreasing MG's operating costs.
Fontenot and Dong (2019)	Various optimization methods and control systems, including rule-based control, optimum control, agent-based modelling, and MPC, were evaluated, and it was determined that MPC is the most efficient for MG systems.
Vašak et al. (2021)	MPC is becoming increasingly popular due to its adaptability, ability to be used in any application independent of field, and accessibility to fast computers. Researchers will be helped by the work presented here as they further investigate the adaptability of this controller for design, analysis, and application in RESs.
Villalón et al. (2020)	To improve performance and dynamic response, this review found that predictive control methods are utilized on MGs for the three control levels and with model adjustments to account for uncertainties. Predictive control is a particularly promising control method for MG applications that need varying levels of control.

**Table 2.1** MPC control approach with main contributions in review articles.

Ref.	Features	Key Findings	Objective
Zhao et al. (2022)	Uncertainty of RES	The capacity to balance MG operation's robustness and economy is provided by EMS modelled as DRMPC technology.	Economical operation
Ma et al. (2022)	Reliability, forecasting uncertainties	Decrease in capital cost and help downsize the system.	Reduce PV curtailment and unmet load
Khokhar and Parmar (2022)	Uncertainty in MG	A MG's frequency variations have a reduced tendency to degrade and reduced cost EV batteries.	Frequency regulation
Dong et al. (2022)	Complexity of MG control	Decrease communication cost	Recovery of voltage/frequency, complexity reduction
Yamashita et al. (2020a)	Uncertainty of battery usage	Reduces annual costs for residential and non-residential building MGs.	Complexity reduction in MG control
Marín et al. (2019)	Uncertainty of RES	Reduce operating cost, reduce peaks, and uniform grid consumption.	Optimal operation considering uncertainty
Ouammi (2021)	Uncertainties of power generation, operational flexibility of EVs	Peak loads are reduced for building MGs	Reduce peak load and optimize power exchange
Lei et al. (2017)	Complexity of MG control	Improve the power quality of PV power plants.	Stabilize the grid import/export
Zhang et al. (2018)	Forecasting of power demand	Decrease in total cost by 22.69%	Minimize the prediction error
Fontenot and Dong (2019)	Forecast RE generation and load	Decentralized approach reduces the risk of system failure.	Decrease congestion and peak loads
Minhas et al. (2022)	Multi-time scale, forecasting of RE uncertainties, load demand	Optimal charge and discharging, reduced annual storage capacity loss of EV batteries by 23%.	Multi-time scale, forecasting of RE uncertainties, load demand
Elkazaz et al. (2020)	Forecasting of load demand	EMS achieves reduction in cost by 30%.	Increase in RE self-consumption within MG

**Table 2.2** MPC control approach with objectives and key findings.

MPC-based techniques are frequently employed to tackle mixed integer nonlinear objectives such as the unit commitment problem of EMS in MGs. The MPC-based control approaches take into account factors, including variability, MG component uncertainty, and the usage of forecasting data. Effective MGs-EMS that can be provided over a considered time horizon in day-ahead or real-time scheduling can also be provided by MPC rolling or receding horizon optimization approaches.

The neuro-fuzzy algorithm utilized by the MPC-inspired EMS takes into consideration the intermittent nature of RES in grid-connected MG with the loads and PV provided in Ulutas et al. (2020). The stochastic-based energy management of MG, which has many control objectives, is solved using the MPC rolling horizon approach in order to overcome the uncertainty issues with RES and loads. Scenario-based stochastic programming with a rolling horizon approach is described in Silvente et al. (2018) as a way to reduce the operational expenses of MGs when there is uncertainty regarding wind speed. The data obtained via deterministic approaches can be updated or modified using the rolling horizon or MPC approaches, which are reactive-based methodologies. A scenario-based MPC was suggested in Parisio et al. (2016) to reduce operating expenses and overall emissions. Wu et al. (2020) presents an opportunity constraint MPC for a grid-connected MG with a gas turbine, battery, and PVs. In this, economical operation over a long-time horizon is achieved at the higher level, while optimal scheduling takes uncertainty into account at the lower level. To ensure cost-effective and adaptable operation, Garcia-Torres and Bordons (2015) provides MPC-based optimal control for hybrid ESS, such as hydrogen ESS, batteries, and capacitors, in renewable energy MGs. For islanded AC MG, a hierarchical MPC-based technique was utilized to overcome concerns with power quality and uneven power-sharing Jayachandran and Ravi (2019). Moreover, EMS-specific MPC techniques that take into account battery ageing have been established (Allahham et al. (2019, 2022)). For residential MGs with grid connection (Nikkhah et al. (2021c,d)) and islanded operation of MGs (Cavus et al. (2022b); Nikkhah et al. (2021b, 2022)), a number of MPC-based building-to-building EMs are also proposed.

In the well-known 3-layer control, rolling or receding optimization, MPC-based processes accomplish the secondary control layer's goals, such as voltage regulation, frequency regulation, and power allocation. Furthermore, self-triggering based on the MPC's predictive capability was used to reduce communication costs (Dong et al. (2022)). In order to improve power flows and lower peak loads while maintaining the quality of service for EVs in a vehicle-to-building (V2B) scenario, MPC is employed in the MG optimization framework (Ouammi (2021)). Centralized energy management for a building-integrated MG (BIM) was developed using MPC and finite horizon planning optimization (Dagdougui et al. (2020)). The BIM operation that satisfies the indoor temperature along with BIM components and electricity exchange with the grid is optimized by this method. A dual decomposition-based distributed MPC for energy management in MGs networks is given in Razzanelli et al. (2020) for a workable power exchange without causing a privacy risk. For standalone MGs with wind, solar, and battery power sources, Kong et al. (2019) presents a hierarchical (upper and lower layer) distributed MPC that offers

great reliability, efficiency, and flexibility in its control. A robust MPC with intraday energy management optimization for islanded MGs was proposed in Yang et al. (2019). In the MG-EMS application that incorporates distributed RES and ESS, MPC and its improvements that are utilized to achieve goals like optimizing energy efficiency, managing import/export power from/to the grid, and economic optimization show a growing trend (Hu et al. (2021)).

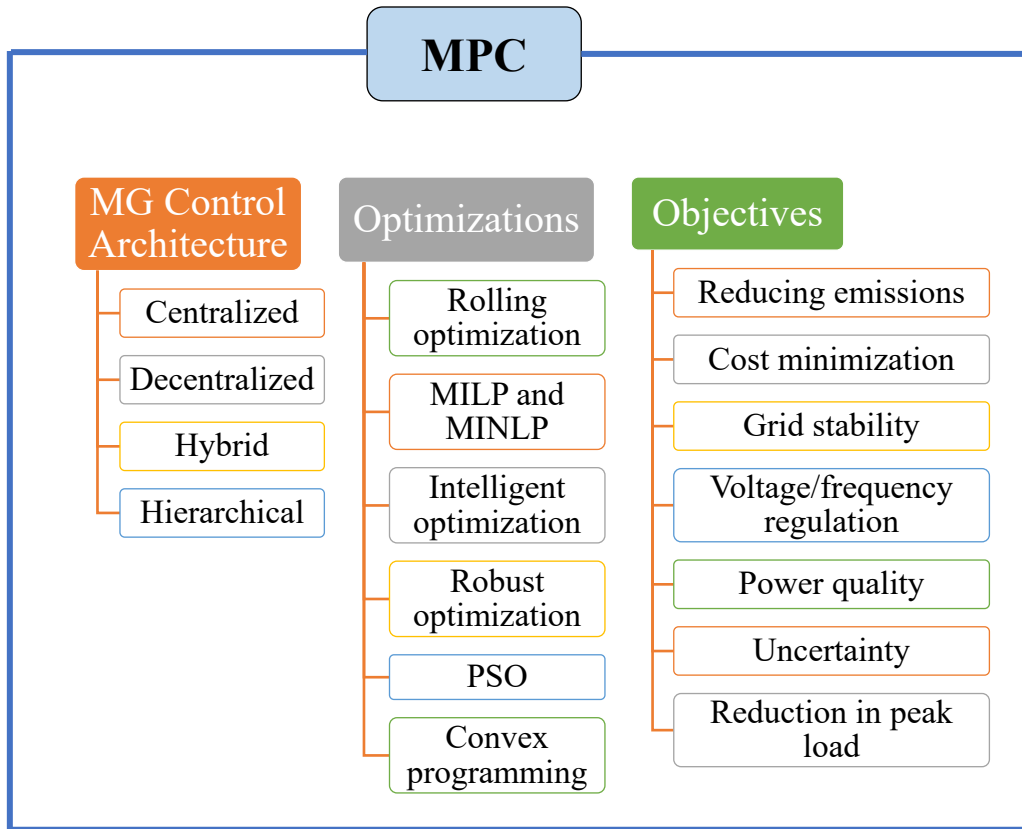


**Figure 2.3** Constituents of MPC for achieving objectives in MGs-EMS

1. Flexibility in EMS of MGs through MPC: The MPC and their variations enable the construction of centralized, decentralized, and hierarchical control structures for energy management in MG. With elements including a rolling or receding horizon approach, accounting uncertainty, forecasting information, and reactive (feedback) mechanism, MPC can successfully accomplish EMS’s control and optimization goals. By supplying the forecasted data connected to the RES generators and load demand, MGs using MPC-based control methods can increase the flexibility of their energy management. The rolling horizon approach makes real-time or day-ahead scheduling viable and allows the DSM and DR approach in the control architecture to lower peak loads. The degree of PnP functionality offered will not lead to an increase in computational complexity. This PnP of ESS and other loads enhances the flexibility and reliability of EMS. With the use of control feedback from the available generation and load demand in the islanded or grid-connected mode of operation, the MG can operate in a flexible manner. Within the anticipated time window, there can be delays in the energy requirements of MG components. This further aids in addressing the MG-changeable EMS’s demand patterns.

2. Affordability in EMS of MGs through MPC: Using MPC-based techniques, the issues relating to the nature of mixed integer linear and nonlinear characteristics considering various operational limitations are successfully resolved. Within the MGs that utilized MPC-based control approaches, combining various optimization strategies, including robust, rolling, and stochastic optimization, aided in obtaining inexpensive and optimal energy management. The MPC's self-triggering function will assist in creating an economical control system for MG-EMS by lowering the need for communication infrastructure. At the control unit, the imports and exports of energy from the grid are continuously tracked. This aids in attaining the grid-connected MG's inexpensive and economical running.
3. Security in EMS of MGs through MPC: The most advantageous feature of MPC control techniques for MG-EMS is their capacity to handle any disruptions and uncertainty. The MPC-based approaches with robust optimization effectively handle the MG-EMS uncertainty issue to improve security. MPC control methods can include new, updated, or predicted information in the EMS and are reactive in nature. For real-time online and stable MG operations, MPC with a rolling horizon method decreases forecast inaccuracy. By doing this, MPC can forecast how the constrained system will behave in the future. The MPC's distributed/decentralized design regulated the complex hybrid power system's power flows. Due to its primary function of integrating newly updated data and forecast information, MPC has a quick transient response. The security of the MG-EMS is also increased by prioritizing the most delicate loads while maintaining supply-demand balance, frequency regulation, and voltage regulation in hierarchical control that uses the MPC approach.

Although there are many advantages of MPC utilization on the MG control, there are some drawbacks of MPC usage. In other words, MPC should be improved for several issues. Several MPC models are restricted to just stable, open-loop systems. Also, MPC frequently requires a high number of model coefficients to characterise a response. Some MPC models are designed for output disturbances and may not handle input disturbances adequately. Some types of MPC make use of the constant output disturbance assumption. This compensates for the fact that the model's anticipated output is not identical to the actual measured output. This method assumes the correction term will be constant in the future, which may not produce excellent results if there is an actual disruption at the plant input. Even if the model is right, control performance will be poor if the prediction horizon is not adequately constructed (Woolf (2009)). Also, these are (i) the complexity of the MPC implementation, (ii) the scalability and adaptability of MPC, and (iii) the control and design of different modes for the ESSs (battery, fuel tank, and water tank).

### 2.2. Objectives of Thesis

This thesis aims to present optimal configuration and control strategies to ensure scalable, reliable, flexible, adaptable, PnP, and efficient operation of a MG, including PV panel, ESSs (battery,

hydrogen tank, and water tank), utility grid, load, fuel cell, electrolyzer, and EVs (three EVs have different kinds of batteries). To obtain these properties for MG, three different kinds of control and energy management of MG are proposed. The objectives of this thesis are described as follows:

- The implementation of MPC is easier.
- Optimal operation of power flows for the MGs are obtained in order to minimize the MG running cost, penalize the usage of accumulators (to avoid the charging from the utility grid), and enhance the practicality of RESs usage.
- The MPC is improved in terms of scalability and adaptability (flexibility). Therefore, an increase in the complex structure in the MG does not affect the MG control because of our scalable method.
- When changing the components of MG, such as removing the utility grid and adding the diesel generator, the MG control can adapt easily due to our adaptable and flexible method.
- Combining the two methods ( $\epsilon$ -variables and S-MPC) will lead to building the S-MPC, allowing optimal control of the MG in all possible modes.
- The PnP ability is an important consideration for MG design, as it allows the system to be easily modified and adapted to changing requirements or operating conditions. By designing MGs with PnP capabilities, system operators can ensure that the MG remains flexible and adaptable while maintaining stable and efficient operation.

### 2.3. Thesis Contributions

The main contributions of this thesis can be listed as follows:

- A hybrid method called MPC- $\epsilon$ -variables is produced. The implementation of MPC has been simplified.
- An extended optimal  $\epsilon$ -variables is developed. Optimal  $\epsilon$ -variables are produced. The  $\epsilon$ -variables can be easily integrated into the S-MPC, allowing for more flexible and adaptable control strategies. This is particularly important for MGs that have varying operating conditions. The merged control strategy can easily adapt to different MG configurations and operating conditions.
- A hybrid method has been developed based on  $\epsilon$ -variables and classical MPC to build the S-MPC of a flexible hybrid MG with PnP assets.

### 2.4. Thesis Organization

The dissertation will be divided into six chapters, each focusing on a particular aspect of the proposed hybrid control method for flexible hybrid MGs.

- Chapter 1 provides an overview of MGs, their control challenges, and the proposed solution in its introduction. In addition, the introduction describes the thesis's aims and objectives.
- Chapter 2 will provide a comprehensive literature review of current control methods employed for MGs, including  $\varepsilon$ -variables-based logic control and MPC. There will be a discussion of the benefits and limitations of each approach, as well as recent advancements in hybrid control methods.
- Chapter 3 will introduce the proposed hybrid control framework that combines  $\varepsilon$ -variables with conventional MPC for MGs. This chapter will describe the implementation of MPC and  $\varepsilon$ -variables. Also, in this chapter, the implementation of the proposed hybrid control will be explained step by step. Lastly, the employment of  $\varepsilon$ -variables and if-else statements will be compared.
- Simulation analysis will be used in Chapter 4 to assess the performance of the extended optimal  $\varepsilon$ -variables. The simulation model will be developed based on a theoretical hybrid MG, and the simulation results will be presented and analyzed in depth. This chapter will utilize S-MPC in the compact form to get optimal  $\varepsilon$ -variables. On the other hand, by merging the  $\varepsilon$ -variables on the S-MPC, the S-MPC is getting more scalable, adaptable, and flexible.
- Chapter 5 provides an enhanced  $\varepsilon$ -variables-based control method for EMS in flexible hybrid MG systems. The S-MPC will be solved using QP. In addition, the methodology will explain how to deal with complex systems with multiple modes or operating conditions of the MG using the S-MPC method. This chapter will suggest a hybrid framework/method based on  $\varepsilon$ -variables and traditional MPC to automatically generate and validate the S-MPC.
- Chapter 6 will provide a summary and conclusion of the thesis, as well as a discussion of the contributions made to the field of MG control. In addition, the method's limitations and future research directions will be discussed.

The next chapter will explain one of our proposed methods called the name "hybrid MPC- $\varepsilon$ -variables. According to this hybrid method, the MPC is improved in terms of implementation by merging  $\varepsilon$ -variables based on the logical control method. Also, in the next chapter, there is a comparison of  $\varepsilon$ -variables and if/else statements. The advantages of  $\varepsilon$ -variables above the if/else statement will be explained using figures and equations.



## Chapter 3. Control of Microgrids using an Enhanced MPC

### 3.1. Overview

$\epsilon$ -variables-based control strategies have allowed for greater scalability and resilience. However, these strategies may not be the most effective. This chapter proposes a hybrid method that combines MPC with  $\epsilon$ -variables in order to simplify the implementation of MPC and make it more effective for complex energy systems. The findings of this chapter indicate that this hybrid method significantly simplifies the control structure, allowing more complex control strategies to provide additional benefits to the energy system, such as scalability and robustness. This chapter contributes to the field of MG control by proposing a method that can facilitate the implementation of advanced control strategies for renewable energy systems that are both practical and effective. In transitioning to more sustainable energy systems, this research has significant implications for MGs' continued development and optimization.

Choosing MPC with  $\epsilon$ -variable involves considering specific advantages and characteristics of this approach. The reasons why one might choose MPC with  $\epsilon$ -variable:

- **Optimization Over a Finite Horizon:** MPC with  $\epsilon$ -variable optimizes control inputs over a finite prediction horizon. This means that it considers future system behaviour and makes decisions by minimizing a cost function over this finite time horizon. This can lead to improved performance compared to purely myopic controllers.
- **Incorporation of Forecast Information:** The  $\epsilon$ -variable extends traditional MPC by incorporating forecast information. This allows the controller to anticipate future disturbances and adapt its control strategy accordingly. This is particularly valuable in scenarios where future events or disturbances are known or can be predicted.
- **Flexibility and Adaptability:** MPC with  $\epsilon$ -variable provides flexibility in handling various types of constraints, including state and input constraints. The  $\epsilon$ -variable acts as a buffer or relaxation factor for constraints, allowing the system to operate within safe limits while still optimizing performance.
- **Integration with Machine Learning Techniques:** The  $\epsilon$ -variable approach can be integrated with machine learning techniques to enhance its capabilities. For example, combining MPC with artificial neural networks (ANN) or other predictive models can improve predictions and adaptability.
- **Reduced Dependency on Plant Model Accuracy:** Traditional MPC relies on an accurate plant dynamics model. The  $\epsilon$ -variable method can reduce the dependency on an accurate

plant model, making it more practical for situations where obtaining a precise model is challenging.

It's important to note that the control strategy choice depends on the system's specific characteristics, the available information, and the desired performance criteria. The  $\varepsilon$ -variable introduces a level of adaptability and robustness to traditional MPC, making it suitable for certain applications.

### 3.2. Introduction

The development of RESs and the increased utilization of energy storage have resulted in transforming the conventional power network into novel topologies such as MGs. Chacko and Sachidanandam (2020) and Tobajas et al. (2022) present MGs that integrate various types of energy sources, including RESs ((PV) panels, wind), ESSs (batteries, hydrogen, pumped hydro (water)), diesel generators, and load and control devices. Also, by operating in a decentralized manner, an MG can reduce network congestion in energy sources, power losses, and operating expenses (Ocanha et al. (2020); Zhang et al. (2022)). However, an MG faces additional controllability challenges due to unexpected power fluctuations during real-time operation, intermittent energy production, and random energy consumption (Hu et al. (2021); Yoldas et al. (2022)). For a satisfactory EMS, advanced control technologies are necessary (Allahham (2008); Giaouris et al. (2015); Xie et al. (2018)).

Fuzzy Logic Controller (FLC), Rule-Based Control (RBC), Linear Quadratic Integrator (LQI), Hysteresis Controller (HC), Power Pinch Analysis (PPA), and other methods for controlling MG systems have been described in the existing literature (Allahham and Alla (2009); Choudhury (2022); Giaouris et al. (2015); Nyong-Bassey et al. (2020)). In addition, Niu et al. (2019) and Terlouw et al. (2019) exploited a complex EMS algorithm using mixed-integer programming. In addition, Wu et al. (2016) made use of stochastic dynamic programming. In contrast, Amoasi Acquah et al. (2018) and Conte et al. (2017) implemented an optimization algorithm based on stochastic variables. However, MPC is a more advanced and effective control strategy than conventional control strategies, which cannot predict uncertainties or disturbances. In addition, MPC has a rapid transient response Hu et al. (2021) because its primary function is to incorporate newly updated data and forecasts. Thus, the MPC is able to make better decisions regarding the future behaviour of the system based on a variety of constraints (Ulutas et al. (2020)).

A MPC consists of three primary elements: the predictive model, the objective (cost) function, and the solving algorithm (Vazifeh et al. (2019)). MPC can be utilized in multiple ways to control the MG system more effectively than other control strategies. For instance, MPC is straightforward and intuitive to comprehend. Additionally, it can be implemented in a variety of power converter topologies. It operates by considering multiple constraints and uncertainties (Villalón et al. (2020)). However, because it employs complex algorithms and imposes a large number of control parameters, it takes longer to solve than the other methods. In other words, it

requires much processing power and time (Dentler (2018)). Consequently, the system needs to be enhanced in terms of complexity and scalability.

On the other hand, a new method for systematically modelling EMSs based on evolution operators and the state of the directed graph that represents the system was introduced for the first time in Ulutas et al. (2020). This method is based on the so-called  $\varepsilon$ -variables, which describe the evolution and, consequently, the control approach of a multi-vector energy system (Giaouris et al. (2018)). Every asset in the system is represented by a node, and an edge represents every energy and/or matter flow between nodes (see Figure 3.1).

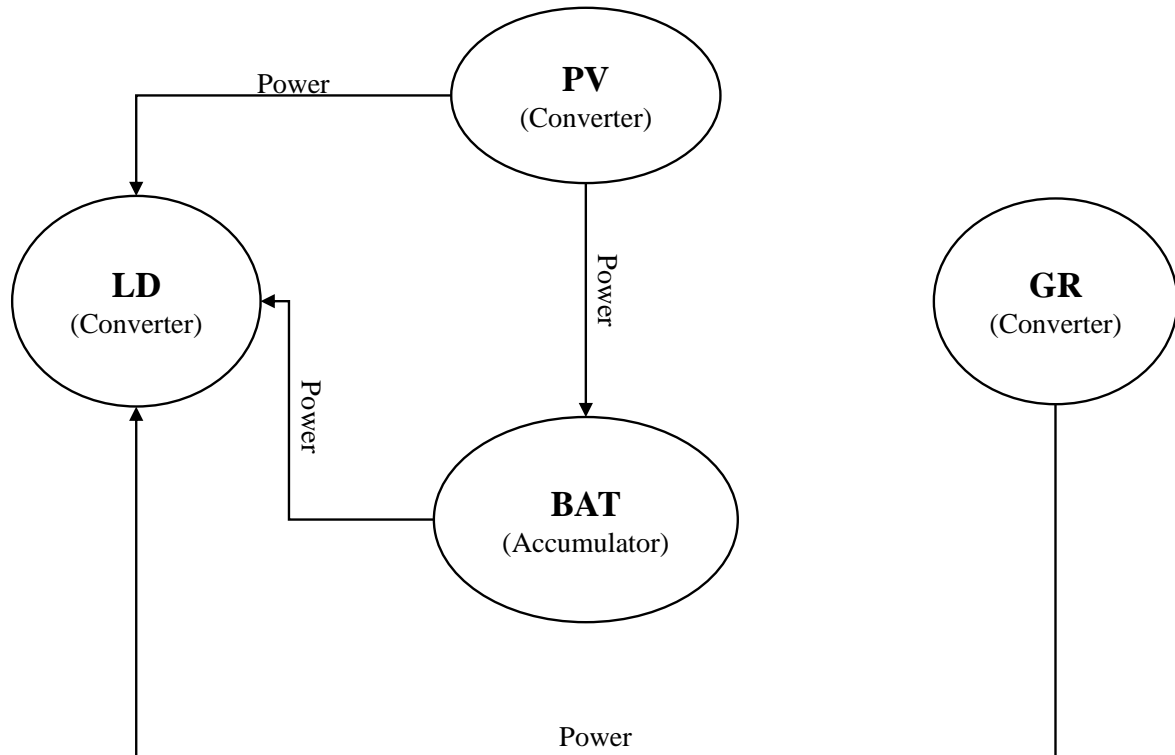


**Figure 3.1** The illustration of directed graph

Specifically, graph theory can be used to easily describe a hybrid energy system, according to Ulutas et al. (2020). In other words, complex energy systems can be depicted in a manner that simplifies their analysis, operation, and management with the aid of graph theory enhanced by the previously mentioned evolution operators. According to this methodology, every energy system consists of three primary components: flows, accumulators, and converters. The flows represent the flow of energy and/or matter, the accumulators store energy or matter, and the converters convert energy and/or matter back into energy and/or matter. The evolution operators describing the EMS of a multi-vector system are the control statements that operate the converters (Giaouris et al. (2013)). This chapter aims to produce a more systematic method for designing MPC for hybrid energy systems using a similar methodology. As a proof of concept, we employ a simple energy system Figure 3.2 in which the flow represents power, the accumulator represents a battery *BAT*, and the converters represent the PV *PV* array, the utility grid, *GR*, and load *LD*. The system's graph is depicted in Figure 3.1, and the MG's assets can be divided into two

groups, such as  $R_s^{Acc} = \{BAT\}$  and  $R_s^{Con} = \{PV, GR, LD\}$  (Ulutas et al. (2020)). The flow can be defined as the connection between two nodes, such as PV to BAT and BAT to LOAD, as shown in Figure 3.1. Consequently, the set of flow discussed in this chapter can be represented as  $Flow = \{(Electrical) Power\}$ .

This section proposes a novel hybrid method for implementing the MPC that retains the same benefits as the MPC while making it more scalable and straightforward through the use of the  $\varepsilon$ -variables. This technique is a hybrid MPC- $\varepsilon$ -variable technique (MPC- $\varepsilon$ -variables).

### 3.3. Motivation for the Proposed Method

The following essential considerations motivate the introduction of the novel hybrid approach, MPC- $\varepsilon$ -variables:

**Simplifying the Control Structure:** One of the biggest difficulties in MG control is managing the inherent complexity associated with varied energy sources, storage technologies, and load fluctuations. While traditional control strategies are successful, they frequently result in convoluted and less scalable control structures. The suggested solution addresses this issue by combining MPC with  $\varepsilon$ -variables, resulting in a simplified yet robust control architecture.

**Improving MPC Practical Implementation:** MPC is well-known for its superior control capabilities, considering different constraints for effective MG operation. The intricacy and processing demands involved with MPC implementation, on the other hand, can provide practical obstacles. The hybrid MPC- $\varepsilon$ -variables method aims to make MPC more accessible and practical by using the  $\varepsilon$ -variables approach's simplicity and scalability. This integration keeps MPC's benefits while simplifying its deployment in complicated energy systems.

**Practical and Effective Implementation:** While traditional control approaches have their advantages, they may fail to deliver practical and efficient solutions for the dynamic and unpredictable character of MGs. The MPC- $\varepsilon$ -variables method was developed in order to provide a more systematic and adaptive methodology. This hybrid method tries to find a compromise between complexity and practicability by merging the strengths of MPC and  $\varepsilon$ -variables, allowing the implementation of advanced control strategies that are both successful and viable in real-world circumstances.

### 3.4. Structure of the PV-Battery-Grid system (PBG)

As depicted in Figure 3.2, the MG system consists of a PV, a battery for energy storage, and a utility grid system. The PV ( $P_{PV}$ ) is used to satisfy the daily load demand of the MG system. When excessive energy is in the PV, the battery is charged by the PV ( $PV_{BAT}$ ) during the MG running. On the other hand, if there is deficit energy in the PV, the battery will be in discharging mode ( $BAT_{LD}$ ) in order to meet the load-generation mismatch. The last option is to power flow from the utility grid ( $GR_{LD}$ ) to the load when there is no energy in the PV and the battery.

The PV generator serves as a crucial component in our MG, contributing to renewable energy generation. The PV generator has a capacity of 14 kW. The efficiency of the power

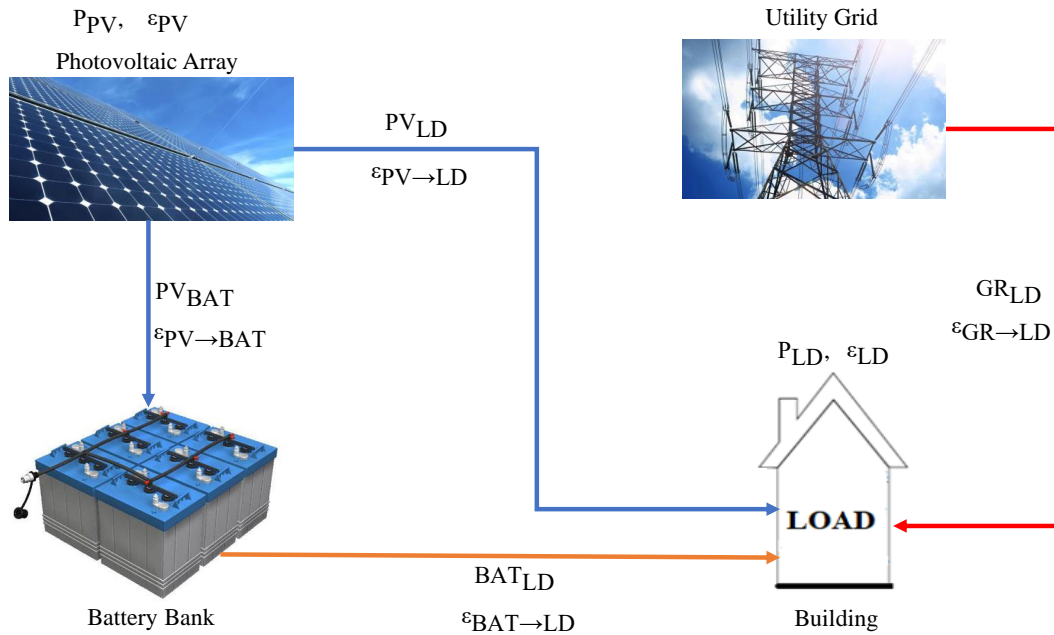


**Figure 3.2** Structure of the PBG system

electronic converter is assumed to be 85% under standard test conditions. The PV panels are oriented to the south at an optimal tilt angle of 30 degrees. Energy storage through batteries is essential for managing fluctuations in energy generation and consumption. The battery system has a storage capacity of 20 kWh. We assume a round-trip efficiency of 85% for the battery system. The maximum charging and discharging rates are set at 10 kW. The load consists of residential consumers. The average power demand on the MG is 3 kW daily. Load demand exhibits daily and seasonal variations. For efficiency calculations, we assume a standard solar irradiance level of 1000 W/m<sup>2</sup>. The PV array comprises 50 solar panels with a total area of 80 m<sup>2</sup>. Our assumptions consider realistic charge-discharge cycles and losses, and the chosen efficiency aligns with typical values for the battery technology used. Load patterns are based on historical data, and the variability considers typical consumption patterns in the chosen locality (Ani (2016); Buchholz and Styczynski (2014); Smets et al. (2016)).

### 3.5. General Information for the Implementation of MPC

As demonstrated in Figure 3.3, the MPC mechanism predicts the system's behaviour and optimizes its performance using the dynamic model, cost function, and constraints to produce the optimal decision (Cavus et al. (2022b)).

The MPC is implemented and calculated using the set point values, past inputs, outputs, and future output value predictions. It computes a set of  $N_c$  values of the input, represented by  $u(k + N_c - 1)$  at the  $k^{th}$  sample. In other words, the set consists of the current and future inputs  $u(k)$  and  $u(k + N_c - 1)$ , respectively. The calculation of a set of  $N_p$  predicted outputs  $y(k + N_p)$  continues until the system reaches its optimal values. In order to gain the dispatching strategy, "receding horizon control" is a notable aspect of MPC. It is important to note that only the initial

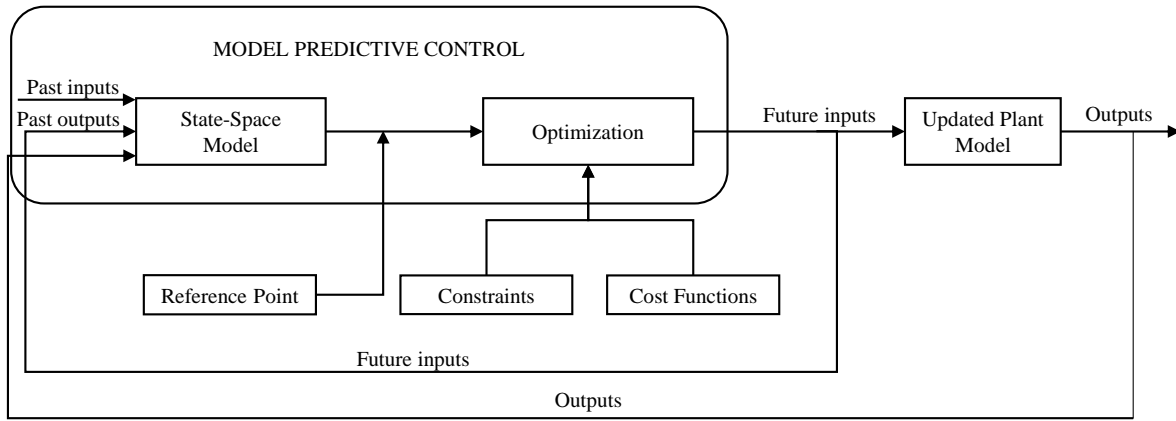


Figure 3.3 The schematic of MPC

move is executed, and a new sequence is estimated at the  $k + 1$  position. As shown in Figure 3.4 (Cavus et al. (2022b)), this step is repeated for every  $k$ -time sampling.

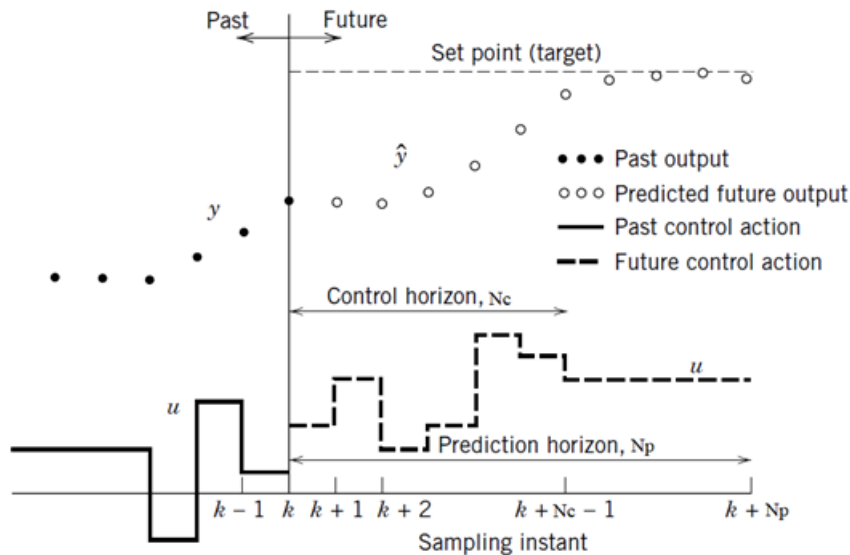


Figure 3.4 The basic idea for MPC (Seborg et al. (2016))

The significance of control and prediction horizons is crucial in the proposed method, and it plays a pivotal role in determining the effectiveness and performance of the control strategy. The control horizon represents the finite time span into the future over which the control inputs are optimized. If the proposed method selects a shorter control horizon, it allows for faster responses to changes in the system but may sacrifice long-term optimization. In contrast, a longer control horizon provides a more accurate long-term prediction but often increases computational complexity. Also, for our proposed method, a well-chosen control horizon enables the MPC controller to adapt to changes in the system and disturbances dynamically. It allows the controller to respond effectively to variations in the operating conditions, ensuring that the system remains stable and meets performance objectives. Our proposed method's control horizon is essential for handling system constraints within the optimization process. By considering future control inputs, the MPC controller can anticipate and prevent violations of constraints, ensuring that the system operates within acceptable limits.

Regarding the prediction horizon, it represents the duration over which the system's future evolution is forecasted. A longer prediction horizon captures a more extended time span of system dynamics, providing a more accurate representation of future states. An appropriate prediction horizon helps mitigate the impact of input delays in the system. By forecasting the system's behaviour over a more extended period, the controller can compensate for delays in implementing control actions. A longer prediction horizon allows the MPC controller to anticipate future changes, enhancing the stability and overall performance of the controlled system. It facilitates proactive decision-making to minimize deviations from the desired trajectory. Similar to the control horizon, the prediction horizon requires a careful balance. A longer prediction horizon may improve accuracy but increases computational load. Therefore, choosing an appropriate prediction horizon is critical for balancing computational efficiency and prediction accuracy.

In terms of the results:

- **Effect of Control Horizon on Operational Cost:** With a control horizon of 2 hours, the operational energy consumption of the MGs is 150 kWh. Increasing the control horizon to 6 hours results in a reduction to 120 kWh. However, computational demands also increase, showcasing a trade-off between energy savings and computational complexity.
- **Impact of Prediction Horizon on BESS Usage:** Suppose that with a short prediction horizon of 30 minutes, the BESS is utilized at 60 kWh capacity. Extending the prediction horizon to 2 hours leads to a more efficient BESS usage at 40 kWh. Beyond this, the benefits diminish, indicating an optimal prediction horizon for BESS management.
- **Influence of Control and Prediction Horizons on PV Usage:** Given a specific combination of control and prediction horizons, the practicality of PV usage increases by 20%. It could be shown that adjusting these horizons optimally enhances the MG's ability to harness solar energy efficiently.
- **Performance of the Extended Optimal  $\epsilon$ -Variable Method:** Present data demonstrating that the extended optimal  $\epsilon$ -variable method reduces the operational energy consumption of the MG by nearly 25%, uses the BESS 35 kWh less, and increases the practicability of PV usage by 20%, compared to traditional methods.
- **Energy Import and Export Optimization in Flexible Hybrid MGs:** Consider that the novel hybrid framework/method combining  $\epsilon$ -variables and conventional MPC results in a 40 kWh reduction in imported energy from the grid and a 42 kWh increase in exported energy. This showcases the effectiveness of the proposed method in optimizing energy flow.

The following section explains how to implement the MPC step by step (Wang (2009)):

### 3.5.1. Defining a State-space Plant Model

We start our research by assuming that the underlying plant is defined by the following:

$$x_m(k+1) = A_m x_m(k) + B_m u(k) \quad (3.1)$$

$$y(k) = C_m x_m(k) \quad (3.2)$$

The triplet  $(A, B, C)$  is known as the augmented model and will be employed in predictive control design. The dimensions of  $A_m$ ,  $B_m$ , and  $C_m$  are  $n_1 \times n_1$ ,  $n_1 \times m$ , and  $q \times n_1$ , respectively.  $u$  is the manipulated or input variable,  $y$  is the process output, and  $x_m$  is the assumed  $n_1$ -dimensional vector for the state variable. Note that the input for this plant model is  $u(k)$ . Therefore, we must modify the model to accommodate the embedded integrator in our design.

Note that a general state-space model formulation has a direct term from the input signal  $u(k)$  to the output  $y(k)$  as follows:

$$y(k) = C_m x_m(k) + D_m u(k)$$

Due to the principle of receding horizon control, which requires current plant information for prediction and control, we have implicitly assumed that the input  $u(k)$  cannot simultaneously affect the output  $y(k)$ . Consequently,  $D_m = 0$  in the plant model. Using a difference operation on both sides of the expression (3.1), we obtain that

$$x_m(k+1) - x_m(k) = A_m(x_m(k) - x_m(k-1)) + B_m(u(k) - u(k-1))$$

Let's represent the difference of the state variable with the symbol:

$$\Delta x_m(k+1) = x_m(k+1) - x_m(k); \quad \Delta x_m(k) = x_m(k) - x_m(k-1),$$

and the difference between the control variable by

$$\Delta u(k) = u(k) - u(k-1),$$

These are the increments of the  $x_m(k)$  and  $u(k)$  variables. The difference between the state-space equation with this transformation is:

$$\Delta x_m(k) = A_m \Delta x_m(k) - B_m \Delta u(k) \quad (3.3)$$

Note that the state-space model's input is  $u(k)$ . The subsequent step is to connect  $\Delta x_m(k)$  to the output  $y(k)$ . To accomplish this, a new state variable vector is selected to be

$$x(k) = [\Delta x_m(k)^T \ y(k)]^T,$$

where superscript  $T$  denotes matrix transposition. Note that

$$y(k+1) - y(k) = C_m(x_m(k+1) - x_m(k)) = C_m\Delta x_m(k+1) \quad (3.4)$$

$$= C_mA_m\Delta x_m(k) + C_mB_m\Delta u(k) \quad (3.5)$$

Combining (3.3) and (3.5) generates the following state-space model:

$$\underbrace{\begin{bmatrix} \Delta x_m(k+1) \\ y(k+1) \end{bmatrix}}_{x(k+1)} = \underbrace{\begin{bmatrix} A_m & 0_m^T \\ C_mA_m & 1 \end{bmatrix}}_A \underbrace{\begin{bmatrix} \Delta x_m(k+1) \\ y(k) \end{bmatrix}}_{x(k)} + \underbrace{\begin{bmatrix} B_m \\ C_mB_m \end{bmatrix}}_B \Delta u(k)$$

$$y(k) = \underbrace{\begin{bmatrix} 0_m & 1 \end{bmatrix}}_C \begin{bmatrix} \Delta x_m(k+1) \\ y(k+1) \end{bmatrix} \quad (3.6)$$

where

$$0_m = \underbrace{\begin{bmatrix} 0 & 0 & \dots & 0 \end{bmatrix}}_{n_1}$$

The  $(A,B,C)$  triplet is referred to as the augmented model, which will be utilized in the design of predictive control.

#### 3.5.2. Predictive Control within One Optimization Window

After formulating the mathematical model, the next step in designing a predictive control system is to calculate the predicted plant output using the future control signal as the adjustable variable. Within an optimization window, this forecast is described. This section examines in depth the optimization performed within this window. Here, we assume that the current time is  $k_i$  and that the length of the optimization window is  $N_p$  samples. First, the case of single-input and single-output systems are considered, and then the results are extended to multi-input, multi-output systems.

##### *Prediction of State and Output Variables*

Assuming that at the sampling instant  $k_i$ ,  $k_i > 0$ , the state variable vector  $x(k_i)$  is available through measurement,  $x(k_i)$  represents the current plant state. The more general case in which the state is not directly measurable will be discussed later. The symbol denotes the future control trajectory.

$$\Delta u(k_i), \Delta u(k_i+1), \dots, \Delta u(k_i+N_c-1),$$

where  $N_c$  is the control horizon dictating the number of parameters used to capture the future trajectory of control. With the information  $x(k_i)$ , future state variables are predicted for  $N_p$  samples, where  $N_p$  is referred to as the prediction horizon.  $N_p$  is also the optimization window's

length. The future state variables are denoted as

$$x(k_i + 1|k_i), x(k_i + 2|k_i), \dots, x(k_i + m|k_i), \dots, x(k_i + N_p|k_i),$$

where  $x(k_i + m|k_i)$  is the predicted state variable at  $k_i + m$  based on the current plant data  $x(k_i)$ . It is decided that the control horizon  $N_c$  will be less than (or equal to) the prediction horizon  $N_p$ . Using the set of future control parameters and the state-space model  $(A,B,C)$ , the future state variables are calculated sequentially:

$$\begin{aligned} x(k_i + 1|k_i) &= Ax(k_i) + B\Delta u(k_i) \\ x(k_i + 2|k_i) &= Ax(k_i + 1|k_i) + B\Delta u(k_i + 1) \\ &= A^2x(k_i) + AB\Delta u(k_i) + B\Delta u(k_i + 1) \\ &\vdots \\ x(k_i + N_p|k_i) &= A^{N_p}x(k_i) + A^{N_p-1}B\Delta u(k_i) + A^{N_p-2}B\Delta u(k_i + 1) + \dots + A^{N_p-N_c}B\Delta u(k_i + N_c - 1) \end{aligned} \quad (3.7)$$

Using the predicted state variables as a substitute for the predicted output variables:

$$\begin{aligned} y(k_i + 1|k_i) &= CAx(k_i) + CB\Delta u(k_i) \\ y(k_i + 2|k_i) &= CA^2x(k_i) + CAB\Delta u(k_i) + CB\Delta u(k_i + 1) \\ y(k_i + 3|k_i) &= CA^3x(k_i) + CA^2B\Delta u(k_i) + CAB\Delta u(k_i + 1) + CB\Delta u(k_i + 2) \\ &\vdots \\ y(k_i + N_p|k_i) &= CA^{N_p}x(k_i) + CA^{N_p-1}B\Delta u(k_i) + CA^{N_p-2}B\Delta u(k_i + 1) + \dots + CA^{N_p-N_c}B\Delta u(k_i + N_c - 1) \end{aligned} \quad (3.8)$$

Note that all predicted variables are derived from the current state variable information  $x(k_i)$  and the future control movement  $u(k_i + j)$ , where  $j = 0, 1, \dots, N_c - 1$ .

Define vectors,

$$\begin{aligned} Y &= [y(k_i + 1|k_i) \ y(k_i + 2|k_i) \ y(k_i + 3|k_i) \ \dots \ y(k_i + N_p|k_i)]^T \\ \Delta U &= [(\Delta u_{k_i+1}) \ (\Delta u_{k_i+2}) \ \dots \ (\Delta u_{k_i+N_c-1})]^T, \end{aligned}$$

where, in the case of a single input and single output, the dimension of  $Y$  is  $N_p$ , and that of  $U$  is  $N_c$ . We collect (3.7) and (3.8) (above two equations) as a compact matrix containing both numbers.

$$Y = Fx(k_i) + \Phi\Delta U \quad (3.9)$$

where

$$F = \begin{bmatrix} CA \\ CA^2 \\ CA^3 \\ \vdots \\ CA^{N_p} \end{bmatrix} \Phi = \begin{bmatrix} CB & 0 & 0 & \cdots & 0 \\ CAB & CB & 0 & \cdots & 0 \\ CA^2B & CAB & CB & \cdots & 0 \\ \vdots & \vdots & \vdots & \ddots & \vdots \\ CA^{N_p-1}B & CA^{N_p-2}B & CA^{N_p-3}B & \cdots & CA^{N_p-N_c}B \end{bmatrix}$$

### 3.5.3. Optimization

For a given set-point signal  $r(k_i)$  at sample time  $k_i$ , the objective of the predictive control system within a prediction horizon is to bring the predicted output as close as possible to the set-point signal, assuming that the set-point signal remains constant in the optimization window. This objective is then translated into a design to identify the "best" control parameter vector  $\Delta U$  such that an error function between the set point and predicted output is minimized.

Assuming the set-point information is present in the data vector

$$R_s^T = \underbrace{\begin{bmatrix} 1 & 1 & \cdots & 1 \end{bmatrix}}_{N_p} r(k_i),$$

The cost function  $J$  that reflects the control objective is defined as

$$J = (R_s - Y)^T (R_s - Y) + \Delta U^T \bar{R} \Delta U \quad (3.10)$$

where the first term is associated with the goal of minimizing errors between the predicted output and the set-point signal, and the second term reflects the consideration given to the size of  $\Delta U$  when the objective function  $J$  is made as small as possible.  $\bar{R}$  is a diagonal matrix with the form  $\bar{R} = r_w I_{N_c N_c}$  ( $r_w \geq 0$ ), where  $r_w$  is a tuning parameter used to achieve the desired closed-loop performance. For the case in which  $r_w = 0$ , the cost function (3.10) is interpreted as a circumstance in which we do not care how large  $U$  may be, and our sole objective is to minimize the error  $(R_s - Y)^T (R_s - Y)$ . The cost function (3.10), in the case of a large  $r_w$ , is interpreted as a scenario in which we would carefully consider how large  $U$  could be and reduce the error  $(R_s - Y)^T (R_s - Y)$  with caution.

Tuning the parameter  $r_w$  in the predictive control system involves finding an appropriate value that achieves the desired closed-loop stability and performance. The choice of  $r_w$  plays a critical role in balancing the trade-off between minimizing errors in the predicted output and controlling the size of the control parameter vector  $\Delta U$ . Here are some general guidelines on how you might approach tuning  $r_w$  for closed-loop stability:

- A higher value of  $r_w$  tends to prioritize the control effort, potentially leading to a more conservative control action. On the other hand, a lower value may focus more on tracking the set-point signal.

- A larger  $r_w$  places more emphasis on minimizing the control input, potentially sacrificing some tracking performance. Conversely, a smaller  $r_w$  may prioritize tracking performance at the expense of higher control effort.
- After adjusting  $r_w$ , observe its impact on stability. This involves analyzing the system's closed-loop response, particularly how changes in  $r_w$  affect stability margins. The goal is to find a range of  $r_w$  values that ensure closed-loop stability.
- Based on observations and analysis, iteratively adjust  $r_w$  values until you achieve a satisfactory balance between closed-loop stability, tracking performance, and control effort.
- The ultimate goal of this stability analysis is to find a suitable range of  $r_w$  values that ensures closed-loop stability. Closed-loop stability means that the system remains stable when the control loop is closed, and the desired performance is achieved without leading to instability or oscillations.

To determine the optimal  $U$  that minimises  $J$ , using Equation (3.9),  $J$  is expressed as

$$J = (R_s - Fx(k_i))^T (R_s - Fx(k_i)) - 2\Delta U^T \Phi^T (R_s - Fx(k_i)) + \Delta U^T (\Phi^T \Phi + \bar{R}) \Delta U \quad (3.11)$$

Using the first derivative of the cost function  $J$ , we obtain:

$$\frac{\partial J}{\partial \Delta U} = -2\Phi^T (R_s - Fx(k_i)) + 2(\Phi^T \Phi + \bar{R}) \Delta U \quad (3.12)$$

The required condition of the minimum  $J$  is derived as

$$\frac{\partial J}{\partial \Delta U} = 0,$$

which we derive the optimal solution for the control signal as

$$\Delta U = (\Phi^T \Phi + \bar{R})^{-1} \Phi^T (R_s - Fx(k_i)) \quad (3.13)$$

with the presumption that  $(\Phi^T \Phi + \bar{R})^{-1}$  exists. In optimization literature, the matrix  $(\Phi^T \Phi + \bar{R})^{-1}$  is referred to as the Hessian matrix. Note that  $R_s$  is a data vector containing the set-point data expressed as

$$R_s = \underbrace{\begin{bmatrix} 1 & 1 & \dots & 1 \end{bmatrix}^T}_{N_p} r(k_i) = \bar{R} s r(k_i),$$

where

$$R_s = \underbrace{\begin{bmatrix} 1 & 1 & \dots & 1 \end{bmatrix}^T}_{N_p},$$

The following equation relates the optimal solution of the control signal to the set-point signal  $r(k_i)$  and the state variable  $x(k_i)$ :

$$\Delta U = (\Phi^T \Phi + \bar{R})^{-1} (R_s r(k_i) - Fx(k_i)) \quad (3.14)$$

#### 3.5.4. Receding Horizon Control (Point 9)

Despite the fact that the optimal parameter vector  $U$  contains the controls  $u(k_i)$ ,  $u(k_i + 1)$ ,  $u(k_i + 2)$ ,  $\dots$ ,  $u(k_i + N_c - 1)$ , we only implement the first sample of this sequence, i.e.,  $u(k_i)$  while ignoring the rest of the sequence. When the subsequent sampling interval arrives, the most recent measurement is used to construct the state vector  $x(k_i + 1)$  for calculating the new control signal sequence. The receding horizon control law is the result of repeating this procedure in real-time.

#### Closed-loop Control System

In Equation (3.13), where  $(\Phi^T \Phi + \bar{R})^{-1} \Phi^T (R_s)$  represents the set-point change and  $(\Phi^T \Phi + \bar{R})^{-1} \Phi^T F$  represents the state feedback control within the context of predictive control. Both matrices are constant for a time-invariant system due to their dependence on the system parameters. Due to the principle of receding horizon control, we only use the first element of  $\Delta U$  at time  $k_i$  as the incremental control, thus:

$$\Delta u(k_i) = \underbrace{\begin{bmatrix} 1 & 0 & \dots & 0 \end{bmatrix}^T}_{N_c} (\Phi^T \Phi + \bar{R})^{-1} \Phi^T (R_s - Fx(k_i))$$

and

$$K_y r(k_i) - K_{mpc} x(k_i) \quad (3.15)$$

where  $K_y$  is the first element of

$$(\Phi^T \Phi + \bar{R})^{-1} \Phi^T (R_s)$$

and  $K_{mpc}$  is the first row of

$$(\Phi^T \Phi + \bar{R})^{-1} \Phi^T F$$

Equation (3.15) is a standard representation of linear time-invariant state feedback control. The gain vector for state feedback control is  $K_{mpc}$ . As a result, the augmented design model:

$$x(k+1) = Ax(k) + B\Delta u(k)$$

Substituting (3.15) into the augmented system equation generates the closed-loop system; changing index  $k_i$  to  $k$  produces the closed-loop system equation.

$$x(k+1) = Ax(k) - BK_{mpc}x(k) + BK_y r(k) \quad (3.16)$$

$$= (A - BK_{mpc})x(k) + BK_y r(k) \quad (3.17)$$

Consequently, the closed-loop eigenvalues can be determined using the closed-loop characteristic equation:

$$\det[\lambda I - (A - BK_{mpc})] = 0$$

### 3.5.5. Formulation of Constrained Control Problems

There are three common types of constraints encountered frequently in application development. The first two types deal with constraints imposed on the control variables  $u(k)$ , while the third type deals with output  $y(k)$  or state variable  $x(k)$  constraints. For clarity, we will first discuss single-input and single-output systems and then extend the discussion to MIMO systems.

#### *Constraints on the Incremental Variation of the Control Variable*

These are hard constraints on the size of control signal movements or the rate of change of control variables ( $u(k)$ ). Suppose the upper limit of a system with a single input is  $\Delta u^{max}$ , and the lower limit is  $\Delta u^{min}$ . The form specifies the constraints in the form as follows:

$$\Delta u^{min} \leq \Delta u(k) \leq \Delta u^{max} \quad (3.18)$$

Note using less than plus equal to in (3.18), where equality plays a crucial role in solving the constrained control problem.

The rate of change constraints can be used to impose directional movement constraints on the control variables; for example, if  $u(k)$  can only increase and cannot decrease, we may choose  $0 \leq \Delta u(k) \leq \Delta u^{max}$ . The constraint on  $\Delta u(k)$  can be utilized in situations where the rate of change of the control amplitude is constrained or limited in value. In a control system implementation, for instance, if the control variable  $u(k)$  may only increase or decrease by a magnitude less than 0.1 unit, then the operational constraint is:

$$-0.1 \leq \Delta u(k) \leq 0.1$$

#### *Constraints on the Control Variable's Amplitude*

These are the most frequently encountered constraints across all types. These are the physical constraints that the system must adhere to. Basically, we require that

$$u^{min} \leq u(k) \leq u^{max}$$

Note that  $u(k)$  is an incremental variable and not the actual physical variable.

#### ***Output Constraints***

We can also specify the plant output operating range. For instance, if the output  $y(k)$  has upper and lower limits  $y^{max}$  and  $y^{min}$ , then the output constraints are specified as follows:

$$y^{min} \leq y(k) \leq y^{max} \quad (3.19)$$

#### ***State Constraints***

The plant state operating range can also be specified. For example, if the state  $x(k)$  has upper and lower bounds  $x^{max}$  and  $x^{min}$ , the output constraints are as follows:

$$x^{min} \leq x(k) \leq x^{max} \quad (3.20)$$

#### **3.5.6. Constraints in Multi-input and Multi-output Plants**

If there are multiple inputs, then the constraints for each input are specified independently. Assume in the case of multiple inputs that the constraints for the upper limits are given as

$$[\Delta u_1^{max} \quad \Delta u_2^{max} \quad \dots \quad \Delta u_m^{max}]$$

and lower limits as

$$[\Delta u_1^{min} \quad \Delta u_2^{min} \quad \dots \quad \Delta u_m^{min}]$$

Each variable with a change rate is denoted as:

$$\begin{aligned} \Delta u_1^{min} &\leq \Delta u_1(k) \leq \Delta u_1^{max} \\ \Delta u_2^{min} &\leq \Delta u_2(k) \leq \Delta u_2^{max} \\ &\vdots \\ \Delta u_m^{min} &\leq \Delta u_m(k) \leq \Delta u_m^{max} \end{aligned} \quad (3.21)$$

Similarly, suppose that the upper limit of the control signal is constrained as follows:

$$u_1^{max} \quad u_2^{max} \quad \dots \quad u_m^{max}$$

and lower limit as

$$u_1^{min} \quad u_2^{min} \quad \dots \quad u_m^{min}$$

The amplitude of each control signal must then satisfy the constraints:

$$\begin{aligned}
 u_1^{min} &\leq u_1(k) \leq u_1^{max} \\
 u_2^{min} &\leq u_2(k) \leq u_2^{max} \\
 &\vdots \\
 u_m^{min} &\leq u_m(k) \leq u_m^{max}
 \end{aligned} \tag{3.22}$$

Similarly, to define the multi-state constraints:

Each input is specified independently. Assume in the case of multiple states that the constraints for the upper limits are given as

$$[\Delta x_1^{max} \quad \Delta x_2^{max} \quad \dots \quad \Delta x_m^{max}]$$

and lower limits as

$$[\Delta x_1^{min} \quad \Delta x_2^{min} \quad \dots \quad \Delta x_m^{min}]$$

Each variable with a change rate is denoted as:

$$\begin{aligned}
 \Delta x_1^{min} &\leq \Delta x_1(k) \leq \Delta x_1^{max} \\
 \Delta x_2^{min} &\leq \Delta x_2(k) \leq \Delta x_2^{max} \\
 &\vdots \\
 \Delta x_m^{min} &\leq \Delta x_m(k) \leq \Delta x_m^{max}
 \end{aligned} \tag{3.23}$$

Similarly, suppose that the upper limit of the state vector is constrained as follows:

$$x_1^{max} \quad x_2^{max} \quad \dots \quad x_m^{max}$$

and lower limit as

$$x_1^{min} \quad x_2^{min} \quad \dots \quad x_m^{min}$$

The amplitude of each state vector must then satisfy the constraints:

$$\begin{aligned}
 x_1^{min} &\leq x_1(k) \leq x_1^{max} \\
 x_2^{min} &\leq x_2(k) \leq x_2^{max} \\
 &\vdots \\
 x_m^{min} &\leq x_m(k) \leq x_m^{max}
 \end{aligned} \tag{3.24}$$

### ***Constraints as Part of the Optimal Solution***

After describing the constraints as part of the design specifications, the next step is to translate them into linear inequalities and relate them to the original MPC problem. The key is to parameterize the constrained variables with the same parameter vector  $\Delta U$  used in the design

of predictive control. Constraints are therefore expressed as a set of linear equations based on the parameter vector  $\Delta U$ . In optimization literature,  $\Delta U$  is frequently referred to as the decision variable. Since the predictive control problem is formulated and solved within the framework of receding horizon control, each moving horizon window's constraints are taken into account. This enables us to modify the constraints at the start of each optimization window and also permits us to solve the constrained control problem numerically. If we wish to impose constraints on the rate of change of the control signal  $\Delta u(k)$  at time  $k_i$ , the constraints at sample time  $k_i$  are expressed as follows:

$$\Delta u^{min} \leq \Delta u(k_i) \leq \Delta u^{max}$$

The predictive control scheme looks to the future based on the time instance  $k_i$ . The constraints on subsequent samples, such as the first three samples,  $\Delta u(k_i)$ ,  $\Delta u(k_i + 1)$ , and  $\Delta u(k_i + 2)$ , are imposed as follows:

$$\begin{aligned} \Delta u^{min} &\leq \Delta u(k_i) \leq \Delta u^{max} \\ \Delta u^{min} &\leq \Delta u(k_i + 1) \leq \Delta u^{max} \\ \Delta u^{min} &\leq \Delta u(k_i + 2) \leq \Delta u^{max} \end{aligned}$$

In principle, each constraint is specified within the prediction horizon. In order to reduce the computational load, we select a subset of future sampling instants rather than all future samples in order to impose constraints.

Comparing different numbers of samples in terms of the time required, such a comparison would typically involve running simulations or experiments with different prediction horizons and observing the computational time required for optimization. The results of such a comparison could provide insights into the computational efficiency of the receding horizon control approach under different scenarios. If we're considering a larger number of samples, it's essential to evaluate whether the increased accuracy in predicting future system behaviour justifies the additional computational cost. In some cases, a relatively small prediction horizon may be sufficient to capture the most critical dynamics of the system, allowing for a computationally efficient control strategy. However, a longer prediction horizon might be necessary for systems with long time constants or complex dynamics. In summary, the decision on the number of samples and the trade-off between computational efficiency and constraint accuracy is often problem-dependent. It requires carefully considering the system dynamics and the specific requirements of the control application.

Numerical results related to the imposition of constraints on future trajectories of control signals and system outputs are explained in the next chapters. These numerical results collectively emphasize the importance and effectiveness of imposing constraints on control signals and system outputs in achieving optimal energy management within the MG:

1. **Constraint on Energy Consumption from the Grid:** With the extended optimal  $\varepsilon$ -variables method, the constraint on the energy consumption from the grid ( $GR_{LD}$ ) was

effectively applied. The reduction in energy consumption, from 2055 kWh to 1529 kWh, signifies the impact of constraints on optimizing the MG's operation.

2. **Battery Usage Constraint:** The extended optimal  $\varepsilon$ -variables method showcased a significant reduction in battery usage ( $BAT_{LD}$ ) by imposing constraints. The battery usage decreased from 2127.1 kWh to 1956.7 kWh, highlighting the effectiveness of constraints in managing energy storage.
3. **Optimized PV Usage:** Constraints played a crucial role in encouraging the practicality of PV usage ( $PV_{GR}$  and  $PV_{BAT}$ ). The energy usage increase from the grid's PV system ( $PV_{GR}$ ), from 620.68 kWh to 791.12 kWh, demonstrates how constraints contribute to the optimal utilization of renewable sources.
4. **Overall Energy Consumption Patterns with Constraints:** The overall energy consumption patterns are a direct result of constraints influencing the control strategies. The imposed constraints contributed to a reduction in grid-supplied energy, improved sustainability, and cost savings.

Now that the constraints have been expressed as linear-in-the-parameter inequalities  $\Delta U$ , the next step is to combine them with the original cost function  $J$  used in the design of predictive control. As optimal solutions will be obtained through QP, the constraints must be split into two parts to reflect the lower and upper limits with the opposite sign. Specifically, the constraints:

$$\Delta U^{min} \leq \Delta U \leq \Delta U^{max}$$

will be represented by two inequalities:

$$-\Delta U \leq -\Delta U^{min} \quad (3.25)$$

$$\Delta U \leq \Delta U^{max} \quad (3.26)$$

In a matrix form, this will be:

$$\begin{bmatrix} -I \\ I \end{bmatrix} \Delta U \leq \begin{bmatrix} -\Delta U^{min} \\ \Delta U^{max} \end{bmatrix} \quad (3.27)$$

where  $\Delta U^{min}$  and  $\Delta U^{max}$  are column vectors that contain  $N_c$  elements for  $\Delta u^{min}$  and  $\Delta u^{max}$ , respectively. The output constraints can be defined regarding  $\Delta U$ :

$$Y^{min} \leq Fx(k_i) + \Phi \Delta U \leq Y^{max} \quad (3.28)$$

In the end, the MPC in the presence of hard constraints is proposed as finding the parameter vector  $\Delta U$  that minimizes Equation (3.11). Then, subject to the inequality constraints as follows:

$$\begin{bmatrix} M_1 \\ M_2 \\ M_3 \end{bmatrix} \Delta U \leq \begin{bmatrix} N_1 \\ N_2 \\ N_3 \end{bmatrix} \quad (3.29)$$

In this Equation (3.11), as mentioned previously,  $\Phi^T \Phi + \bar{R}$  is a Hessian matrix and must be positive definite. Because the cost function  $J$  is quadratic and the constraints are linear inequalities, the problem of determining the optimal predictive control becomes one of determining the optimal solution to a standard QP problem.

Equation (3.29) is denoted by for compactness as below:

$$M\Delta U \leq \gamma \quad (3.30)$$

where  $M$  and  $\gamma$  are a compatible matrix and vectors expressing the constraints, with its number of rows equal to the variety of constraints and a number of columns equal to the dimension of  $\Delta U$ . When the constraints are fully implemented, the variety of constraints is equal to  $4 \times m \times N_c + 2 \times q \times N_p$ , where  $m$  is the several of inputs and  $q$  is the several of outputs. The total number of constraints is generally greater than the dimension of the decision variable  $\Delta U$ . Because the receding horizon control law only implements the initial control movement and disregards the remaining calculated future control signals, the question arises as to whether it is necessary to impose constraints on all future control signals and system output trajectories.

When dealing with control systems and optimization problems, imposing constraints on future trajectories is often necessary to ensure the system behaves in a desired manner and satisfies specific requirements. Here are a few key reasons for imposing constraints:

Introducing constraints can lead to improved system performance by preventing undesirable behaviours. For instance, limiting overshoot or ensuring smooth transitions between states can be achieved by imposing constraints on the trajectories. Many systems have physical limits or operational constraints that must be respected to avoid damage, instability, or violation of safety standards. Examples include limits on control input amplitudes, velocity constraints, or temperature thresholds. Constraining trajectories ensure that these limits are not violated over time. For our proposed method, the constraints imposed on power flows, state-of-charge (SOC) of the battery, and other variables help prevent the system from operating beyond its specified limits. For example, constraints on battery SOC prevent overcharging or over-discharging, prolonging the battery life and ensuring its long-term reliability. Constraints contribute to the stability of the microgrid by preventing the system from entering unstable or oscillatory modes. They help in avoiding control actions that could lead to instability, ensuring a smooth and controlled response to disturbances. Constraints on power flows and energy storage help optimise resource allocation. For instance, by limiting the power sent to the grid or defining constraints on the use of non-renewable sources, the method can promote the efficient use of renewable energy

and reduce dependency on external grids. In summary, the constraints on future trajectories can involve both control signals (inputs) and system outputs. Considering the system's evolution over time, these constraints contribute to the formulation of optimization problems that seek to find the best control signals while adhering to the defined limitations.

### 3.5.7. Numerical Solutions Using QP

The standard QP problem has been investigated thoroughly (see, for example, Boyd et al. (2004); Luenberger et al. (1984)). Due to the fact that this is a distinct field of study, it requires considerable effort to fully comprehend the relevant theory and algorithms. The required numerical solution for MPC is frequently viewed as an obstacle to its application. Nonetheless, we can comprehend the essence of QP in order to generate the necessary computational programs. The advantage of doing so is that we can access the code if anything goes wrong; we can also write safety 'jacket' software for real-time applications. These aspects are very important in an industrial environment. To be consistent with the literature on QP, the decision variable is denoted by  $u$ . The objective function  $J$  and constraints are written as follows:

$$J = 1/2u^T E x + u^T F \tag{3.31}$$

$$M u \leq \gamma \tag{3.32}$$

Quadratic Term:

$$J = \frac{1}{2} u^T E u$$

where:

- $u$  is a vector of variables (could be a column vector).
- $E$  is a positive definite matrix.
- The term  $u^T E u$  represents the dot product of  $u$  with  $E u$ . Here,  $E u$  is another vector obtained by multiplying the matrix  $E$  with  $u$ . The multiplication  $E u$  results in a vector and the dot product  $u^T E u$  is a scalar.

By multiplying the dot product by  $\frac{1}{2}$ , it is a common practice in optimization problems (like quadratic programming) to use this term, and it has the same effect on the optimization as the original quadratic term (without the  $\frac{1}{2}$ ).

Linear Term:

$$u^T F$$

where:

- $F$  is a vector.

This term is a linear term because it involves a linear combination of the variables  $u$  with the coefficients given by the vector  $F$ .

This is a standard form for a quadratic function in optimization problems. The goal in many optimization contexts is to minimize or maximize such quadratic functions subject to certain constraints, which seems to be the case here given the constraint  $Mu \leq \gamma$ .

### 3.5.8. Predictive Control of MIMO Systems

In the preceding section, the predictive control system was developed as a single-input and single-output system for ease of demonstration. Because of the state-space formulation, this design process can easily be extended to MIMO systems with not much extra work.

#### General Formulation of the Model

Consider the plant to have  $m$  inputs,  $q$  outputs, and  $q_1$  states. Furthermore, we assume that the number of outputs is fewer than or equal to the number of inputs (i.e.,  $q, m$ ). If the number of outputs exceeds the number of inputs, we cannot hope to independently regulate each measured output with zero steady-state errors. We consider plant noise and disturbance in the general formulation of the predictive control problem.

$$x_m(k+1) = A_m x_m(k) + B_m u(k) + B_d w(k) \quad (3.33)$$

$$y(k) = C_m x_m(k) \quad (3.34)$$

$w(k)$  denotes the input disturbance, which is believed to be a sequence of integrated white noise. This indicates that the difference equation relates the input disturbance  $w(k)$  to a zero-mean, white noise sequence  $\varepsilon(k)$ .

$$w(k) - w(k-1) = \varepsilon(k) \quad (3.35)$$

It is worth noting that the following difference equation follows from 3.33:

$$x_m(k) = A_m x_m(k-1) + B_m u(k-1) + B_d w(k-1) \quad (3.36)$$

Equation 3.36 can be converted to Eq.3.37:

$$\Delta x_m(k+1) = A_m \Delta x_m(k) + B_m \Delta u(k) + B_d \varepsilon(k) \quad (3.37)$$

To link the output  $y(k)$  to the state variable  $\Delta x_m(k)$ , we derive that

$$\Delta y(k+1) = C_m \Delta x_m(k+1) = C_m A_m \Delta x_m(k) + C_m B_m \Delta u_m(k) + C_m B_d \varepsilon(k) \quad (3.38)$$

Choosing a new vector of state variables  $x(k) = [\Delta x_m(k)^T, y(k)^T]^T$ , we have:

$$\underbrace{\begin{bmatrix} \Delta x_m(k+1) \\ y(k+1) \end{bmatrix}}_{x(k+1)} = \underbrace{\begin{bmatrix} A_m & 0_m^T \\ C_m A_m & 1 \end{bmatrix}}_A \underbrace{\begin{bmatrix} \Delta x_m(k) \\ y(k) \end{bmatrix}}_{x(k)} + \underbrace{\begin{bmatrix} B_m \\ C_m B_m \end{bmatrix}}_{B_m} \Delta u(k) + \underbrace{\begin{bmatrix} B_d \\ C_m B_d \end{bmatrix}}_{B_d} \varepsilon(k)$$

$$y(k) = \underbrace{\begin{bmatrix} 0_m & 1 \end{bmatrix}}_C \begin{bmatrix} \Delta x_m(k) \\ y(k) \end{bmatrix} \quad (3.39)$$

### Solution of Predictive Control for MIMO Systems

The predictive control method can be easily extended, but we must pay attention to the dimensions of the state, control, and output vectors in a MIMO context.

The future state variables are derived sequentially utilising the set of future control parameters based on the state-space model  $(A,B,C)$ .

$$\begin{aligned} x(k_i + 1|k_i) &= Ax(k_i) + B\Delta u(k_i) + B_d\varepsilon(k_i) \\ x(k_i + 2|k_i) &= Ax(k_i + 1|k_i) + B\Delta u(k_i + 1) + B_d\varepsilon(k_i + 1|k_i) \\ &= A^2x(k_i) + AB\Delta u(k_i) + B\Delta u(k_i + 1) + AB\varepsilon(k_i) + B_d\varepsilon(k_i + 1|k_i) \\ &\vdots \\ x(k_i + N_p|k_i) &= A^{N_p}x(k_i) + A^{N_p-1}B\Delta u(k_i) + A^{N_p-2}B\Delta u(k_i + 1) + A^{N_p-N_c}B\Delta u(k_i + N_c - 1) \\ &\quad + A^{N_p-1}B_d\varepsilon(k_i) + A^{N_p-2}B_d\varepsilon(k_i + 1|k_i) + \dots + B_d\varepsilon(k_i + N_p - 1|k_i) \end{aligned} \quad (3.40)$$

The expected value of  $\varepsilon(k_i + i|k_i)$  at future sample  $i$  is assumed to be zero if  $\varepsilon(k)$  is a zero-mean white noise sequence. The noise effect on the anticipated values is zero since the state and output variables' predictions are calculated as the corresponding variables' expected values.

Finally, the PBG system can be modelled by employing the MPC method in the following section.

### 3.6. The modelling of PBG using the MPC

The state-space linear equation can be defined using the battery equation. The linear state-space equation can generally be represented as follows (**Point 1**):

$$x(k+1) = Ax(k) + Bu(k) \quad (3.41)$$

where  $x$  is the state vector and  $SOC$  of the battery in this system,  $u$  is the input vector, also known as the control vector, and  $PV_{LD}$ ,  $PV_{BAT}$ , and  $BAT_{LD}$ . In the system,  $y$  represents the output vector and  $GR_{LD}$ .  $A$  and  $B$  can be defined in accordance with Eq (3.34). The following illustrates  $x$ ,  $u$ , and  $y$  (**Point 2-4**):

$$x(k) = [SOC(k)] \quad (3.42)$$

$$u(k) = [PV_{LD}(k); PV_{BAT}(k); BAT_{LD}(k)] \quad (3.43)$$

$$y(k) = [GR_{LD}(k)] \quad (3.44)$$

3.6.1. *The constraints of the components of PBG (Point 5)*

The PV system supplies the load demand and charges the battery. It operates based on the following constraints at sampling time  $k$ :

$$0 \leq P_{PV} \leq P_{PV}^{max} \quad (3.45)$$

$$0 \leq PV_{LD} \leq PV_{LD}^{max} \quad (3.46)$$

$$0 \leq PV_{BAT} \leq PV_{BAT}^{max} \quad (3.47)$$

where  $P_{PV}^{max}$ ,  $PV_{LD}^{max}$ , and  $PV_{BAT}^{max}$  represent the maximum amount of energy supplied by the PV to the load, the battery, and the grid, respectively.  $P_{PV}$  can also be used to represent the total energy required to meet the load demand and charge the battery.

$$P_{PV}(k) = PV_{LD}(k) + PV_{BAT}(k) \quad (3.48)$$

The battery is utilized in both charging and discharging modes depending on the amount of available sunlight. Consequently, the charging and discharging of the battery can be defined by the following equation:

$$SOC(k) = SOC(k+1) + \frac{PV_{BAT}(k)\eta_{ch}}{C_l} - \frac{BAT_{LD}(k)}{C_l\eta_{dis}} \quad (3.49)$$

In addition, constraints regarding the battery are depicted below:

$$SOC^{min} \leq SOC(k) \leq SOC^{max} \quad (3.50)$$

$$0 \leq BAT_{LD} \leq BAT_{LD}^{max} \quad (3.51)$$

where  $SOC$  represents the battery's state of charge,  $SOC^{min}$  and  $SOC^{max}$  represent the minimum and maximum  $SOC$  values, respectively.  $BAT_{LD}^{max}$  and  $C_l$  are the hourly maximum allowable discharging power and battery capacity, respectively.  $\eta_{ch}$  and  $\eta_{dis}$  represent the battery's charging and discharging efficiencies, respectively.

When the PV panel and the battery are insufficient, the utility grid is utilized to meet the load demand. This is the final option because it is more expensive and environmentally harmful. The only benefit of its utilization is its availability at all times, barring blackouts.

In addition, the constraints associated with the grid system and load can be expressed as follows:

$$0 \leq GR_{LD} \leq GR_{LD}^{max} \quad (3.52)$$

$$P_{LD}(k) = PV_{LD}(k) + BAT_{LD}(k) + GR_{LD}(k) \quad (3.53)$$

where  $GR_{LD}^{max}$  represents the maximum quantity of power from the utility grid.

### 3.6.2. Objective Functions of PBG (Point 6)

The cost functions of the PBG system are:

1. To minimize the energy consumption from non-RES:  $\sum_k^{k+N_p} w_1^2 GR_{LD}(k)^2 = J_1$
2. To increase the life cycle of the battery:  $\sum_k^{k+N_p} w_2^2 (PV_{BAT}(k)^2 + BAT_{LD}(k)^2) = J_2$
3. To maximize the practicality of renewable energy usage:  $\sum_k^{k+N_p} w_3^2 (PV_{LD}(k)^2 + PV_{BAT}(k)^2) = J_3$

where  $N_p$  is the prediction horizon and  $w_1$ ,  $w_2$ , and  $w_3$  are cost weighting factors.

The selection of cost weighting factors ( $w_1$ ,  $w_2$ , and  $w_3$ ) in the objective function is a crucial aspect of designing a MPC system. These weighting factors determine the relative importance of each objective in the optimization process. The choice of these factors is often based on the specific priorities and requirements of the MG system and the goals of the control strategy. Here are some general considerations and methods for selecting these weighting factors:

- Consider the primary goals and objectives of the MG system. For example, if minimizing energy consumption from non-renewable sources is a top priority, a higher weight might be assigned to the corresponding term in the objective function.
- Identify key performance metrics that reflect the desired behaviour of the MG. Each term in the objective function corresponds to a specific metric. Assign higher weights to the metrics that are more critical to the overall system performance.
- Evaluate trade-offs between conflicting objectives. For instance, there might be a trade-off between maximizing the use of renewable energy and extending the battery life. The weighting factors should reflect the importance of achieving a balance between such objectives.

### 3.6.3. Reference Matrix for the PBG

Define the reference matrix ( $R$ ) for the PBG (**Point 7**):

$$R(k) = [w_1(P_{LD}(k); w_3(P_{PV}(k); 0; w_1(P_{LD}(k+1); w_3(P_{PV}(k+1); 0; \dots; w_1(P_{LD}(k+N_p-1); w_3(P_{PV}(k+N_p-1); 0] \quad (3.54)$$

### 3.6.4. The calculation of receding horizon control:

In the MPC principle, the optimization problem is solved during each sampling time  $k$ , and the first element of  $U(k)$  is employed to the MG (**Point 8**):

$$u(k) = U(k+1|k) \quad (3.55)$$

### 3.7. The Implementation of $\varepsilon$ -variables for the PBG

The main idea behind the  $\varepsilon$ -variable method is that every asset is symbolized by a node, and every flow of matter/energy is symbolized by an edge in the complicated MG system, as demonstrated in Figure 3.2. This theory and the aforementioned evolution operators can simplify this power system's analysis, management, and operation. This method states that any hybrid power system consists of three key factors: converters, accumulators, and flows. The converters are used to convert the energy/matter to matter/energy, the accumulators accumulate energy/matter, and the flows symbolize the flow of energy/matter. Lastly, the control statements are the evolution operators based on the logical operators, illustrating the different types of EMSs exploited by the multi-vector system (Giaouris et al. (2013)).

As evidence of the idea, Figure 3.2 illustrates the complicated hybrid MG system. According to the graph theory, the converters are the PV array, load (LD), and utility grid (GR); the battery (BAT) can be considered as an accumulator, and power can be regarded as flows. As can be seen in Figure 3.2, the assets of the MG system can be split into two sets as follows:

- The set of converters:  $Rs^{Con} = \{PV, LD, GR\}$
- The set of accumulator:  $Rs^{Acc} = \{BAT\}$

In addition, the connection between two nodes can be called a *flow*, such as PV to BAT and BAT to PV as a power flow.

Therefore, the set of flow for the complicated hybrid power system can be illustrated as follows Giaouris et al. (2018):

- The set of flow:  $Flows = \{Power\}$

To identify any dynamical system, we require two tasks: (a) the set of its possible states (state space -  $S$ ) and (b) an evolution operator ( $\phi$ ) that determines which specific state the system will be in at any given time (**Point 16**). In this regard, the state  $s$  (**Point 11**) of a graph (i.e., of the MG) at a specific instant is given by the states of the nodes and edges specified as follows (**Point 9**):

- A state (**Point 13**) must specify its presence and the type/amount of flow it includes for the edges. This is symbolized by variable  $F_{a \rightarrow b}^j$  with  $j \in Flow$  and  $m, n$  two adjacent nodes. If there is no edge,  $F_{a \rightarrow b}^j$  is zero.
- The state (**Point 14**) of an accumulator is the normalized amount of stored matter or energy, represented by variable  $SOAcc^l \in [0,1], l \in Rs^{Acc}$ .
- The state (**Point 15**) of the converters is their status (whether they are activated or not), which is indicated by variable  $\varepsilon_i(k) \in 0,1, i \in Rs^{Con}$ .

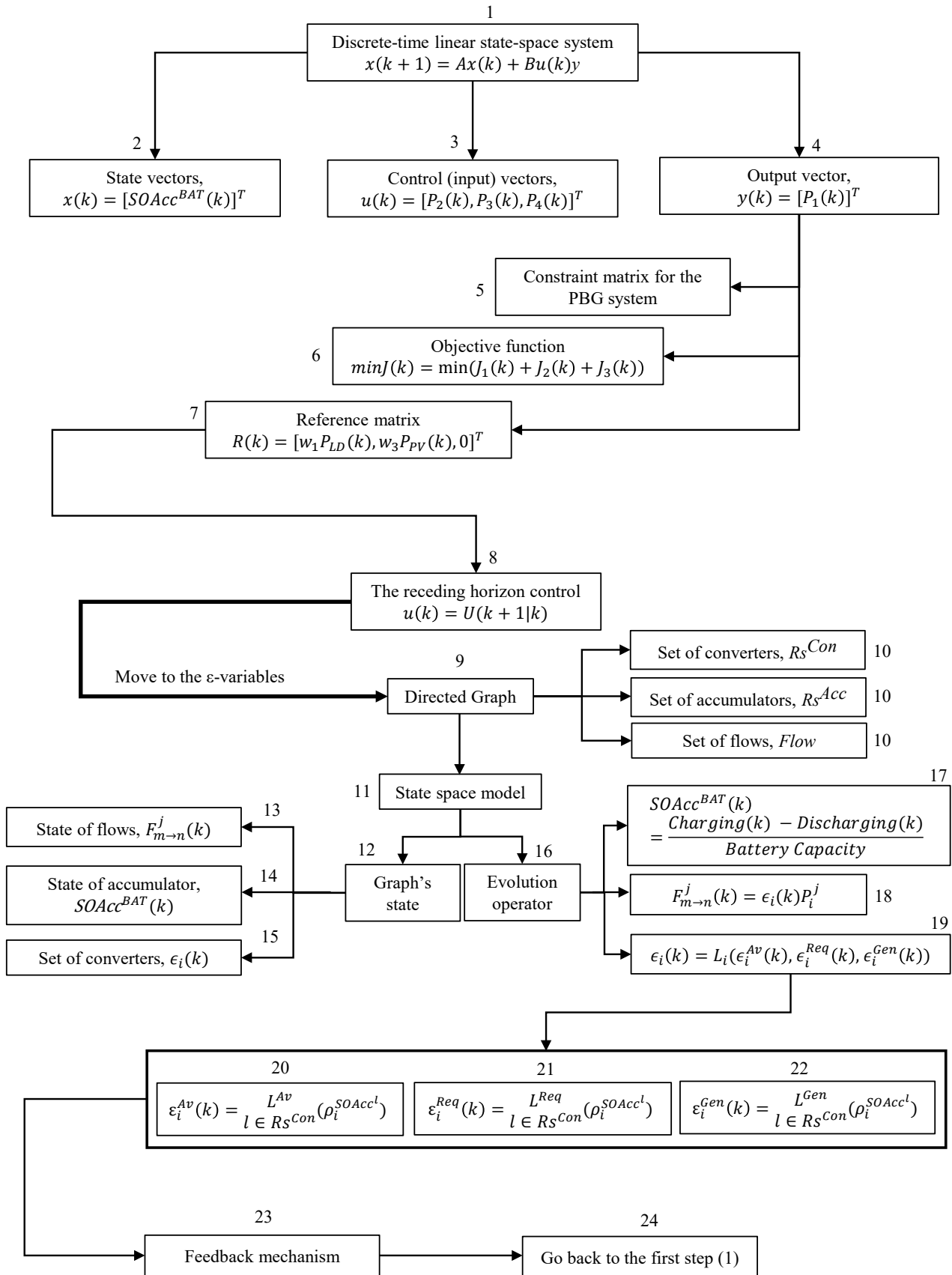


Figure 3.5 A graph shown in state space; points addressed in the text are indicated by numbers.

Hence, the states  $s \in S$  of the graph are (**Point 11**):

$$s = \{F_{a \rightarrow b}^j, SOAcc^l(k), \varepsilon_i(k)\} \quad l = \text{BAT}, \quad (3.56)$$

$$l \in R_s^{Acc}, i \in R_s^{Con}, a, b \in R_s^{Acc} \times R_s^{Con}, j \in Flow$$

The next step is constructing the evolution operator  $\Phi$  (**Point 16**) to give a state  $s$  in the state space  $S$  at an instant  $t_0$ . We can calculate the state at the instant  $t$  as  $s(t) = \phi(t, s(t_0))$  where  $\phi: S \rightarrow S$ .

This evolution operator is the energy management approach utilized to control the MG and the accumulator operation principle for our purposes. As in dynamical systems, we require a different evolution operator for each state variable, i.e., an evolution operator for each  $s \in S$  in our graph.

The evolution operator (**Point 18**) for an accumulator  $l$  with a state variable  $SOAcc^l$  is effectively an integrator and is dependent on its capacity  $C_l$  and the flows  $F_{a \rightarrow b}^j(k)$  that are directed towards and away from the accumulator (**Point 17**):

$$SOAcc^l(k) = SOAcc^l(k-1) + \frac{\sum_{k_1 \in R_s^{Con}} F_{k_1 \rightarrow l}^j(k) - \sum_{k_2 \in R_s^{Con}} F_{l \rightarrow k_2}^j(k)}{C_l} \quad (3.57)$$

An edge with the evolution operator  $F_{a \rightarrow b}^j(k)$  (**Point 10**) has the following definition (**Point 18**):

$$F_{a \rightarrow b}^j(k) = \varepsilon_i \cdot P_i^j, \quad i \in \{m, n\}, \quad j \in Flow \quad (3.58)$$

where  $\varepsilon_i$  is the state of the corresponding converter and  $P_i^j$  is the amount of energy or matter that can be converted by the  $k^{th}$  unit per unit of time. Variables  $P_i^j$  might be either uncontrollable (like the PV energy flow) or controlled by the grid's designer or the energy management strategy (for example, the flow of energy from the BAT).

Depending on the energy management technique, the evolution operator for the converters (i.e., the variables  $\varepsilon_i$ ) can be a complex function (**Point 20**). Nonetheless, it depends on three variables that have a binary representation:

1.  $\varepsilon_i^{Av}(k)$ , which stands for the availability of the material or energy to be transformed (**Point 21**).
2. A conversion's demand for materials or energy is represented by the symbol  $\varepsilon_i^{Req}(k)$  (**Point 22**).
3. Other potential desired conditions (such as not operating the FC when the EVs are activated) that are not connected to the aforementioned are represented by  $\varepsilon_i^{Gen}(k)$  (**Point 23**).

The state of the accumulators determines whether materials or energy are available or required to complete a conversion. A binary variable that is 1 when there is availability or demand and 0

otherwise is used to assess this **(Point 20-22)**:

$$\varepsilon_i^{Av}(k) = L^{Av}(\rho_i^{SOAcc^l}) \quad (3.59)$$

$$\varepsilon_i^{Req}(k) = L^{Req}(\rho_i^{SOAcc^l}) \quad (3.60)$$

where the logical operators  $L^{Av}$  and  $L^{Req}$  are used on the variables to quantify the need for and the supply of/from the accumulator  $l$ . The binary variable  $\rho$  is either 0 or 1 depending on the accumulators (see Eq. 3.56-3.59).

The general condition may be dependent on a node or an edge, but it is typically dependent on the state of other converters and can be characterized as follows:

$$\varepsilon_i^{Gen}(k) = L^{Gen}(\rho_i^{SOAcc^l}) \quad (3.61)$$

where  $L^{Gen}$  is a logical operator.

Using a logical operator  $L_i$ , the device  $i$ 's final evolution operator is found **(Point 19)**:

$$\varepsilon_i(k) = L_i(\varepsilon_i^{Av}(k), \varepsilon_i^{Req}(k), \varepsilon_i^{Gen}(k)) \quad (3.62)$$

### **3.8. The Implementation of hybrid MPC- $\varepsilon$ -variables technique (Point 23-24)**

As depicted in Figure 3.6, the 'data' utilized as input data by the hybrid MPC- $\varepsilon$ -variables technique are initially obtained using the MPC method. In Figure 3.6, the 'data' are  $GR_{LD}$ ,  $PV_{LD}$ ,  $PV_{BAT}$  and  $BAT_{LD}$ . The evolution operators are then computed using the state of the accumulators and converters. To be more specific:

- As illustrated in Figure 3.6, the evolution operator for converters can be defined by three factors represented by binary variables:  $\varepsilon_i^{Av}$ ,  $\varepsilon_i^{Req}$ , and  $\varepsilon_i^{Gen}$  represent the availability of power, the load requirement, and the potentially desired condition, respectively. The energy supply is dependent on the condition of the accumulators. As shown below, the binary variable  $\rho$  is either 0 or 1 depending on the accumulators:

$$\varepsilon_i^{Av}(k) = L_{Acc}^{Av}(\rho_i^{SOAcc^{BAT}}(k)) \quad (3.63)$$

$$\varepsilon_i^{Req}(k) = L_{Acc}^{Req}(\rho_i^{SOAcc^{BAT}}(k)) \quad (3.64)$$

$$\varepsilon_i^{Gen}(k) = L_{Acc}^{Gen}(\rho_i^{SOAcc^{BAT}}(k)) \quad (3.65)$$

$$\varepsilon_i(k) = \varepsilon_i^{Av}(k) \wedge \varepsilon_i^{Req}(k) \wedge \varepsilon_i^{Gen}(k) \quad (3.66)$$

where  $L^{Av}$  and  $L^{Req}$  are the logical operators 'and' or 'or', and the general condition relies on the general condition of converters.  $i(k)$  is also the state of converter  $i$  while  $\varepsilon_i^{Av}(k)$  and  $\varepsilon_i^{Req}(k)$  are boolean variables that determine the availability and requirement of converter  $i$  respectively.

- Power flows are computed by multiplying Equations (3.37) and (3.36) by Equation (3.53).

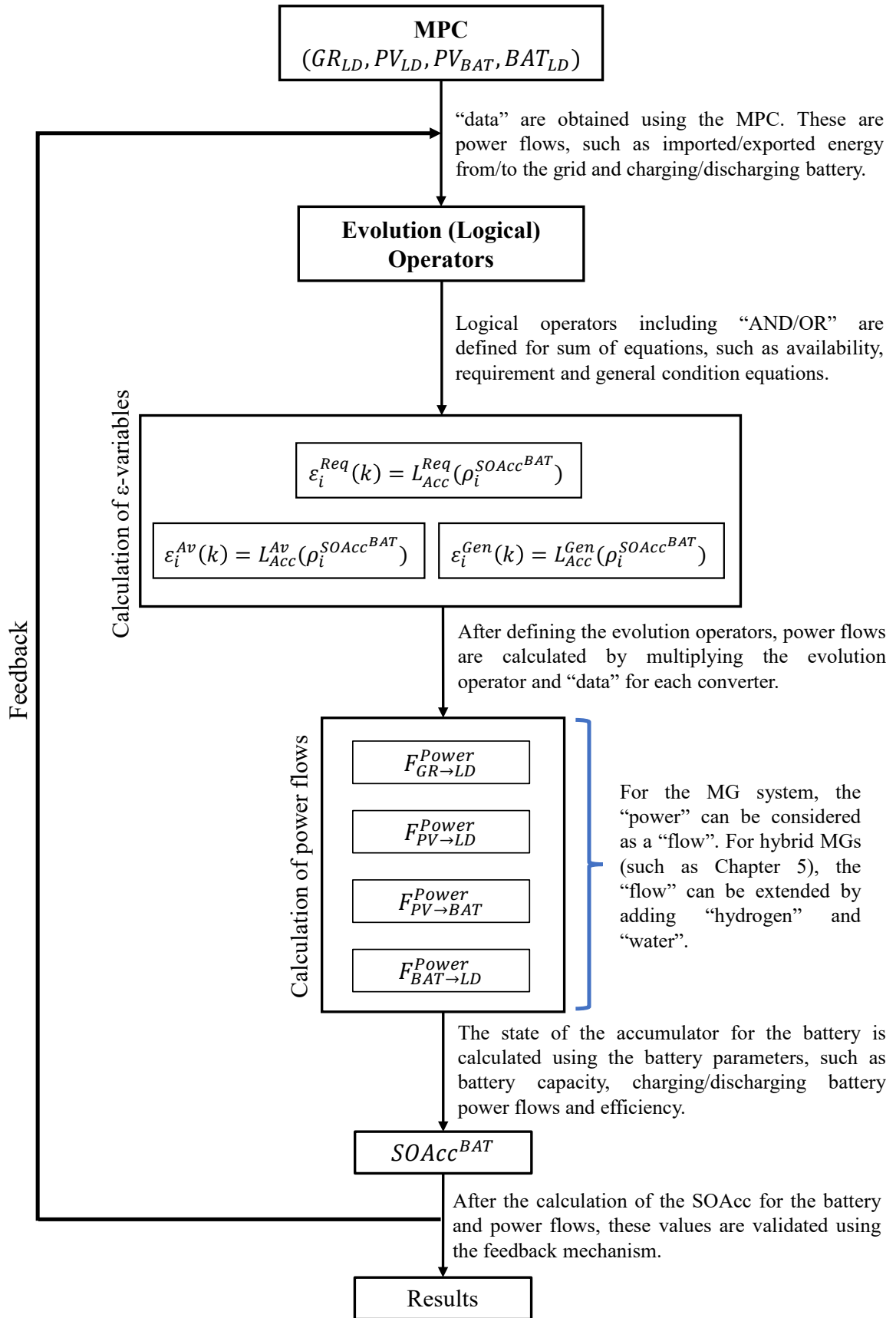


Figure 3.6 The flow-chart of the proposed method (MPC- $\epsilon$ -variables)

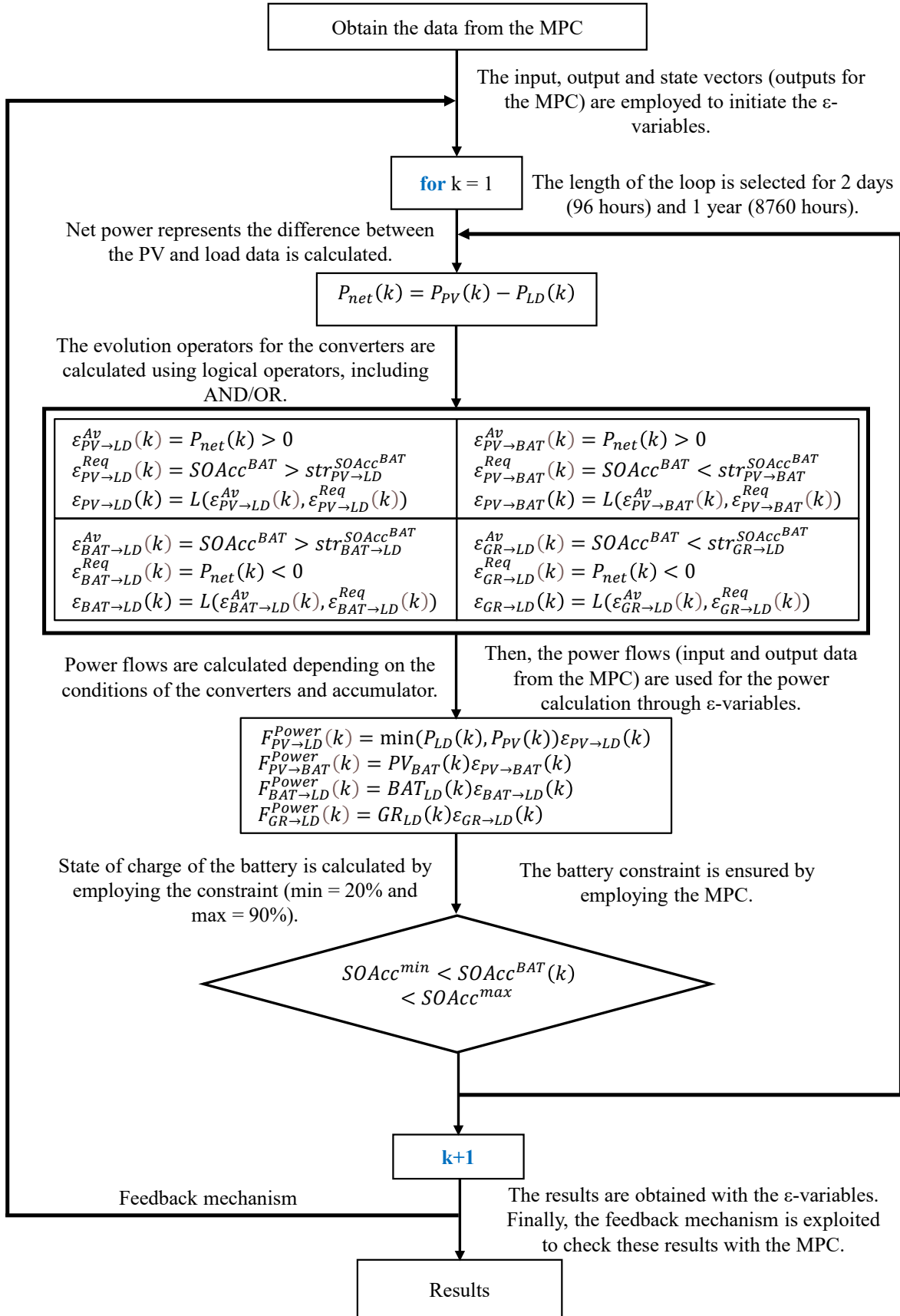


Figure 3.7 The detailed flow chart of the hybrid MPC- $\varepsilon$ -variables technique.

$$\begin{aligned}
 & - F_{GR \rightarrow LD}^{Power}(k) = y.\varepsilon_i(k) \\
 & - F_{PV \rightarrow LD}^{Power}(k) = u(1).\varepsilon_i(k) \\
 & - F_{PV \rightarrow BAT}^{Power}(k) = u(2).\varepsilon_i(k) \\
 & - F_{BAT \rightarrow LD}^{Power}(k) = u(3).\varepsilon_i(k)
 \end{aligned}$$

- The final step is to compute the accumulator's evolution operator:

$$SOAcc^{BAT}(k+1) = SOAcc^{BAT}(k) + \frac{F_{PV \rightarrow BAT}^{Power} - F_{BAT \rightarrow LD}^{Power}}{BatteryCapacity} \quad (3.67)$$

$$SOAcc^{BAT}(k) \in [0, 1]$$

Depending on their operational status (active or inactive), the converters are depicted as  $\varepsilon_i(k) \in \{0, 1\}$  where  $i \in R_s^{Con}$ .

After finding the control decisions, the results are checked by employing the feedback mechanism of our proposed method (**Point 23**). According to our results, the control decisions of alone MPC and that of MPC- $\varepsilon$ -variables are the same. This is an expected and reasonable outcome. However, if these results are not the same, the controller returns to the first step to modify or change something (**Point 24**).

If, after checking the results using the feedback mechanism in **Point 23**, it is found that the control decisions of the alone MPC and MPC- $\varepsilon$ -variables are not the same, it indicates a discrepancy or inconsistency in the control strategy. In such a scenario, the controller would need to return to **Point 1** and modify or adjust certain aspects of the system or the control algorithm. Here are some potential aspects that might need modification:

- **Algorithm Parameters:** Review and adjust parameters used in the algorithm, such as prediction horizons, weights in the objective function, or tuning parameters. Small changes in these parameters can significantly impact the optimization results.
- **Constraints:** Reevaluate the constraints imposed on the system. If the constraints are too restrictive or do not adequately capture the system dynamics, they might need to be modified.
- **Evolution Operators:** Examine the evolution operators, especially those associated with  $\varepsilon$ -variables. These operators play a crucial role in determining the system's behaviour and responses to different conditions. Adjustments might be needed to ensure they accurately represent the system dynamics.
- **Logical Operators:** If logical operators are used in the  $\varepsilon$ -variables, review and modify them as needed. Logical conditions that determine the activation or deactivation of converters should align with the system's requirements.
- **Initial Conditions:** Check the initial conditions of the system. The system's starting state can significantly impact the optimization results. Ensure that the initial conditions are realistic and appropriate for the given scenario.

The detail for implementing the second step of our method has been explained in Figure 3.7. This figure explains the evolution operator's calculation and the logical operators' definitions for each converter. Moreover, Figure 3.7 illustrates the calculation of the power flows for  $PV_{LD}$ ,  $PV_{BAT}$ ,  $GR_{LD}$ , and  $BAT_{LD}$ .

### 3.9. The comparison of $\varepsilon$ -variables and if/else statement

Figure 3.8 shows that the if/else statement implementation consists of several steps in the MATLAB 'for' loop. Initially, the loop calculates the net values of equal PV power minus load demand. The condition of  $SOC$  is then evaluated to determine whether it is greater or less than the minimum/maximum values of  $SOC$ . At that time, both negative and positive values are examined. This technique operates based on the four distinct situations formulated within  $\varepsilon$ -variables, as shown in Figure 3.8's large rectangular area. These conditions include:

- if  $P_{net}(k) > 0$  }  $SOAcc^{BAT} > SOC^{max}$   $SOAcc^{BAT} < SOC^{max}$
- if  $P_{net}(k) < 0$  }  $SOAcc^{BAT} > SOC^{min}$   $SOAcc^{BAT} < SOC^{min}$

The if/else statement results are evaluated based on these four conditions. The results are binary variables (0 or 1) using logical operators, including AND and OR. Finally, the power flows are calculated by incorporating the battery's  $SOC$  constraint. Concerning the feedback line, the if/else statement's results are compared to those obtained by the MPC. As depicted in Figure 3.8, despite the fact that we get the same results with  $\varepsilon$ -variables, the if/else statement is neither straightforward nor practical. To make it clear, supposing that we decide to change the value for the initial  $SOC$  or remove one of the power flows, the controller is required to be re-modified. Nevertheless, in the  $\varepsilon$ -variables, we do not need to re-modify too many things in this controller, supposing that we decided to change something in this controller. Therefore,  $\varepsilon$ -variables are primarily used to make the MG system more practical and simple to implement, particularly hybrid MG systems.

### 3.10. Results and Discussions

#### 3.10.1. Simulation results of hybrid MPC- $\varepsilon$ -variables technique

Figure 3.9 depicts the PV and load data obtained from a building in the UK during the autumn season. Energy generation starts at the beginning of the morning (different morning times depending on sunlight) during these days. Also, the peak energy generation occurs at 1 PM and 2 PM. On the other hand, there is no PV generation in the course of the non-sunlight times. Regarding the load demand, it fluctuates due to several parameters such as the number of occupants, special days, and colder/warmer days, e.g., For instance, the load demand peaks on the first day between 7 PM and 8 PM since the occupants may return from their works or special day along with Christmas or Easter days. When sunlight is insufficient, or there is excessive load-generation mismatch, especially on nights, the battery (as a priority), then the utility grid is

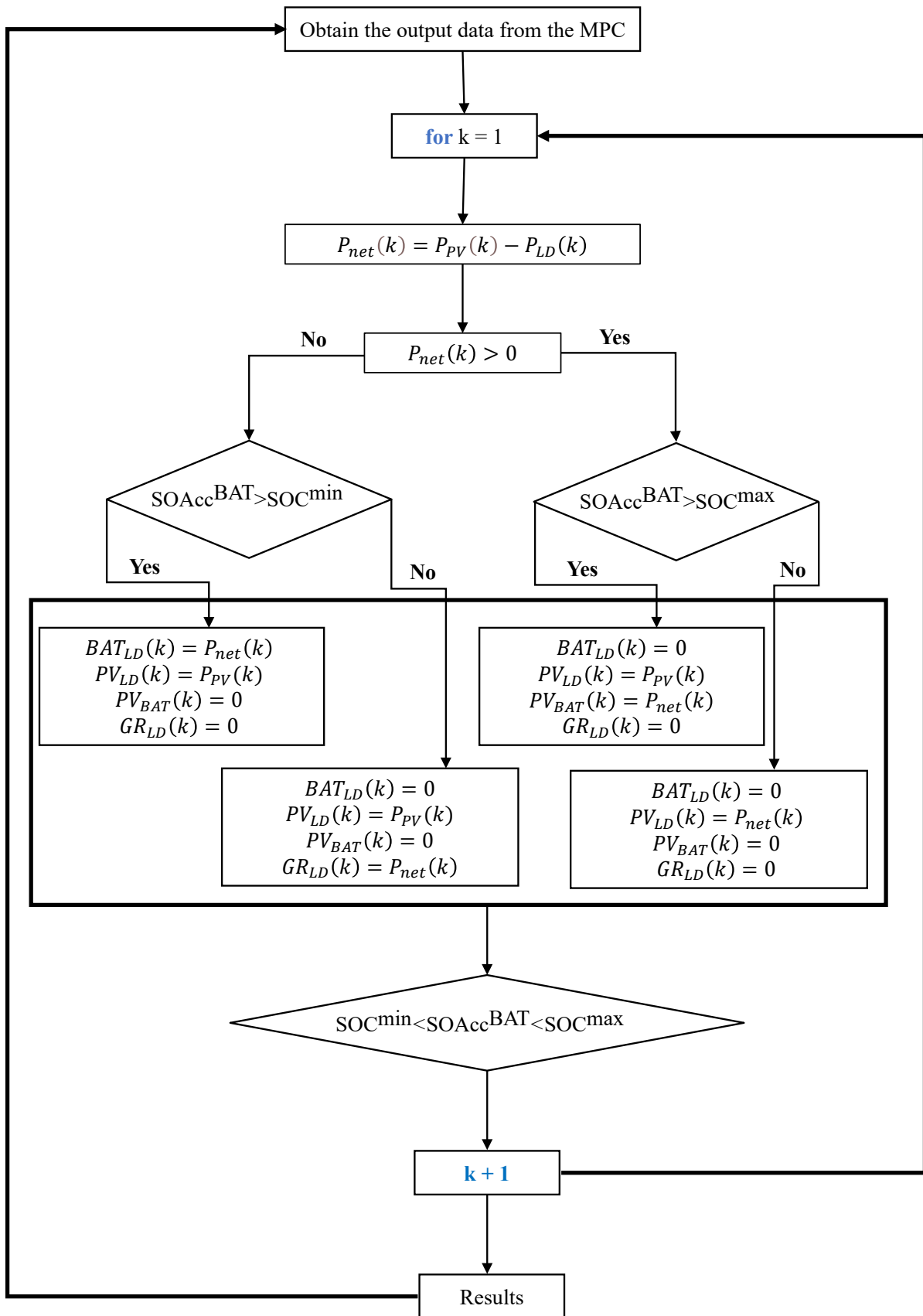
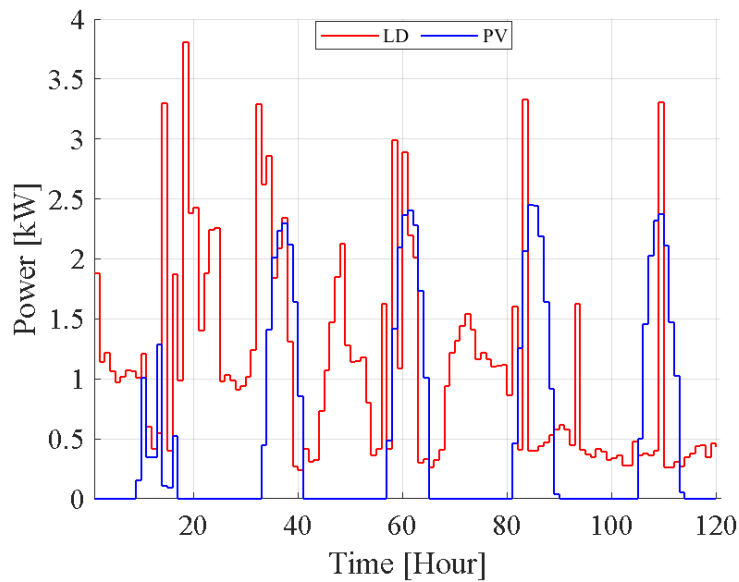


Figure 3.8 The illustration of the if/else statement



**Figure 3.9** Hourly PV and load demand (120 hours) for the building in the UK during the autumn season.

utilized. On the other hand, if the PV generates excess energy after covering the load-generation mismatch, the energy is exploited in order to charge the battery. The following figures will effectively demonstrate energy usage using the MPC and MPC- $\varepsilon$  variables.

Initially, the MPC is implemented, and then the MPC is merged with the  $\varepsilon$ -variables to compare each strategy's results. According to our results, the standard MPC and the merged MPC- $\varepsilon$ -variables have the same results. Moreover, our results indicate that the proposed method does not alter the fundamental goals and behaviour of the MPC. It is simple to extend the use of  $\varepsilon$ -variables to more complex systems and control constraints by modifying their logical operators.

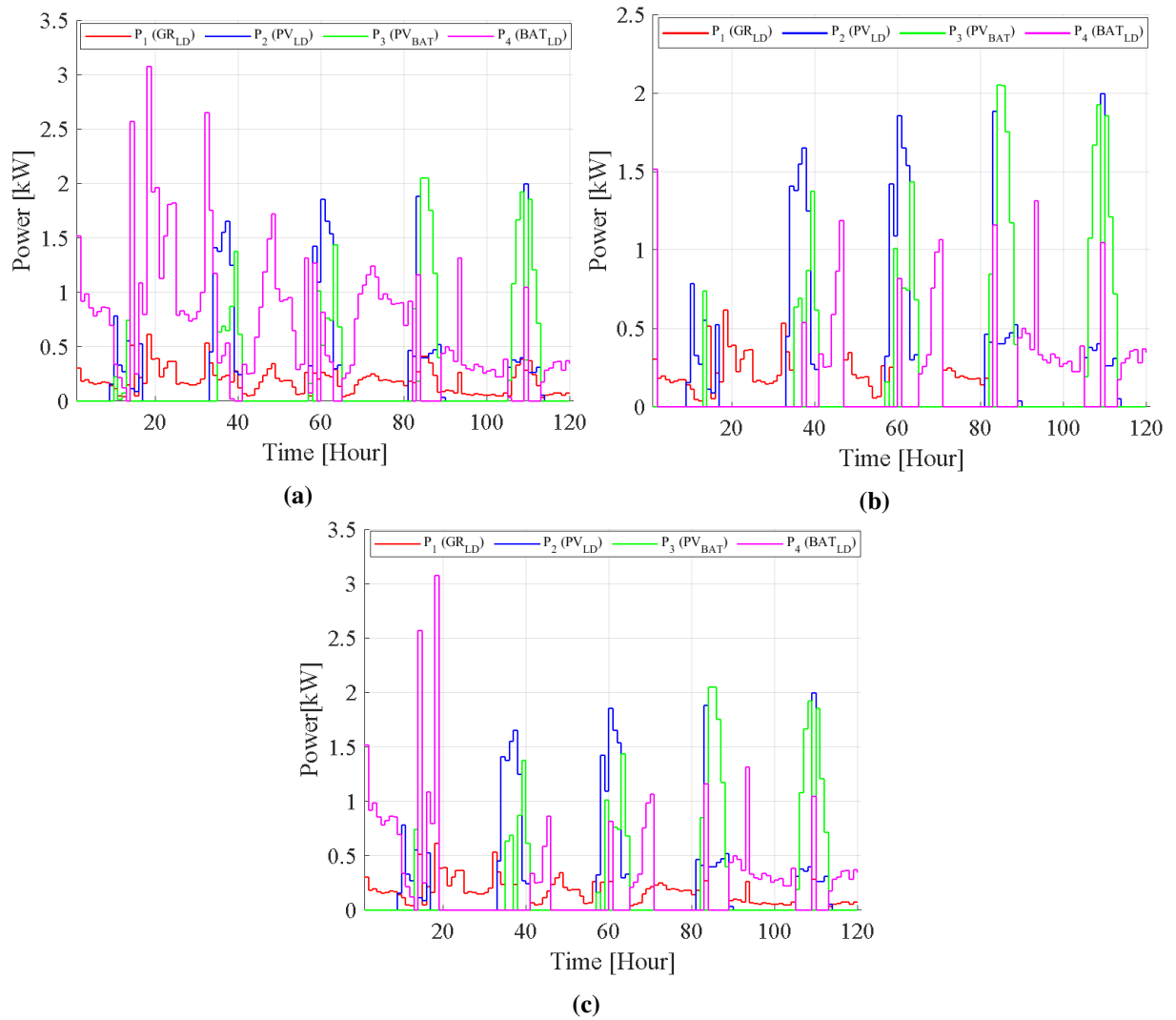


**Figure 3.10** The results of power flows using (a) the MPC, (b) the MPC- $\epsilon$ -variables, and (c) the MPC- $\epsilon$ -variables when  $SOAcc(1) = 0.55$  during the autumn.

As shown in Figure 3.10a, the MPC imports energy from the battery  $BAT_{LD}$  and utility grid  $GR_{LD}$  when the  $SOC$  falls below 30%. It is worth noting that the MPC does not fall below the critical value (20%) in order to protect the battery from over-discharging. When the battery works to meet the load-generation mismatch, it is in discharging mode  $BAT_{LD}$ . On the other hand, the battery is in charging mode when the PV generates excessive energy,  $PV_{BAT}$ . Furthermore, by modifying the evolution operator of  $\epsilon_{GR \rightarrow LD}$ , the energy consumption from the utility grid can be decreased, as demonstrated in Figure 3.10b. In this case, the binary variables of  $\epsilon_{GR \rightarrow LD}$  are converted from 1 to 0. If the initial value of  $SOC$  is chosen as 55%, the energy from the battery to the load  $\epsilon_{BAT \rightarrow LD}$  is increasing initially. After the first day, the binary variables of  $\epsilon_{BAT \rightarrow LD}$  are converted from 1 to 0. Therefore, the value starts to decrease, as demonstrated in Figure 3.10c. On the contrary, the utility grid works instead of the battery. In this case, the logical operators of the  $\epsilon_{GR \rightarrow LD}$  are turned from AND to OR. By doing that, the binary variables of  $\epsilon_{GR \rightarrow LD}$  are converted to 1. Hence, energy imported from the utility grid  $GR_{LD}$  is increased, whereas energy imported from the battery is decreased  $BAT_{LD}$ .

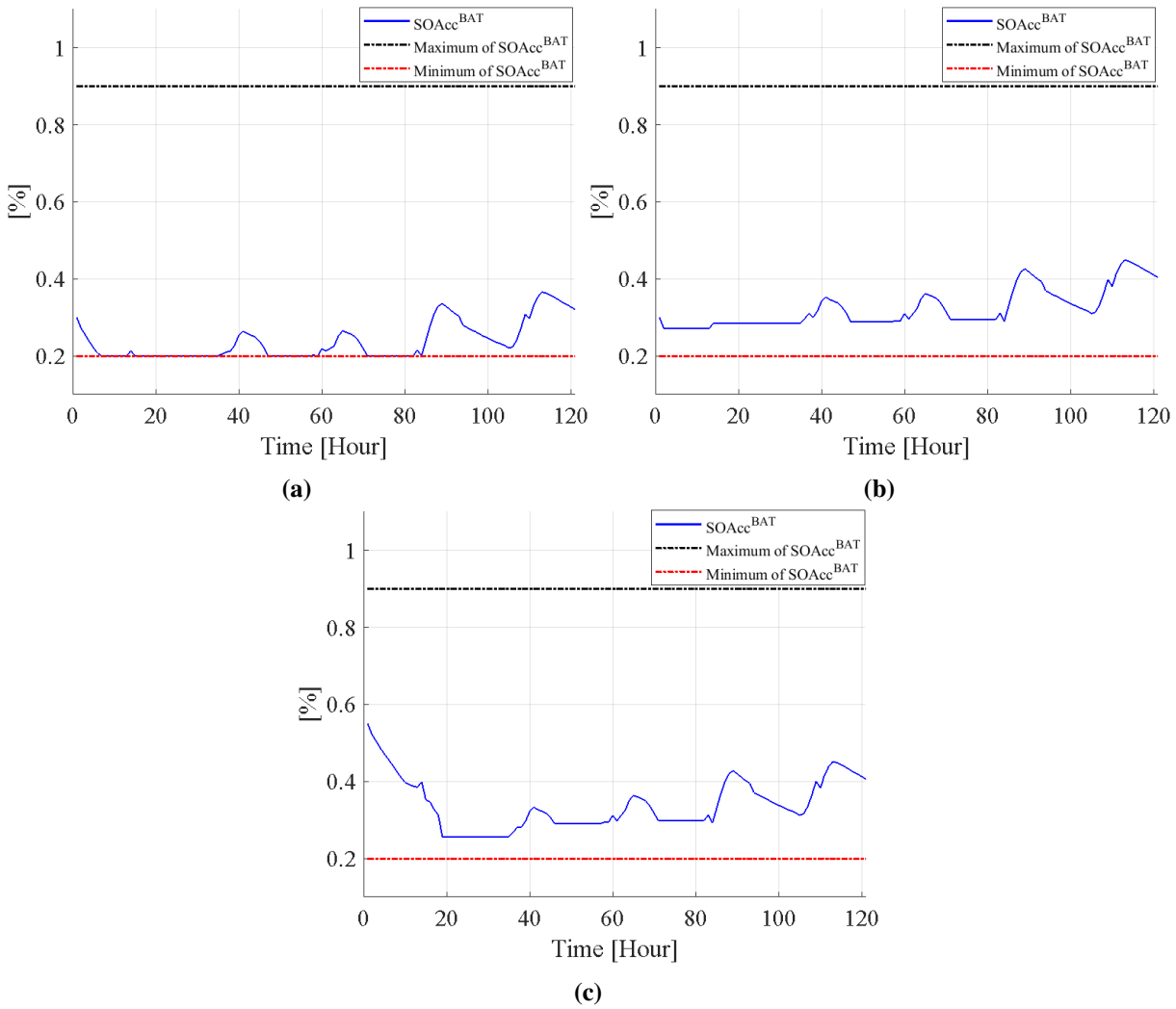


**Figure 3.11** The results of power flows and *SOC* of the battery using the MPC- $\epsilon$ -variables

However, there are instances in which this can occur close to the point where PV will produce sufficient energy to compensate for the slight drop in *SOC* below 30% (see Figure 3.11b), thereby increasing the system’s independence from the main grid. Therefore, in this instance, and without modifying the MPC structure, the evolution operator of the converter "Grid" will contain an additional term that is logically 0 when it is anticipated that the PV will produce sufficient power within 1 or 2 samples. Since, in this work, this evolution operator utilizes the AND logical gate, when this new binary variable equals zero, the evolution operator will also equal zero, as indicated in Figure 3.11a. To clearly explain it, if the evolution operators change for the asset (battery), the case of the battery changes. For instance, to protect the battery from over-discharging, the logical operators of  $\epsilon_{BAT \rightarrow LD}$  are converted from 1 to 0. For this reason, the *SOC* of the battery behaves differently from the previous one, as shown in Figure 3.11b. The *SOC* of the battery is dramatically decreasing during the first day (see Figure 3.11c), but it does not pass critical value due to the evolution operator of  $\epsilon_{BAT \rightarrow LD}$ . In summary, the MG system is re-modified when changing the initial value of *SOC* of the battery because of  $\epsilon$ -variables. In order to meet the load-generation mismatch, the utility grid runs much more than before rather than the battery usage.

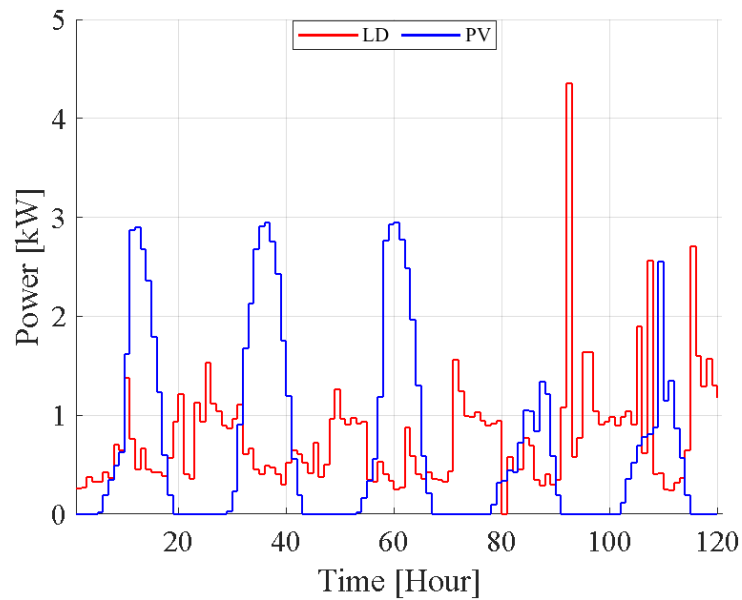


**Figure 3.12** Hourly PV and load demand (120 hours) for the building in the UK during summer.

On the other hand, Figure 3.12 displays the PV and load data collected from a building in the UK during summer. During these days, energy production begins earlier than the winter season because of much more sunlight days. In addition, the peak energy production starts to occur at the beginning of 11 AM. During non-sunlight hours, however, there is no PV generation. These non-sunlight hours start much later (after 8 PM) than the winter session. Regarding load demand, this amount is much less since the occupants have planned for outside activities during hot nights.

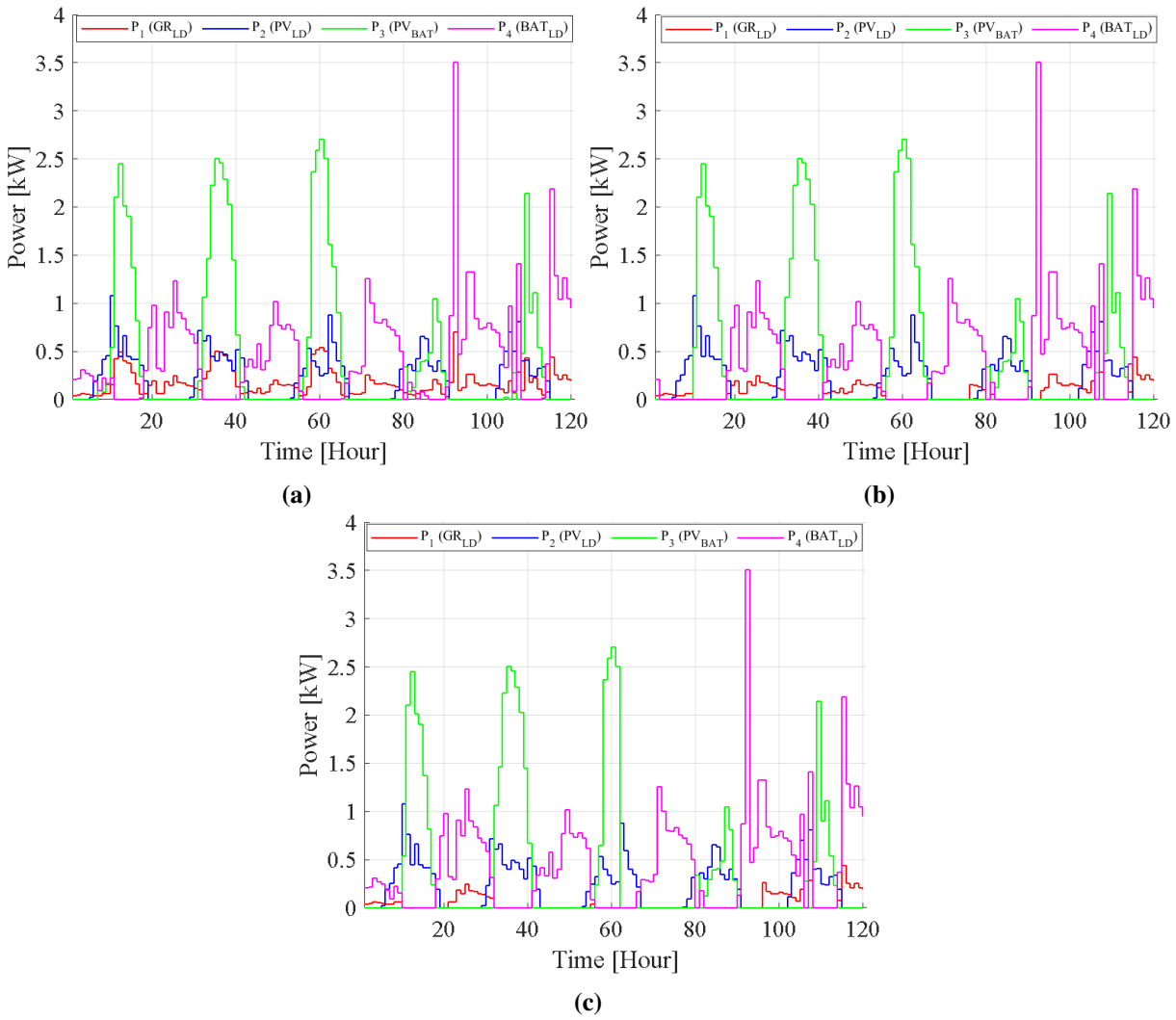


**Figure 3.13** The results of power flows using (a) the MPC, (b) the MPC- $\epsilon$ -variables, and (c) the MPC- $\epsilon$ -variables when  $SOAcc(1) = 0.55$  during the summer.

During the summer season, the PV generation is much greater than in the winter season. Hence, the values of charging battery  $PV_{BAT}$  are much greater than can be when compared to Figure 3.10a and Figure 3.13a. The main reason for the increase in  $SOC$  of the battery (see Figure 3.13a) is the increase in the  $PV_{BAT}$ . In contrast, the discharging battery  $BAT_{LD}$  decreases due to the much more sunlight days. As mentioned earlier, when there is excessive energy in the PV, the energy is employed for the charging battery. Notably, there is not enough energy in PV and battery, and the utility grid  $GR_{LD}$  is utilized in order to meet the load-generation mismatch. Regarding the  $\epsilon$ -variable method, when the  $SOAcc$  of the battery falls below the initial value of the  $SOAcc$ , the evolution operators (logical operators) of the  $\epsilon_{BAT \rightarrow LD}$  are converted AND, initially. After the first day, the binary variables of  $BAT_{LD}$  are turned from 0 to 1, as illustrated in Figure 3.13b. If the initial value of  $SOAcc$  is set to 55%, the power transferred from the battery to the load  $\epsilon_{BAT \rightarrow LD}$  initially increases. Concerning the utility grid  $GR_{LD}$ , the values decrease depending on the initial value of  $SOAcc$ , as can be seen when compared to Figure 3.13b and Figure 3.13c. As a result of  $\epsilon$ -variables, the MG system must be modified when the initial  $SOAcc$  value of the battery is changed. In order to compensate for the mismatch between load and

generation, the utility grid runs significantly more than it did previously, rather than utilizing batteries.

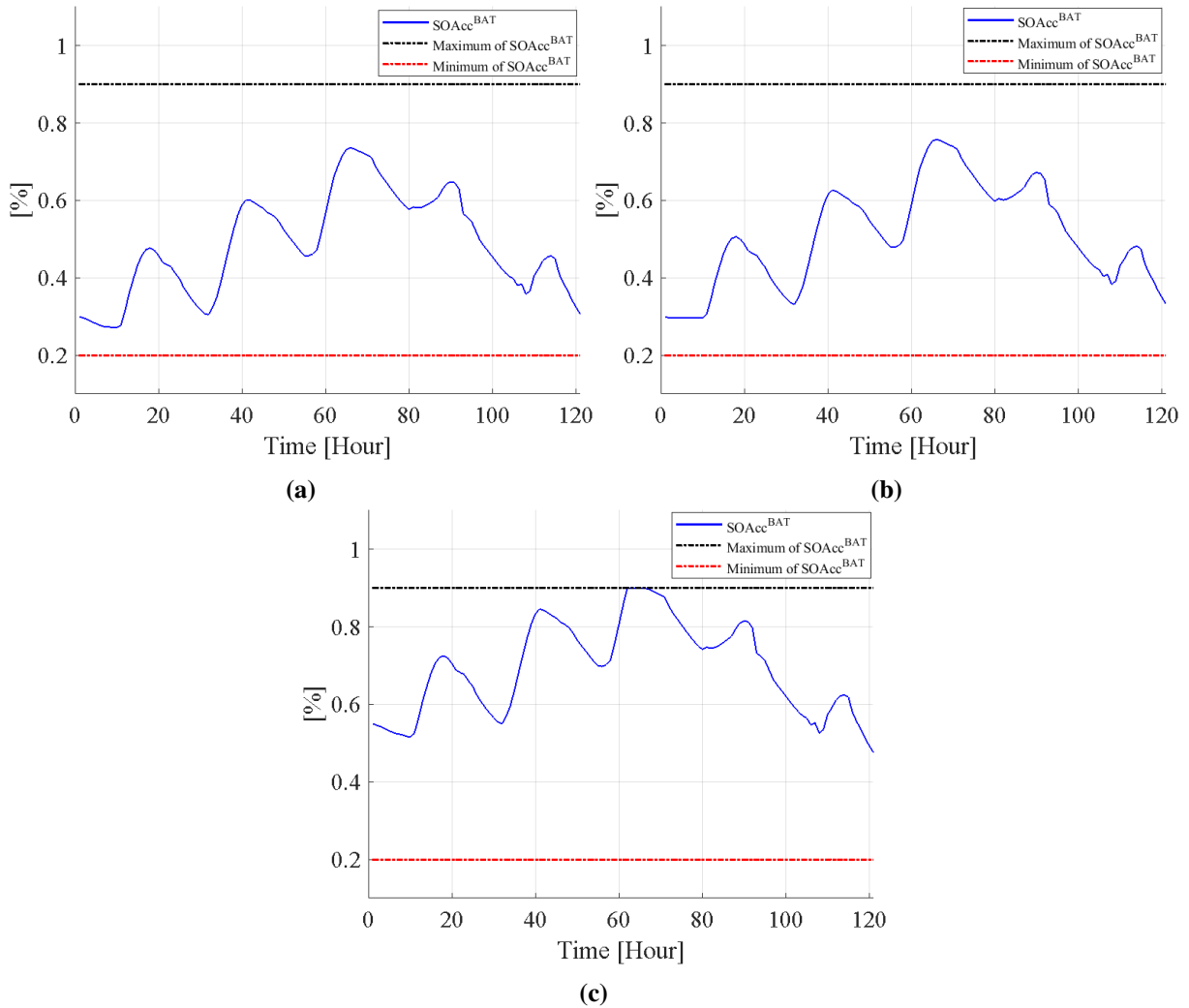


**Figure 3.14** The results of power flows and  $SOC$  of the battery using the MPC- $\epsilon$ -variables during summer.

Furthermore, the logical operators of  $\epsilon_{GR \rightarrow LD}$  are converted to 0 during the first day since the  $SOAcc$  of the battery drops below 30% (see Figure 3.14a). To clarify, if the evolution operator of the asset (battery) changes, the battery's case also changes. For example, the logical operators of  $\epsilon_{BAT \rightarrow LD}$  are converted from 1 to 0 to prevent over-charging. Due to this, the  $SOAcc$  of the battery behaves differently compared to the previous one, as depicted in Figure 3.14b. Figure 3.14b demonstrates that by modifying the evolution operator of  $\epsilon_{GR \rightarrow LD}$ , the energy consumption from the utility grid can be reduced. The binary variables of  $\epsilon_{GR \rightarrow LD}$  are converted from 1 to 0 in this instance. The  $SOAcc$  of the battery increases significantly during the MG operation (see Figure 3.14c) but does not go above the critical value (90%) due to the evolution operator  $\epsilon_{BAT \rightarrow LD}$ . For instance, the  $SOAcc$  of the battery is at the peak at the end of the 3rd day. In this case, the evolution operator of  $\epsilon_{BAT \rightarrow LD}$  is converted to AND. By doing that, the binary variables of  $\epsilon_{BAT \rightarrow LD}$  are turned from 1 to 0.

The building is simulated for 8760 hours (one year) and compared to the results of these methods ( $\epsilon$ -variables and the merged MPC- $\epsilon$ -variables). All these values of  $SOC$  work at desired

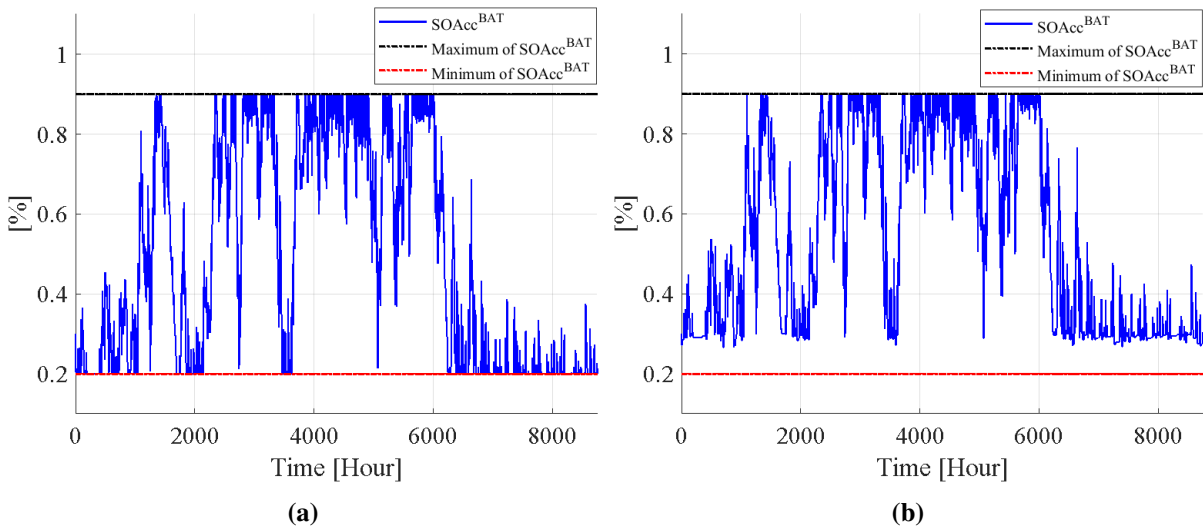


**Figure 3.15** The results of power flows and *SOC* of the battery using the MPC -  $\epsilon$ -variables

conditions; namely, it does not over-charging/over-discharging because of the constraints and evolution operator of an asset for the battery, as illustrated in Figure 3.15. To clarify, when the battery approaches over-charging, the binary variables of  $\epsilon_{BAT \rightarrow LD}$  are converted from 1 to 0. After that, the *SOC* value is increased or stabilized. On the other hand, supposing that the battery is getting close to over-charging, the logical gate of the  $\epsilon_{PV \rightarrow BAT}$  is turned from 1 to 0. By doing that, the value of  $\epsilon_{PV \rightarrow BAT}$  is started to decrease or be stable. It is noted that the standard MPC and merged MPC- $\epsilon$ -variables are the same results in terms of *SOC* of the battery and power flows. In brief, these desired conditions are assessed with constraints and evolution operators through the MPC and  $\epsilon$ -variables.

### 3.11. Conclusion

In conclusion, there are various reasons to use MPC to manage the MG power system. Using cost functions and constraints, the MPC is able to predict power generation and consumption as well as deal with uncertainty and disturbances. However, MPC implementation is not simple, particularly in complex MG systems. In addition, it requires a great deal of processing power and time. In this chapter, the  $\epsilon$ -variables have been combined with the MPC technique to address these issues. This hybrid method reduces the complexity of the MPC implementation and improves the scalability and controllability of the PBG system at any given time. The MPC- $\epsilon$ -variables technique simplifies the system's control, so to speak. In this chapter, we first demonstrated that the MPC and the MPC- $\epsilon$ -variables produce identical results. Then, as a case study, we demonstrated how the EMS could be easily modified without requiring MPC modifications.

The next chapter will explain several case studies to prove improved the MPC in terms of scalability and adaptability (flexibility) by merging  $\epsilon$ -variables. The proposed method is called "extended optimal  $\epsilon$ -variables". However, the main downside of  $\epsilon$ -variables is not being optimal. Therefore, the next chapter will illustrate how to overcome the downside of the  $\epsilon$ -variables. The

imported energy from the utility grid is decreased, whereas the exported energy to the RES (such as PV) is increased. In addition, the adaptability and scalability with the changes or modifications in the MG structure are significantly improved using the extended optimal  $\varepsilon$ -variables in the next chapter.



## Chapter 4. Energy Management of Grid-Connected Microgrids using an Optimal Systems Approach

### 4.1. Overview

MGs have emerged as a result of the increasing adoption of RESs to combat global warming, which has caused a significant shift in the topologies of traditional power networks. Localized power generation and distribution systems are a new paradigm for energy industry segments. However, controlling them can be difficult due to their complexity and the diverse properties of each asset in the MG. Various approaches have been proposed to address the control challenges of MGs, including the optimal operation of MG assets and systems-based approaches for synthesizing an MG's EMS. Systems-based approaches aim to simplify the control structure and enhance the adaptability and scalability of MG's EMS. In contrast, optimal operation methods aim to maximize the efficiency and dependability of each asset in the MG.  $\epsilon$ -variables-based logical control strategy is a promising systems-based approach. This method models control strategies in MGs and simplifies the control structure, enabling greater scalability and robustness. Nonetheless, control based on  $\epsilon$ -variables is not optimal and does not always provide the best solution.

On the other hand, S-MPC is a sophisticated method for controlling power systems that satisfy multiple constraints to achieve an optimal solution based on multiple criteria. However, implementing S-MPC can be computationally intensive and complex. To overcome the difficulties of implementing both  $\epsilon$ -variables based control and S-MPC, the extended optimal  $\epsilon$ -variable method is proposed in this chapter. This method combines  $\epsilon$ -variables based control with S-MPC to optimize the energy management of an MG and improve its adaptability and scalability.

The extended optimal  $\epsilon$ -variable method has shown significant improvements in optimizing the EMS of an MG. Our findings indicate that this method reduces the operational cost of an MG by nearly 35%, reduces the use of the BESS by 42%, and improves the viability of PV use by 28%. In addition, this method improves the adaptability and scalability of the MG's control structure by translating S-MPC results to the  $\epsilon$ -variable method. The extended optimal  $\epsilon$ -variable method is a promising approach for managing complex and diverse energy systems, as the conclusion demonstrates. The method increases the effectiveness and efficiency of MG control, making it an invaluable resource for the energy sector. This chapter provides a comprehensive overview of the development, implementation, and effectiveness of the extended optimal  $\epsilon$ -variable method in optimizing the energy management of MGs.

### 4.2. Introduction

PV and WT power generators are increasingly integrated into MGs due to their renewable and eco-friendly characteristics (Xu et al. (2019)). MG integrates diverse energy sources, such as RESs (PV panels, wind), ESSs (batteries, hydrogen, pumped hydro (water)), diesel generators, and load and control devices (Tobajas et al. (2022)). In addition, an MG can schedule DR programs in order to maintain a balance between generation and demand. DR programs have the capability of modifying customer load profiles (Kakran and Chanana (2018)). This capability increases the MGs' dependability and decreases their energy consumption. The MG is considered an advanced power network topology for these reasons (Cheng et al. (2018)).

However, an MG faces additional controllability challenges due to abrupt power fluctuations during real-time operation, intermittent energy production, and irregular energy consumption (Hu et al. (2021); Yoldas et al. (2022)). To properly manage the power flow between the main grid and MGs, (i) the scalability and (ii) the optimal operation of MG assets with increases in the complexity of control frames (Ghasemi et al. (2023)) are the most significant challenges. Consequently, a practical method is required to ensure efficient energy management. In contrast, a new method for systematically modelling EMSs based on evolution operators and the state of the directed graph representing the system was first proposed in Giaouris et al. (2015). This method is based on the so-called  $\varepsilon$ -variables that describe the evolution and, consequently, the control strategy of a multi-vector energy system (Giaouris et al. (2018)). A node represents each asset in the system, and an edge between the nodes defines each energy and/or matter flow.

Specifically, graph theory can be used to easily describe a hybrid energy system, as stated in Giaouris et al. (2018). In other words, energy systems can be depicted in a manner that simplifies their analysis, operation, and management with the aid of graph theory augmented by the evolution operators mentioned previously. The evolution operators describing the multi-vector system's EMS are the control statements that operate the converters (Giaouris et al. (2013)). The MG's scalability problem has been resolved using the  $\varepsilon$ -variables method. Nonetheless, this approach is not optimal.

Several optimization and control algorithms have been presented in Table 4.1 in order to optimize the operation of the MGs. Several authors have also employed stochastic dynamic programming and optimization algorithms (Aaslid et al. (2022); Alipour et al. (2022); Wang et al. (2022a); Zhu et al. (2021)). Using the Cuckoo Search (CS) algorithm and the GOA, the operation of renewable energy systems has been optimized to minimize the overall losses in the distribution network (Suresh and Edward (2020)). In Wang et al. (2022b), distributed proximal primal–dual (PD) was used to optimize a distributed energy management problem for responsive loads and distributed generators with transmission losses. To achieve optimal energy management with tolerable operational costs and GHG emissions, a PD-based distributed algorithm with dynamic weights is introduced. Moreover, the technique proposed has lower computational complexity than distributed optimization algorithms Liu and Yang (2022). The teaching learning-based optimization (TLBO) algorithm was used to solve a multi-objective optimization problem that reduced costs and enhanced the reliability of the MG. The findings demonstrated how charging

and discharging ESSs could reduce MG costs while improving system performance and reliability (Rahmani et al. (2023)). The simulation results presented in Zhang et al. (2016) demonstrate the efficiency of the master-slave (MS) peer-to-peer integration MG control method based on communication in achieving stable operation of the MG in grid-connected and islanded states, as well as smooth switching between these two modes. Multi-commodity flow (MCF) and Single-commodity flow (SCF) were employed to provide flexible and adaptable operations for MG generation. Regardless of the difficulty of the optimization problem, this study demonstrated that MCF-based formulations and enumeration formulations are typically less effective (Pang et al. (2022)). PSO has been incorporated for the optimal design of a hybrid renewable energy system (HRES), including PVs, WTs, and battery units while minimizing the system's overall cost (Mansouri Kouhestani et al. (2020)).

A novel extended optimal  $\varepsilon$ -variable technique is produced. With the help of this method:

- The operational cost of the MG is decreased.
- The practicality of renewable generator usage is encouraged.
- The adaptability and scalability with the changes in the MG structure are improved.

The scalability and adaptability of the MPC with optimal  $\varepsilon$ -variable in response to changes in the MG structure can be attributed to several key features and methodologies. Here are some aspects that contribute to its scalability and adaptability:

**Scalability:**

1. **Ease of Integration with New Components:** The optimal  $\varepsilon$ -variable MPC is designed to integrate new components into the MG easily. This includes renewable energy sources, storage systems, or other elements. The control strategy can adapt to changes in the MG's topology without requiring extensive reconfiguration.
2. **Flexible Control Horizons:** The predictive nature of MPC allows for flexibility in control horizons. This flexibility is valuable when adding or removing components from the MG. The control horizon can be adjusted to seamlessly accommodate the characteristics and dynamics of new elements.
3. **Modular Design:** The modular control architecture allows for adding or replacing modules corresponding to different MG components. This modularity ensures the control system can scale with the MG's growth or changes.
4. **Parameter Adaptability:** The MPC's parameters, including the prediction horizon and other optimization settings, can be adjusted to suit the scale of the MG. This adaptability is crucial when expanding or modifying the MG infrastructure.

**Adaptability:**

Optimization method	Scalable	Reliable	Adaptable	Optimal	ImPLY	Ref.
$\epsilon$ -variable	Outstanding	Poor	Outstanding	No	Easy	Giaouris et al. (2018)
MCF	Poor	Good	Good	Yes	Easy	Ahmadi and Martí (2015); Borghetti (2012); Pang et al. (2022)
SCF	Poor	Good	Good	Yes	Easy	Chen et al. (2015); Ding et al. (2017)
PD	Good	Good	Good	Yes	Complex	Liu and Yang (2022); Wang et al. (2022b)
MS	Poor	Poor	Good	Yes	Complex	Delghavi and Yazdani (2017); Zhang et al. (2016); Zheng and Weiye (2021)
PSO	Poor	Poor	Poor	Yes	Complex	Mansouri Kouhestani et al. (2020)
GOA	Poor	Good	Good	Yes	Complex	Fossati et al. (2015); Hakimi et al. (2019); Suresh and Edward (2020)
TLBO	Poor	Outstanding	Outstanding	Yes	Moderate	Rahmani et al. (2023)
MPC	Outstanding	Poor	Outstanding	Yes	Complex	Hu et al. (2021); Su et al. (2014); Villalón et al. (2020)
Extended optimal $\epsilon$ -variable	Outstanding	Outstanding	Outstanding	Yes	Easy	Cavus et al. (2023)

**Table 4.1** The Comparison of Optimization Methods

1. **Dynamic Model Updating:** The MPC with optimal  $\epsilon$ -variable employs a dynamic model that can be updated to reflect changes in the MG’s structure. This adaptability ensures that the control system continues to make accurate predictions and optimal decisions, even with modifications to the system.
2. **Scenario-Based Optimization:** The  $\epsilon$ -variable method allows for the consideration of multiple scenarios or operating modes. As the microgrid structure changes, the MPC can select the most appropriate scenario, adapting its control strategy accordingly.

3. **Real-Time Monitoring and Feedback:** Real-time monitoring of the MG's performance allows the MPC to receive feedback on the effectiveness of its control decisions. This feedback loop enables adaptive adjustments in response to changes or unexpected events.

S-MPC, on the other hand, is an innovative and more effective control strategy than conventional control strategies. In addition, S-MPC has a rapid transient response (Hu et al. (2021)) because its primary function is to incorporate newly updated data and forecasts. By doing so, the S-MPC is able to make better decisions regarding the future behaviour of the system using various constraints (Su et al. (2014); Ulutas et al. (2020); Wang (2009)). In addition, S-MPC can be utilized in multiple ways to control the MG system more effectively than other control strategies. For instance, S-MPC is straightforward and intuitive to comprehend. It operates by considering multiple constraints and uncertainties (Villalón et al. (2020)). However, it is difficult to implement and modify if the structure of the MG has changed due to a sudden change in the MG during operation.

As shown in Table 4.1, although these optimization strategies are optimal, some of them are neither scalable nor simple. This chapter employs an innovative methodology to produce a more systematic method for bridging the gap between the simplicity of implementation, scalability, and optimal operation of the MG. The approach implements the combination of the  $\epsilon$ -variable method and S-MPC, retaining the benefits of the  $\epsilon$ -variable method while making it more effective and robust by incorporating S-MPC.

The rest of the chapter are organized as follows: Section 4.3 presents the implementation of S-MPC with Finite-horizon Linear Quadratic regulator (LQR) in the compact formulation. In Section 4.4, the methodology for developing an optimal systems-based EMS for the MG is outlined. Section 4.5 describes the MG utilized in this study and explains the steps required to implement the optimal method proposed. In Section 4.6, the simulation results of the proposed EMS are discussed. Section 4.7 concludes with a summary of the conclusions.

1. **Reduction in Operational Energy Cost:** For instance, consider the operational energy cost of the MG with the traditional method as 200 kWh. After implementing MPC with optimal  $\epsilon$ -variables, the cost is reduced to 150 kWh. This 25% reduction signifies improved cost-effectiveness in managing the MG.
2. **Improved Battery Energy Storage System (BESS) Utilization:** Suppose the BESS previously operated at 100 kWh without the proposed methodology. After implementing MPC with optimal  $\epsilon$ -variables, the BESS usage is reduced to 58 kWh. This 42% decrease indicates more efficient utilization of the energy storage system, leading to potential cost savings and enhanced system performance.
3. **Cost Reduction Summary:** By integrating MPC with optimal  $\epsilon$ -variables, the thesis demonstrates a comprehensive cost reduction strategy. The 25% decrease in operational energy cost, the 42% reduction in BESS usage, and the 28% improvement in PV utilization collectively contribute to a more economical and sustainable MG operation.

4. **Energy Utilization Improvement Summary:** The improvements in BESS and PV utilization contribute to a more efficient and sustainable energy management system. The 42% decrease in BESS usage indicates better storage system efficiency, while the 28% increase in PV usage highlights enhanced harnessing of RESs. Together, these improvements signify a more optimized and sustainable energy utilization strategy for the MG.

### 4.3. General Information for the Implementation of S-MPC with Finite-horizon LQR in Compact Formulation

The constraints set of the states and control vectors can be represented by the set of  $\mathbb{X}$  and  $\mathbb{U}$  as follows (usually characterized by linear inequalities):

$$\mathbb{X} = x \in \mathbb{R}^n : a_x x \leq b_x \quad (4.1)$$

$$\mathbb{U} = u \in \mathbb{R}^m : a_u u \leq b_u \quad (4.2)$$

It is noted that  $\mathbb{R}$  is the set of real numbers;  $\mathbb{R}^n$  and  $\mathbb{R}^{m \times n}$  symbolize n-dimensional Euclidean space and the space of  $m \times n$  real matrices.  $a_x$  and  $b_x$  are vectors or matrices that represent coefficients for the linear inequalities constraining the state vector  $x(k)$ .  $a_u$  and  $b_u$  are vectors or matrices that define the right-hand side of the linear inequalities for the control vector  $u(k)$ .

The cost function (objective function) is selected as a quadratic sum of the system states and system-control inputs:

$$J = x(T_H)^T Q(T_H) x(T_H) + \sum_{k=0}^{T_H-1} x(k)^T Q x(k) + u(k)^T R u \quad (4.3)$$

where  $Q(T_H) \in \mathbb{R}^{n \times n}$  and  $Q \in \mathbb{R}^{n \times n}$ , are the weighting matrices exploited for weighting the states;  $R \in \mathbb{R}^{m \times m}$ , is another weighting matrix utilized for weighting control inputs. In Eq. (4.3),  $R$  and  $Q$  symbolize the input penalty symmetric matrix and the state penalty symmetric matrix, respectively. Furthermore,  $Q(T_H)$  represents the terminal predictive state in order to obtain the final response of the system.

The system-state and system-control sequences are stated as follows:

$$\begin{aligned} \mathbf{X} &= (x(0), x(1), x(2), \dots, x(T_H)) & \mathbf{X} &\in \mathbb{X}^{T_H+1} \\ \mathbf{U} &= (u(0), u(1), u(2), \dots, u(T_H)) & \mathbf{U} &\in \mathbb{U}^{T_H+1} \end{aligned}$$

To minimise the cost function, S-MPC computes the control sequence for the next  $N_p$  instants. It is worth noting that a prediction horizon  $N_p$  should be smaller than or equal to the time horizon  $T_H$ . The cost function with a  $N_p$  at time instant  $k$  can be stated as:

$$J = x(k + N_p | k)^T Q(k + N_p | k) x(T_H) + \sum_{i=k}^{k+N_p-1} x(i | k)^T Q x(i | k) + u(i | k)^T R u(i | k) \quad (4.4)$$

### 4.3 General Information for the Implementation of S-MPC with Finite-horizon LQR in Compact Formulation

where  $x(i|k)$  and  $u(i|k)$  represent the state and control input at time  $i$  predicted at time instant  $k$ .  $k$  are the time instants within the time horizon  $T_H$ ;  $i$  are the time instants within the prediction horizon  $N_P$ .

Similarly, the system-state and system-control sequence for the S-MPC at time instant  $k$  can be defined as:

$$\begin{aligned}\mathbf{X} &= (x(k|k), x(k+1|k), x(k+2|k), \dots, x(k+N_P|k)) \\ \mathbf{U} &= (u(k|k), u(k+1|k), u(k+2|k), \dots, u(k+N_P-1|k))\end{aligned}$$

Then, the S-MPC problem for the linear system Eq. (4.1) with the current state  $x(k|k) = x(k)$  given, compute the system-control sequence  $\mathbf{U}(k)$ , by solving the optimization problem:

$$\begin{aligned}\mathbf{U}(k) &\in \mathbb{U}^{N_P} & \mathbf{X}(k) &\in \mathbb{X}^{N_P+1} \\ x(i+1|k) &= Ax(i|k) + Bu(i|k) & i &= k, \dots, k+N_P-1\end{aligned}$$

From the solution of the state equation for the discrete-time linear state-space system:

$$\begin{bmatrix} x(k|k) \\ x(k+1|k) \\ x(k+2|k) \\ \vdots \\ x(k+N_P|k) \end{bmatrix} = \begin{bmatrix} I \\ A \\ A^2 \\ \vdots \\ A^{N_P} \end{bmatrix} x(k) + \begin{bmatrix} 0 & 0 & \dots & 0 \\ B & 0 & \dots & 0 \\ AB & B & \dots & \vdots \\ \vdots & \vdots & \ddots & 0 \\ A^{N_P-1}B & A^{N_P-2}B & \dots & B \end{bmatrix} \begin{bmatrix} u(k|k) \\ u(k+1|k) \\ u(k+2|k) \\ \vdots \\ u(k+N_P-1|k) \end{bmatrix} \quad (4.5)$$

By defining the following matrices:

$$\mathbf{X}(k) = \begin{bmatrix} x(k|k) \\ x(k+1|k) \\ x(k+2|k) \\ \vdots \\ x(k+N_P|k) \end{bmatrix}; \quad \mathbf{U}(k) = \begin{bmatrix} u(k|k) \\ u(k+1|k) \\ u(k+2|k) \\ \vdots \\ u(k+N_P-1|k) \end{bmatrix}; \quad \mathbf{A}_x = \begin{bmatrix} I \\ A \\ A^2 \\ \vdots \\ A^{N_P} \end{bmatrix}; \quad \mathbf{B}_u = \begin{bmatrix} 0 & 0 & \dots & 0 \\ B & 0 & \dots & 0 \\ AB & B & \dots & \vdots \\ \vdots & \vdots & \ddots & 0 \\ A^{N_P-1}B & A^{N_P-2}B & \dots & B \end{bmatrix}$$

The equation (4.59) is re-written as:

$$\mathbf{X}(k) = \mathbf{A}_x x(k) + \mathbf{B}_u \mathbf{U}(k) \quad (4.6)$$

The predicted state  $\mathbf{X}(k)$  can be considered as a function of the current state  $x(k)$  and control sequence  $\mathbf{U}(k)$ . Similarly, by defining:

$$Q_x = \begin{bmatrix} Q & 0 & \cdots & 0 \\ 0 & Q & \cdots & 0 \\ 0 & 0 & \cdots & \vdots \\ \vdots & \vdots & \ddots & 0 \\ 0 & 0 & \cdots & Q_{N_P}; \end{bmatrix} \quad R_u = \begin{bmatrix} R & 0 & \cdots & 0 \\ 0 & R & \cdots & 0 \\ 0 & 0 & \cdots & \vdots \\ \vdots & \vdots & \ddots & 0 \\ 0 & 0 & \cdots & R_{N_P} \end{bmatrix} \quad (4.7)$$

Then, the cost function (4.4) can be stated using  $\mathbf{X}(k)$  and  $\mathbf{U}(k)$  as

$$J(k) = \mathbf{X}(k)^T Q_x \mathbf{X}(k) + \mathbf{U}(k)^T R_u \mathbf{U}(k) \quad (4.8)$$

Finally, by defining:

$$a_X = \begin{bmatrix} a_x & 0 & \cdots & 0 \\ 0 & a_x & \cdots & 0 \\ 0 & 0 & \cdots & \vdots \\ \vdots & \vdots & \ddots & 0 \\ 0 & 0 & \cdots & a_x; \end{bmatrix} \quad b_X = \begin{bmatrix} b_x & 0 & \cdots & 0 \\ 0 & b_x & \cdots & 0 \\ 0 & 0 & \cdots & \vdots \\ \vdots & \vdots & \ddots & 0 \\ 0 & 0 & \cdots & b_x; \end{bmatrix} \quad a_U = \begin{bmatrix} a_u & 0 & \cdots & 0 \\ 0 & a_u & \cdots & 0 \\ 0 & 0 & \cdots & \vdots \\ \vdots & \vdots & \ddots & 0 \\ 0 & 0 & \cdots & a_u; \end{bmatrix} \quad b_U = \begin{bmatrix} b_u & 0 & \cdots & 0 \\ 0 & b_u & \cdots & 0 \\ 0 & 0 & \cdots & \vdots \\ \vdots & \vdots & \ddots & 0 \\ 0 & 0 & \cdots & b_u; \end{bmatrix} \quad (4.9)$$

The system-state and system-control constraints in (4.1) and (4.2) can be demonstrated in terms of  $\mathbf{X}(k)$  and  $\mathbf{U}(k)$  as:

$$a_X \mathbf{X}(k) \leq b_X \quad (4.10)$$

$$a_U \mathbf{U}(k) \leq b_U \quad (4.11)$$

By combining  $\mathbf{X}(k)$  and  $\mathbf{U}(k)$ , the cost function with a single decision vector will be:

$$z = \begin{bmatrix} \mathbf{X}(k) \\ \mathbf{U}(k) \end{bmatrix}; H = \begin{bmatrix} Q_x & 0 \\ 0 & R_u \end{bmatrix}; a = \begin{bmatrix} a_X & 0 \\ 0 & a_U \end{bmatrix}; b = \begin{bmatrix} b_X \\ b_U \end{bmatrix} \quad (4.12)$$

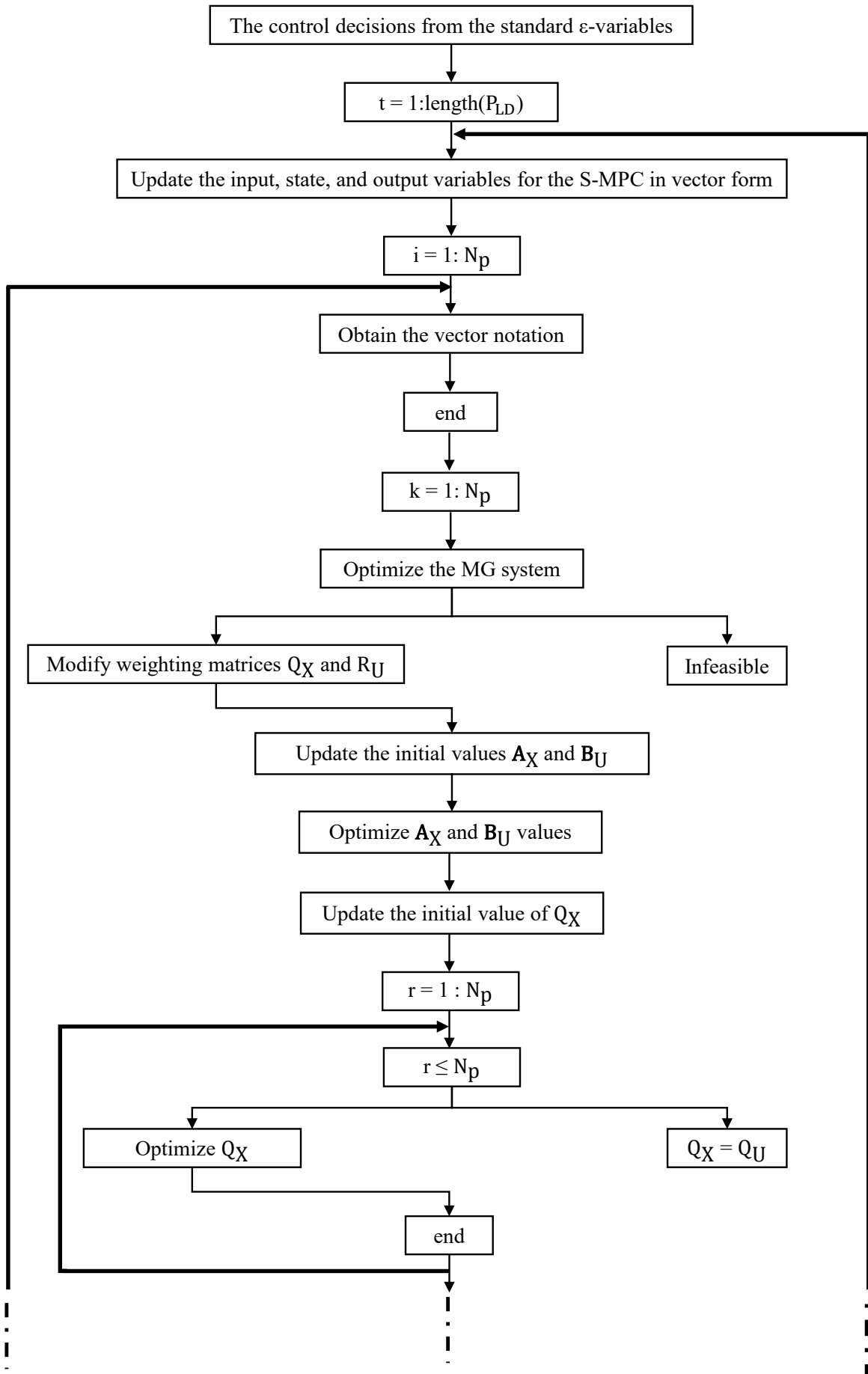
The cost function (4.8), and constraints (4.6), (4.10), and (4.11), and optimization problem can be re-written as a quadratic problem as below:

$$\min z^T H z \quad \text{subject to} \quad a z \leq b \quad (4.13)$$

In S-MPC, this optimization problem is solved during each time instant  $k$  and the first element of  $U(k)^*$  is applied to the system, i.e., the control input with S-MPC is:

$$u(k) = [U(k)^*](1) = u(k|k)^* \quad (4.14)$$

### 4.3 General Information for the Implementation of S-MPC with Finite-horizon LQR in Compact Formulation



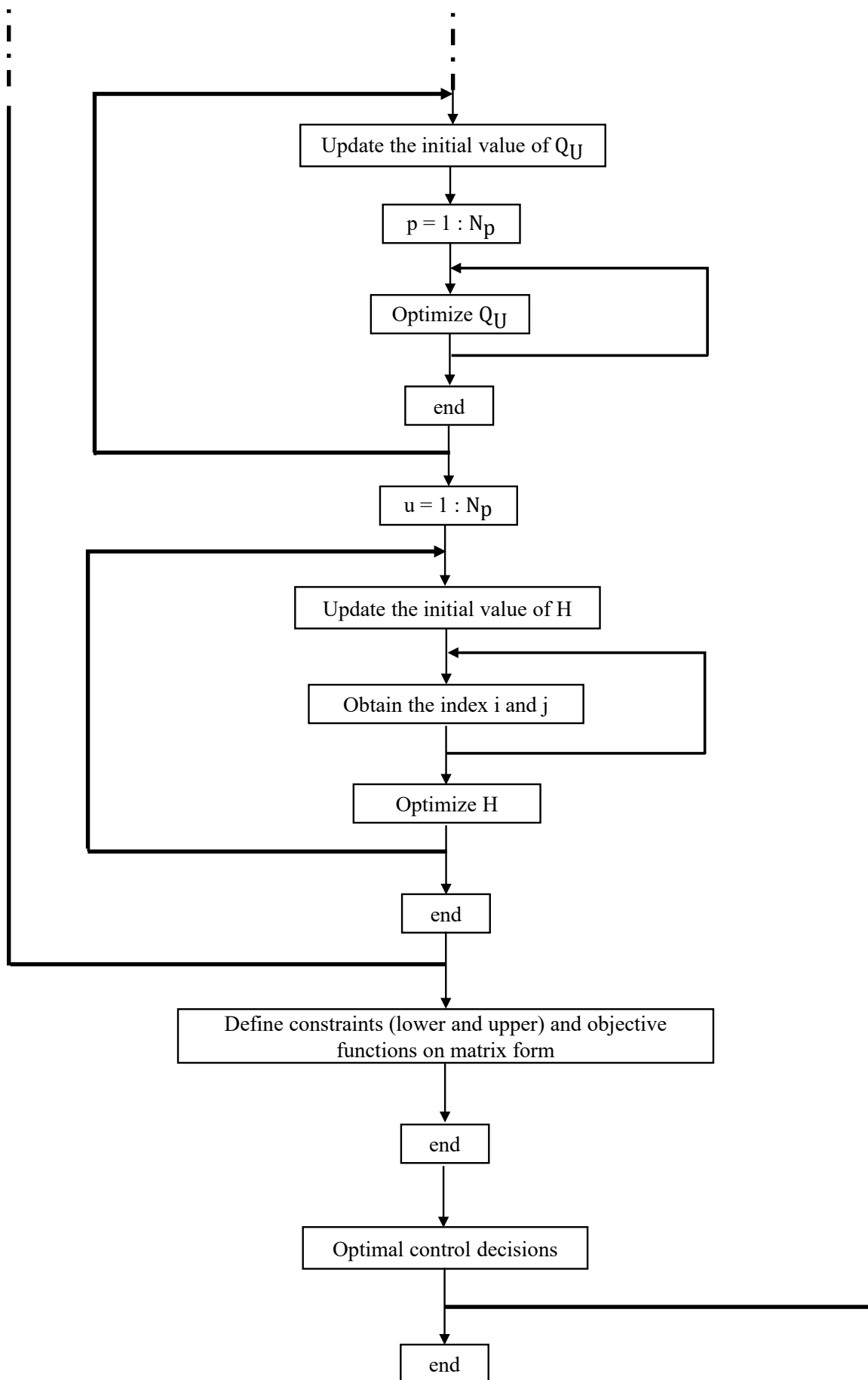


Figure 4.1 The flowchart of the implementation of MPC in a compact form

4.4. Methodology of building optimal systems-based EMS of a MG

As depicted in Figure 4.2, the method for constructing MG’s EMS consists of three primary steps. In the initial phase, the EMS will be constructed using a system approach based on the MG’s specifications and operational constraints. The  $\epsilon$ -variables method (Cavus et al. (2022b); Giaouris et al. (2018)) is the system approach utilized in this chapter. The output of the initial step is an EMS that is not optimal. In the second step, the obtained EMS will be used as input to generate the equivalent mathematical problem to meet optimally the objective(s) specified by the MG operators, taking into account the operational condition already incorporated into the obtained EMS in Step 1. The optimal problem will be expressed in S-MPC format. After determining the optimal decisions in Step 2, these will be incorporated into the  $\epsilon$ -variables-based EMS in Step 3. Therefore, the output of Step 3 is the extended optimal  $\epsilon$ -variables-based EMS. At the beginning of each time step during the operational phase of the EMS, the MG specification and inputs from the MG operator will be verified. If this information has changed, the operational states of the MG assets will be updated, and the three steps of EMS construction will be repeated to account for the new information. If not, the extended optimal  $\epsilon$ -variables-based EMS is utilized to control the MG for the subsequent time step. Notably, the proposed method determines if the system specifications/inputs of the MG operator have changed for the subsequent time step.

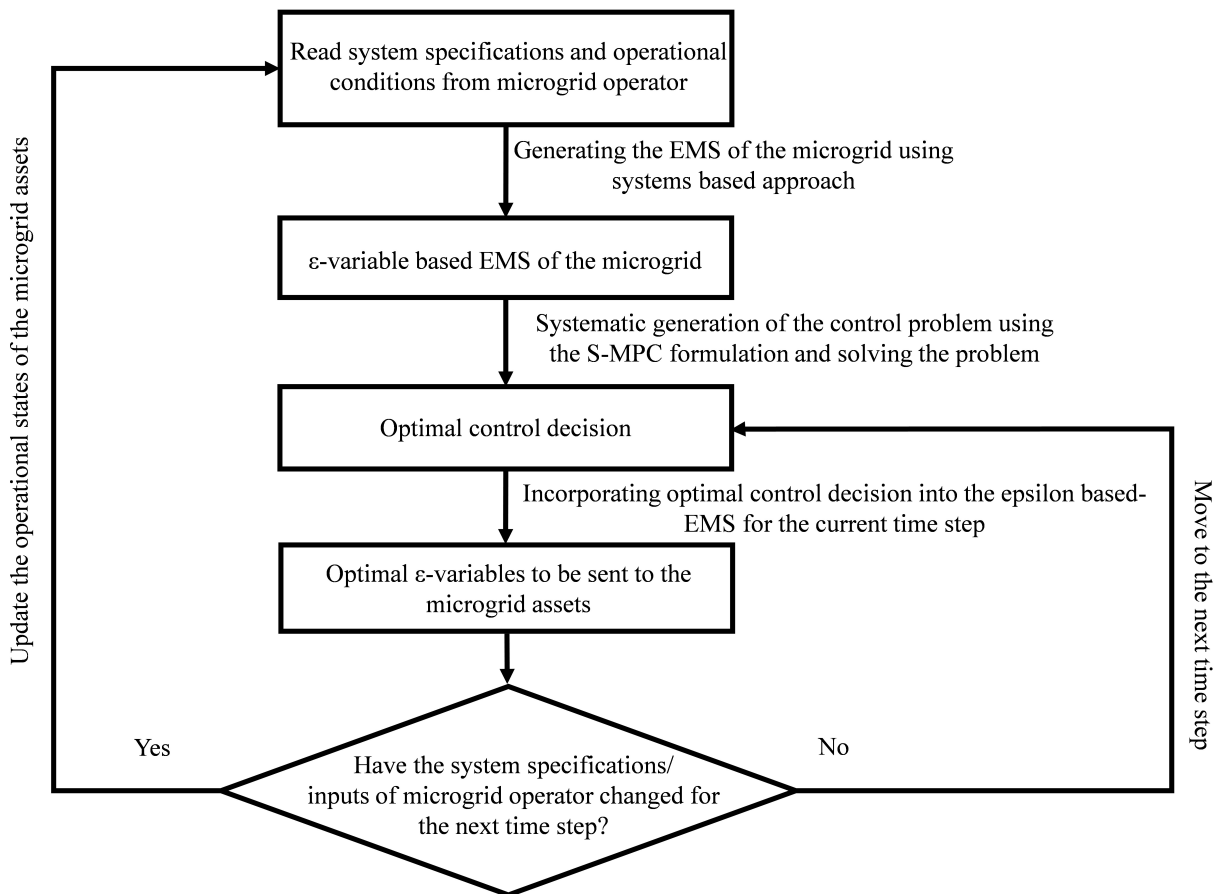


Figure 4.2 Flow chart of the optimal system based on EMS.

#### 4.5. The building optimal system based EMS

This section describes the three steps to construct the optimal systems-based EMS using the simple MG. The MG system includes a 14 kW PV array, 20 kWh of battery storage (Sökmen and Çavuş (2017)), a 5.4 kW diesel generator, and the utility grid, as depicted in Figure 4.3.

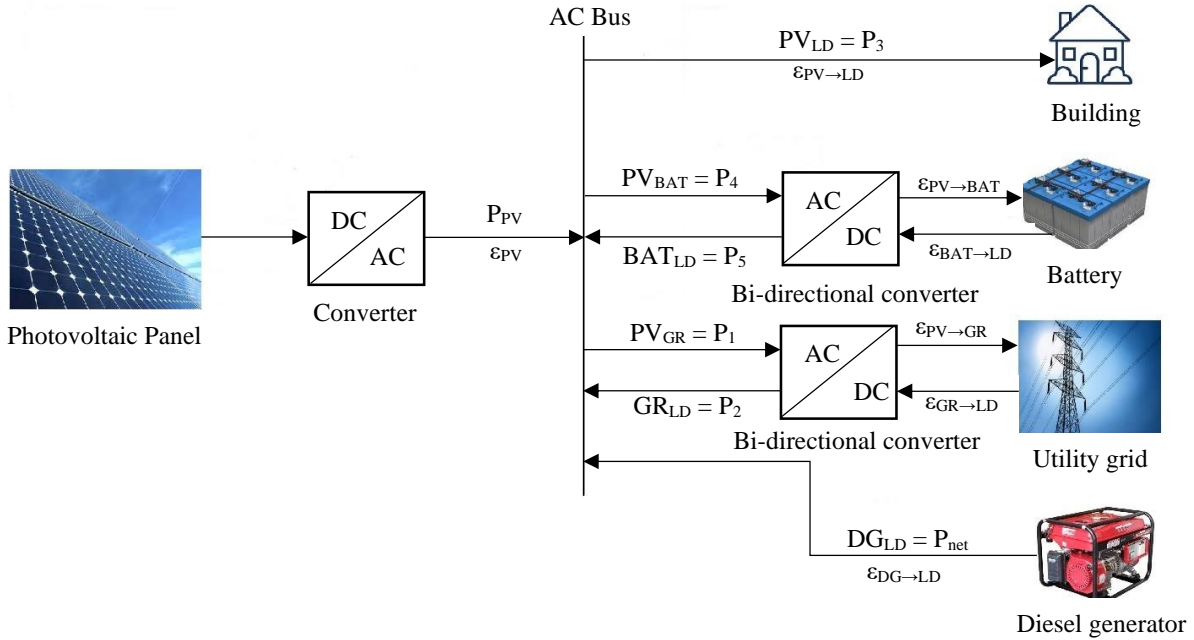


Figure 4.3 Conceptual microgrid structure proposed in this work.

##### 4.5.1. A. Step 1: Building the EMS using $\varepsilon$ -variables

The power flow is computed by multiplying  $P_{net}$  by Eq. (3.56).

$$F_{PV \rightarrow GR}^{Power}(k) = P_{net}(k) \varepsilon_{PV \rightarrow GR}(k) \quad (4.15)$$

$$F_{GR \rightarrow LD}^{Power}(k) = P_{net}(k) \varepsilon_{GR \rightarrow LD}(k) \quad (4.16)$$

$$F_{PV \rightarrow LD}^{Power}(k) = P_{net}(k) \varepsilon_{PV \rightarrow LD}(k) \quad (4.17)$$

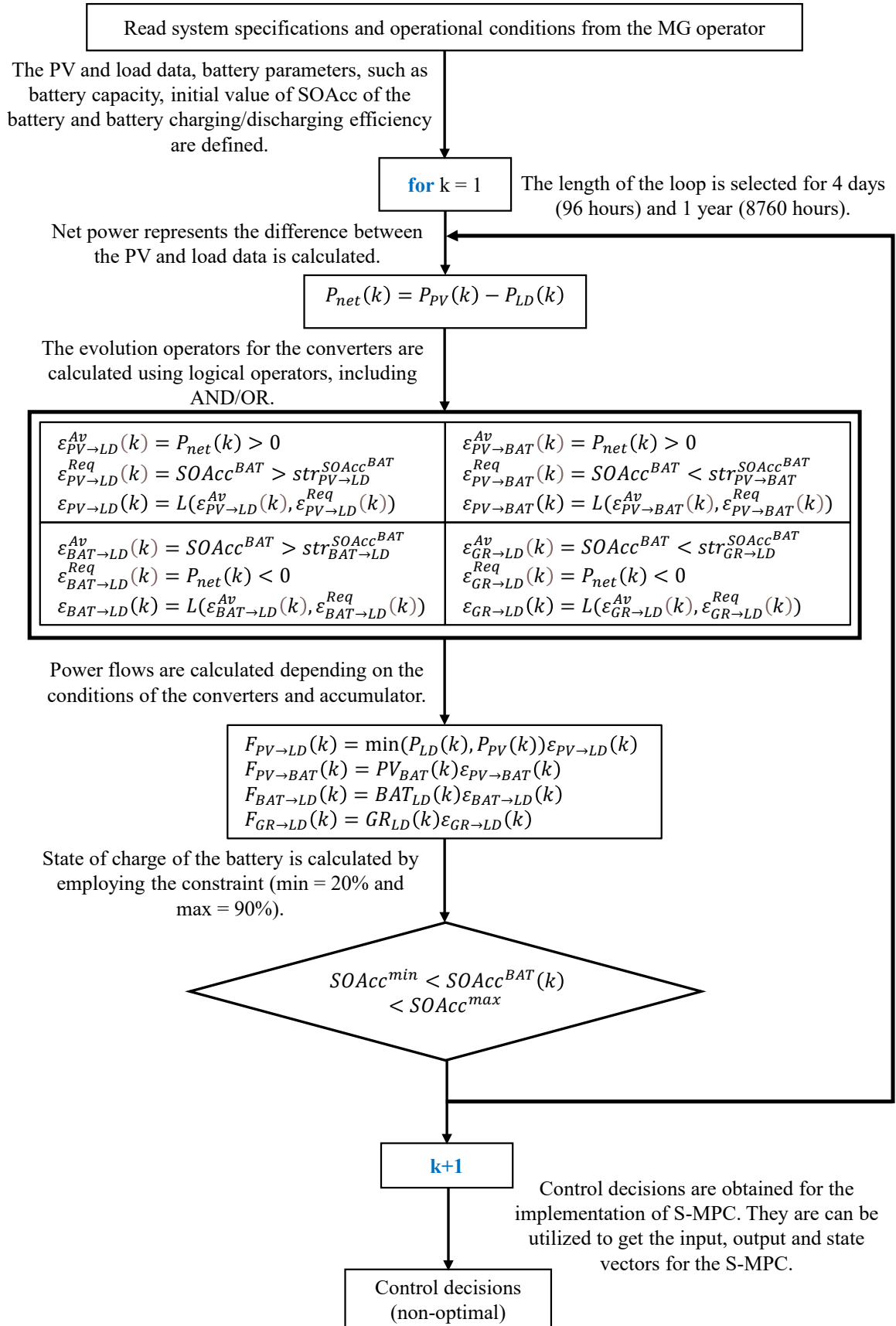
$$F_{PV \rightarrow BAT}^{Power}(k) = P_{net}(k) \varepsilon_{PV \rightarrow BAT}(k) \quad (4.18)$$

$$F_{BAT \rightarrow LD}^{Power}(k) = P_{net}(k) \varepsilon_{BAT \rightarrow LD}(k) \quad (4.19)$$

$$F_{DG \rightarrow LD}^{Power}(k) = P_{net}(k) \varepsilon_{DG \rightarrow LD}(k) \quad (4.20)$$

In these equations mentioned above, we did not consider the power flow between GR to BAT ( $GR_{BAT}$ ) or BAT to GR ( $BAT_{GR}$ ). The constraints related to grid charging and discharging batteries can be defined. By doing so, pricing (running cost) can be changed. Considering constraints for charging batteries using the grid, especially in the event of negative pricing, involves careful management of power flows and pricing dynamics. Here are some key considerations:

1. Charging Constraints during Negative Pricing: Implementing constraints for charging batteries during negative pricing is a strategic approach. The MG can take advantage


 Figure 4.4 Flow chart for the standard  $\varepsilon$ -variables

of low or negative pricing by allowing charging during these periods, optimizing energy costs.

2. **Bidirectional Power Flow Constraints:** Constraints should be defined for bidirectional power flows between the grid and the battery (both charging and discharging). This includes defining charging rate limits when the MG imports electricity from the grid.
3. **Dynamic Pricing Impact:** The pricing structure and constraints should reflect the impact of charging on the overall running cost. During negative pricing, the MG may maximize charging to store energy for future use, considering the potential economic benefits.
4. **Grid Stability and Congestion Management:** While maximizing charging during negative pricing can be economically beneficial, it's crucial to consider grid stability and potential congestion issues. Charging constraints should prevent excessive power flows that may impact grid reliability.

The final step is to compute the accumulator's evolution operator:

$$SOAcc^{BAT}(k+1) = SOAcc^{BAT}(k) + \frac{(char-dis)\Delta t}{C_i} \quad (4.21)$$

#### **4.5.2. B. Step 2: Systematic Generation of the Extended Optimal Control Problem Using S-MPC Formulation**

The S-MPC method is implemented subsequent to the  $\varepsilon$ -variables method. Before the S-MPC is implemented, the system-state, system-input, and system-output vectors are defined. Let's start by discussing the definition of the discrete-time linear state-space system using Equation (3.30) (see  $x(k+1) = Ax(k) + Bu(k)$  (Zhu et al. (2014)).  $k = 0, 1, 2, \dots, T_H - 1$  is the discrete-time instant, and  $x(k) \in \mathbb{X} \subseteq \mathbb{R}^n$  and  $u(k) \in \mathbb{U} \subseteq \mathbb{R}^m$  are the state and control vector, respectively.  $A \in \mathbb{R}^{n \times n}$  is the state-system matrix and  $B \in \mathbb{R}^{n \times m}$  is the input-system matrix.

For the MG, system-control (input) vectors are energy consumption from the grid  $GR_{LD}, (P_2(k))$ ; power flow from the PV to the load  $PV_{LD}, (P_3(k))$ ; PV to the battery (charging)  $PV_{BAT}, (P_4(k))$ ; battery to the load (discharging)  $BAT_{LD}, (P_5(k))$ . On the other hand, the system-output vectors are exported energy from PV to the grid  $PV_{GR}, (P_1(k))$ ; the battery exploitation (charging and discharging situation)  $PV_{BAT} + BAT_{LD}, (P_4(k) + P_5(k))$ , and the practical utilization of PV,  $PV_{LD} + PV_{BAT}, (P_3(k) + P_4(k))$ .

The hybrid power system's system-state vector and system-control vector can be expressed as follows:

$$x_a(k) = SOC(k) \quad (4.22)$$

$$u(k) = [P_2(k); P_3(k); P_4(k); P_5(k)] \quad (4.23)$$

$$u(k) = [GR_{LD}(k); PV_{LD}(k); PV_{BAT}(k); BAT_{LD}(k)] \quad (4.24)$$

where subscription "a" in the equations represents a matrix assumed to have dimension  $m_1$ . The following elements define the battery's dynamic process:

$$\begin{aligned} x_a(k) &= x_a(k-1) + b_a u(k-1) \\ \Delta x_a(k) &= b_a u(k-1) \end{aligned} \quad (4.25)$$

where  $b_a = [0 \ 0 \ \eta_{ch} \ \eta_{dis}]$ . Define the system-output vectors  $y_a$ ,  $y_b$  and  $y_c$ :

$$y_a(k) = c_a x_a(k-1) + d_a u(k) \quad (4.26)$$

where  $c_a = 0$  and  $d_a = [w_1 \ w_1 \ 0 \ w_1]$ . From the definition of  $y_a$ ;

$$\sum w_1^2 P_2^2(k) = \sum (w_1 P_{LD}(k) - y_a(k))^2 \quad (4.27)$$

With respect to  $y_b$ ;

$$y_b(k) = w_3(P_3(k) + P_4(k)) = c_b x_a(k-1) + d_b u(k) \quad (4.28)$$

where  $c_b = 0$  and  $d_b = [0 \ w_3 \ w_3 \ 0]$ . To encourage the practicality of PV utilization, the definition of  $y_b$ ;

$$\sum (w_3 P_{PV}(k) - y_b(k))^2 \quad (4.29)$$

Regarding  $y_c$ ,

$$y_c(k) = w_2(P_4(k) + P_5(k)) = c_c x_a(k-1) + d_c u(k) \quad (4.30)$$

where  $c_c = 0$  and  $d_c = [0 \ 0 \ w_2 \ w_2]$ . To increase the life cycle of the battery, the definition of  $y_c = 0$ ;

$$\sum y_c(k)^2 \quad (4.31)$$

Finally, the augmented system-state and the system output of the hybrid power system will be:

$$x(k) = [x_a(k) \ y_a(k-1) \ y_b(k-1) \ y_c(k-1)]^T \quad (4.32)$$

$$y(k) = [y_a(k-1) \ y_b(k-1) \ y_c(k-1)]^T \quad (4.33)$$

The linear state-space can be defined according to the battery (4.33). In general, the linear state-space (3.30) can be represented as follows:

$$SOC(k+1) = SOC(k) + \frac{\eta_{ch} P_4(k) \Delta t}{C_l} - \frac{P_5(k) \Delta t}{C_l (\eta_{dis})} \quad (4.34)$$

Because of the dynamic equation of  $SOC$  in (4.34),  $A$  and  $B$  in (3.41) will be:

$$A = \begin{bmatrix} 1 & 0 & 0 & 0 \\ 0 & 0 & 0 & 0 \\ 0 & 0 & 0 & 0 \\ 0 & 0 & 0 & 0 \end{bmatrix} \quad B = \begin{bmatrix} 0 & 0 & \eta_{ch} & -\eta_{dis} \\ w_1 & w_1 & 0 & w_1 \\ 0 & w_3 & w_3 & 0 \\ 0 & 0 & w_2 & w_2 \end{bmatrix} \quad (4.35)$$

### ***The Inequalities Constraints of the MG***

The PV system supplies the load demand and charges the battery. It operates based on several types of constraints at sampling time  $k$ , as follows:

$$0 \leq P_{PV}(k) \leq P_{PV}^{max} \quad (4.36)$$

$$0 \leq PV_{GR}(k) \leq PV_{GR}^{max} \quad (4.37)$$

$$0 \leq PV_{LD}(k) \leq PV_{LD}^{max} \quad (4.38)$$

$$0 \leq PV_{BAT}(k) \leq PV_{BAT}^{max} \quad (4.39)$$

Additionally, the total energy required to meet the load demand and charge the battery must be equal to or less than  $P_{PV}$  as below:

$$P_{PV}(k) \geq PV_{LD}(k) + PV_{BAT}(k) \quad (4.40)$$

Also, constraints associated with the battery are depicted below:

$$SOC^{min} \leq SOC(k) \leq SOC^{max} \quad (4.41)$$

$$0 \leq BAT_{LD}(k) \leq BAT_{LD}^{max} \quad (4.42)$$

The utility grid is utilised when solar panels and batteries are insufficient to meet load requirements. This is the last option, as it is more expensive and detrimental to the environment. The only benefit of exploiting this resource is that it is always available, except for blackouts.

Furthermore, the constraints associated with the grid system and load can be expressed as follows:

$$0 \leq GR_{LD}(k) \leq GR_{LD}^{max} \quad (4.43)$$

$$PV_{LD}(k) + BAT_{LD}(k) + GR_{LD}(k) = P_{LD}(k) \quad (4.44)$$

### ***Objectives Functions of the MG***

The cost functions of the MG consist of three components:

- To minimize the energy consumption from non-RES:

$$\sum_k^{k+N_p} w_1^2 GR_{LD}(k)^2 \quad (4.45)$$

- To increase the life cycle of the battery:

$$\sum_k^{k+N_p} w_2^2 (PV_{BAT}(k)^2 + BAT_{LD}(k)^2) \quad (4.46)$$

- To encourage the exported energy to the utility grid:

$$\sum_k^{k+N_p} w_3^2 (PV_{LD}(k)^2 + PV_{BAT}(k)^2) \quad (4.47)$$

### *The Implementation of S-MPC Using Persistence of Excitation (PE)*

Undoubtedly, the battery cannot be simultaneously charged and discharged, so (4.48) can be written as follows (Zhu et al. (2014)):

$$PV_{BAT}(k)BAT_{LD}(k) = 0 \quad (4.48)$$

Contrary to the other constraints, constraint (4.48) is not convex. In order to accomplish convex optimization in S-MPC design, the system must be split into two cases. These are the charging situation ( $PV_{BAT}=0$ ) and discharging situation ( $BAT_{LD}=0$ ).

**Charging situation:** The constraint can be written as follows (Zhu et al. (2014)):

$$\begin{aligned} BAT_{LD}(k) &\leq 0 \\ BAT_{LD}(k) &\geq 0 \end{aligned} \quad (4.49)$$

Constraints (4.36), (4.37), (4.38), (4.39), (4.40), (4.42), (??), (4.43), and (4.49) can be expressed in a compact form by (Zhu et al. (2014)):

$$f_{ch}u(k) \leq \gamma_{ch} \quad (4.50)$$

where

$$f_{ch} = \begin{bmatrix} -1 & 0 & 0 & 0 \\ 0 & -1 & 0 & 0 \\ 0 & 0 & -1 & 0 \\ 0 & 0 & 0 & -1 \\ \mathbf{0} & \mathbf{0} & \mathbf{0} & \mathbf{1} \\ 1 & 1 & 0 & 1 \\ 0 & 1 & 1 & 0 \\ 1 & 0 & 0 & 0 \\ 0 & 1 & 0 & 0 \\ 0 & 0 & 1 & 0 \\ 0 & 0 & 0 & -1 \\ -1 & -1 & 0 & -1 \end{bmatrix}; \gamma_{ch} = \begin{bmatrix} 0 \\ 0 \\ 0 \\ 0 \\ \mathbf{0} \\ P_{LD}(k) \\ P_{PV}(k) \\ PV_{GR}^{max} \\ PV_{LD}^{max} \\ PV_{BAT}^{max} \\ BAT_{LD}^{max} \\ GR_{LD}(k) - P_{LD}(k) \end{bmatrix} \quad (4.51)$$

Equation (4.51) requires to be converted to matrix form with respect to  $U(k)$  and  $N_p$  by Zhu et al. (2014):

$$\bar{f}_{ch}U(k) \leq \bar{\gamma}_{ch} \quad (4.52)$$

where

$$\bar{f}_{ch} = \begin{bmatrix} f_{ch} & \cdots & 0 \\ \vdots & \ddots & \vdots \\ 0 & \cdots & f_{ch} \end{bmatrix}; \bar{\gamma}_{ch} = \begin{bmatrix} \gamma_{ch} \\ \vdots \\ \gamma_{ch} \end{bmatrix} \quad (4.53)$$

**Discharging situation:** The constraint can be written as follows (Zhu et al. (2014)):

$$\begin{aligned} PV_{BAT}(k) &\leq 0 \\ PV_{BAT}(k) &\geq 0 \end{aligned} \quad (4.54)$$

Constraints (4.36), (4.37), (4.38), (4.39), (4.40), (4.42), (??), (4.43), and (4.48) can be written in a compact form by (Zhu et al. (2014)):

$$f_{dis}u(k) \leq \gamma_{dis} \quad (4.55)$$

where

$$f_{dis} = \begin{bmatrix} -1 & 0 & 0 & 0 \\ 0 & -1 & 0 & 0 \\ 0 & 0 & -1 & 0 \\ 0 & 0 & 0 & -1 \\ \mathbf{0} & \mathbf{0} & \mathbf{1} & \mathbf{0} \\ 1 & 1 & 0 & 1 \\ 0 & 1 & 1 & 0 \\ 1 & 0 & 0 & 0 \\ 0 & 1 & 0 & 0 \\ 0 & 0 & 1 & 0 \\ 0 & 0 & 0 & -1 \\ -1 & -1 & 0 & -1 \end{bmatrix}; \gamma_{dis} = \begin{bmatrix} 0 \\ 0 \\ 0 \\ 0 \\ \mathbf{0} \\ P_{LD}(k) \\ P_{PV}(k) \\ PV_{GR}^{max} \\ PV_{LD}^{max} \\ PV_{BAT}^{max} \\ BAT_{LD}^{max} \\ GR_{LD}(k) - P_{LD}(k) \end{bmatrix} \quad (4.56)$$

Equation (4.56) requires to be converted to matrix form with respect to  $U(k)$  and  $N_p$  by (Zhu et al. (2014)):

$$\bar{f}_{dis}U(k) \leq \bar{\gamma}_{dis} \quad (4.57)$$

where

$$\bar{f}_{dis} = \begin{bmatrix} f_{dis} & \cdots & 0 \\ \vdots & \ddots & \vdots \\ 0 & \cdots & f_{dis} \end{bmatrix}; \bar{\gamma}_{dis} = \begin{bmatrix} \gamma_{dis} \\ \vdots \\ \gamma_{dis} \end{bmatrix} \quad (4.58)$$

#### 4.5.3. C. Step 3: Translating the Optimal Control Decisions of S-MPC to $\varepsilon$ -variables

The power flows are calculated by multiplying (4.24) and (3.56), and (4.33) and (3.56).

$$F_{PV \rightarrow LD}^{Power}(k) = u(2) \varepsilon_i(k) \quad (4.59)$$

$$F_{PV \rightarrow BAT}^{Power}(k) = u(3) \varepsilon_i(k) \quad (4.60)$$

$$F_{BAT \rightarrow LD}^{Power}(k) = u(4) \varepsilon_i(k) \quad (4.61)$$

$$F_{DG \rightarrow LD}^{Power}(k) = P_{net}(k) \varepsilon_i(k) \quad (4.62)$$

Then, another step is to estimate the evolution operator for the accumulator:

$$SOAcc^{BAT}(k+1) = SOAcc^{BAT}(k) + \frac{(F_{PV \rightarrow BAT}^{Power}(k) - F_{BAT \rightarrow LD}^{Power}(k))\Delta t}{Battery\ Capacity} \quad (4.63)$$

#### 4.5.4. Summary of the Building the Extended Optimal $\varepsilon$ -variables Method

As represented in Figure 4.4, the S-MPC technique uses as input data 'control decisions from the  $\varepsilon$ -variables method,' which are initially obtained using the  $\varepsilon$ -variables method. In Figure 4.5, the "control decisions" are  $PV_{GR}$ ,  $GR_{LD}$ ,  $PV_{LD}$ ,  $PV_{BAT}$ , and  $BAT_{LD}$ . Then, using "quadratic programming" in S-MPC, the input (control), output, and state variables of the hybrid power system are recalculated and optimized. It is imperative to note that charging and discharging cannot occur simultaneously. Therefore, the battery is subjected to persistent excitation. Finally, the  $SOC$  of the battery and "optimal control decisions" are determined and compared to "control decisions" derived using the  $\varepsilon$ -variables method. To be more specific:

In summary, as depicted in Figure 4.5, the extended optimal  $\varepsilon$ -variables technique is comprised of the following steps:

1. The system requirements and operational conditions are read from the MG operator.
2. The net energy (differences between the PV and load data) for 96 and 8760 hours is determined.
3. The evolution operators and power flows for PV, the battery, the load, and the utility grid are computed.
4. The  $SOAcc^{BAT}$  is estimated as the final step in the  $\varepsilon$ -variables.
5. The initial step of the extended optimal  $\varepsilon$ -variables technique is to evaluate the "control decisions" derived from the  $\varepsilon$ -variables.

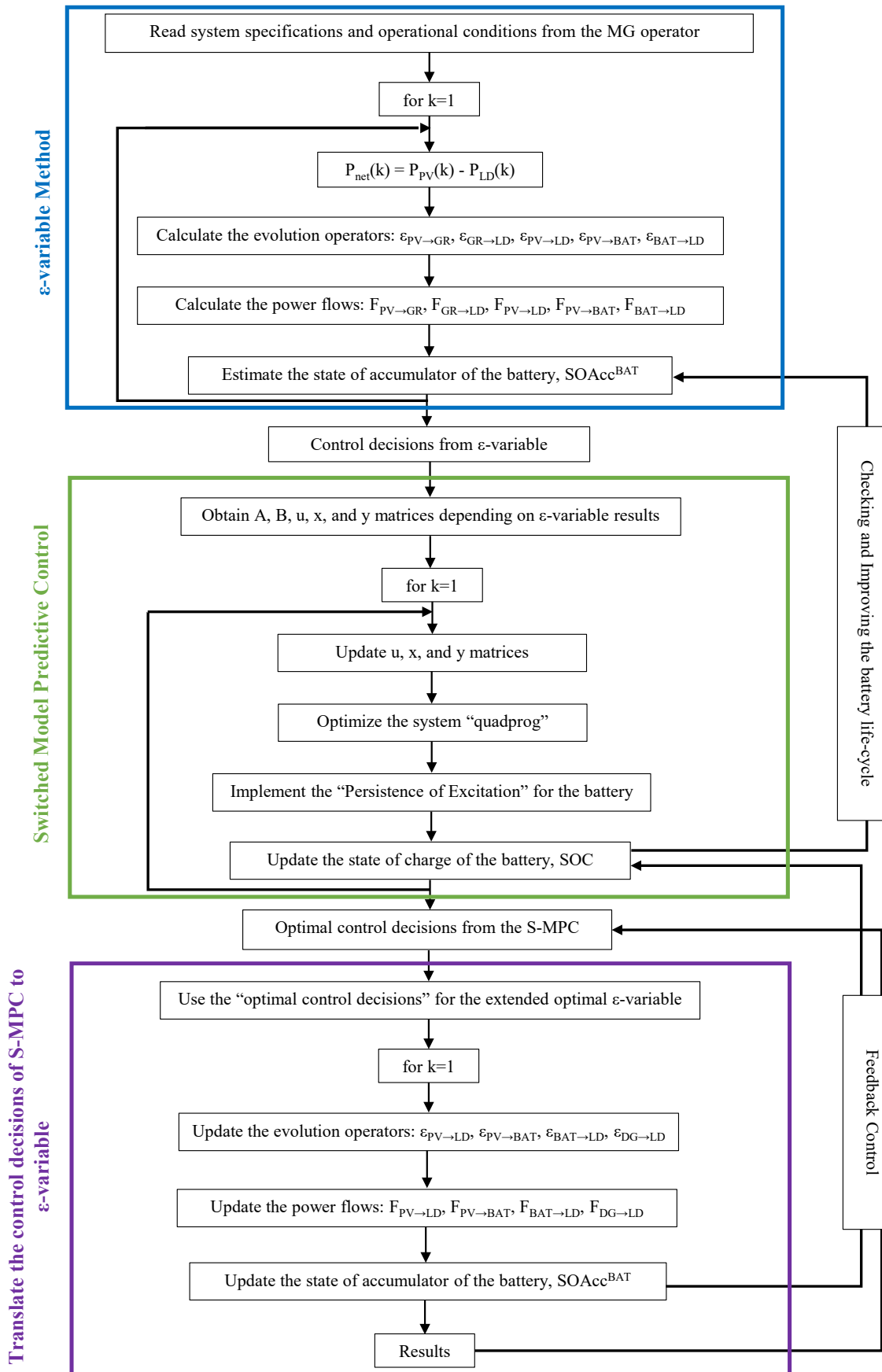


Figure 4.5 The flowchart of building the extended optimal  $\epsilon$ -variables technique for the MG is shown in Figure 4.2.

6.  $A$ ,  $B$ ,  $u$ ,  $x$ , and  $y$  matrices are dependent on "control decisions."
7. The persistence of excitation is then implemented in order to prevent the battery from being simultaneously charged and discharged.
8. MG operations are optimized and simulated using QP in MATLAB/Simulink on a CoreTM i7 4500U (2.40GHz) computer with 8GB of RAM and Windows 10 Professional.
9. All "optimal control decisions" are revised and compared to antecedent "control variables."
10. Regarding the section converting S-MPC results to  $\varepsilon$ -variables, the utility grid is eliminated, and the diesel generator is added. The "optimal control variables" are then modified as input data for the  $\varepsilon$ -variables method.
11. Evolution operators and power flows are revised in accordance with the "optimal control variables" obtained from the S-MPC.
12. The last step entails estimating and updating the  $SOAcc^{BAT}$  and power results and implementing feedback control.

All steps above are demonstrated in Figure 4.5. As shown, initially, PV and load demand for the building are obtained, and some parameters for battery and power are defined. The next step is to implement the S-MPC algorithm. It consists of the predictive algorithm, optimization, and receding horizon control. According to Figure 4.5,  $Q_X$  and  $R_U$  are modified and optimized at a given instant  $k$  time. Then,  $A_X$  and  $B_U$  are updated depending on the QP optimization. Next is optimising the "Hessian matrix ( $H$ )" and defining the objective functions. The last step is to update the system-state, system-control, and system-output.

Ensuring the optimality of the  $\varepsilon$ -variable in the context of MPC often relies on the specific formulation of the optimization problem, the choice of the cost function, and the underlying assumptions about the system dynamics. The optimality of the  $\varepsilon$ -variable is generally inferred from the principles of MPC and the  $\varepsilon$ -variable method. Here are some points that contribute to the perceived optimality:

- **Cost Function Formulation:** The optimal  $\varepsilon$ -variable method involves the formulation of a cost function that quantifies the performance objectives and constraints. The choice of this cost function is crucial, as it guides the optimization process. Our cost function is appropriately defined to represent the desired system behaviour, so the resulting  $\varepsilon$ -variable is optimal with respect to those objectives.
- **Optimization Algorithm:** The optimization algorithm used to solve the MPC problem, considering the  $\varepsilon$ -variable, plays a significant role. The algorithm is designed to handle the specific constraints and objectives of the system accurately, so the resulting  $\varepsilon$ -variable is to be considered optimal under the given conditions.

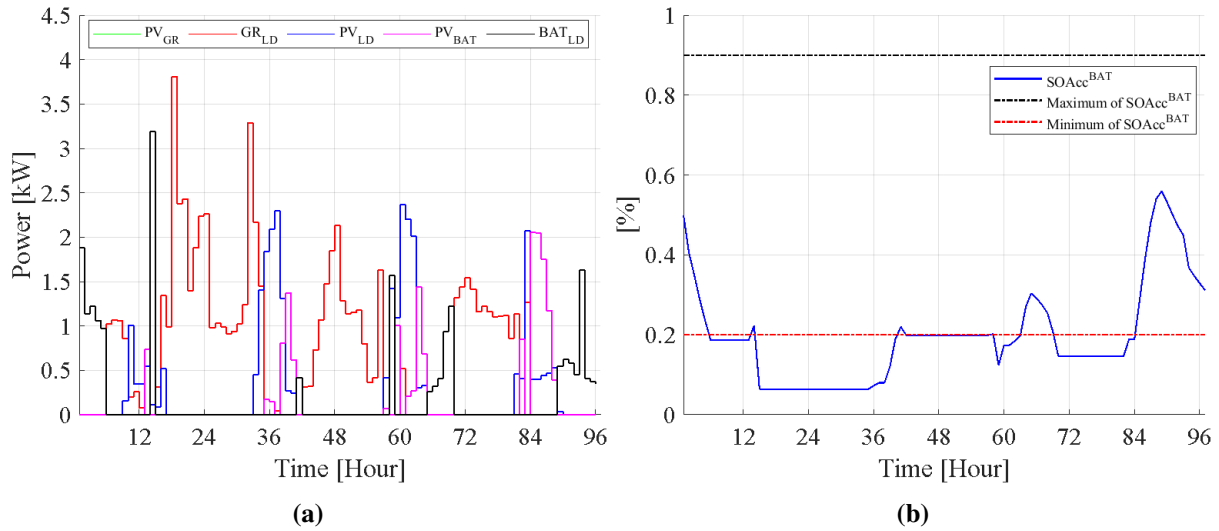


**Figure 4.6** (a) Power flows and (b) SOAcc of the accumulators for four days (96 hours) using the standard  $\epsilon$ -variables method.

- **Consistency with MPC Principles:** MPC, by nature, is designed to provide optimal control actions based on predictions of future system behaviour. The optimal  $\epsilon$ -variable method is consistent with the principles of MPC, leveraging predictive modelling and optimization, so it is implied that the resulting control decisions are optimal within the framework of the chosen optimization problem.

#### 4.6. Results and Discussions

##### 4.6.1. Simulation Results of the Extended Optimal $\epsilon$ -variables Method

Before the simulation, some parameters were defined, as shown in Table 4.2 Kostopoulos et al. (2020); Zhu et al. (2014).

Notations	Values	Notations	Values
$PV_{GR}^{max}$	5 kW	$w_1$	1.0
$PV_{LD}^{max}$	5 kW	$w_2$	0.2
$PV_{BAT}^{max}$	5 kW	$w_3$	0.8
$BAT_{LD}^{max}$	5 kW	$\eta_{ch}$	0.85
$GR_{LD}^{max}$	5 kW	$\eta_{dis}$	0.95
$SOAcc_{min}^{BAT}(1)$	30%	$C$	20 kWh
$SOAcc_{min}^{BAT}$	20%	$SOAcc_{max}^{BAT}$	90%

**Table 4.2** Values of System Parameters

The PV array and load data for the simulation were obtained from the building in the UK for four days (96 hours) and one year (8760 hours) (Makonin (2019)).

To see explicitly how to perform our method, the  $\epsilon$ -variables method is applied and obtained the results as shown in Figure 4.6. Then,  $\epsilon$ -variables-S-MPC is applied and gets the results as shown in Figure 4.7. From the results, (i) the energy consumption from the grid  $GR_{LD}$  significantly decreased when compared to Figure 4.6a and Figure 4.7a, (ii) the practicality of PV

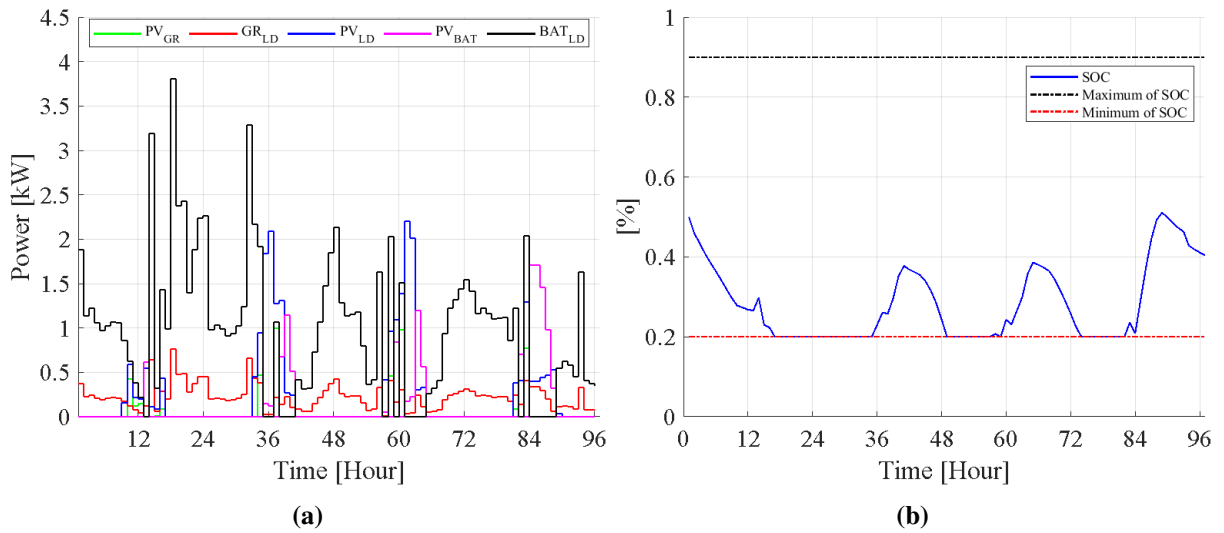


**Figure 4.7** (a) Power flows and (b) SOAcc of the accumulators for four days (96 hours) using the extended optimal  $\varepsilon$ -variables method.

usage ( $PV_{GR}$  and  $PV_{BAT}$ ) is encouraged, (iii) the battery usage  $BAT_{LD}$  is penalized. On the other hand, the state of charge of the battery is working at the desired conditions in Figure 4.7b using the extended optimal  $\varepsilon$ -variables technique. After translating the results of S-MPC to  $\varepsilon$ -variables methods, the same results were obtained with the extended optimal  $\varepsilon$ -variables technique.

Based on the simulation results presented in Figure 4.8 and Table 4.3, the overall energy consumption from the grid exhibited a significant decrease, transitioning from 2055 kWh to 1529 kWh for both the  $\varepsilon$ -variables and extended optimal  $\varepsilon$ -variables methods. This reduction underscores the effectiveness of both control strategies in minimizing grid-supplied energy, contributing to improved energy sustainability and cost savings.

Furthermore, the energy usage from the PV system for the GR ( $PV_{GR}$ ) experienced an encouraging increase, rising from 791.12 kWh to 620.68 kWh. This upward trend is attributed to the optimized control decisions implemented by both the  $\varepsilon$ -variables and extended optimal  $\varepsilon$ -variables techniques, enhancing the utilization of RES within the MG.

In terms of battery charging, the results indicate that the extended optimal  $\varepsilon$ -variables technique outperforms the traditional  $\varepsilon$ -variables method. The usage of the battery, accounting for 2127.1 kWh and 1956.7 kWh for the  $\varepsilon$ -variables and extended optimal  $\varepsilon$ -variables methods, respectively, reflects a more efficient and judicious management of the energy storage system. With its advanced optimisation strategies, the extended optimal  $\varepsilon$ -variables technique proves to be more effective in reducing battery consumption while ensuring optimal performance and longevity.

These observed results align with expectations, as the extended optimal  $\varepsilon$ -variables technique, with its enhanced optimization capabilities, demonstrates superior performance in achieving energy efficiency, reducing grid dependence, and maximizing the use of RES. The presented bar chart in Figure 4.8 provides a visual representation of the energy consumption patterns for each method, highlighting the impact of these control strategies on various energy sources within the MG.

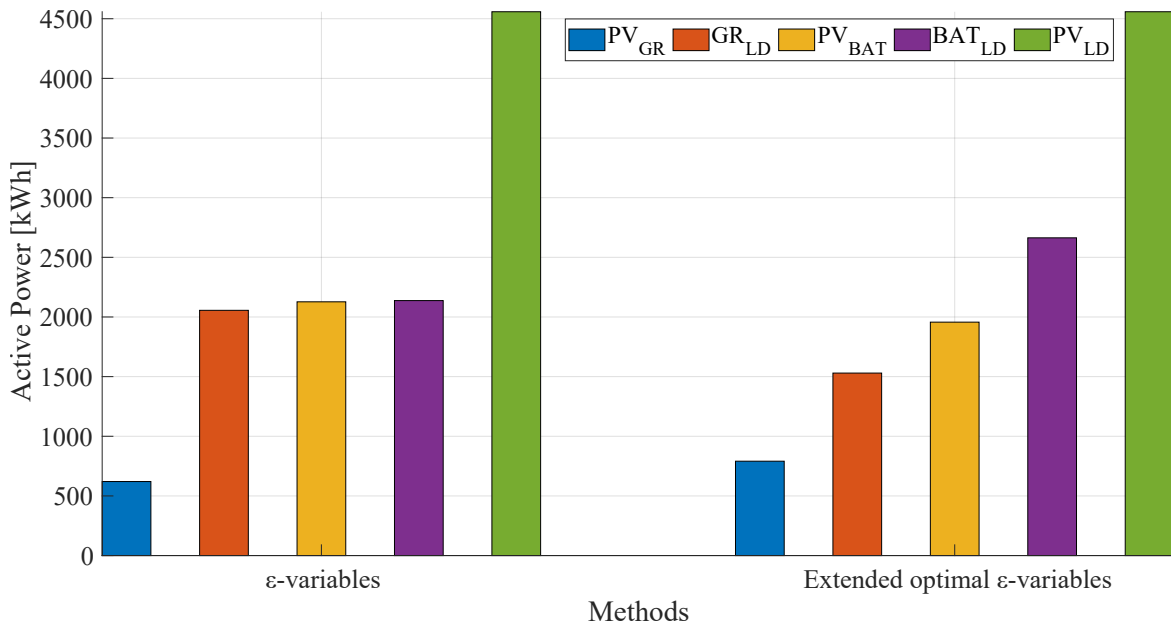


**Figure 4.8** Power flows for one year (8760 hours) using the standard  $\epsilon$ -variables method and the extended optimal  $\epsilon$ -variables method.

Methods	$PV_{GR}$ [kWh]	$GR_{LD}$ [kWh]	$PV_{BAT}$ [kWh]	$BAT_{LD}$ [kWh]	$PV_{LD}$ [kWh]
$\epsilon$ -variables	620.68	2055.8	2127.1	2137.4	4558.6
Extended optimal $\epsilon$ -variables	791.12	1529.8	1956.7	2663.4	4558.6

**Table 4.3** Numerical comparisons of  $\epsilon$ -variables method and extended optimal  $\epsilon$ -variables method

**4.6.2. The Illustrating the Adaptability and Scalability of the Extended Optimal  $\epsilon$ -variables Method**

Some processes have been fulfilled to show how our structure becomes more adaptable and scalable using our proposed method: (i) changing evolution operators and (ii) adding a diesel generator standalone.

**Changing Evolution Operators on the Extended Optimal  $\epsilon$ -variables Method**

To demonstrate how our structure becomes more flexible and scalable, the evolution operator for the utility grid  $\epsilon_{GR}$  was modified by switching the logical operator from "OR" to "AND." As depicted in Figure 4.9b, when the  $SOC$  falls below 50%, the S-MPC will import energy from the grid. In some instances, however, this may occur close to the point where PV will produce enough energy to compensate for the slight drop in  $SOC$  below 40%, thereby increasing the system's independence from the main grid. In this instance, and without modifying the S-MPC structure, the evolution operator of the converter "Grid" will contain another term that is logical 0 when it is anticipated that the PV will produce sufficient power in 1 or 2 samples. Since this evolution operator in this work employs the AND logical gate, when this new binary variable is 0,  $\epsilon_{GR}$  will also be 0. Consequently, the system will not import energy from the main grid,

as shown in Figure 4.9a. Regarding the  $\epsilon_{BAT}$ , its binary variables (black line in Figure 4.9a are changed from 1 to 0 when the utility grid operates for battery charging. (red line). In other words, if the battery is depleted, the evolution operator of grid  $\epsilon_{GR}$  will change from 0 to 1 in the grid. Therefore,  $\epsilon_{GR \rightarrow BAT}$  runs and the  $GR_{BAT}$  connection is active.

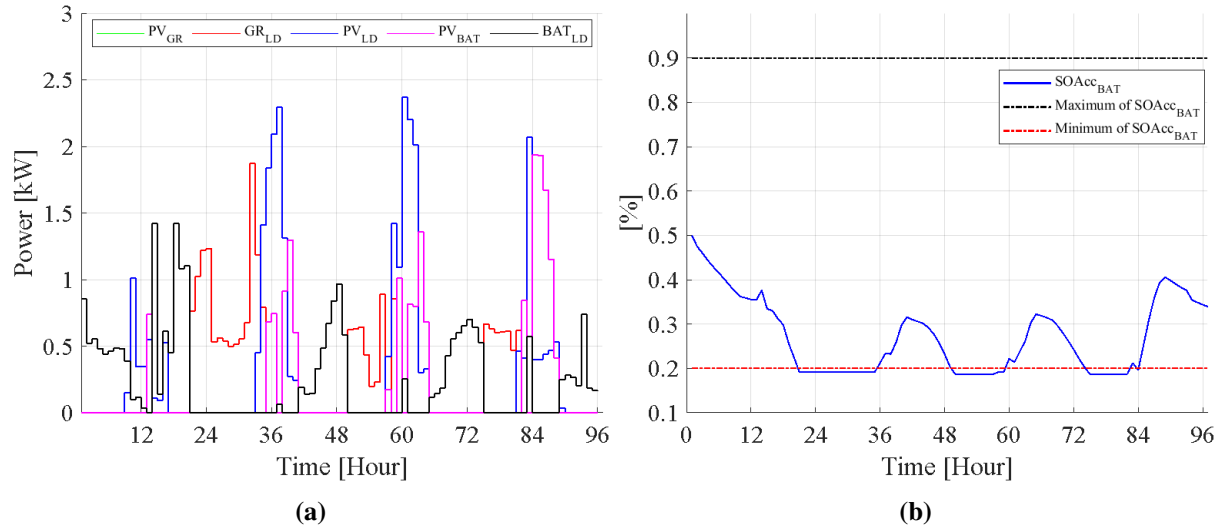


**Figure 4.9** The translating of results of S-MPC to the  $\epsilon$ -variables method for (a) power flows and (b) SOAcc of the accumulator.

#### *Adding a Diesel Generator by Standalone*

During the second step (S-MPC section) of the extended optimal  $\epsilon$ -variables technique, a diesel generator is added, the utility grid is removed, and the algorithm is updated, as depicted in Figure 4.5.  $PV_{GR}$  and  $GR_{LD}$  are excluded in this instance, whereas  $DG_{LD}$  is present. The  $\epsilon$ -variables can be easily incorporated into the system and utilized for the hybrid power system in the event of an emergency, such as a blackout or an imbalance in load demand. As depicted in Figure 4.10a, the results of the extended optimal  $\epsilon$ -variables technique reveal that the PV, battery, and diesel generator meet the load demand, respectively. In the morning and afternoon, the PV is sufficient to meet the load demand. (blue line). If there is excess energy from the PV system, the battery is charged from the PV system. (pink line). The unbalanced load is covered by the battery (black line) and the diesel generator. (red line). Notably, during the operation of the diesel generator, the battery (pink line) has not been charged at all (red line). The battery operates as expected, and the SOC of the battery does not exceed the critical values, as shown in Figure 4.10b With the help of the extended optimal  $\epsilon$ -variables technique, the adaptability/flexibility and scalability of the S-MPC have been enhanced.

#### *Applying a hysteresis zone in order to increase the lifetime of various assets using the starting and stopping values of the accumulators*

The condition of the devices (ON-OFF switching of the devices) depends on a connection between two devices based on a simple condition imposed on  $SOAcc$ . The decision whether or

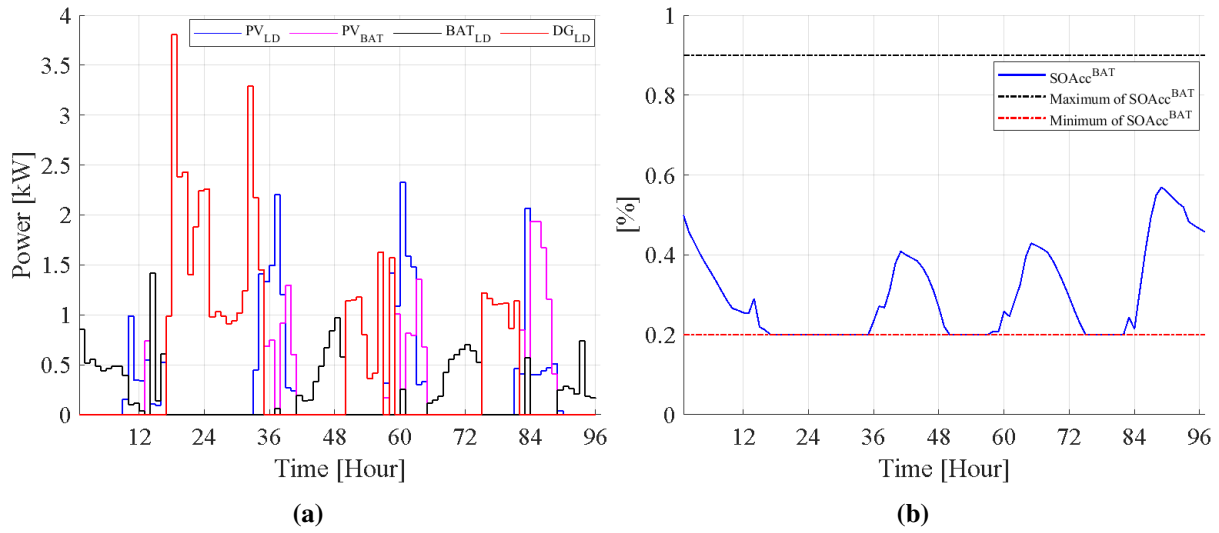


**Figure 4.10** The illustration of the scalability of the extended optimal  $\varepsilon$ -variables method when adding the diesel generator

not passive/activate a connection between two devices in the sight of a hysteresis zone is the outcome of the succeeding logical tests. These tests rely on the stored energy/material as shown in Figure 4.11:

- If a pre-specific limit  $stp_{a \rightarrow b}^{SOAcc^l}(k)$  is lower than  $SOAcc^l$ , the connection is passive.
- If a pre-specific limit  $str_{a \rightarrow b}^{SOAcc^l}(k)$  is higher than  $SOAcc^l$ , the connection is active.
- If  $SOAcc^l$  is at the between  $str_{a \rightarrow b}^{SOAcc^l}(k)$  and  $stp_{a \rightarrow b}^{SOAcc^l}(k)$ , the result of the connection will be:
  - Active if it was previously activated.
  - Passive if it was previously passive.

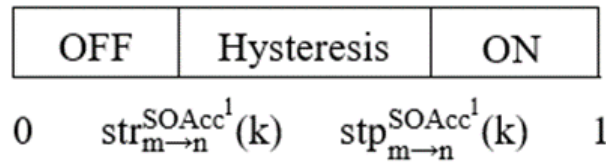


**Figure 4.11** The hysteresis zone for the extended optimal  $\varepsilon$ -variables technique in the MG

With the help of the above parameters, variable  $\rho$  can be stated as a function of the related situations imposed on  $SOAcc^l$  by:

$$\rho_{a \rightarrow b}^{SOAcc^{BAT}} = [SOAcc^l(k) < str_{a \rightarrow b}^{SOAcc^{BAT}}(k)] \vee [[str_{a \rightarrow b}^{SOAcc^{BAT}}(k) < SOAcc^{BAT}(k) < stp_{a \rightarrow b}^{SOAcc^{BAT}}(k)] \wedge [\varepsilon_{a \rightarrow b}(k-1)]] \quad (4.64)$$

Equation (4.63) says that the left side of the expression represents the simple ON-OFF behaviour of the devices, whereas the rest of the expression illustrates the hysteresis behaviour. Besides, it is

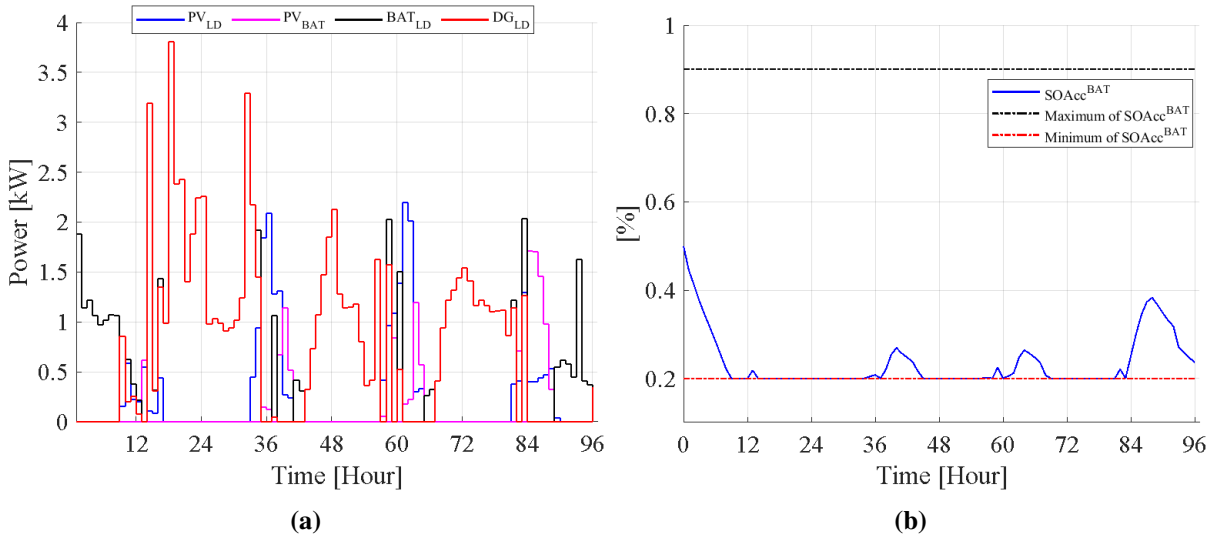


**Figure 4.12** The results of power flows and  $SOAcc^{BAT}$  when changing  $stp_{DG \rightarrow LD}^{SOAcc^{BAT}}$ .

worth noting that there are three accumulation areas related to the battery. In other words, below  $str_{a \rightarrow b}^{SOAcc^{BAT}}(k)$ , between  $str_{a \rightarrow b}^{SOAcc^{BAT}}(k)$  and  $stp_{a \rightarrow b}^{SOAcc^{BAT}}(k)$ , and above  $stp_{a \rightarrow b}^{SOAcc^{BAT}}(k)$  in order to determine whether a connection will be activated/passive. This process basically repeated for every connection. This process is very beneficial for especially complicated hybrid power systems since it is much easier to control many basic rules (Calderón et al. (2010)). It can be understood from this process that the values of the limits  $str_{a \rightarrow b}^{SOAcc^{BAT}}(k)$  and  $stp_{a \rightarrow b}^{SOAcc^{BAT}}(k)$  can be considered as decision variables for the overall system performance of the complicated hybrid power system (Giaouris et al. (2013)).

To show the effect of the hysteresis zone on the extended optimal, the value of  $\varepsilon$ -variables,  $stp_{DG \rightarrow LD}^{SOAcc^{BAT}}$  is decreased from the 25% to 20%. In this case, the usage of the diesel generator  $DG_{LD}$  is increased since its evolution operator is turned to be activated, as illustrated in Figure 4.12a. In other words, the connection of  $\varepsilon_{DG \rightarrow LD}$  is activated because of the hysteresis zone (see Figure 4.11). On the other hand, the  $SOAcc$  values are changing compared to the previous one in order to meet the load-generation mismatch. It is worth noting that the  $SOAcc$  of the battery does not go below the critical value because of the extended optimal  $\varepsilon$ -variables, as shown in Figure 4.12b. In addition, the battery is charged by employing the PV,  $PV_{BAT}$ , when there is excessive energy in the PV.

Regarding the changing of the hysteresis zone of  $BAT_{LD}$ , the value of  $str_{BAT \rightarrow LD}^{SOAcc^{BAT}}$  is increased from 20% to 25%. By doing that, the hysteresis zone of the  $\varepsilon_{BAT \rightarrow LD}$  is approaching the left side (see Figure 4.11). Therefore, the connection of the  $\varepsilon_{BAT \rightarrow LD}$  is passive. In this case, the binary variables of  $\varepsilon_{BAT \rightarrow LD}$  are converted from 1 to 0. As can be understood from Figure 4.12a, the battery discharging ( $BAT_{LD}$ ) is decreasing. According to this value, the  $SOAcc$  of the battery fluctuates. However, it has not decreased as much as the previous one (compare Figure 4.12b and Figure 4.13b). In summary, the extended optimal  $\varepsilon$ -variables can achieve the desired objective functions such as minimization of the imported energy from the grid, increase in the exported energy to the battery and utility grid, and penalization of the battery usage in two cases.

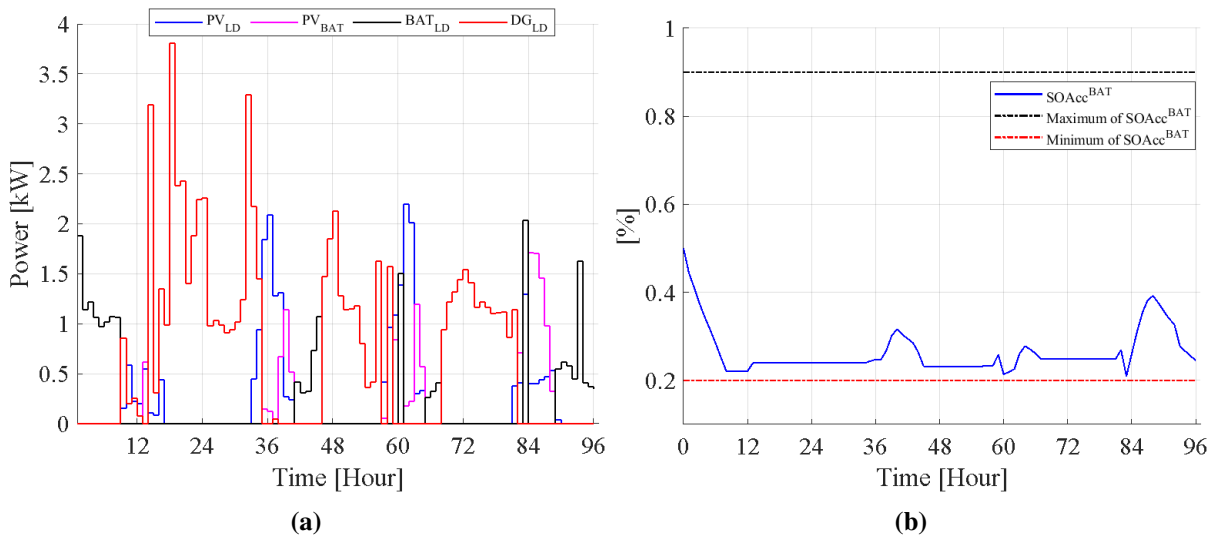


Figure 4.13 The results of power flows and  $SOAcc^{BAT}$  when changing  $str_{BAT \rightarrow LD}^{SOAcc^{BAT}}$ .

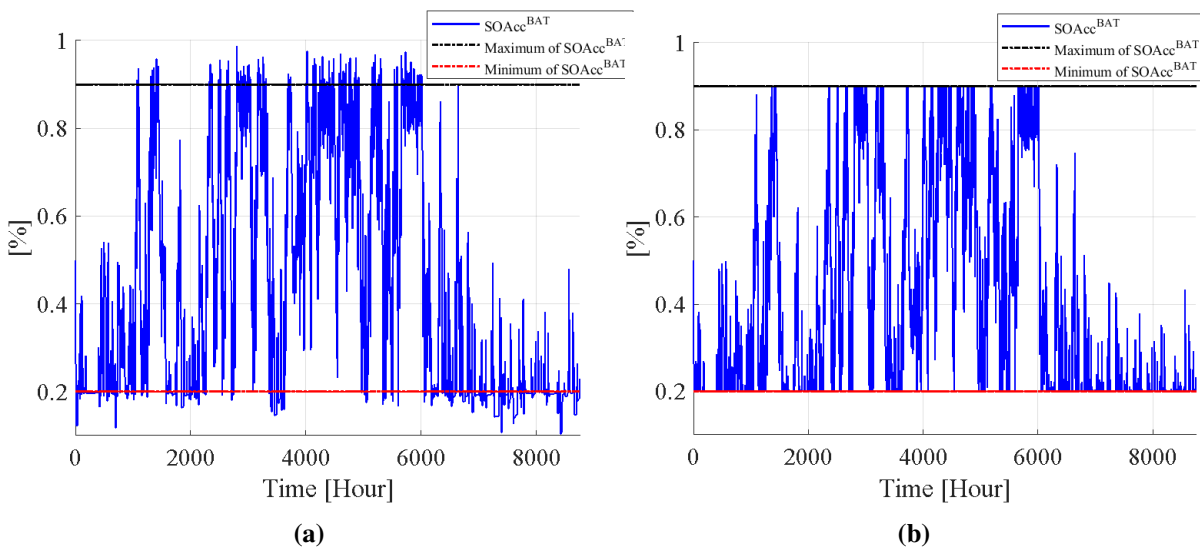


Figure 4.14 The results of the state of charge of the battery using (a)  $\epsilon$ -variables and (b) extended optimal  $\epsilon$ -variables

To compare the standard  $\varepsilon$ -variables and extended optimal  $\varepsilon$ -variables, the MG system is simulated for one year (8760 hours) as demonstrated in Figure 4.14a and Figure 4.14b. Since the standard  $\varepsilon$ -variables are not optimal techniques, they do not have any constraints and optimization methods. To explain it clearly, Figure 4a illustrates that the  $SOAcc$  of the battery can exceed the maximum critical value (such as  $>90\%$ ) or go below the minimum critical value (such as  $<20\%$ ). On the other hand, Figure 4.14b shows that the battery can work at the desired conditions by employing the extended optimal  $\varepsilon$ -variables. This is vitally important that the health of the battery can deteriorate when the battery is exploited during over-charging and over-discharging. Therefore, the essential importance of the extended optimal  $\varepsilon$ -variables is to enhance the battery's health. One of the objective functions of the extended optimal  $\varepsilon$ -variables is to penalize the usage of the battery by avoiding the battery charging from the non-RESs, such as the diesel generator and the utility grid. Hence, the results of the  $SOAcc$  (see Figure 4.14b) are expected and reasonable through the extended optimal  $\varepsilon$ -variables.

#### 4.7. Conclusion

There are several reasons for utilizing the variable method to manage the MG power system; however, this method is not the most effective. In contrast, S-MPC employs cost functions and constraints in conjunction with various optimization techniques to forecast power generation and consumption. However, implementing S-MPC is not simple, especially in complex MG systems. To address the shortcomings of the  $\varepsilon$ -variables and S-MPC methods, we developed an extended optimal  $\varepsilon$ -variables technique that effectively: (i) reduces the operational cost of MG by nearly 35%, (ii) reduces the usage of the BESS by 42%, and (iii) increases the practicability of PV usage by 28%. The computational capacity of the new method is roughly equivalent (+2%) to the S-MPC. This significantly improved the scalability and adaptability of the existing S-MPC implementation by extending optimal  $\varepsilon$ -variables. The adaptability and scalability of the extended optimal  $\varepsilon$ -variables technique were improved by modifying a number of evolution operators and introducing a diesel generator. Consequently, the proposed extended technique simplifies and optimizes the control of the system.

The next chapter will demonstrate the scalability of the proposed method on a real system constructed in Xanthi, Greece. It will utilize fuel cells and electrolyzers to be completely independent of the main power grid. In this instance, hydrogen and water tanks can be viewed as accumulators, whereas fuel cells, electrolyzers, PVs, etc., can be viewed as converters. Also, the next chapter will consist of developing a hybrid method based on  $\varepsilon$ -variables and conventional MPC to construct the S-MPC of a flexible hybrid MG with PnP assets.



## **Chapter 5. A Hybrid Method Based on Logic Predictive Controller for Flexible Hybrid Microgrid with Plug-and-Play Capabilities**

### **5.1. Overview**

Flexible hybrid MGs with PnP assets have gained popularity recently due to their ability to incorporate RESs and storage systems. However, controlling these systems can be challenging due to their complexity and the diverse characteristics of each asset in the MG. Various control strategies have been proposed to address these difficulties. One such strategy is  $\varepsilon$ -variables-based logic control, which simplifies the control structure of MGs and enables greater scalability and resilience. However, the resulting controller is not optimal and may be incapable of managing multiple MG models. MPC, which employs a mathematical model of the system to predict its behaviour and determine the optimal control action, is another advanced control strategy. However, MPC cannot design and control multiple models, rendering it unsuitable for flexible hybrid MGs. Alternatively, S-MPC employs multiple models to represent system operating modes or scenarios. S-MPC selects a model and control strategy based on the system state and performance objectives, enabling it to manage systems with mode-dependent dynamics. However, developing and validating the design and management of multiple MG models is difficult. Moreover, S-MPC is more complicated to implement due to its multiple steps (Cavus et al. (2024)).

This chapter proposes a novel hybrid framework/method based on  $\varepsilon$ -variables and traditional MPC to automatically generate and validate the S-MPC. The proposed strategy enhances the optimization of the energy management of a flexible hybrid MG and reduces computational complexity. S-MPC implementation is simplified by translating S-MPC decisions into  $\varepsilon$ -variables. The proposed hybrid method is validated using a QP strategy that minimizes or maximizes objective functions under the constraints of bounds, linear equality, and inequality to solve the S-MPC optimization problem in a compact form. The results indicate that the suggested control method decreases the amount of energy imported from the grid by approximately 46.7% and increases the amount of energy exported to the grid by approximately 50.8%. This thesis contributes to the field of MG control by proposing a method that can facilitate the implementation of advanced control strategies for flexible hybrid MGs with PnP assets.

### **5.2. Introduction**

A hybrid flexible MG is a small-scale power system that integrates and manages multiple energy sources, including RESs such as solar, wind, and hydro, as well as conventional sources such

## **A Hybrid Method Based on Logic Predictive Controller for Flexible Hybrid Microgrid with Plug-and-Play Capabilities**

---

as diesel generators Emad et al. (2020); Yoldaş et al. (2017). MG is designed to operate either connected or disconnected from the main power grid, providing a reliable and sustainable power supply for various applications Ishaq et al. (2022); Nshuti (2022). The flexibility of a MG refers to the MG's capability to vary energy demand and its ability to optimize the available energy sources Herc et al. (2022); Hirsch et al. (2018).

Adding the PnP capability to the MG's assets facilitates the system's installation and operation. PnP assets can enhance the MG's flexibility Veneri (2017). For instance, incorporating PnP EVs into a MG can increase the MG's flexibility Anthony Jnr (2021); Ravi and Aziz (2022) by varying the size of available storage capacity dynamically. PnP EVs can be added or removed from the MG system without extensive reconfiguration Sadabadi et al. (2017). However, having assets with PnP capabilities allows the MG to operate in multiple operational modes. This makes the design of optimal control of the MG challenging.

### **5.2.1. Literature Review**

MPC is widely used in the literature to control MGs (Nikkhah et al. (2021a); Pamulapati et al. (2022b)). A rolling horizon approach is applied in Silvente et al. (2018) to reduce the operational cost of the MG and to maximize the income from exporting power to the utility grid. A scenario-based MPC is presented in Parisio et al. (2016) with an objective to reduce carbon emission. The authors in Cheng et al. (2020) used the interval predictions to reduce the impact of the uncertainty in renewable energy generation, which, in its turn, reduced the operational cost significantly. To reduce the impact of uncertainty of energy demand and renewable energy generation, a robust MPC (R-MPC) was developed in Marín et al. (2019). A robust rolling-horizon MPC is presented in Nikkhah et al. (2021c,d) to control in real time a community of buildings represented as MGs. The control philosophy in Nikkhah et al. (2021c,d) improves the robustness of the residential MGs in the face of real-time weather and energy price prediction errors. Nawaz et al. (2023) presents a distributed MPC-based energy scheduling problem for multi-island microgrids. Energy coordination aims to achieve supply-demand equilibrium in an individual MG and reduce battery degradation for its extended cycle life. To solve the MPC optimization problem, a mixed-integer quadratic programming strategy is utilized. Fang et al. (2022) proposes a multiple-time-scale energy management solution for a hydrogen-based multi-energy MG to supply electricity, hydrogen, and heating loads to minimize the multi-energy MG operational cost. The proposed solution consists of day-ahead energy scheduling and MPC-based real-time energy dispatch. The numerical results demonstrate that the proposed solution outperforms the benchmark solution, with mean daily operational costs 37.08% less than the benchmark solution.

It is important to notice that all these MPC methods can control the MG only in one operational mode, allow it to meet different objectives in this operational mode, and can consider the impact of the uncertainty of renewable generation and energy demand. These methods do not allow for control of the MG with different operational modes. On the other hand, many methods are developed to control complex systems with different operational modes. These methods are based on system state and use Petri Nets (Allahham and Alla (2008)) and/or automata (Allahham

and Alla (2009); Javaid et al. (2019); Khawaja et al. (2019); Pamulapati et al. (2022a)). Other methods are based on the evolution/logical operators and the states graph (Cavus et al. (2022b); Giaouris et al. (2013)). The authors in Giaouris et al. (2013) and Cavus et al. (2022b) used the  $\varepsilon$ -variables to define the system evolution and the system graph to model the operational states/modes of the energy system. The mutual use of graph theory and the evolution operators presented in Cavus et al. (2022b); Giaouris et al. (2013) allows us to address the problem of system scalability, and this is by considering all the possible operational modes of the system assets in the system graph. It is important to highlight that the PnP feature of the system's assets will change the system's size dynamically. This means the MG controller must deal with the scalability issue. The main drawback of these methods is that the resultant controller does not operate the MG in its different operational modes optimally.

S-MPC is a variation of MPC that employs multiple models, each representing a distinct mode of system operation. S-MPC chooses the appropriate model and associated optimal control strategy based on the current state of the system and the system objectives. This enables S-MPC to deal with systems with mode-dependent dynamics. The main difference between MPC and S-MPC is that MPC uses a single model to control the system (Cavus et al. (2023)); however, S-MPC uses multiple models and switches between them according to the current state of the system (Maślak and Orłowski (2022); Zhu et al. (2014)). The authors in Wang (2009) demonstrated the development of S-MPC to control a MG.

It is important to highlight that the construction of S-MPC is challenging, especially for MG, which has many operational modes. The challenge arises from the following factors:

- S-MPC development requires the development of multiple models that represent the system's behaviour in the different operational modes. In addition, the MG can have different objectives; in each operational mode, the MG can have an objective different from the other operational modes.
- S-MPC development requires the design of switching logic that maps the system's current state to the appropriate model and the switching conditions between the operational modes.

Dealing with these challenges requires an exhaustive knowledge of the system and its desired behaviour in each operational mode. All this knowledge must be systematically combined to build the S-MPC.

### 5.2.2. *Contributions and research questions*

Controlling the flexible hybrid MG in which the assets have PnP capabilities requires building a controller that is able to consider all the possible operating modes of the MG. The classical MPC allows the control of the MG optimally in a specific operational mode but cannot represent the different possible operational modes. On the other hand, the control methods based on the mutual use of graph theory and the evolution operators can control the MG in its different operational modes, but the resultant operation of the MG is not optimal. S-MPC can control the MG optimally in its different operational modes; however, the construction of this controller

## **A Hybrid Method Based on Logic Predictive Controller for Flexible Hybrid Microgrid with Plug-and-Play Capabilities**

---

is complex and requires a strong knowledge of the system and its desired behaviour in each operational mode. The complexity of the S-MPC arises from the need to put all this knowledge to produce the final S-MPC. The main contribution of this section is to present a systematic method to build the switched MPC of a flexible hybrid MG with PnP assets. This method is based on combining logical control, graph theory, and classical MPC. In this method,

- The system graph and the evolution parameters allow us to define the operational modes, the switching conditions, and the state variables in each operational mode.
- The classical MPC allows us to find the optimal control decisions in each operational mode according to the objective defined for each operational mode.

Based on the method of controller synthesis proposed in this section, the following research questions can be addressed:

- How can S-MPC be generated in a systematic way to control flexible hybrid MGs in which the assets have PnP capabilities?
- How the decisions from S-MPC can be implemented in a simple way?

### **5.2.3. Organization of this chapter**

The rest of the section is organized as follows: Section 5.3 presents the methodology of the hybrid method based on controlling flexible MG with PnP capabilities. Section 5.4 illustrates a detailed description of the hybrid method implementation. The simulation results of four case studies with the hybrid method based on controlling flexible MG are discussed in Section 5.5. Finally, Section 5.6 outlines the conclusions and addresses future work.

### **5.3. Hybrid method based to control flexible MG with PnP capabilities**

The methodology of building the EMS of flexible hybrid MG comprises three key steps, as illustrated in Figure 5.1. In the first step, the EMS will be built utilizing a systems approach based on the MG conditions and the operational constraints of the MG. The system approach exploited in this chapter is the  $\varepsilon$ -variables (Cavus et al. (2023, 2022b); Giaouris et al. (2018)). “Control decisions” have been found at the end of this step. The output of the first step is a non-optimal EMS. In the second step, the obtained EMS will be used as input to generate the equivalent mathematical problem to optimally meet the objectives specified by the MG operators, considering the operational condition already included in the EMS gained from Step 1. The optimal problem will be formulated in the form of S-MPC. The S-MPC is solved using the QP approach. During the solving, the system input, state, and output weights are produced so as to make the problem compact form. Then, the S-MPC designs and controls the multiple models depending on the net energy (difference between PV energy and load) and the condition of the accumulators. If there is a deficit or excess power, the  $SOAcc$  of the accumulators is considered. If one of the  $SOAcc$  of the accumulators is greater than the minimum value of the  $SOAcc$ , the

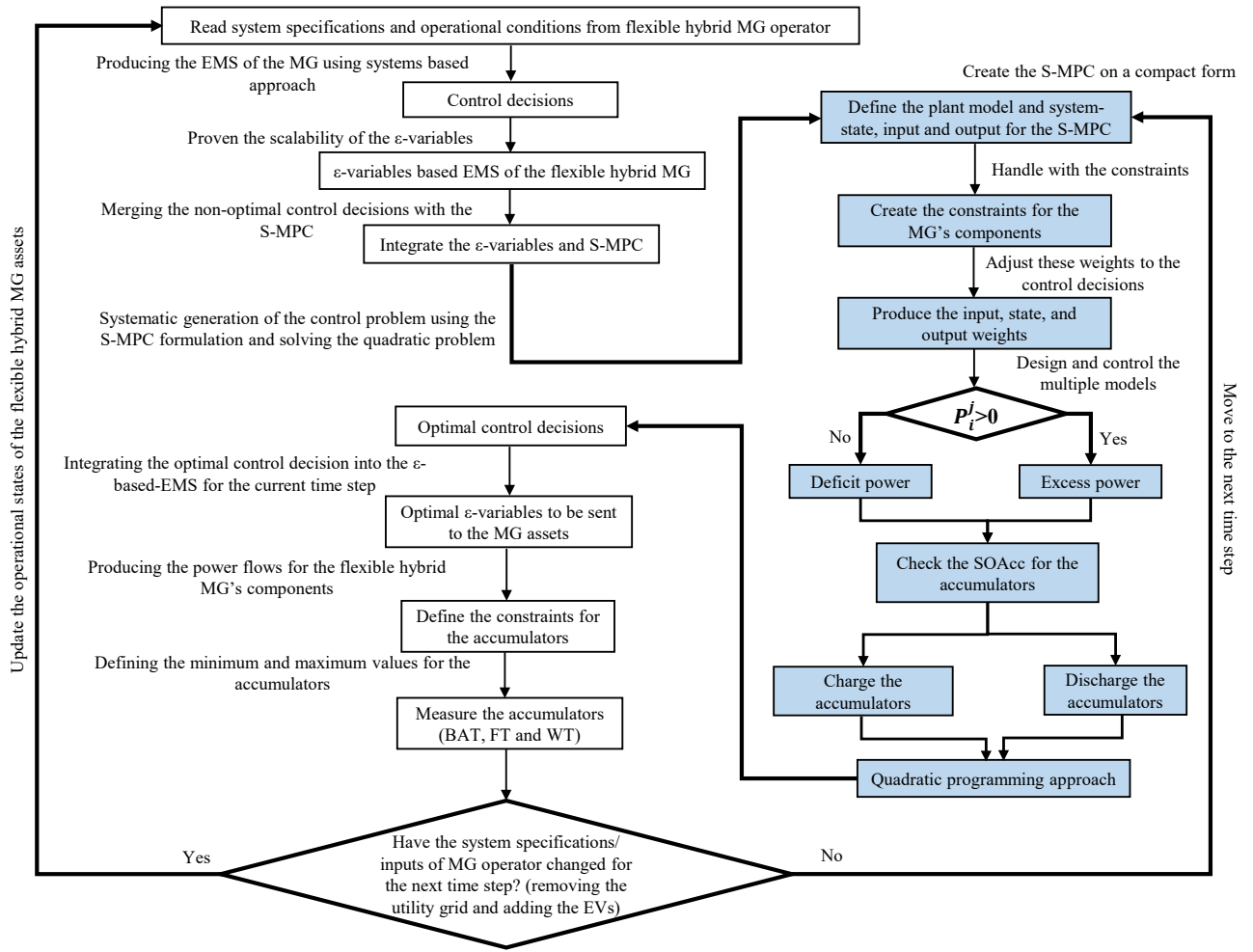
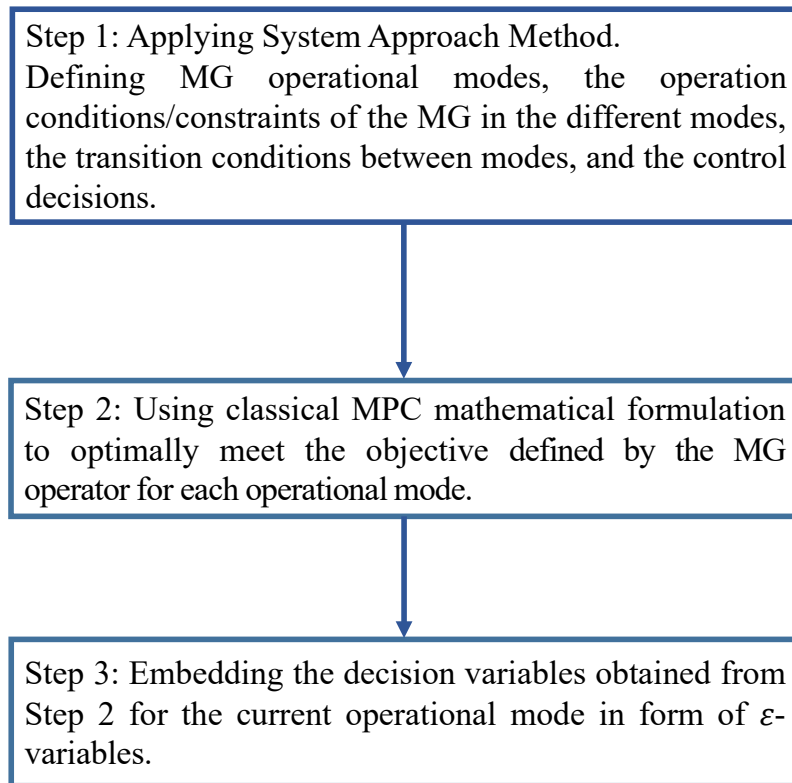


Figure 5.1 Flow chart of the algorithm generating S-MPC from the MPC automatically.

accumulator is in charging mode; otherwise, it is in discharging mode. After finding the “optimal control decisions” in Step 2, these decisions will be embedded in the  $\varepsilon$ -variables-based EMS in Step 3. Then, the accumulators are measured and evaluated. The output of Step 3 will be hence optimal  $\varepsilon$ -variables EMS. During the operational phase of the EMS, the MG specifications and inputs from the flexible hybrid MG operator will be checked at the beginning of each time step. If this information has been modified/changed, the operational states of the MG assets will be updated, and the three steps of the EMS building will be repeated to consider the new input. If not, the optimal  $\varepsilon$ -variables-based EMS can be used to control the MG for the next time step. Notably, the proposed method checks whether the MG operator’s system specifications/inputs change for the next time step. These steps have been explained in Figure 5.2.

#### 5.4. The Proposed Optimal Systems-Based EMS

This is a case study, and this is a real system that was built in Xanthi, Greece (Giaouris et al. (2018)). As shown in Figure 5.3, the MG consists of a 15 kW PV array, a BAT, a WT, and a FT used as ESSs, an EL, a FC, and the GR. The PV can be used as a priority energy source on the MG. If the PV is not able to provide enough power, then either the BAT or the FC will ensure



**Figure 5.2** A brief flow chart of our proposed method.

that the load is satisfied. The GR will supply the energy if the battery is empty and there is no available hydrogen. On the other hand, when the BAT is full, and there is a surplus, the EL will be used if there is space in the WT and the FT. Then, the energy will be sent to the GR. The implementation of the methodology presented in Section 5.3 is summarised by the flowchart given in Figure 5.2. In the following, each step of the implementation method will be explained for the MG shown in Figure 5.3.

### **5.4.1. Step 1: Defining the operational modes and switching conditions (the logical control system approach)**

The main idea behind the  $\varepsilon$ -variables is that a node symbolizes every asset. Every flow of matter/energy is symbolized by an edge in the flexible hybrid MG system, as demonstrated in Figure 5.5. In **Point 1**, the state graph is generated. Then, in **Point 2**, the different assets in each state will be classified as a converter, energy flow, or accumulator. The output of **Point 2** is the graph shown in Figure 5.4. In **Point 3**, the dynamical state-space model is for each asset in each state. Using this theory and the evolution operators (calculated in 5.6), this power system's analysis, management, and operation can be simplified. Lastly, the control statements are the evolution operators based on the logical operators, illustrating the different types of EMSs exploited by the multi-vector system (Giaouris et al. (2013)).

To control the flexible hybrid MG using logic control, state transition diagrams, also known as state machines or automata, can be used to represent the different operating modes of the accumulators. Different operational modes, switching conditions, and state variables in each

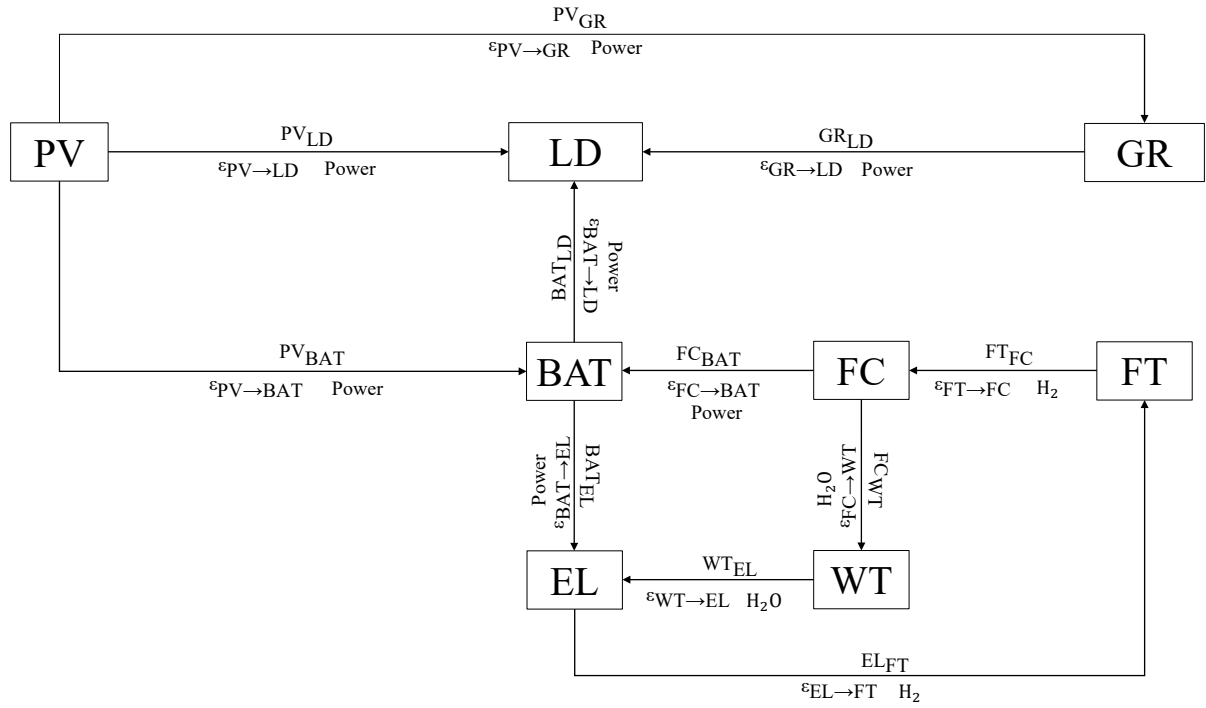


Figure 5.3 Hybrid MG Structure.

mode are determined using binary notation. Each state in this diagram represents the particular mode or condition of the accumulators. The transitions between states represent the actions or events that cause the accumulators' mode to change. Figure 5.4 depicts the various operating modes and relationships between them for a system comprised of a battery, a fuel tank, and a water tank via an automata graph. A three-digit binary number on the graph represents each of the eight possible states. The state "000" indicates that the system is completely off, whereas the state "111" indicates that all three components are charged or filled, and the system is fully operational. The remaining six states represent various combinations of component charging or filling. Notably, the graph also displays the relationships between the various states. For instance, when the battery is charged, and the water tank fills, the system can transition from state "000" to state "110." The system can transition from state "110" to state "010" if the battery is discharged while the water tank fills.

As evidence of the idea, Figure 5.3 illustrates the hybrid MG system. According to the graph theory, the converters are the PV array, LD, GR, FC, and EL; the BAT, FT, and WT can be considered as accumulators, and power, hydrogen, and water can be regarded as flows. As can be seen in Figure 5.3, the assets of the MG system can be split into two sets as follows:

- The set of converters:  $R_s^{Con} = \{PV, LD, GR, EL, FC\}$
- The set of accumulators:  $R_s^{Acc} = \{BAT, FT, WT\}$

In addition, the connection between two nodes can be called a *flow*, such as FC to BAT and BAT to EL as a power flow, EL to FT and FT to FC as a hydrogen flow, and FC to WT and WT to EL as a hot water flow.

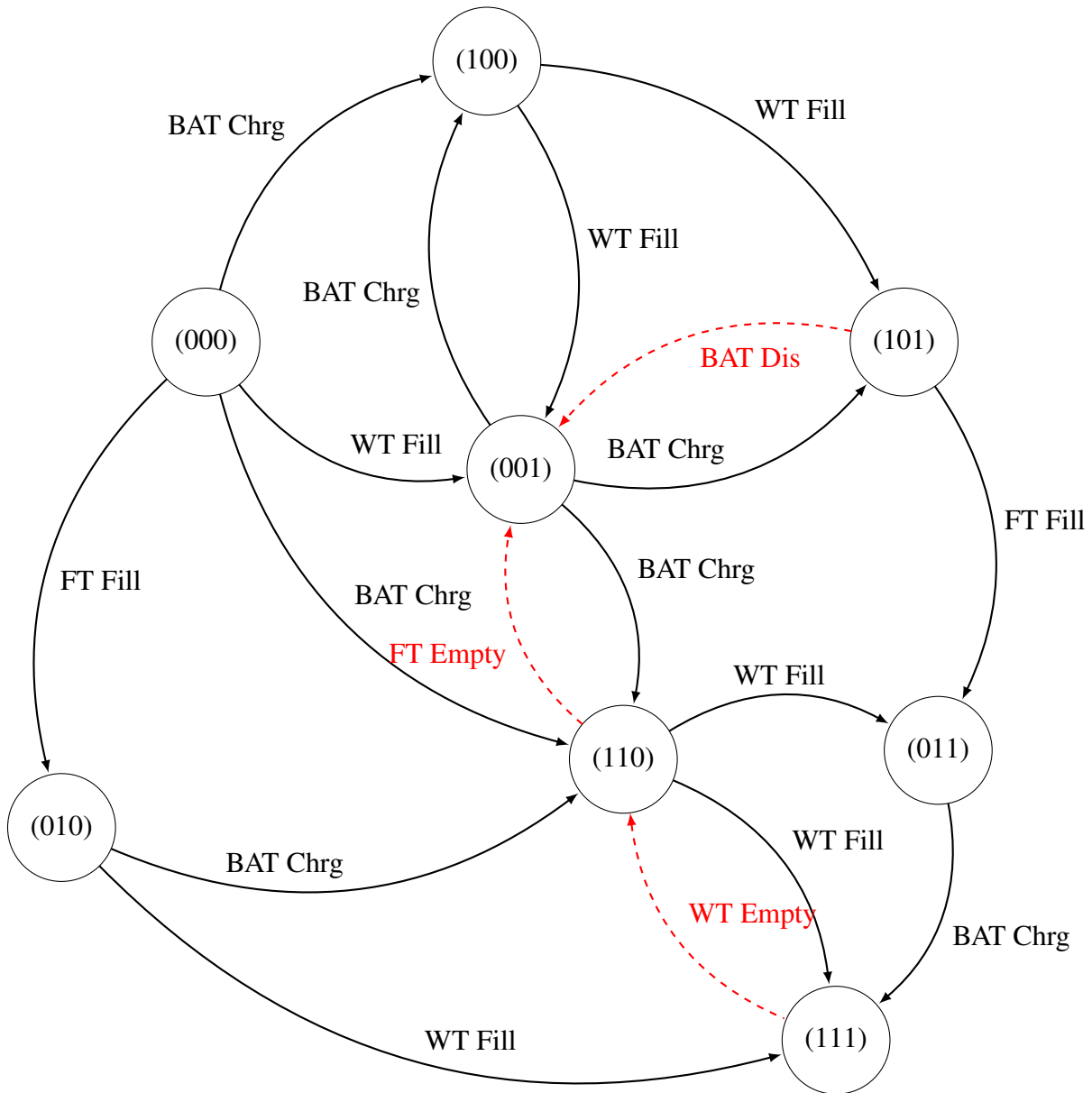


**Figure 5.4** The illustration of the different operational modes, the switching conditions, and the state variables in each mode using the automata/graph method.

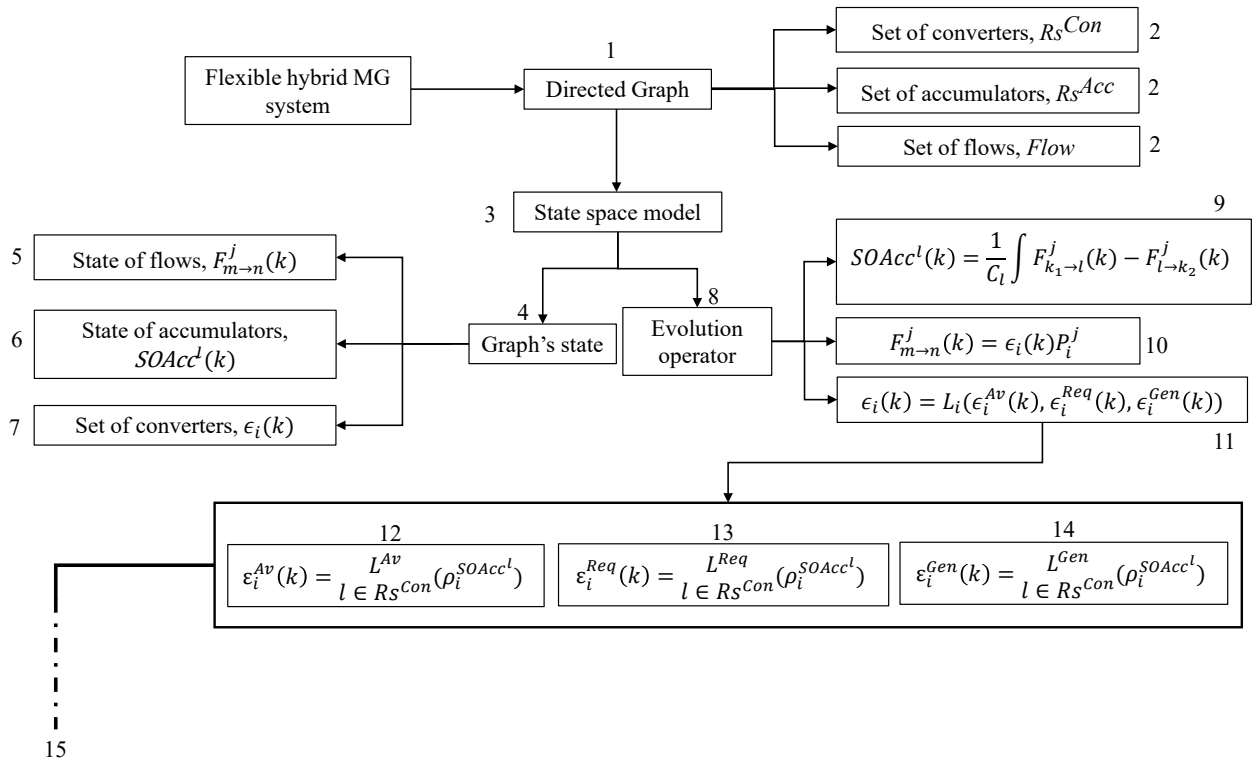


**Figure 5.5** A graph shown in state space (in the first step) for the hybrid control method; numbers indicate points addressed in the text.

Therefore, the set of flows for the hybrid power system can be illustrated as follows (Giaouris et al. (2018)):

- The set of flows:  $Flows = \{Power, Hydrogen, Water\}$

The detailed implementation of the  $\epsilon$ -variables has already been explained step by step in Section 3.5.4 (**Point 4-14**).

As shown in Figure 5.6, this step is composed of sub-steps which are:

- Initially, evolution operators are defined.
- The power flows are calculated by multiplying equation  $P_i^j$  and Eq. (5.7). However, to calculate the EL and FC, some equations need to be as follows:

According to Faraday's Law, the generation rate of  $H_2$  in the EL and production rate of hot water in the FC can be calculated by respectively (Cheng et al. (2020)):

$$n_{H_2} = n_F(n_c I_{elec}) / (n_e F)$$

$$n_{H_2O} = (n_{c_{FC}} I_{FC}) / (n_F)(n_e F)$$

$n_F$  symbolizes that Faraday's efficiency can be defined as the ratio between the actual and theoretical amount of  $H_2$  generated and is generally between 80-100%.  $I_{elec}$  is the operating current for the EL,  $F$  is the Faraday's constant;  $n_c$  and  $n_{c_{FC}}$  is the number of cells for the EL and FC, respectively; lastly,  $n_e$  is the number of electrons.

## A Hybrid Method Based on Logic Predictive Controller for Flexible Hybrid Microgrid with Plug-and-Play Capabilities

When the battery is fully charged, excess energy from the PV can potentially be exploited to run the electrolyzer at 4 kW. On the other hand, the PV does not accomplish to meet the load-generation mismatch; the fuel cell rated at 1 kW can be utilized in order to store hydrogen. It can be used as an alternative energy. The generated water from the fuel cell is stored in the water tank. Optionally, the utility grid can be used in austere conditions, such as a lack of energy in the PV or accumulators. The power flows (in Figure 5.3) of FC and EL can be calculated as follows:

- For the FC in Figure 5.3;

$$F_{out\_FC_{H_2O}}(k) = \varepsilon_{FC}(k)n_{H_2O} \quad (5.1)$$

$$F_{out\_FC_{Power}}(k) = \varepsilon_{FC}(k)F_{FC} \quad (5.2)$$

$$F_{in\_FT_{H_2}}(k) = F_{out\_EL_{H_2}}(k) \quad (5.3)$$

where  $F_{out\_FC_{H_2O}}$  represents the flow of water from the FC to the water tank,  $F_{out\_FC_{Power}}$  is the power from the FC to the battery, and  $F_{in\_FT_{H_2}}$  is the flow of hydrogen from the FT to the FC.

- For the EL in Figure 5.3;

$$F_{in\_BAT_{Power}}(k) = F_{out\_PV_{Power}}(k) + F_{out\_GR_{Power}}(k) + F_{out\_FC_{Power}}(k) \quad (5.4)$$

$$F_{in\_WT_{H_2O}}(k) = F_{out\_FC_{H_2O}}(k) \quad (5.5)$$

$$F_{out\_EL_{H_2}}(k) = \varepsilon_{EL}(k)n_{H_2} \quad (5.6)$$

where  $F_{in\_BAT_{Power}}$  is the total power in the BAT.  $F_{out\_PV_{Power}}$  is the power for the load, battery, and utility grid.  $F_{out\_GR_{Power}}$  is the power for the load.  $F_{in\_WT_{H_2O}}$  is the water from the FC.  $F_{out\_EL_{H_2}}$  is the flow from the EL to the FT.

Also, consider these equations:

$$F_{out\_FT_{H_2}}(k) = \varepsilon_{FC}(k)n_{H_2O} \quad (5.7)$$

$$F_{out\_BAT_{Power}}(k) = \varepsilon_{EL}(k)F_{EL} \quad (5.8)$$

$$F_{out\_WT_{H_2O}}(k) = \varepsilon_{EL}(k)n_{H_2} \quad (5.9)$$

$$F_{out\_PV_{Power}}(k) = \varepsilon_{PV}(k)F_{out\_PV}(k) \quad (5.10)$$

$$F_{out\_GR_{Power}}(k) = \varepsilon_{GR}(k)F_{out\_GR}(k) \quad (5.11)$$

where  $F_{out\_FT_{H_2}}$  represents the flow of hydrogen from FT to the EL,  $F_{out\_BAT_{Power}}$  is the power from the BAT to the EL,  $F_{out\_WT_{H_2O}}$  is the flow of water from the WT to the EL.

- The last step is to calculate the evolution operator for the accumulator (see Eq. (3.47)).

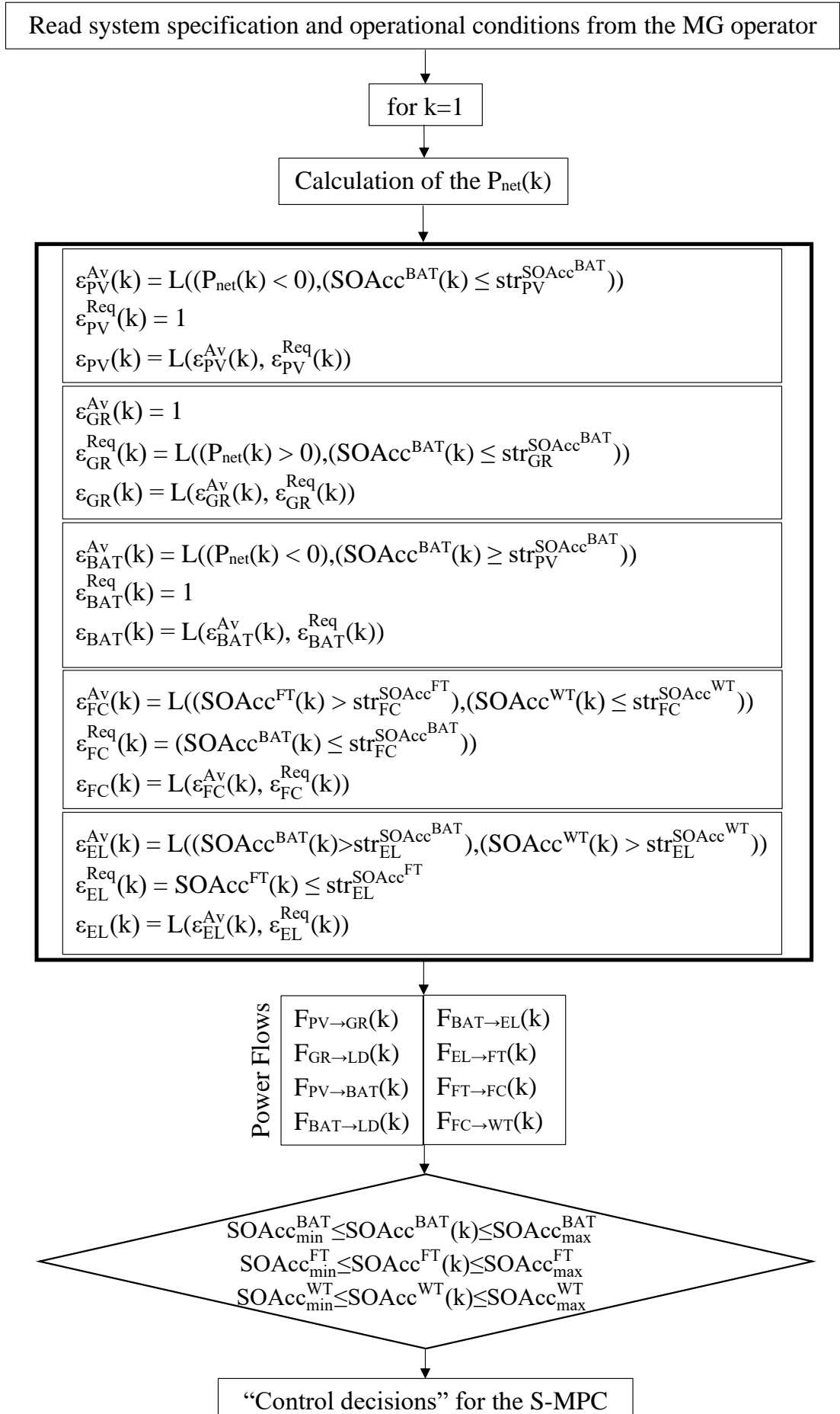
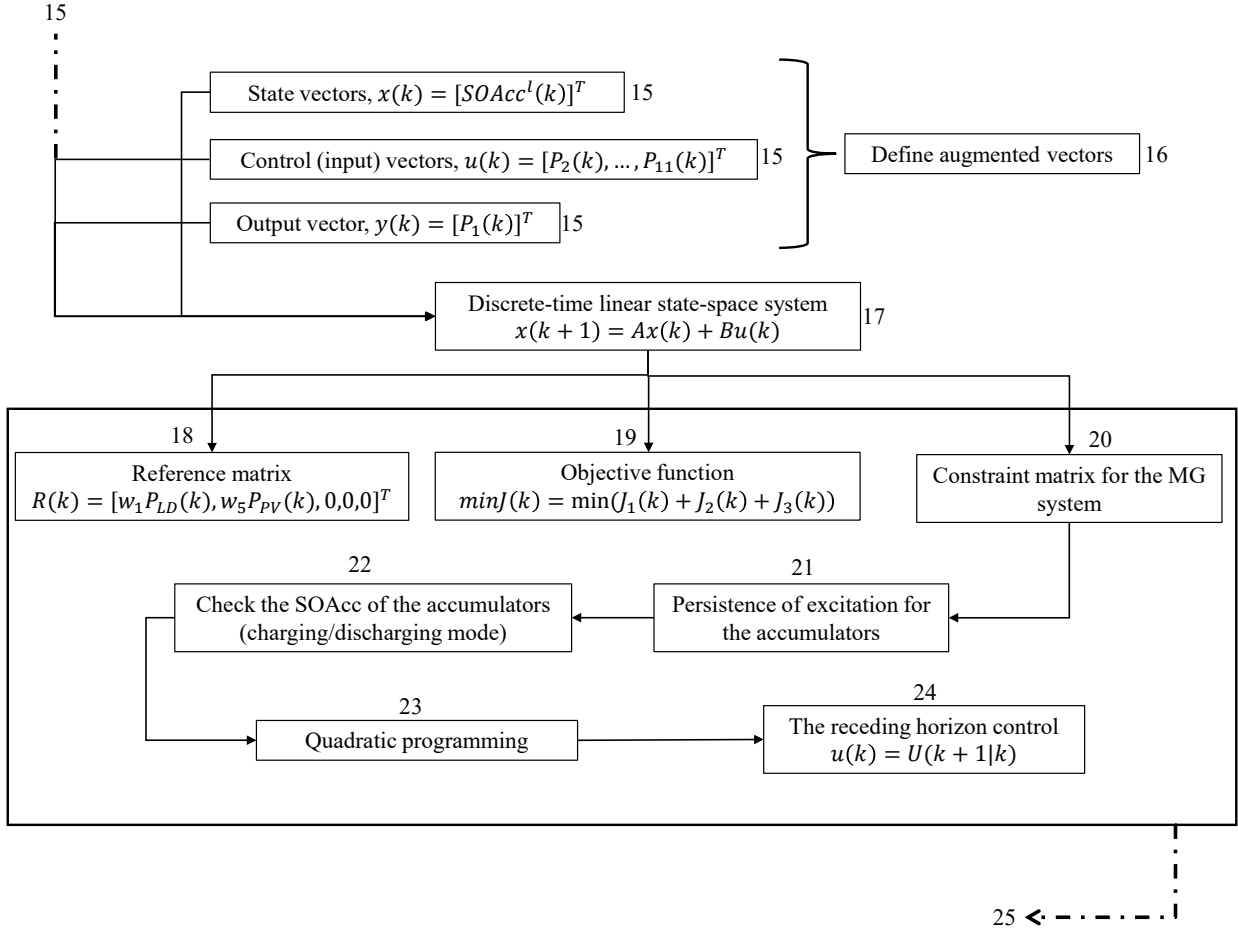


Figure 5.6 The flow chart of the ε-variables

**5.4.2. Step 2: Generating the optimal controller for each operational mode**

From Step 1, the control decisions obtained are utilized to find the optimum system control, state, and output vectors for the S-MPC. There are several stages as follows (**Point 15**): Define the system-state, control, and output vectors for the MG with the help of Equation (3.47-3.49) and Eq. (3.52):



**Figure 5.7** A graph is shown in the second step for the hybrid control method; points addressed in the text are indicated by numbers.

From Eq. (3.52), the system-state vector of the MG is obtained as follows (**Point 15**):

$$x_{a1}(k) = [SOAcc^{BAT}(k)] \quad (5.12)$$

$$x_{a2}(k) = [SOAcc^{FT}(k)] \quad (5.13)$$

$$x_{a3}(k) = [SOAcc^{WT}(k)] \quad (5.14)$$

$SOAcc^{BAT}(k)$ ,  $SOAcc^{FT}(k)$ , and  $SOAcc^{WT}(k)$  are the state of accumulators for the battery, hydrogen tank, and water tank, respectively. From Eq. (3.49) and Eq. (5.1-5.11), the system-control (input) vector of the MG is found as follows (**Point 15**):

$$u(k) = [PV_{LD}(k); GR_{LD}(k); PV_{BAT}(k); BAT_{LD}(k); FC_{BAT}(k); BAT_{EL}(k); EL_{FT}(k); FT_{FC}(k); WT_{EL}(k)] \quad (5.15)$$

The dynamic process equations of the battery, hydrogen, and water tank can be represented by:

$$\begin{aligned} x_{a_1}(k) &= x_{a_1}(k-1) + b_{a_1}u(k-1) \\ \Delta x_{a_1}(k) &= b_{a_1}u(k-1) \end{aligned} \quad (5.16)$$

where  $b_{a_1} = [0 \ 0 \ \eta_{ch} \ -\eta_{dis} \ \eta_{ch} \ -\eta_{dis} \ 0 \ 0 \ 0 \ 0]$ .

$$\begin{aligned} x_{a_2}(k) &= x_{a_2}(k-1) + b_{a_2}u(k-1) \\ \Delta x_{a_2}(k) &= b_{a_2}u(k-1) \end{aligned} \quad (5.17)$$

where  $b_{a_2} = [0 \ 0 \ 0 \ 0 \ 0 \ 0 \ \eta_{ch_{H_2}} \ -\eta_{dis_{H_2}} \ 0 \ 0]$ .

$$\begin{aligned} x_{a_3}(k) &= x_{a_3}(k-1) + b_{a_3}u(k-1) \\ \Delta x_{a_3}(k) &= b_{a_3}u(k-1) \end{aligned} \quad (5.18)$$

where  $b_{a_3} = [0 \ 0 \ 0 \ 0 \ 0 \ 0 \ 0 \ 0 \ \eta_{ch_{H_2O}} \ -\eta_{dis_{H_2O}}]$ .

The system-output vector of the MG is as follows (**Point 15**):

$$y_a(k) = c_a x_a(k-1) + d_a u(k) \quad (5.19)$$

where  $c_a = 0$  and  $d_a = [w_1 \ w_1 \ 0 \ w_1 \ 0 \ 0 \ 0 \ 0 \ 0 \ 0]$ . From the definition of  $y_a$ ,

$$\sum (w_1 P_{LD}(k) - y_a(k))^2 \quad (5.20)$$

where  $w_1$  is a positive weight coefficient for the minimization of the operational cost of the hybrid MG.

$$y_b(k) = w_3(P_2(k) + P_4(k)) = c_b x_a(k-1) + d_b u(k) \quad (5.21)$$

With respect to  $y_b$ ,

where  $c_b = 0$  and  $d_b = [w_3 \ 0 \ w_3 \ 0 \ 0 \ 0 \ 0 \ 0 \ 0 \ 0]$ . To increase the exported energy, the definition of  $y_b$ ,

$$\sum (w_5 P_{PV}(k) - y_b(k))^2 \quad (5.22)$$

where  $w_3$  is a positive weight coefficient for the enhancement of usage of the PV generator.

Regarding  $y_c$ ,  $y_d$ , and  $y_e$ ,

$$y_c(k) = w_2(P_4(k) + P_5(k) + P_6(k) + P_7(k)) = c_c x_a(k-1) + d_c u(k) \quad (5.23)$$



1. The utilization of the utility grid is minimized.

$$\min J_1(k) = \min \sum_k^{k+N_p} (w_1 P_{LD}(k) - y_a(k))^2 \quad (5.28)$$

2. The usage of the accumulators is penalized so as to prevent the charging from the utility grid

$$\min J_2(k) = \min \sum_k^{k+N_p} y_c(k)^2 + y_d(k)^2 + y_e(k) \quad (5.29)$$

3. The exported energy to the utility grid is encouraged.

$$\min J_3(k) = \min \sum_k^{k+N_p} (w_3 P_{PV}(k) - y_b(k))^2 \quad (5.30)$$

Define the overall cost function (objective function) for the MG:

$$\min J(k) = \min (J_1(k) + J_2(k) + J_3(k)) \quad (5.31)$$

Define the constraints for the MG (**Point 20**): Energy/matter flows from the PV array, utility grid, battery, fuel tank, electrolyzer, fuel cell, and water tank are non-negative values and are subject to their maximum values:

$$\begin{aligned} 0 \leq P_1(k) = P_{LD}(k) - y_a(k) \leq P_1^{max} \\ 0 \leq P_m(k) \leq P_m^{max} \end{aligned} \quad (5.32)$$

where  $P_m^{max}$  ( $m = 1, 2, \dots, 11$ ) imply the maximum values of energy/matter flows. The sum of PV energy supplied directly for the load ( $P_2(k)$ ) and the battery for the charging ( $P_4(k)$ ) should be smaller than the energy flow from the PV array, ( $P_{PV}(k)$ ).

$$P_2(k) + P_4(k) \leq P_{PV}(k) \quad (5.33)$$

The  $SOAcc^{BAT}$  for the battery,  $SOAcc^{FT}$  for the fuel tank, and  $SOAcc^{WT}$  for the water tank are restricted between their minimum and maximum values (Cavus et al. (2023)).

$$\begin{aligned} SOAcc^{BAT^{min}} \leq SOAcc^{BAT} \leq SOAcc^{BAT^{max}} \\ SOAcc^{FT^{min}} \leq SOAcc^{FT} \leq SOAcc^{FT^{max}} \\ SOAcc^{WT^{min}} \leq SOAcc^{WT} \leq SOAcc^{BAT^{WT}} \end{aligned} \quad (5.34)$$





## A Hybrid Method Based on Logic Predictive Controller for Flexible Hybrid Microgrid with Plug-and-Play Capabilities

Then, minimize the quadratic cost function as follows (**Point 23**):

$$J(U) = \sum_{k=0}^{N_p-1} (x(k)^T Q x(k) + u(k)^T C x(k)) + x(N)^T Q_f x(k) \quad (5.43)$$

where  $N$  is called the horizon of the quadratic problem.  $Q$  is the state weight  $Q = Q^T \geq 0$ ;  $C$  is the control weight  $C = C^T > 0$  and  $Q_f$  is the final cost weight  $Q = Q_f^T \geq 0$ .

Note that  $X = (x(0), x(1), \dots, x(N))$  is a linear function of  $x(0)$  and  $U = (u(0), u(1), \dots, u(N-1))$ .

$$\begin{bmatrix} x(0) \\ x(1) \\ \vdots \\ x(N) \end{bmatrix} = \begin{bmatrix} 0 & 0 & \dots & 0 \\ B & 0 & \dots & 0 \\ AB & B & 0 & \vdots \\ \vdots & \vdots & \ddots & 0 \\ A^{N-1}B & A^{N-2}B & \dots & B \end{bmatrix} \begin{bmatrix} u(0) \\ u(1) \\ \vdots \\ u(N-1) \end{bmatrix} + \begin{bmatrix} I \\ A \\ A^2 \\ \vdots \\ A^N \end{bmatrix}$$

This matrix can be expressed as:

$$X = GU + Hx(0) \quad (5.44)$$

where  $G \in \mathbb{R}^{Nn.Nm}$  and  $H \in \mathbb{R}^{Nn.Nn}$ .

Equation (5.43) can be re-written as follows:

$$J(U) = X^T \underbrace{\begin{bmatrix} Q & 0 & \dots & 0 \\ 0 & \ddots & 0 & \vdots \\ \vdots & 0 & Q & 0 \\ 0 & \dots & 0 & Q_f \end{bmatrix}}_{Q_1} X + U^T \underbrace{\begin{bmatrix} R & 0 & \dots & 0 \\ 0 & \ddots & 0 & \vdots \\ \vdots & 0 & R & 0 \\ 0 & \dots & 0 & R_f \end{bmatrix}}_{Q_2} U$$

These matrices are combined with Eq. (5.44) to obtain Eq. (5.45) using the QP:

$$J(U) = (GU + Hx(0))^T Q_1 (GU + Hx(0)) + U^T Q_2 U \quad (5.45)$$

The calculation of receding horizon control (**Point 24**):

In the S-MPC principle, the optimization problem is solved during each sampling time  $k$ , and the first element of  $U(k)$  is employed to the MG:

$$u(k) = U(k+1|k) \quad (5.46)$$

### 5.4.3. Step 3: Implementing the optimal decisions using the logic control

As illustrated in Figure 5.17, in this section, the utility grid ( $PV_{GR}$  and  $GR_{LD}$ ) is removed, and the EV fleet that their batteries have 45 kWh, 55 kWh, and 60 kWh ( $EV_{LD}$ ) are added, and the state space is updated (**Point 25**). Then, the power flows are re-calculated by multiplying Eq.

(5.15) and (3.52) (**Point 26**).

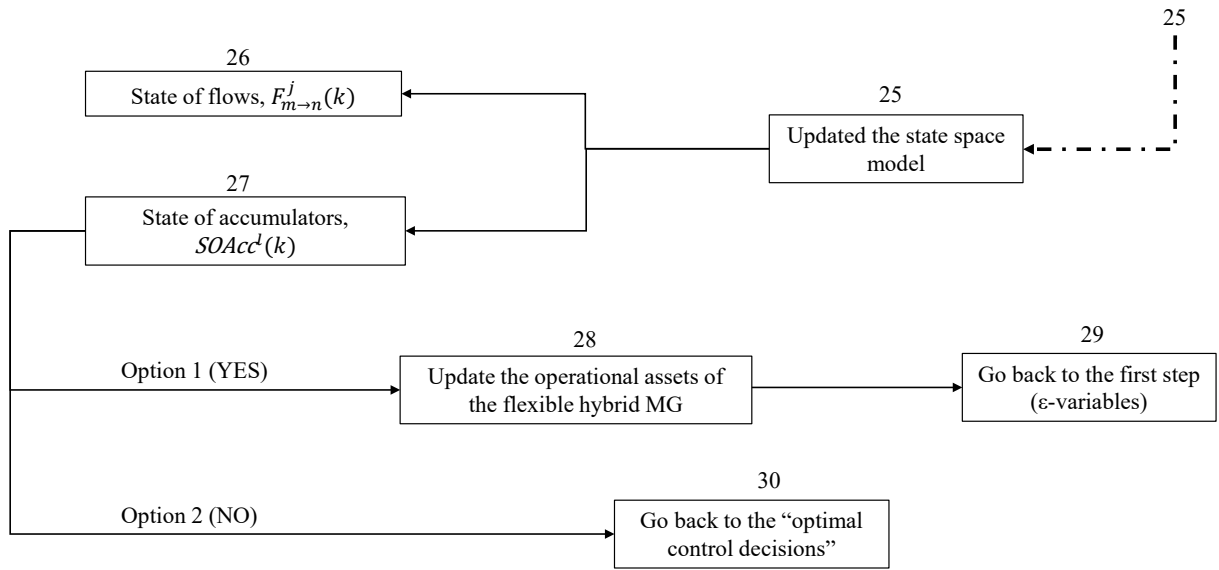


**Figure 5.8** A graph shown in the third step for the hybrid control method; points addressed in the text are indicated by numbers.

$$F_{a \rightarrow b}^j(k) = u(m)\varepsilon_i(k) \quad (5.47)$$

$$F_{EV \rightarrow LD}^{Power}(k) = P_{net}(k)\varepsilon_i(k) \quad (5.48)$$

$$F_{PV \rightarrow EV}^{Power}(k) = P_{net}(k)\varepsilon_i(k) \quad (5.49)$$

where  $u(m)$  is the control variables of the S-MPC for  $m=2,4,\dots,11$ . After that, another step is to measure the evolution operator for the accumulators ( $BAT$ ,  $FT$ , and  $WT$ ) (see Eq.(5.2)) (**Point 27**).

Finally, the hybrid control method is checked to determine whether the system specifications/inputs of the flexible hybrid MG operator changed for the next time step or not (removing the utility grid and adding the EVs).

If YES, the operational assets of the flexible hybrid MG are updated (**Point 28**), and the system goes back to the first step to implement the standard  $\varepsilon$ -variables (**Point 29**). Then, all 3 steps are re-implemented.

If NO, the next step is to go back to the "optimal control decisions" (**Point 30**). Then, the third step (optimal  $\varepsilon$ -variables) is re-implemented.

In summary, to simply the hybrid control method is composed of several phases, as shown in Figure 5.9:

- Some system specifications and operational conditions from the MG operator, such as PV and load data, and some parameters, including battery, fuel tank, and water tank, are defined.

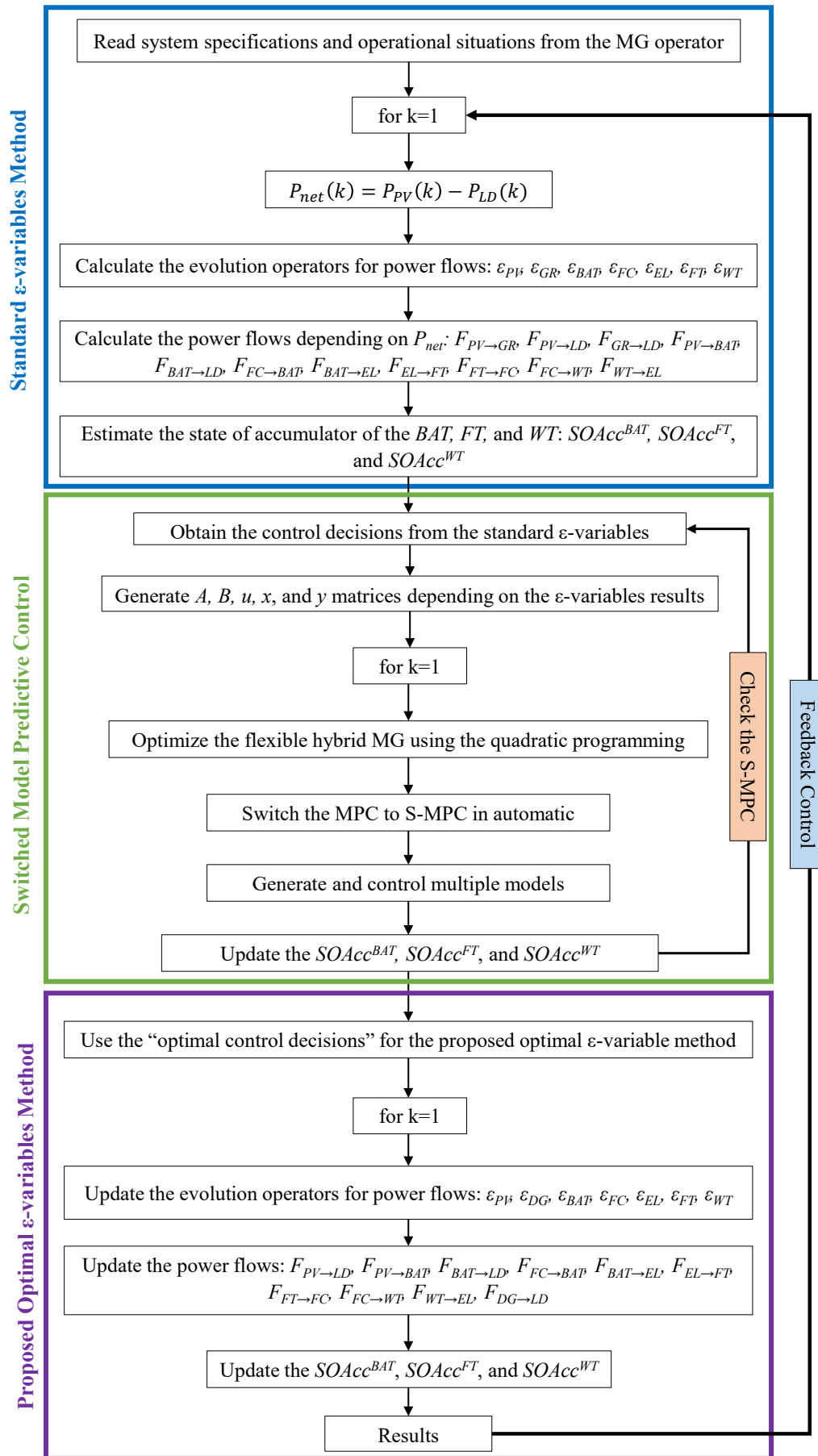


**Figure 5.9** Flow-chart of the proposed hybrid optimal method for the flexible hybrid MG.

- Net energy  $P_{net}$  (differences between the PV and the load data for 48 hours and 8760 hours) is calculated. However, net energy for the FC and EL is calculated according to Eq.(5.1-5.11)
- The evolution operators for the accumulators and converters are calculated; then, the power flows among the components of the hybrid MG are calculated.
- The last step in the  $\varepsilon$ -variables is the measurement of the  $SOAcc$  for the  $BAT$ ,  $FT$ , and  $WT$ .
- The first step in the S-MPC is to evaluate the "control decisions" obtained by exploiting the standard (non-optimal)  $\varepsilon$ -variables.
- The  $A$ ,  $B$ ,  $u$ ,  $x$ , and  $y$  matrices are obtained depending on the "control decisions".
- Multiple models are evaluated for the accumulators, depending on the amount of power  $P_i^j$  and  $SOAcc^l$ .
- After that, the persistence of excitation for the accumulators ( $BAT$ ,  $FT$ , and  $WT$ ) is implemented in order not to allow the charging and discharging conditions for the accumulators simultaneously.
- The hybrid MG system is optimized with the help of "quadratic programming".
- The state of the accumulators for the battery, fuel tank, and water tank is updated.
- "Optimal control decisions" are measured and compared with former "control decisions".
- In the final step, these "optimal control decisions" are embedded in the  $\varepsilon$ -variables-based EMS.
- The  $SOAcc$  for the  $BAT$ ,  $FT$ , and  $WT$  is measured and updated. The output of the last step will be thus optimal  $\varepsilon$ -variables-based EMS.
- The MG requirements and inputs from the MG operator will be checked at the start of each time step during the operating phase of the EMS. If this information is adjusted or changed, the operating states of the MG assets are updated, and the three steps of EMS construction are performed to take the new input into account. If this is not the case, the best  $\varepsilon$ -variables-based EMS can be utilized to regulate the MG for the following time step. It is worth noting that the suggested method determines whether or not the MG operator's system specifications/inputs change for the next time step.

### 5.5. Use Cases: Simulation results and discussions

Before the simulation, several parameters have been defined, as shown in Table 5.1. The weighting factors assigned to each extra term in the cost function are used to adjust the term's

## A Hybrid Method Based on Logic Predictive Controller for Flexible Hybrid Microgrid with Plug-and-Play Capabilities

priority or cost concerning the other control targets Cortés et al. (2009). The PV system's energy generation data and demand were obtained from Makonin (2019).

It is important to note that the control action is continuously adjusted based on feedback from the system being controlled. In the case of MPC, the control action is determined by solving an optimization problem at each time step, taking into account the current state of the system, the predicted future states, and the desired performance objectives. The optimization problem incorporates feedback information to minimize a cost function or achieve a specific control objective. MPC relies on feedback information to update control actions over time. It uses predictions of future states to optimize the control action sequence. The feedback information allows MPC to adapt and respond to changes and disturbances in the system, improving its performance and robustness.

While MPC is a form of closed-loop control, it is important to note that the optimization problem is solved based on a prediction of future system behaviour. This prediction is based on the model and assumptions about the system dynamics and constraints. Therefore, MPC can be seen as a combination of open-loop and closed-loop control, where the optimization problem is solved based on an open-loop prediction, and the resulting control action is adjusted in a closed-loop manner based on the feedback information.

Notations	Notations	Notations
$w_1 = 1.0$	$SOAcc^{BAT}(1) = 0.3$	$P_m^{max} = 5 \text{ kW}$
$w_2 = 0.4$	$SOAcc^{FT}(1) = 0.9$	$C_{BAT}^{max} = 96 \text{ kWh}$
$w_3 = 0.3$	$SOAcc^{WT}(1) = 0.5$	$C_{FT}^{max} = 10.1 \text{ kWh}$
$w_4 = 0.5$	$F_{EL} = 4 \text{ kW}$	$C_{WT}^{max} = 39.7 \text{ kWh}$
$w_5 = 0.5$	$F_{FC} = 1 \text{ kW}$	$SOAcc_{max}^l = 0.9$
$nc_{EL} = 15$	$nc_{FC} = 40$	$SOAcc_{min}^l = 0.2$
$\eta_{ch}^l = 0.9$	$\eta_{dis}^l = 0.85$	$\Delta t = 1 \text{ s}$
$C_{EV_1}^{max} = 45 \text{ kWh}$	$C_{EV_2}^{max} = 55 \text{ kWh}$	$C_{EV_3}^{max} = 60 \text{ kWh}$

**Table 5.1** Parameters for the real system (Ipsakis et al. (2009)).

### 5.5.1. Use Case 1: Control of the flexible hybrid MG using logic control

The system's behaviour is analyzed during the simulation of the flexible hybrid MG with logic control. Initially, the battery is in a discharging mode, as indicated by the digit 0 in the first position of the three-digit code, as shown in Figure 5.10. As the simulation progressed, the PV system's output was utilized to satisfy the mismatch load demand. If the PV system generates excess energy, it is used to charge the battery, which occurred at the 13th time step. Consequently, the three-digit code is changed to (100) to indicate that the battery is in charging mode. At the 15th time step, the battery continued to charge, and the WT reached its maximum output. In this instance, the three-digit code is changed to (101) to indicate that the battery was in charging mode while the WT was being filled. After one hour, the battery is neither charging nor discharging, but the WT still is filling, so the three-digit code was updated to (001). Between the 16th and 22nd time steps, the battery is discharged. At the beginning of the 22nd and 30th-time steps,

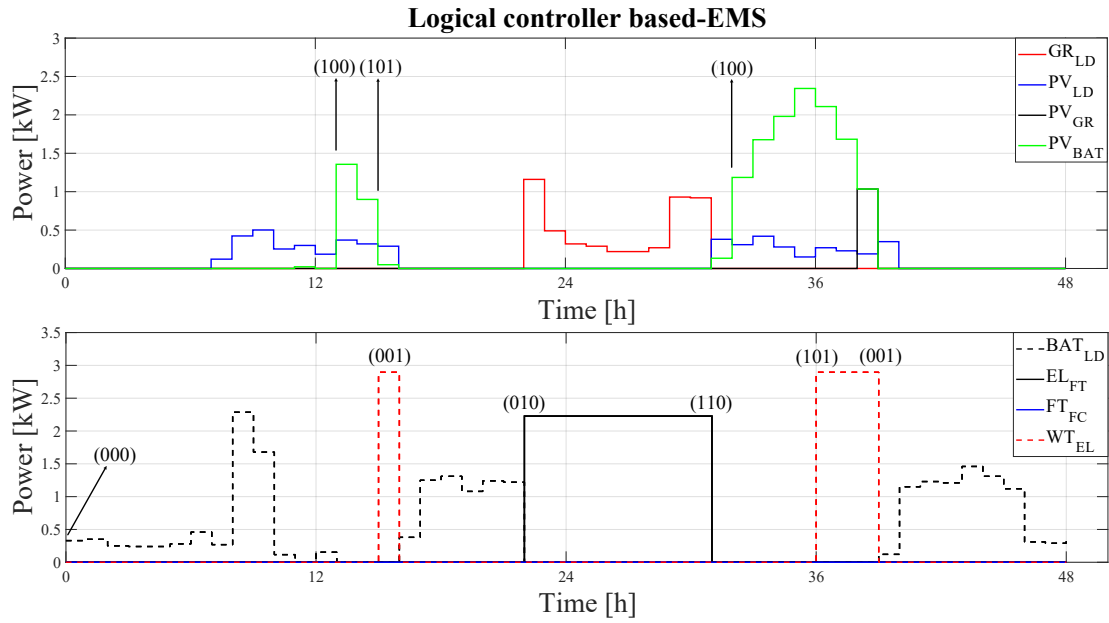


**Figure 5.10** The results of working of logical controller based-EMS

the FT is filling, and the utility grid is also used to compensate for the imbalance between load and generation. Throughout this time frame, the three-digit code was changed to (010). The three-digit code is updated to (110) after the PV system supplies power to the battery for one hour. The WT is fully filled at the 32nd time step, but the battery remains in charging mode. The three-digit code is therefore changed to (100). At the start of the 36th time step, the WT reached its maximum capacity, and the battery continued to charge, resulting in the update of the three-digit code to (101). The battery is neither charged nor discharged after three hours, while the WT remains at its maximum capacity. As a result, the three-digit code for these states was changed to (001).

The logic control approach in the control of the flexible hybrid microgrid exhibited distinct behaviour, as indicated by the changing three-digit code, which reflected the operational modes of the accumulators and converters' utilization to manage load-generation imbalances. The analysis of these code variations provides valuable insights into the effectiveness of the control strategy in managing energy flow.

$F_{EL}$  and  $F_{FC}$  were selected as 4 kW and 1 kW. The evolution operator of  $\varepsilon_{PV}$  is working in order to meet the load-generation mismatch for the building and charge the battery in the case of excess energy, as shown in Figure 5.11. If the PV is unable to generate sufficient power, either the battery or the FC will ensure that the load is met. If the battery is depleted and there is no accessible hydrogen, the grid will supply energy. In other words, when there is no energy from the PV, the evolution operator of  $\varepsilon_{BAT}$ ,  $\varepsilon_{FC}$  or  $\varepsilon_{EL}$  is converted from 0 to 1 to compensate for the load-generation mismatch. If there is still insufficient energy in the battery, fuel cell, and electrolyzer, the utility grid will start to work. Hence, the evolution operator of  $\varepsilon_{GR \rightarrow LD}$  is converted from 0 to 1, as illustrated in Figure 5.11. On the other hand, FC will work to hot the water tank when the  $SOAcc^{WT}$  of the water tank is less than the critical value (<20%). Therefore, the evolution operator of  $\varepsilon_{FC \rightarrow WT}$  turns from 0 to 1, as demonstrated in Figure 5.11. When the

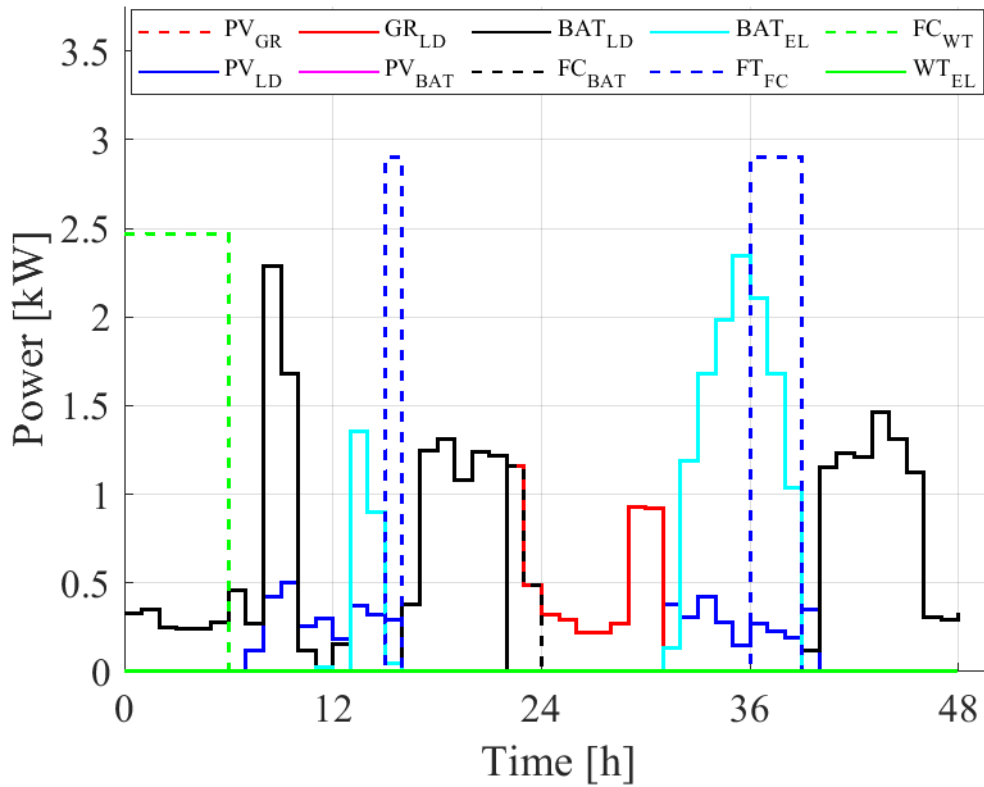


**Figure 5.11** The results of power flows using standard  $\varepsilon$ -variables

$SOAcc^{FT}$  has enough energy to give FC, the evolution operator  $\varepsilon_{FT \rightarrow FC}$  converts to 1. On the other hand, the evolution operator  $\varepsilon_{FC \rightarrow BAT}$  is activated to charge the battery when excessive energy is in the FC. Hence the binary variables of  $\varepsilon_{FC \rightarrow BAT}$  are turned to 1 at the end of the control (see Figure 5.10).

### 5.5.2. Use Case 2: Controlling the flexible hybrid MG using S-MPC

The results of the standard  $\varepsilon$ -variable method are utilized to obtain the components of the S-MPC, such as coefficient  $A$  and  $B$ , control (input) vector  $u$ , state vector  $x$ , and output vector  $y$ . At the end of the second step of the proposed method, the optimal LQ control decisions are obtained.

As shown in Figure 5.12, the PV works not only for the load but also for the utility grid and battery  $PV_{GR}$  and  $PV_{BAT}$ . Hence, the practicality of PV usage is enhanced. Moreover, the discharging of the accumulators decreases. The accumulator's utilization is penalized in order to prevent the charging from the utility grid. The energy consumption from the utility grid  $GR_{LD}$  (running cost of the MG) is decreased, as illustrated in Figure 5.12.

The increase in the exported energy and the decrease in the imported energy are the main differences between the logic control and optimal  $\varepsilon$ -variables. To prove that, the controller has been simulated for one year (8760 hours). Our results illustrate that the exported energy to the utility grid  $PV_{GR}$  is encouraged from 1705.35 kWh to 2571.01 kWh. Energy imported from the grid significantly decreased from 1494.36 kWh to 796.46 kWh, as demonstrated in Figure 5.13. These results are expected and desired since the optimal control decisions are obtained using optimal  $\varepsilon$ -variables.

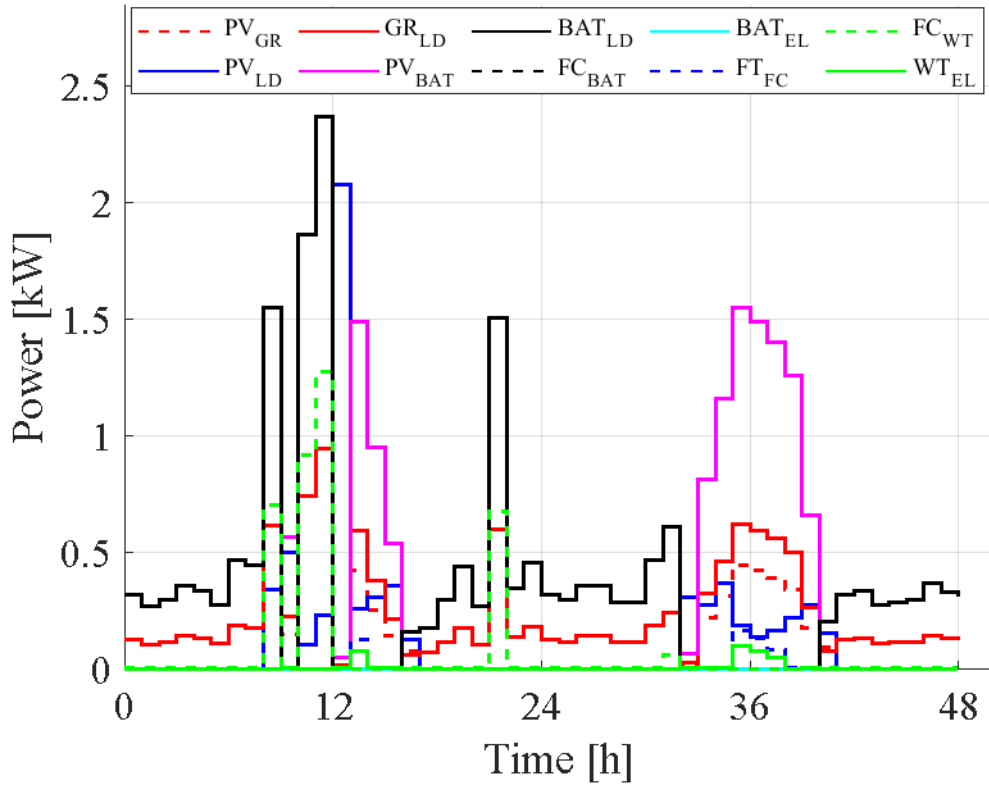


Figure 5.12 The results of power flows using the S-MPC method

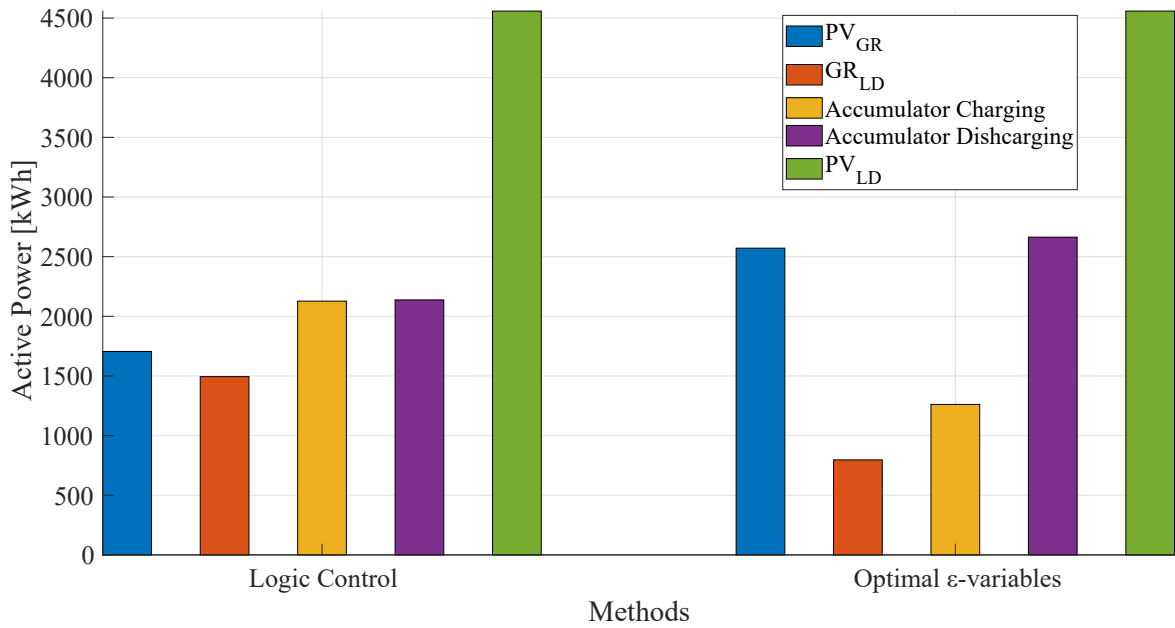


Figure 5.13 The results for the standard  $\epsilon$ -variables and optimal  $\epsilon$ -variables for one year.

Quantitatively, the decrease in grid-supplied energy imports is approximately 46.9%, indicating a significant reduction in reliance on grid-supplied energy. In addition, the increased exported energy demonstrates a substantial increase of approximately 50.8% in the use of RESs, emphasizing the enhanced integration of RESs into the MG system. From a cost perspective, the implementation of optimal  $\varepsilon$ -variables yields substantial advantages. The decreased dependence on imported energy reduces the costs associated with grid-supplied electricity. While the specific cost reduction percentage can vary based on individual circumstances, the overall cost savings attributable to optimal  $\varepsilon$ -variables-optimized control decisions are evident.

In summary, the implementation of optimal  $\varepsilon$ -variables demonstrates its effectiveness in optimizing the energy management system of the microgrid. This is evidenced by a significant reduction in energy imported from the grid, an impressive increase in the use of RESs, and the resulting cost savings. The application of optimal  $\varepsilon$ -variables establishes it as a viable and advantageous strategy for improving the performance and sustainability of flexible hybrid MGs.

### ***5.5.3. Use Case 3: Incorporating plug-and-play EV fleet***

We observe slight variations in the power profiles of EVs between the two controllers in Figure 5.14. The distinctive control strategies employed by each controller account for these distinctions. The MPC-based EMS Controller uses the plug-and-play capability of S-MPC to optimise the power allocation adaptively based on the current system state and EV fleet characteristics. The plug-and-play capability of S-MPC enables the seamless integration of new EVs into the system without extensive modifications to the control algorithm. It takes into account the variability and unpredictability of EV fleet behaviour, making it flexible and adaptable to fleet composition changes. This feature enables the MPC-based EMS Controller to manage the EV fleet efficiently and optimise power flows, even as new EVs are added or removed.

The logical based-EMS Controller manages the EV fleet and distributes power based on predefined rules and heuristics. However, manual adjustments or modifications may be necessary when integrating new EVs into the system. The MPC based-EMS Controller, on the other hand, leverages the plug-and-play capability of S-MPC to enable the seamless integration of new EVs into the system without extensive reconfiguration. The MPC algorithm adapts to changes in the composition of the EV fleet and optimises power distribution based on the current state of the system, taking into account factors such as EV load requirements, grid constraints, and forecasts. MPC Based-EMS Controller scalability and adaptability are enhanced by the plug-and-play capability of S-MPC. It simplifies the incorporation of new EVs into the fleet and ensures efficient utilisation of their variable energy resources. This capability allows the controller to effectively manage the variability and unpredictability of the EV fleet, resulting in optimised power flows and enhanced system performance. In conclusion, the plug-and-play capability of S-MPC in the MPC-based-EMS Controller improves its adaptability and scalability, allowing for seamless integration of new EVs and efficient fleet management. The choice between these controllers depends on the specific system requirements, the desired control approach, and the importance placed on adaptability, optimisation, and integration simplicity.

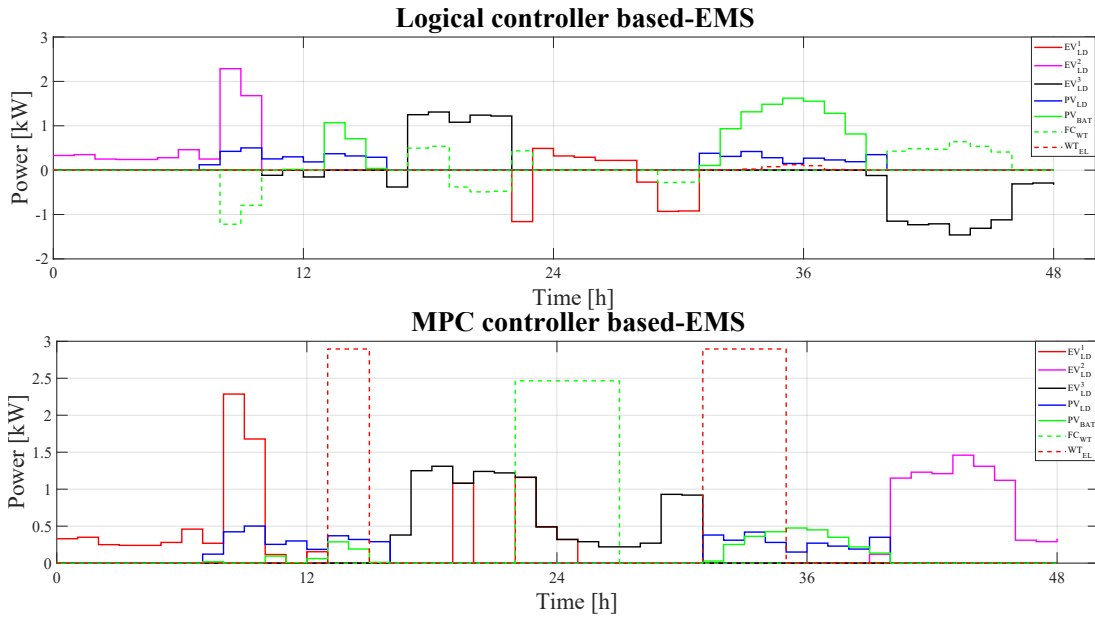


**Figure 5.14** Incorporating plug-and-play EV fleet using the logical controller and MPC controller based-EMS

The  $SOAcc$  variables play a crucial role in the decision-making processes of the energy management system, allowing for the efficient utilisation of energy resources. By monitoring and controlling  $SOAcc$  levels, the system can ensure optimal charging and discharging of the battery and EVs, thereby balancing supply and demand for energy. In Figure 5.15, variations in  $SOAcc$  indicate the dynamic nature of the system's operation. These variations denote substantial modifications to the control strategy, such as switching between battery discharging and grid running modes or battery discharging and EV running modes. Overall, the  $SOAcc$  variables provide valuable information about the energy storage levels of the system's battery and EVs. Their fluctuations and patterns highlight the dynamic nature of the energy management system, which enables the efficient use of available energy resources and the effective adaptation to changing system conditions and control strategies.

To make it clear, in the third step of the optimal  $\varepsilon$ -variables, the MG is working in islanded mode. Three different EVs have been added separately and at different times. To show the capability of our proposed method, the conditions of EL and FC are switched OFF. When the PV and BAT do not have enough energy for the building, the EV meets the load-generation mismatch through the evolution operator of  $\varepsilon_{EV \rightarrow LD}$ . On the other hand, when there is excessive energy in the PV, the PV charges the BAT employing the  $\varepsilon_{PV \rightarrow BAT}$ . The battery stores the energy and uses it for the building with the evolution operator of  $\varepsilon_{BAT \rightarrow LD}$  when there is a load-generation mismatch, as shown in Figure 5.16. Our results show that when removing the utility grid and adding the EV fleet, the controller works properly through the flexible hybrid MG. The  $SOAcc$  of the battery and EV fleet are working at desired conditions, as shown in Figure 5.15. In other words, their  $SOAcc$  does not below or exceed the critical values during operation because our proposed method is optimal.

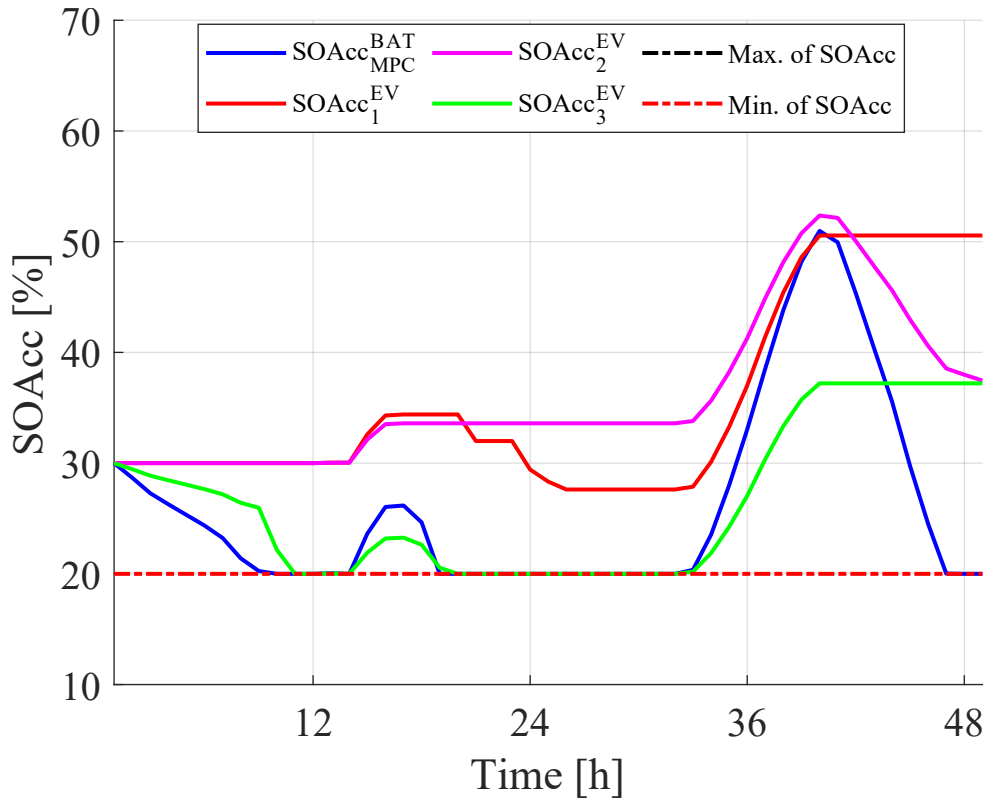


**Figure 5.15** The illustration of the SOAcc of the battery is the hybrid control method.

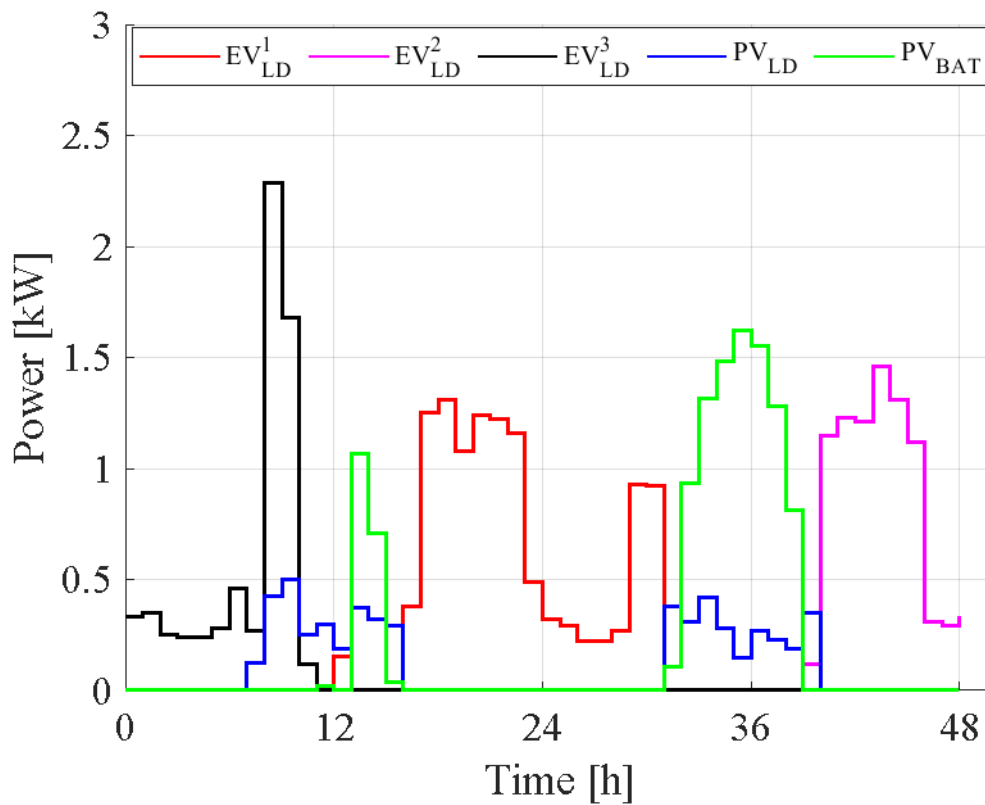


**Figure 5.16** The results of power flows (adding the EV fleet and removing the utility grid).

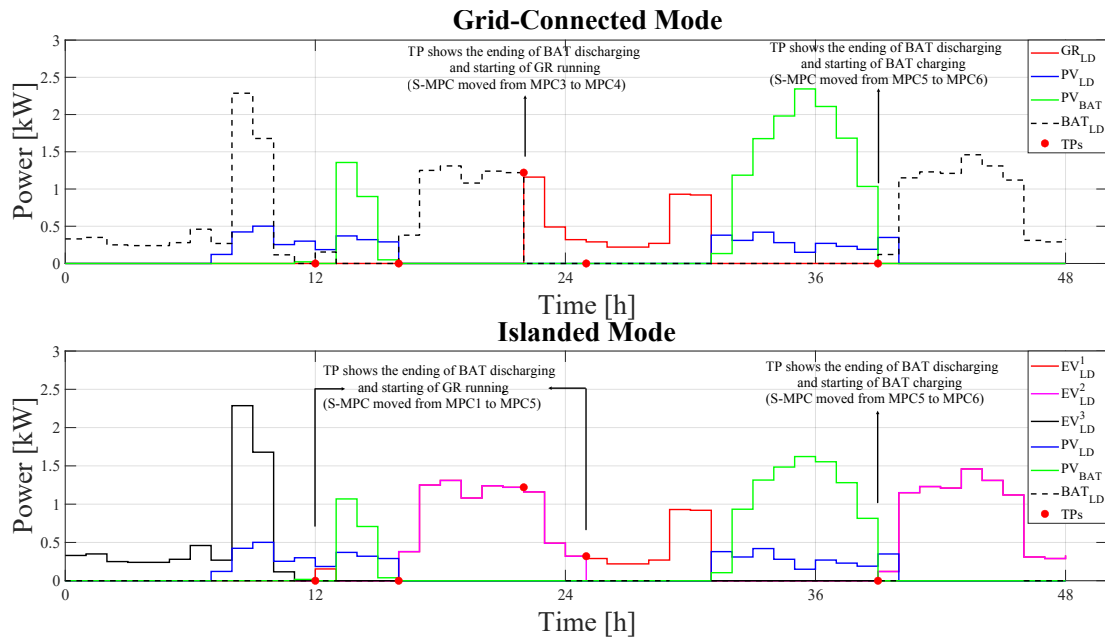


**Figure 5.17** The results of power flow when the MG is in grid-connected mode and islanded mode

#### 5.5.4. Use Case 4: Islanded MG

**Grid-Connected Mode:** The results for grid-connected mode display the transition points (TPs) at specific time steps, indicating significant changes in system operation. In this mode, the TP indicates the transition from the battery (BAT) discharging to the GR operation, as well as the transition from BAT discharging to BAT charging. As shown in Figure 5.17, at 12h, 16h, 22h, and 25h, the TP signifies the end of BAT charging and the start of GR running. This indicates that the battery has reached capacity, and the system has switched to grid power. The transition from BAT discharge to GR operation indicates the capacity limitations of the battery and the need to rely on the grid to meet the load requirements. In addition, the TP at 39h indicates the end of BAT discharging and the beginning of BAT charging. This indicates that the battery is depleted and requires recharging, possibly in preparation for future grid instability or increased load demand. The transition from BAT discharging to BAT charging demonstrates the system's adaptability and capacity to optimise its operation by recharging the battery energy storage.

**Islanded Mode:** Similar TPs are observed in the islanded mode, indicating significant changes in system operation. The TP represents the transition from BAT discharge to GR operation and from BAT discharge to EV operation. As demonstrated in Figure 5.17, the TPs at 12h, 16h, 22h, and 25h indicate the conclusion of BAT discharge and the start of GR running. This indicates that, in the absence of a grid connection, the battery has reached its minimum capacity, and the system switches to utilising power from a nearby generator or renewable sources. In the islanded mode, the switch from BAT discharge to GR operation signifies the system's reliance on alternative power sources. In addition, the TP at 39h indicates the end of BAT discharge and the beginning of EV operation. This indicates that the battery has been depleted, and the system has resorted to using power from EVs to meet load requirements. The transition from BAT discharge

## **A Hybrid Method Based on Logic Predictive Controller for Flexible Hybrid Microgrid with Plug-and-Play Capabilities**

---

to EV operation exemplifies the system's flexibility and plug-and-play capability, allowing EVs to contribute to the power supply in islanded mode.

These transition points illustrate the adaptive nature of the S-MPC algorithm and its capacity to make informed decisions based on the system's state and evolving requirements. The S-MPC can seamlessly transition between different control modes to ensure efficient energy management in both grid-connected and islanded modes by detecting specific conditions, such as low battery levels or the availability of alternative energy sources. The presence of transition points in both grid-connected and isolated modes demonstrates the efficacy of the S-MPC algorithm in managing power flows and optimising system operation. The ability to switch between different control modes enables the system to adapt to changing conditions and optimally utilise available energy sources, thereby enhancing grid stability and ensuring a reliable power supply.

### **5.6. Conclusions**

In conclusion, the proposed hybrid control method is entirely illustrated in the flexible hybrid MGs in which assets with PnP capabilities are constructed in Xanthi, Greece (Giaouris et al. (2018)). This method exploits a fuel cell and an electrolyzer so as to accomplish complex autonomy from the main grid. These studies demonstrate that the standard (non-optimal)  $\varepsilon$ -variables have several advantages, such as being scalable and practical for flexible hybrid MGs, especially complex hybrid power systems. However,  $\varepsilon$ -variables are not optimal. On the other hand, MPC predicts the system's future behaviour and chooses the optimal control action using a mathematical model. At each time step, MPC solves an optimization problem using the system's current state, predicted future states, and a cost function that reflects performance objectives and constraints. Nevertheless, it cannot control the flexible hybrid MG because of multiple operating models. S-MPC is a variation of MPC that uses multiple models to represent different system operating modes or scenarios. Based on the system's state and performance goals, S-MPC chooses a model and control strategy. However, S-MPC requires many more steps, making it harder to implement. Through the S-MPC, the amount of grid consumption is minimized by almost 46.7%, and the exported energy to the utility grid is encouraged by nearly 50.8%. Nonetheless, implementing the proposed hybrid control method has numerous steps, especially for complex hybrid MG. This issue makes the hybrid MG system more complicated in terms of controllability. In order to cope with this issue, the decisions of S-MPC are translated into the  $\varepsilon$ -variables. By doing so, a systematic methodology is obtained, and the control structure can be significantly simplified. Also, the computational complexity of the S-MPC is reduced. In other words, this hybrid control method model systematically and practically the control regulations that supervise the complex hybrid MG. Thus, it has the ability to permit more complex EMSs to be adopted readily.

The next chapter will be a conclusion and future works for all studies. Implementing MPC is difficult due to the requirement of a plant model with high computational and algorithmic complexity and numerous control parameters. Several machine learning (ML) techniques, such

as an RNN with long short-term memory (LSTM) and CNN, can be combined with the MPC to address these issues.



## Chapter 6. Conclusions

To summarise, there are many reasons in support of utilizing the MPC technique in order to manage the MG power system effectively. Utilizing cost functions and constraints, the MPC can make predictions regarding the generation and consumption of power and deal with unpredictability and disturbances. MPC, on the other hand, is not an accessible technology to put into practice, particularly in more complicated MG systems. In addition to this, a significant amount of processing power and time is required. In order to solve these issues, the MPC technique has been combined with the  $\varepsilon$ -variables used in this thesis. By utilizing this hybrid approach, the complexity of the MPC implementation can be reduced. At the same time, the scalability and controllability of the PBG system can be improved at any given point in time. Putting it another way, the MPC- $\varepsilon$ -variables technique makes the control of the system much easier to understand and implement. In this thesis, we first demonstrated that the MPC and the MPC- $\varepsilon$ -variables produce the same results. Next, as a case study, we gave an example of how the EMS can easily be altered without making any changes within the MPC. Finally, we concluded this article by demonstrating that the MPC and the MPC- $\varepsilon$ -variables produce the same results.

There are a number of reasons for utilizing the  $\varepsilon$ -variable method to manage the MG power system, but it is not the most effective method. On the other hand, S-MPC employs cost functions and constraints in conjunction with various optimization techniques to predict power generation and consumption. Nonetheless, S-MPC implementation is not simple, particularly in complex MG systems. To overcome the shortcomings of the  $\varepsilon$ -variable and S-MPC methods, we developed an extended optimal  $\varepsilon$ -variable technique that effectively: (i) reduces the operational cost of MG by nearly 35%, (ii) reduces the battery energy storage system usage by 42%, and (iii) increases the practicability of PV usage by 28%. The computational capability of the new method is comparable (+2%) to that of the S-MPC. This extended optimal  $\varepsilon$ -variable (i) improved the existing  $\varepsilon$ -variable method, (ii) reduced the complexity of the existing S-MPC implementation, and (iii) significantly enhanced the scalability and adaptability of the existing S-MPC implementation. The adaptability and scalability of the extended optimal  $\varepsilon$ -variable technique were improved by modifying a number of evolution operators and incorporating a diesel generator. Consequently, the proposed extended technique makes the system's control more straightforward and optimal.

In other chapters, the proposed hybrid control method is fully exemplified by the flexible hybrid MGs constructed in Xanthi, Greece (Giaouris et al. (2018)). This method employs a fuel cell and an electrolyzer to achieve complex independence from the main power grid. These studies demonstrate that the standard (non-optimal)  $\varepsilon$ -variables have a number of benefits, such

as being scalable and applicable to flexible hybrid MGs, particularly hybrid power systems with complex architectures. Nonetheless,  $\varepsilon$ -variables are non-optimal. Using a mathematical model, MPC predicts the system's future behaviour and selects the optimal control action. MPC solves an optimization problem at each time step by utilizing the system's current state, predicted future states, and a cost function that reflects performance objectives and constraints. However, it is unable to control the flexible hybrid MG due to the existence of multiple operating models. S-MPC is a variant of MPC that employs multiple models to represent various modes or scenarios of system operation. S-MPC selects a model and control strategy based on the system's state and performance goals. However, S-MPC requires many more steps, making its implementation more difficult. Through the S-MPC, the amount of energy consumed from the utility grid is reduced by nearly 53.3%, and the amount of energy exported to the utility grid is increased by nearly 50.8%. However, implementing the proposed hybrid control method involves numerous steps for hybrid MG that are particularly complex. This issue makes the hybrid MG system's controllability more complicated. In order to address this issue, the S-MPC decisions are translated into  $\varepsilon$ -variables. In this manner, a systematic methodology is obtained, and the control structure can be simplified considerably. Also, the S-MPC's computational complexity is reduced. In other words, this hybrid control method models the control regulations that supervise the complex hybrid MG systematically and practically. Thus, it has the capacity to facilitate the adoption of more complex EMSs. By eliminating the prediction horizon, the computational power of S-MPC can be decreased for future research. By doing so, S-MPC's steps can be reduced. This can be accomplished by combining the S-MPC with one artificial neural network (ANN) method, including RNNs and CNNs.

In summary, to highlight key findings:

### **MPC Advantages and Challenges:**

- MPC offers effective management of MG power systems through cost functions and constraints, handling unpredictability and disturbances.
- However, MPC is challenging to implement in complex MG systems, demanding significant processing power and time.

### **Hybrid Approach - MPC- $\varepsilon$ -Variables:**

- A hybrid approach combining MPC with  $\varepsilon$ -variables is introduced to address MPC implementation complexities.
- This approach enhances system controllability and scalability, simplifying implementation without sacrificing results.

### **Equivalence of MPC and MPC- $\varepsilon$ -Variables:**

- Demonstrated that MPC and MPC- $\varepsilon$ -Variables produce equivalent results, validating the effectiveness of the hybrid approach.

- 
- Highlighted flexibility in altering EMS without changes in MPC settings, showcasing practicality.

#### **Extended Optimal $\varepsilon$ -Variable Technique:**

- Introduced an extended optimal  $\varepsilon$ -variable technique to overcome limitations of  $\varepsilon$ -variable and S-MPC methods.
- Achieved significant improvements: 35% reduction in MG operational cost, 42% less battery usage, and 28% increased PV usage.

#### **Improved Scalability and Adaptability:**

- Modified evolution operators and incorporated a diesel generator to enhance the adaptability and scalability of the extended technique.
- Simplified system control, making it more straightforward and optimal.

#### **Application to Flexible Hybrid MGs:**

- Applied the proposed hybrid control method to flexible hybrid MGs in Xanthi, Greece.
- Demonstrated scalability and applicability to complex architectures, emphasizing benefits even with non-optimal  $\varepsilon$ -variables.

#### **Comparison with S-MPC:**

- Compared with S-MPC, the proposed hybrid method reduced energy consumption from the grid by 53.3% and increased energy export by 50.8%.
- Acknowledged the complexity of hybrid MG systems and proposed translating S-MPC decisions into  $\varepsilon$ -variables for simplification.
- Overall, the conclusions highlight the advantages of the hybrid approach, the success of the extended optimal  $\varepsilon$ -variable technique, and the practical implications for managing complex MG systems effectively.

### **6.0.1. Future Works**

#### **The issues of MPC:**

- **Prediction horizon:** MPC and ANN are predictive controllers, regardless of whether they incorporate disturbance forecasting into their control logic. MPC employs explicit optimization along a finite prediction horizon, whereas ANN learns behaviours to maximize the sum of immediate and discounted future rewards. The finite horizon is a weakness of MPC, which is most noticeable in jobs with sparse rewards, where a short horizon can render the agent excessively myopic (Bhardwaj et al. (2020)). Furthermore, larger prediction horizons cause MPC to suffer since they increase the number of state and

input variables in the optimization. Although infinite prediction horizons may profit from enhanced behaviour in the long run, it should be highlighted that ANN algorithms employ forecast information inefficiently. This is because all forecast data is flattened and given to the agent's observations without the time dependency. Throughout the learning process, the agent must determine the temporal dependency not explicitly mentioned in the problem formulation. MPC automatically preserves the time dependency (and hence the chronology) by considering the system dynamics computed in the controller model. A proposed synergistic method could address an optimization problem for MPC using small prediction horizons while benefiting from the infinite horizons that characterize ANN (Arroyo et al. (2022)).

- **Computational effort:** The burden of solving an optimization problem on-line, which might be complex and involve many optimization variables, is a significant disadvantage of implicit MPC. This is why MPC controller models are frequently simplified at the expense of optimality, and efficiency advances in optimization solutions are widely desired. Furthermore, state estimation and forecasting must be performed at each control step. Explicit MPC seeks to alleviate this load by generating a control strategy through behaviour cloning, whereas implicit MPC must be constructed first (Arroyo et al. (2022)).
- **Plant model:** Because MPC uses a system model to optimize actions for each control step, it requires knowledge of the current value of the state vector, which system measurements may not establish. As a result, state estimation is required to estimate the controller model's hidden states, i.e., those not monitored during operation (Akbulut et al. (2024); Arroyo et al. (2022)).

In summary, the MPC's implementation is difficult since the plant model is required and has high computational and algorithmic complexity and many control parameters. To solve these issues, a few of the ML techniques, such as a RNN with LSTM and CNN, can be merged with the MPC. Our proposed method suggests that some parameters in the MPC, such as the prediction horizon and rolling horizon approach, can be eliminated. Then the RNN-LSTM and CNN can work as a prediction task. By doing that, the MPC has not required a correct plant model. Also, the computational power and algorithm complexity are decreased (Cavus et al. (2023)).

Moreover, in addressing uncertainties in future works, several considerations and approaches can be explored:

### **Data-Driven Approaches:**

- Leverage ML techniques, such as neural networks, to capture and model uncertainties in the system.
- Train models using historical data to learn the patterns of uncertainties and enhance the predictive capabilities of the controller.

### **Robust MPC:**

- 
- Implement Robust MPC techniques that inherently consider uncertainties in the system parameters and disturbances.
  - Develop methods to systematically handle uncertainties and variations to ensure system stability and performance.

#### **Hybrid MPC-ML Approaches:**

- Combine MPC with machine learning algorithms, such as reinforcement learning or ensemble methods, to adaptively respond to uncertainties.
- Develop hybrid control strategies that seamlessly switch between MPC and machine learning approaches based on the prevailing uncertainties.

#### **Online Learning:**

- Develop MPC variants with online learning capabilities, allowing the controller to adapt and improve its predictions over time as it receives new data and experiences uncertainties.

By addressing uncertainties through these avenues, future works can enhance the robustness, adaptability, and overall performance of the MPC-based control system in the face of unpredictable factors.



## **Appendix A. Appendix**

### **A.1. Microgrid Configuration Details for Chapter 3**

For Chapter 3, the microgrid (MG) configuration details are as follows:

- **PV Generator:**
  - Capacity: 14 kW
  - Orientation: South at an optimal tilt angle of 30 degrees
- **Batteries:**
  - Storage Capacity: 20 kWh
  - Round-Trip Efficiency: 85%
  - Max Charging/Discharging Rates: 50 kW
- **Load:**
  - Residential Consumers
  - Average Power Demand: 30 kW daily
  - Daily and Seasonal Variations
- **PV Array:**
  - 50 Solar Panels
  - Total Area: 80 m<sup>2</sup>
  - Assumed Solar Irradiance: 1000 W/m<sup>2</sup>



## Appendix B.

### B.1. System Parameter Details for Chapter 4

For Chapter 4, the details of the system parameters are provided below:

- **MG System Components:**
  - PV Array Capacity: 14 kW
  - Battery Storage Capacity: 20 kWh
  - Diesel Generator Capacity: 5.4 kW
- **PV Generator:**
  - Maximum Power to Grid ( $PV_{GR}^{max}$ ): 5 kW
  - Maximum Power to Load ( $PV_{LD}^{max}$ ): 5 kW
  - Maximum Power to Battery ( $PV_{BAT}^{max}$ ): 5 kW
- **Battery and Load:**
  - Maximum Power from Battery to Load ( $BAT_{LD}^{max}$ ): 5 kW
  - Maximum Power from Grid to Load ( $GR_{LD}^{max}$ ): 5 kW
- **State of Charge for Accumulators:**
  - Initial State of Charge for Battery ( $SOAcc^{BAT}(1)$ ): 30%
  - Initial State of Charge for Fuel tank ( $SOAcc^{FT}(1)$ ): 90%
  - Initial State of Charge for Water tank ( $SOAcc^{WT}(1)$ ): 50%
  - Minimum State of Charge for Accumulator  $l$  ( $SOAcc_{min}^l$ ): 20%
  - Maximum State of Charge for Accumulator  $l$  ( $SOAcc_{max}^l$ ): 90%
- **Weighting Factors:**
  - Weight for Operational Cost Minimization ( $w_1$ ): 1.0
  - Weight for PV Generator Usage Enhancement ( $w_3$ ): 0.8
  - Weight for Battery Utilization Penalization ( $w_2$ ): 0.2



## Appendix C.

### C.1. Parameters for the Real System for Chapter 5 (Ipsakis et al. (2009))

For Chapter 5, the parameters for the real system are detailed below:

- **Weighting Factors:**

- Weight for Operational Cost Minimization  $w_1$ : 1.0
- Weight for Battery Utilization Penalization  $w_2$ : 0.4
- Weight for PV Generator Usage Enhancement  $w_3$ : 0.3
- Weight for Fuel tank Utilization Penalization  $w_4$ : 0.5
- Weight for Water tank Utilization Penalization  $w_5$ : 0.5

- **Power and Capacity Limits:**

- Maximum Power Output ( $P_m^{max}$ ): 5 kW
- Battery Capacity ( $C_{BAT}^{max}$ ): 96 kWh
- Flywheel Capacity ( $C_{FT}^{max}$ ): 10.1 kWh
- Wind Turbine Capacity ( $C_{WT}^{max}$ ): 39.7 kWh
- Maximum Load Power ( $F_{EL}$ ): 4 kW
- Fuel Cell Power ( $F_{FC}$ ): 1 kW

- **Other Parameters:**

- Number of Cycles for Electric Load ( $nc_{EL}$ ): 15
- Number of Cycles for Fuel Cell ( $nc_{FC}$ ): 40
- Charging Efficiency for Load ( $\eta_{ch}^l$ ): 0.9
- Discharging Efficiency for Load ( $\eta_{dis}^l$ ): 0.85
- Time Step ( $\Delta t$ ): 1 s
- Maximum Capacity for Electric Vehicles ( $C_{EV_1}^{max}, C_{EV_2}^{max}, C_{EV_3}^{max}$ ): 45 kWh, 55 kWh, 60 kWh



## References

- Aaslid, P., Korpås, M., Belsnes, M. M., and Fosso, O. B. (2022). Stochastic optimization of microgrid operation with renewable generation and energy storages. *IEEE Transactions on Sustainable Energy*, 13(3):1481–1491.
- Aghajani, G., Shayanfar, H., and Shayeghi, H. (2015). Presenting a multi-objective generation scheduling model for pricing demand response rate in micro-grid energy management. *Energy Conversion and Management*, 106:308–321.
- Ahmadi, H. and Martí, J. R. (2015). Mathematical representation of radiality constraint in distribution system reconfiguration problem. *International journal of electrical power & energy systems*, 64:293–299.
- Akbulut, O., Cavus, M., Cengiz, M., Allahham, A., Giaouris, D., and Forshaw, M. (2024). Hybrid intelligent control system for adaptive microgrid optimization: Integration of rule-based control and deep learning techniques. *Energies*, 17(10):2260.
- Alavi, S. A., Ahmadian, A., and Aliakbar-Golkar, M. (2015). Optimal probabilistic energy management in a typical micro-grid based-on robust optimization and point estimate method. *Energy Conversion and Management*, 95:314–325.
- Ali, S., Zheng, Z., Aillerie, M., Sawicki, J.-P., Pera, M.-C., and Hissel, D. (2021). A review of dc microgrid energy management systems dedicated to residential applications. *Energies*, 14(14):4308.
- Alipour, M., Gharehpetian, G. B., Ahmadihangar, R., Rosin, A., and Kilter, J. (2022). Energy storage facilities impact on flexibility of active distribution networks: Stochastic approach. *Electric Power Systems Research*, 213:108645.
- Aljohani, T. M., Ebrahim, A. F., and Mohammed, O. (2020). Hybrid microgrid energy management and control based on metaheuristic-driven vector-decoupled algorithm considering intermittent renewable sources and electric vehicles charging lot. *Energies*, 13(13):3423.
- Allahham, A. (2008). *Surveillance des systèmes à événements discrets commandés: Conception et implémentation en utilisant l'automate programmable industriel*. PhD thesis, Université Joseph-Fourier-Grenoble I.
- Allahham, A. and Alla, H. (2008). Post and pre-initialized stopwatch petri nets: Formal semantics and state space computation. *Nonlinear Analysis: Hybrid Systems*, 2(4):1175–1186.
- Allahham, A. and Alla, H. (2009). Monitoring of timed discrete events systems with interrupts. *IEEE transactions on automation science and engineering*, 7(1):146–150.
- Allahham, A., Greenwood, D., and Patsios, C. (2019). Incorporating ageing parameters into optimal energy management of distribution connected energy storage.
- Allahham, A., Greenwood, D., Patsios, C., and Taylor, P. (2022). Adaptive receding horizon control for battery energy storage management with age-and-operation-dependent efficiency and degradation. *Electric Power Systems Research*, 209:107936.
- Alzahrani, A., Shamsi, P., Dagli, C., and Ferdowsi, M. (2017). Solar irradiance forecasting using deep neural networks. *Procedia Computer Science*, 114:304–313.

## References

---

- Amoasi Acquah, M., Kodaira, D., and Han, S. (2018). Real-time demand side management algorithm using stochastic optimization. *Energies*, 11(5):1166.
- Ani, V. A. (2016). Design of a reliable hybrid (pv/diesel) power system with energy storage in batteries for remote residential home. *Journal of Energy*, 2016:1–16.
- Anthony Jnr, B. (2021). Integrating electric vehicles to achieve sustainable energy as a service business model in smart cities. *Frontiers in sustainable cities*, 3:685716.
- Anvari-Moghaddam, A., Rahimi-Kian, A., Mirian, M. S., and Guerrero, J. M. (2017). A multi-agent based energy management solution for integrated buildings and microgrid system. *Applied energy*, 203:41–56.
- Arroyo, J., Manna, C., Spiessens, F., and Helsen, L. (2022). Reinforced model predictive control (rl-mpc) for building energy management. *Applied Energy*, 309:118346.
- Azizi, A., Peyghami, S., Mokhtari, H., and Blaabjerg, F. (2019). Autonomous and decentralized load sharing and energy management approach for dc microgrids. *Electric Power Systems Research*, 177:106009.
- Azuataram, D., Lee, W.-L., de Nijs, F., and Liebman, A. (2020). Reinforcement learning for whole-building hvac control and demand response. *Energy and AI*, 2:100020.
- Babayomi, O., Zhang, Z., Dragicevic, T., Heydari, R., Li, Y., Garcia, C., Rodriguez, J., and Kennel, R. (2022). Advances and opportunities in the model predictive control of microgrids: Part ii—secondary and tertiary layers. *International Journal of Electrical Power & Energy Systems*, 134:107339.
- Belgana, A., Rimal, B. P., and Maier, M. (2014). Open energy market strategies in microgrids: A stackelberg game approach based on a hybrid multiobjective evolutionary algorithm. *IEEE Transactions on Smart Grid*, 6(3):1243–1252.
- Bhardwaj, M., Handa, A., Fox, D., and Boots, B. (2020). Information theoretic model predictive q-learning. In *Learning for Dynamics and Control*, pages 840–850. PMLR.
- Bogaraj, T. and Kanakaraj, J. (2016). Intelligent energy management control for independent microgrid. *Sādhanā*, 41(7):755–769.
- Borazjani, P., Wahab, N. I. A., Hizam, H. B., and Soh, A. B. C. (2014). A review on microgrid control techniques. *2014 IEEE Innovative Smart Grid Technologies-Asia (ISGT ASIA)*, pages 749–753.
- Bordons, C., Teno, G., Marquez, J. J., and Ridao, M. A. (2019). Effect of the integration of disturbances prediction in energy management systems for microgrids. In *2019 International Conference on Smart Energy Systems and Technologies (SEST)*, pages 1–6. IEEE.
- Borghetti, A. (2012). A mixed-integer linear programming approach for the computation of the minimum-losses radial configuration of electrical distribution networks. *IEEE Transactions on Power Systems*, 27(3):1264–1273.
- Boudoudouh, S. and Maâroufi, M. (2018). Multi agent system solution to microgrid implementation. *Sustainable cities and society*, 39:252–261.
- Boyd, S., Boyd, S. P., and Vandenberghe, L. (2004). *Convex optimization*. Cambridge university press.
- Buchholz, B. M. and Styczynski, Z. (2014). *Smart Grids-fundamentals and technologies in electricity networks*, volume 396. Springer.

- Buyak, N., Deshko, V., and Sukhodub, I. (2017). Buildings energy use and human thermal comfort according to energy and exergy approach. *Energy and buildings*, 146:172–181.
- Cagnano, A., De Tuglie, E., and Mancarella, P. (2020). Microgrids: Overview and guidelines for practical implementations and operation. *Applied Energy*, 258:114039.
- Calderón, M., Calderón, A., Ramiro, A., and González, J. (2010). Automatic management of energy flows of a stand-alone renewable energy supply with hydrogen support. *International Journal of hydrogen energy*, 35(6):2226–2235.
- Cannata, N., Cellura, M., Longo, S., Montana, F., Sanseverino, E. R., Luu, Q., and Nguyen, N. (2019). Multi-objective optimization of urban microgrid energy supply according to economic and environmental criteria. In *2019 IEEE Milan PowerTech*, pages 1–6. IEEE.
- Cavus, M., Adhikari, A. A. K., Zangiabadi, M., and Giaouris, D. (2022a). Energy management of microgrids using a flexible hybrid predictive controller.
- Cavus, M., Allahham, A., Adhikari, K., and Giaouris, D. (2024). A hybrid method based on logic predictive controller for flexible hybrid microgrid with plug-and-play capabilities. *Applied Energy*, 359:122752.
- Cavus, M., Allahham, A., Adhikari, K., Zangiabadi, M., and Giaouris, D. (2023). Energy management of grid-connected microgrids using an optimal systems approach. *IEEE Access*.
- Cavus, M., Allahham, A., Adhikari, K., Zangiabadi, M., and Giaouris, D. (2022b). Control of microgrids using an enhanced model predictive controller. *PEMD*.
- Chacko, P. J. and Sachidanandam, M. (2020). Optimization & validation of intelligent energy management system for pseudo dynamic predictive regulation of plug-in hybrid electric vehicle as donor clients. *ETransportation*, 3:100050.
- Chamorro, H. R., Pazmino, C., Paez, D., Jiménez, F., Guerrero, J. M., Sood, V. K., and Martinez, W. (2020). Multi-agent control strategy for microgrids using petri nets. In *2020 IEEE 29th International Symposium on Industrial Electronics (ISIE)*, pages 1141–1146. IEEE.
- Chaouachi, A., Kamel, R. M., Andoulsi, R., and Nagasaka, K. (2012). Multiobjective intelligent energy management for a microgrid. *IEEE transactions on Industrial Electronics*, 60(4):1688–1699.
- Chen, C., Duan, S., Cai, T., Liu, B., and Hu, G. (2011). Smart energy management system for optimal microgrid economic operation. *IET renewable power generation*, 5(3):258–267.
- Chen, C., Wang, J., Qiu, F., and Zhao, D. (2015). Resilient distribution system by microgrids formation after natural disasters. *IEEE Transactions on smart grid*, 7(2):958–966.
- Cheng, J., Duan, D., Cheng, X., Yang, L., and Cui, S. (2020). Probabilistic microgrid energy management with interval predictions. *Energies*, 13(12):3116.
- Cheng, Z., Duan, J., and Chow, M.-Y. (2018). To centralize or to distribute: That is the question: A comparison of advanced microgrid management systems. *IEEE Industrial Electronics Magazine*, 12(1):6–24.
- Chenghui, Z., Qingsheng, S., Naxin, C., and Wuhua, L. (2007). Particle swarm optimization for energy management fuzzy controller design in dual-source electric vehicle. In *2007 IEEE Power Electronics Specialists Conference*, pages 1405–1410. IEEE.
- Chiang, Y.-H., Sean, W.-Y., Wu, C.-H., and Huang, C.-Y. (2017). Development of a converterless energy management system for reusing automotive lithium-ion battery applied in smart-grid balancing. *Journal of Cleaner Production*, 156:750–756.

## References

---

- Choudhury, S. (2022). Review of energy storage system technologies integration to microgrid: Types, control strategies, issues, and future prospects. *Journal of Energy Storage*, 48:103966.
- Conte, F., Massucco, S., Saviozzi, M., and Silvestro, F. (2017). A stochastic optimization method for planning and real-time control of integrated pv-storage systems: Design and experimental validation. *IEEE Transactions on Sustainable Energy*, 9(3):1188–1197.
- Cortés, P., Kouro, S., La Rocca, B., Vargas, R., Rodríguez, J., León, J. I., Vazquez, S., and Franquelo, L. G. (2009). Guidelines for weighting factors design in model predictive control of power converters and drives. In *2009 IEEE International Conference on Industrial Technology*, pages 1–7. IEEE.
- Dagdougui, Y., Ouammi, A., and Benchrifa, R. (2020). Energy management-based predictive controller for a smart building powered by renewable energy. *Sustainability*, 12(10):4264.
- Datta, U., Kalam, A., and Shi, J. (2020). Frequency performance analysis of multi-gain droop controlled dfig in an isolated microgrid using real-time digital simulator. *Engineering Science and Technology, an International Journal*, 23(5):1028–1041.
- Dawoud, S. M., Lin, X., and Okba, M. I. (2018). Hybrid renewable microgrid optimization techniques: A review. *Renewable and Sustainable Energy Reviews*, 82:2039–2052.
- Delghavi, M. B. and Yazdani, A. (2017). Sliding-mode control of ac voltages and currents of dispatchable distributed energy resources in master-slave-organized inverter-based microgrids. *IEEE Transactions on Smart Grid*, 10(1):980–991.
- Dentler, J. E. (2018). *Real-time Model Predictive Control for Aerial Manipulation*. PhD thesis, University of Luxembourg.
- Ding, T., Lin, Y., Li, G., and Bie, Z. (2017). A new model for resilient distribution systems by microgrids formation. *IEEE Transactions on Power Systems*, 32(5):4145–4147.
- Dong, J., Nie, S., Huang, H., Yang, P., Fu, A., and Lin, J. (2019). Research on economic operation strategy of chp microgrid considering renewable energy sources and integrated energy demand response. *Sustainability*, 11(18):4825.
- Dong, X., Gan, J., Wu, H., Deng, C., Liu, S., and Song, C. (2022). Self-triggered model predictive control of ac microgrids with physical and communication state constraints. *Energies*, 15(3):1170.
- Dou, C.-X. and Liu, B. (2013). Multi-agent based hierarchical hybrid control for smart microgrid. *IEEE transactions on smart grid*, 4(2):771–778.
- EI-Bidairi, K. S., Nguyen, H. D., Jayasinghe, S., and Mahmoud, T. S. (2018). Multiobjective intelligent energy management optimization for grid-connected microgrids. In *2018 IEEE International Conference on Environment and Electrical Engineering and 2018 IEEE Industrial and Commercial Power Systems Europe (EEEIC/I&CPS Europe)*, pages 1–6. IEEE.
- Elkazaz, M., Sumner, M., and Thomas, D. (2020). Energy management system for hybrid pv-wind-battery microgrid using convex programming, model predictive and rolling horizon predictive control with experimental validation. *International Journal of Electrical Power & Energy Systems*, 115:105483.
- Elmouatamid, A. et al. (2020). Mapcast: An adaptive control approach using predictive analytics for energy balance in micro-grid systems. *International Journal of Renewable Energy Research (IJRER)*, 10(2):945–954.
- Elmouatamid, A., Naitmalek, Y., Ouladsine, R., Bakhouya, M., El kamoun, N., Khaidar, M., and Zine-Dine, K. (2021). A microgrid system infrastructure implementing iot/big-data technologies for efficient energy management in buildings. In *Advanced Technologies for Solar Photovoltaics Energy Systems*, pages 571–600. Springer.

- Elsied, M., Oukaour, A., Youssef, T., Gualous, H., and Mohammed, O. (2016). An advanced real time energy management system for microgrids. *Energy*, 114:742–752.
- Emad, D., El-Hameed, M., Yousef, M., and El-Fergany, A. (2020). Computational methods for optimal planning of hybrid renewable microgrids: a comprehensive review and challenges. *Archives of Computational Methods in Engineering*, 27:1297–1319.
- Esmat, A., Magdy, A., ElKhattam, W., and ElBakly, A. M. (2013). A novel energy management system using ant colony optimization for micro-grids. In *2013 3rd International Conference on Electric Power and Energy Conversion Systems*, pages 1–6. IEEE.
- Espina, E., Llanos, J., Burgos-Mellado, C., Cardenas-Dobson, R., Martinez-Gomez, M., and Saez, D. (2020). Distributed control strategies for microgrids: An overview. *IEEE Access*, 8:193412–193448.
- Fang, X., Dong, W., Wang, Y., and Yang, Q. (2022). Multiple time-scale energy management strategy for a hydrogen-based multi-energy microgrid. *Applied Energy*, 328:120195.
- Fontenot, H. and Dong, B. (2019). Modeling and control of building-integrated microgrids for optimal energy management—a review. *Applied Energy*, 254:113689.
- Fossati, J. P., Galarza, A., Martín-Villate, A., and Fontan, L. (2015). A method for optimal sizing energy storage systems for microgrids. *Renewable Energy*, 77:539–549.
- Gaiceanu, M., Arama, I. N., and Ghenea, I. (2020). Dc microgrid control. *Microgrid architectures, control and protection methods*, pages 357–380.
- Garcia-Torres, F. and Bordons, C. (2015). Optimal economical schedule of hydrogen-based microgrids with hybrid storage using model predictive control. *IEEE Transactions on Industrial Electronics*, 62(8):5195–5207.
- Garcia-Torres, F., Vilaplana, D. G., Bordons, C., Roncero-Sanchez, P., and Ridao, M. A. (2018). Optimal management of microgrids with external agents including battery/fuel cell electric vehicles. *IEEE Transactions on Smart Grid*, 10(4):4299–4308.
- Garcia Vera, Y. E., Dufolopez, R., and Bernal-Agustin, J. L. (2019). Energy management in microgrids with renewable energy sources: A literature review. *Applied Sciences*, 9(18):3854.
- Ghasemi, N., Ghanbari, M., and Ebrahimi, R. (2023). Intelligent and optimal energy management strategy to control the micro-grid voltage and frequency by considering the load dynamics and transient stability. *International Journal of Electrical Power & Energy Systems*, 145:108618.
- Giaouris, D., Papadopoulos, A. I., Patsios, C., Walker, S., Ziogou, C., Taylor, P., Voutetakis, S., Papadopolou, S., and Seferlis, P. (2018). A systems approach for management of microgrids considering multiple energy carriers, stochastic loads, forecasting and demand side response. *Applied energy*, 226:546–559.
- Giaouris, D., Papadopoulos, A. I., Voutetakis, S., Papadopolou, S., and Seferlis, P. (2015). A power grand composite curves approach for analysis and adaptive operation of renewable energy smart grids. *Clean Technologies and Environmental Policy*, 17:1171–1193.
- Giaouris, D., Papadopoulos, A. I., Ziogou, C., Ipsakis, D., Voutetakis, S., Papadopolou, S., Seferlis, P., Stergiopoulos, F., and Elmasides, C. (2013). Performance investigation of a hybrid renewable power generation and storage system using systemic power management models. *Energy*, 61:621–635.
- Giraldo, J. S., Castrillon, J. A., Lopez, J. C., Rider, M. J., and Castro, C. A. (2018). Microgrids energy management using robust convex programming. *IEEE Transactions on Smart Grid*, 10(4):4520–4530.

## References

---

- González-Romera, E., Romero-Cadaval, E., Roncero-Clemente, C., Ruiz-Cortés, M., Barrero-González, F., Milanés Montero, M.-I., and Moreno-Muñoz, A. (2020). Secondary control for storage power converters in isolated nanogrids to allow peer-to-peer power sharing. *Electronics*, 9(1):140.
- Grisales-Noreña, L. F., Montoya, O. D., and Ramos-Paja, C. A. (2020). An energy management system for optimal operation of bss in dc distributed generation environments based on a parallel pso algorithm. *Journal of Energy Storage*, 29:101488.
- Guerrero, J. M., Chandorkar, M., Lee, T.-L., and Loh, P. C. (2012). Advanced control architectures for intelligent microgrids—part i: Decentralized and hierarchical control. *IEEE Transactions on Industrial Electronics*, 60(4):1254–1262.
- Haidar, A. M., Fakhar, A., and Helwig, A. (2020). Sustainable energy planning for cost minimization of autonomous hybrid microgrid using combined multi-objective optimization algorithm. *Sustainable Cities and Society*, 62:102391.
- Hakimi, S. M., Hasankhani, A., Shafie-khah, M., and Catalão, J. P. (2019). Optimal sizing and siting of smart microgrid components under high renewables penetration considering demand response. *IET Renewable power generation*, 13(10):1809–1822.
- Hannan, M., Tan, S. Y., Al-Shetwi, A. Q., Jern, K. P., and Begum, R. (2020). Optimized controller for renewable energy sources integration into microgrid: Functions, constraints and suggestions. *Journal of Cleaner Production*, 256:120419.
- Herc, L., Pfeifer, A., Duić, N., and Wang, F. (2022). Economic viability of flexibility options for smart energy systems with high penetration of renewable energy. *Energy*, 252:123739.
- Hirsch, A., Parag, Y., and Guerrero, J. (2018). Microgrids: A review of technologies, key drivers, and outstanding issues. *Renewable and sustainable Energy reviews*, 90:402–411.
- Hu, J., Shan, Y., Guerrero, J. M., Ioinovici, A., Chan, K. W., and Rodriguez, J. (2021). Model predictive control of microgrids—an overview. *Renewable and Sustainable Energy Reviews*, 136:110422.
- Ipsakis, D., Voutetakis, S., Seferlis, P., Stergiopoulos, F., and Elmasides, C. (2009). Power management strategies for a stand-alone power system using renewable energy sources and hydrogen storage. *International journal of hydrogen energy*, 34(16):7081–7095.
- Ishaq, S., Khan, I., Rahman, S., Hussain, T., Iqbal, A., and Elavarasan, R. M. (2022). A review on recent developments in control and optimization of micro grids. *Energy Reports*, 8:4085–4103.
- Jabarnejad, M. (2020). Facilitating emission reduction using the dynamic line switching and rating. *Electric Power Systems Research*, 189:106600.
- Javaid, C. J., Allahham, A., Giaouris, D., Blake, S., and Taylor, P. (2019). Modelling of a virtual power plant using hybrid automata. *The Journal of Engineering*, 2019(17):3918–3922.
- Javaid, N., Naseem, M., Rasheed, M. B., Mahmood, D., Khan, S. A., Alrajeh, N., and Iqbal, Z. (2017). A new heuristically optimized home energy management controller for smart grid. *Sustainable cities and society*, 34:211–227.
- Jayachandran, M. and Ravi, G. (2019). Decentralized model predictive hierarchical control strategy for islanded ac microgrids. *Electric Power Systems Research*, 170:92–100.
- Jiménez-Fernández, S., Camacho-Gómez, C., Mallol-Poyato, R., Fernández, J. C., Del Ser, J., Portilla-Figueras, A., and Salcedo-Sanz, S. (2018). Optimal microgrid topology design and siting of distributed generation sources using a multi-objective substrate layer coral reefs optimization algorithm. *Sustainability*, 11(1):169.

- Joung, K. W., Kim, T., and Park, J.-W. (2018). Decoupled frequency and voltage control for stand-alone microgrid with high renewable penetration. *IEEE Transactions on Industry Applications*, 55(1):122–133.
- Ju, L., Tan, Z., Yuan, J., Tan, Q., Li, H., and Dong, F. (2016). A bi-level stochastic scheduling optimization model for a virtual power plant connected to a wind–photovoltaic–energy storage system considering the uncertainty and demand response. *Applied energy*, 171:184–199.
- Kakran, S. and Chanana, S. (2018). Smart operations of smart grids integrated with distributed generation: A review. *Renewable and Sustainable Energy Reviews*, 81:524–535.
- Kamal, F. and Chowdhury, B. (2022). Model predictive control and optimization of networked microgrids. *International Journal of Electrical Power & Energy Systems*, 138:107804.
- Kamboj, V. K., Bath, S., and Dhillon, J. (2016). Solution of non-convex economic load dispatch problem using grey wolf optimizer. *Neural computing and Applications*, 27:1301–1316.
- Karavas, C.-S., Arvanitis, K., and Papadakis, G. (2017). A game theory approach to multi-agent decentralized energy management of autonomous polygeneration microgrids. *Energies*, 10(11):1756.
- Kermani, M., Carnì, D. L., Rotondo, S., Paolillo, A., Manzo, F., and Martirano, L. (2020). A nearly zero-energy microgrid testbed laboratory: Centralized control strategy based on scada system. *Energies*, 13(8):2106.
- Kerr, D. (2022). Net zero electricity market design expert group report-report for the climate change committee.
- Khan, A. A., Naeem, M., Iqbal, M., Qaisar, S., and Anpalagan, A. (2016). A compendium of optimization objectives, constraints, tools and algorithms for energy management in microgrids. *Renewable and Sustainable Energy Reviews*, 58:1664–1683.
- Khan, A. H., Li, S., Chen, D., and Liao, L. (2020). Tracking control of redundant mobile manipulator: An rnn based metaheuristic approach. *Neurocomputing*, 400:272–284.
- Khan, Z. A., Zafar, A., Javaid, S., Aslam, S., Rahim, M. H., and Javaid, N. (2019). Hybrid meta-heuristic optimization based home energy management system in smart grid. *Journal of Ambient Intelligence and Humanized Computing*, 10:4837–4853.
- Khawaja, Y., Allahham, A., Giaouris, D., Patsios, C., Walker, S., and Qiqieh, I. (2019). An integrated framework for sizing and energy management of hybrid energy systems using finite automata. *Applied Energy*, 250:257–272.
- Khokhar, B. and Parmar, K. S. (2022). A novel adaptive intelligent mpc scheme for frequency stabilization of a microgrid considering soc control of evs. *Applied Energy*, 309:118423.
- Kong, X., Liu, X., Ma, L., and Lee, K. Y. (2019). Hierarchical distributed model predictive control of standalone wind/solar/battery power system. *IEEE Transactions on Systems, Man, and Cybernetics: Systems*, 49(8):1570–1581.
- Konneh, K. V., Adewuyi, O. B., Lotfy, M. E., Sun, Y., and Senjyu, T. (2022). Application strategies of model predictive control for the design and operations of renewable energy-based microgrid: A survey. *Electronics*, 11(4):554.
- Kostopoulos, E. D., Spyropoulos, G. C., and Kaldellis, J. K. (2020). Real-world study for the optimal charging of electric vehicles. *Energy Reports*, 6:418–426.
- Koussa, D. S. and Koussa, M. (2015). A feasibility and cost benefit prospection of grid connected hybrid power system (wind–photovoltaic)–case study: An algerian coastal site. *Renewable and Sustainable Energy Reviews*, 50:628–642.

## References

---

- Kumar, R. and Pathak, M. K. (2020). Distributed droop control of dc microgrid for improved voltage regulation and current sharing. *IET Renewable Power Generation*, 14(13):2499–2506.
- Kuznetsova, E., Li, Y.-F., Ruiz, C., and Zio, E. (2014). An integrated framework of agent-based modelling and robust optimization for microgrid energy management. *Applied Energy*, 129:70–88.
- Lei, M., Yang, Z., Wang, Y., Xu, H., Meng, L., Vasquez, J. C., and Guerrero, J. M. (2017). An mpc-based ess control method for pv power smoothing applications. *IEEE Transactions on Power Electronics*, 33(3):2136–2144.
- Leonori, S., De Santis, E., Rizzi, A., and Mascioli, F. F. (2016). Optimization of a microgrid energy management system based on a fuzzy logic controller. In *IECON 2016-42nd Annual Conference of the IEEE Industrial Electronics Society*, pages 6615–6620. IEEE.
- Li, B., Roche, R., and Miraoui, A. (2017). Microgrid sizing with combined evolutionary algorithm and milp unit commitment. *Applied energy*, 188:547–562.
- Lin, P., Jin, C., Xiao, J., Li, X., Shi, D., Tang, Y., and Wang, P. (2018). A distributed control architecture for global system economic operation in autonomous hybrid ac/dc microgrids. *IEEE Transactions on Smart Grid*, 10(3):2603–2617.
- Liu, L.-N. and Yang, G.-H. (2022). Distributed optimal energy management for integrated energy systems. *IEEE Transactions on Industrial Informatics*, 18(10):6569–6580.
- Liu, Y., Yuen, C., Hassan, N. U., Huang, S., Yu, R., and Xie, S. (2014). Electricity cost minimization for a microgrid with distributed energy resource under different information availability. *IEEE Transactions on Industrial Electronics*, 62(4):2571–2583.
- Luenberger, D. G., Ye, Y., et al. (1984). *Linear and nonlinear programming*, volume 2. Springer.
- Luna, A. C., Diaz, N. L., Graells, M., Vasquez, J. C., and Guerrero, J. M. (2016). Mixed-integer-linear-programming-based energy management system for hybrid pv-wind-battery microgrids: Modeling, design, and experimental verification. *IEEE Transactions on Power Electronics*, 32(4):2769–2783.
- Luo, A., Xu, Q., Ma, F., and Chen, Y. (2016). Overview of power quality analysis and control technology for the smart grid. *Journal of Modern Power Systems and Clean Energy*, 4(1):1–9.
- Ma, G., Li, J., and Zhang, X.-P. (2022). A review on optimal energy management of multimicrogrid system considering uncertainties. *IEEE Access*, 10:77081–77098.
- Mahmoud, M. S., Alyazidi, N. M., and Abouheaf, M. I. (2017). Adaptive intelligent techniques for microgrid control systems: A survey. *International Journal of Electrical Power & Energy Systems*, 90:292–305.
- Makonin, S. (2019). Hue: The hourly usage of energy dataset for buildings in british columbia. *Data in brief*, 23.
- Mansouri Kouhestani, F., Byrne, J., Johnson, D., Spencer, L., Brown, B., Hazendonk, P., and Scott, J. (2020). Multi-criteria pso-based optimal design of grid-connected hybrid renewable energy systems. *International Journal of Green Energy*, 17(11):617–631.
- Marín, L. G., Sumner, M., Muñoz-Carpintero, D., Köbrich, D., Pholboon, S., Sáez, D., and Núñez, A. (2019). Hierarchical energy management system for microgrid operation based on robust model predictive control. *Energies*, 12(23):4453.
- Marzband, M., Azarinejadian, F., Savaghebi, M., and Guerrero, J. M. (2015). An optimal energy management system for islanded microgrids based on multiperiod artificial bee colony combined with markov chain. *IEEE systems journal*, 11(3):1712–1722.

- Marzband, M., Ghadimi, M., Sumper, A., and Domínguez-García, J. L. (2014). Experimental validation of a real-time energy management system using multi-period gravitational search algorithm for microgrids in islanded mode. *Applied energy*, 128:164–174.
- Maślak, G. and Orłowski, P. (2022). Microgrid operation optimization using hybrid system modeling and switched model predictive control. *Energies*, 15(3):833.
- Mei, R. N. S., Sulaiman, M. H., Mustafa, Z., and Daniyal, H. (2017). Optimal reactive power dispatch solution by loss minimization using moth-flame optimization technique. *Applied Soft Computing*, 59:210–222.
- Mendes, P. R., Isorna, L. V., Bordons, C., and Normey-Rico, J. E. (2016). Energy management of an experimental microgrid coupled to a v2g system. *Journal of Power Sources*, 327:702–713.
- Meng, L., Sanseverino, E. R., Luna, A., Dragicevic, T., Vasquez, J. C., and Guerrero, J. M. (2016). Microgrid supervisory controllers and energy management systems: A literature review. *Renewable and Sustainable Energy Reviews*, 60:1263–1273.
- Minhas, D. M., Meiers, J., and Frey, G. (2022). Electric vehicle battery storage concentric intelligent home energy management system using real life data sets. *Energies*, 15(5):1619.
- Mohammadi, J. and Ajaei, F. B. (2019). Improved mode-adaptive droop control strategy for the dc microgrid. *IEEE Access*, 7:86421–86435.
- Mohseni, S. and Moghaddas-Tafreshi, S. M. (2018). A multi-agent system for optimal sizing of a cooperative self-sustainable multi-carrier microgrid. *Sustainable cities and society*, 38:452–465.
- Molzahn, D. K., Dörfler, F., Sandberg, H., Low, S. H., Chakrabarti, S., Baldick, R., and Lavaei, J. (2017). A survey of distributed optimization and control algorithms for electric power systems. *IEEE Transactions on Smart Grid*, 8(6):2941–2962.
- Motevasel, M. and Seifi, A. R. (2014). Expert energy management of a micro-grid considering wind energy uncertainty. *Energy Conversion and Management*, 83:58–72.
- Mousazadeh Mousavi, S. Y., Jalilian, A., Savaghebi, M., and Guerrero, J. M. (2018). Power quality enhancement and power management of a multifunctional interfacing inverter for pv and battery energy storage system. *International Transactions on Electrical Energy Systems*, 28(12):e2643.
- Nasr, M.-A., Nikkhah, S., Gharehpetian, G. B., Nasr-Azadani, E., and Hosseinian, S. H. (2020). A multi-objective voltage stability constrained energy management system for isolated microgrids. *International Journal of Electrical Power & Energy Systems*, 117:105646.
- Nawaz, A., Wu, J., Ye, J., Dong, Y., and Long, C. (2023). Distributed mpc-based energy scheduling for islanded multi-microgrid considering battery degradation and cyclic life deterioration. *Applied energy*, 329:120168.
- Nemati, M., Braun, M., and Tenbohlen, S. (2018). Optimization of unit commitment and economic dispatch in microgrids based on genetic algorithm and mixed integer linear programming. *Applied energy*, 210:944–963.
- Nikkhah, S., Allahham, A., Bialek, J. W., Walker, S. L., Giaouris, D., and Papadopoulou, S. (2021a). Active participation of buildings in the energy networks: Dynamic/operational models and control challenges. *Energies*, 14(21):7220.
- Nikkhah, S., Allahham, A., Giaouris, D., Bialek, J. W., and Walker, S. (2021b). Application of robust receding horizon controller for real-time energy management of reconfigurable islanded microgrids. In *2021 IEEE Madrid PowerTech*, pages 1–6. IEEE.

## References

---

- Nikkhah, S., Allahham, A., Royapoor, M., Bialek, J. W., and Giaouris, D. (2021c). A community-based building-to-building strategy for multi-objective energy management of residential microgrids. In *2021 12th International Renewable Engineering Conference (IREC)*, pages 1–6. IEEE.
- Nikkhah, S., Allahham, A., Royapoor, M., Bialek, J. W., and Giaouris, D. (2021d). Optimising building-to-building and building-for-grid services under uncertainty: A robust rolling horizon approach. *IEEE Transactions on Smart Grid*, 13(2):1453–1467.
- Nikkhah, S., Sarantakos, I., Zografou-Barredo, N.-M., Rabiee, A., Allahham, A., and Giaouris, D. (2022). A joint risk-and security-constrained control framework for real-time energy scheduling of islanded microgrids. *IEEE Transactions on Smart Grid*, 13(5):3354–3368.
- Niu, J., Tian, Z., Lu, Y., and Zhao, H. (2019). Flexible dispatch of a building energy system using building thermal storage and battery energy storage. *Applied Energy*, 243:274–287.
- Nshuti, H. M. (2022). Centralized and decentralized control of microgrids.
- Nunna, H. K. and Doolla, S. (2013). Energy management in microgrids using demand response and distributed storage—a multiagent approach. *IEEE Transactions on Power Delivery*, 28(2):939–947.
- Nyong-Bassey, B. E., Giaouris, D., Patsios, C., Papadopoulou, S., Papadopoulos, A. I., Walker, S., Voutetakis, S., Seferlis, P., and Gadoue, S. (2020). Reinforcement learning based adaptive power pinch analysis for energy management of stand-alone hybrid energy storage systems considering uncertainty. *Energy*, 193:116622.
- Ocanha, E. S., Zinani, F. S. F., Modolo, R. C. E., and Santos, F. A. (2020). Assesment of the effects of chemical and physical parameters in the fluidization of biomass and sand binary mixtures through statistical analysis. *Energy*, 190:116401.
- Ontiveros, L. J., Suvire, G. O., and Mercado, P. E. (2017). A new control strategy to integrate flow batteries into ac micro-grids with high wind power penetration. *Redox Princ. Adv. Appl*, 83.
- Ouammi, A. (2021). Peak loads shaving in a team of cooperating smart buildings powered solar pv-based microgrids. *IEEE Access*, 9:24629–24636.
- Pamulapati, T., Allahham, A., Walker, S. L., and Giaouris, D. (2022a). Evolution operator-based automata control approach for ems in active buildings.
- Pamulapati, T., Cavus, M., Odigwe, I., Allahham, A., Walker, S., and Giaouris, D. (2022b). A review of microgrid energy management strategies from the energy trilemma perspective. *Energies*, 16(1):289.
- Pang, K., Wang, C., Hatziargyriou, N. D., Wen, F., and Xue, Y. (2022). Formulation of radiality constraints for optimal microgrid formation. *IEEE Transactions on Power Systems*.
- Papari, B., Edrington, C., Vu, T., and Diaz-Franco, F. (2017). A heuristic method for optimal energy management of dc microgrid. In *2017 IEEE Second International Conference on DC Microgrids (ICDCM)*, pages 337–343. IEEE.
- Parisio, A., Rikos, E., and Glielmo, L. (2016). Stochastic model predictive control for economic/environmental operation management of microgrids: An experimental case study. *Journal of Process Control*, 43:24–37.
- Parisio, A., Rikos, E., Tzamalīs, G., and Glielmo, L. (2014). Use of model predictive control for experimental microgrid optimization. *Applied Energy*, 115:37–46.

- Pedro, H. T. and Coimbra, C. F. (2015). Short-term irradiance forecastability for various solar micro-climates. *Solar Energy*, 122:587–602.
- Pourbabak, H., Chen, T., and Su, W. (2019). Centralized, decentralized, and distributed control for energy internet. In *The Energy Internet*, pages 3–19. Elsevier.
- Prabaharan, N., Jerin, A. R. A., Najafi, E., and Palanisamy, K. (2018). An overview of control techniques and technical challenge for inverters in micro grid. *Hybrid-Renewable Energy Systems in Microgrids*, pages 97–107.
- Qing, X. and Niu, Y. (2018). Hourly day-ahead solar irradiance prediction using weather forecasts by lstm. *Energy*, 148:461–468.
- Qiu, X., Nguyen, T. A., and Crow, M. L. (2015). Heterogeneous energy storage optimization for microgrids. *IEEE Transactions on Smart Grid*, 7(3):1453–1461.
- Rabiee, A., Sadeghi, M., Aghaei, J., and Heidari, A. (2016). Optimal operation of microgrids through simultaneous scheduling of electrical vehicles and responsive loads considering wind and pv units uncertainties. *Renewable and Sustainable Energy Reviews*, 57:721–739.
- Radosavljević, J., Jevtić, M., and Klimenta, D. (2016). Energy and operation management of a microgrid using particle swarm optimization. *Engineering Optimization*, 48(5):811–830.
- Rahim, S., Iqbal, Z., Shaheen, N., Khan, Z. A., Qasim, U., Khan, S. A., and Javaid, N. (2016). Ant colony optimization based energy management controller for smart grid. In *2016 IEEE 30th International Conference on Advanced Information Networking and Applications (AINA)*, pages 1154–1159. IEEE.
- Rahmani, E., Mohammadi, S., Zadehbagheri, M., and Kiani, M. (2023). Probabilistic reliability management of energy storage systems in connected/islanding microgrids with renewable energy. *Electric Power Systems Research*, 214:108891.
- Rahmani-Andebili, M. and Shen, H. (2017). Cooperative distributed energy scheduling for smart homes applying stochastic model predictive control. In *2017 IEEE international conference on communications (ICC)*, pages 1–6. IEEE.
- Ramsami, P. and Oree, V. (2015). A hybrid method for forecasting the energy output of photovoltaic systems. *Energy Conversion and Management*, 95:406–413.
- Rathor, S. K. and Saxena, D. (2020). Energy management system for smart grid: An overview and key issues. *International Journal of Energy Research*, 44(6):4067–4109.
- Ravi, S. S. and Aziz, M. (2022). Utilization of electric vehicles for vehicle-to-grid services: Progress and perspectives. *Energies*, 15(2):589.
- Raza, M. Q., Mithulananthan, N., Li, J., Lee, K. Y., and Gooi, H. B. (2018). An ensemble framework for day-ahead forecast of pv output power in smart grids. *IEEE Transactions on Industrial Informatics*, 15(8):4624–4634.
- Razi, R., Iman-Eini, H., and Hamzeh, M. (2019). An impedance-power droop method for accurate power sharing in islanded resistive microgrids. *IEEE Journal of Emerging and Selected Topics in Power Electronics*, 8(4):3763–3771.
- Razzanelli, M., Crisostomi, E., Pallottino, L., and Pannocchia, G. (2020). Distributed model predictive control for energy management in a network of microgrids using the dual decomposition method. *Optimal Control Applications and Methods*, 41(1):25–41.
- Riffonneau, Y., Bacha, S., Barruel, F., and Ploix, S. (2011). Optimal power flow management for grid connected pv systems with batteries. *IEEE Transactions on sustainable energy*, 2(3):309–320.

## References

---

- Roslan, M., Hannan, M., Ker, P. J., and Uddin, M. (2019). Microgrid control methods toward achieving sustainable energy management. *Applied Energy*, 240:583–607.
- Roy, K., Mandal, K. K., and Mandal, A. C. (2019). Ant-lion optimizer algorithm and recurrent neural network for energy management of micro grid connected system. *Energy*, 167:402–416.
- Rutter, J. and Sasse, T. (2022). Net zero: agenda 2022.
- Sadabadi, M. S., Shafiee, Q., and Karimi, A. (2017). Plug-and-play robust voltage control of dc microgrids. *IEEE Transactions on Smart Grid*, 9(6):6886–6896.
- Sahoo, B., Routray, S. K., and Rout, P. K. (2021). A novel centralized energy management approach for power quality improvement. *International Transactions on Electrical Energy Systems*, 31(10):e12582.
- Sahoo, S. K., Sinha, A. K., and Kishore, N. (2017). Control techniques in ac, dc, and hybrid ac–dc microgrid: a review. *IEEE Journal of Emerging and Selected Topics in Power Electronics*, 6(2):738–759.
- Sao, C. K. and Lehn, P. W. (2008). Control and power management of converter fed microgrids. *IEEE Transactions on Power Systems*, 23(3):1088–1098.
- Sarabi, S., Davigny, A., Riffonneau, Y., and Robyns, B. (2016). V2g electric vehicle charging scheduling for railway station parking lots based on binary linear programming. In *2016 IEEE International Energy Conference (ENERGYCON)*, pages 1–6. IEEE.
- Seborg, D. E., Edgar, T. F., Mellichamp, D. A., and Doyle III, F. J. (2016). *Process dynamics and control*. John Wiley & Sons.
- Shayeghi, H., Shahryari, E., Moradzadeh, M., and Siano, P. (2019). A survey on microgrid energy management considering flexible energy sources. *Energies*, 12(11):2156.
- Shekari, T., Gholami, A., and Aminifar, F. (2019). Optimal energy management in multi-carrier microgrids: an milp approach. *Journal of Modern Power Systems and Clean Energy*, 7(4):876–886.
- Silvente, J., Kopanos, G. M., Dua, V., and Papageorgiou, L. G. (2018). A rolling horizon approach for optimal management of microgrids under stochastic uncertainty. *Chemical Engineering Research and Design*, 131:293–317.
- Singh, S., Chauhan, P., and Singh, N. (2020). Capacity optimization of grid connected solar/fuel cell energy system using hybrid abc-pso algorithm. *International Journal of Hydrogen Energy*, 45(16):10070–10088.
- Smets, A., Jäger, K., Isabella, O., Van Swaaij, R., and Zeman, M. (2016). *Solar Energy: The physics and engineering of photovoltaic conversion, technologies and systems*. Bloomsbury Publishing.
- Sökmen, K. F. and Çavuş, M. (2017). Review of batteries thermal problems and thermal management systems. *Journal of Innovative Science and Engineering (JISE)*, 1(1):35–55.
- Solanki, B. V., Raghurajan, A., Bhattacharya, K., and Canizares, C. A. (2015). Including smart loads for optimal demand response in integrated energy management systems for isolated microgrids. *IEEE Transactions on Smart Grid*, 8(4):1739–1748.
- Su, W., Wang, J., Zhang, K., and Huang, A. Q. (2014). Model predictive control-based power dispatch for distribution system considering plug-in electric vehicle uncertainty. *Electric Power Systems Research*, 106:29–35.

- Sukumar, S., Mokhlis, H., Mekhilef, S., Naidu, K., and Karimi, M. (2017). Mix-mode energy management strategy and battery sizing for economic operation of grid-tied microgrid. *Energy*, 118:1322–1333.
- Sultana, U., Khairuddin, A. B., Aman, M., Mokhtar, A., and Zareen, N. (2016). A review of optimum dg placement based on minimization of power losses and voltage stability enhancement of distribution system. *Renewable and Sustainable Energy Reviews*, 63:363–378.
- Suresh, M. and Edward, J. B. (2020). A hybrid algorithm based optimal placement of dg units for loss reduction in the distribution system. *Applied Soft Computing*, 91:106191.
- Tarragona, J., Pisello, A. L., Fernández, C., de Gracia, A., and Cabeza, L. F. (2021). Systematic review on model predictive control strategies applied to active thermal energy storage systems. *Renewable and Sustainable Energy Reviews*, 149:111385.
- Terlouw, T., AlSkaif, T., Bauer, C., and van Sark, W. (2019). Optimal energy management in all-electric residential energy systems with heat and electricity storage. *Applied Energy*, 254:113580.
- Thirunavukkarasu, G. S., Seyedmahmoudian, M., Jamei, E., Horan, B., Mekhilef, S., and Stojcevski, A. (2022). Role of optimization techniques in microgrid energy management systems—a review. *Energy Strategy Reviews*, 43:100899.
- Tobajas, J., Garcia-Torres, F., Roncero-Sánchez, P., Vázquez, J., Bellatreche, L., and Nieto, E. (2022). Resilience-oriented schedule of microgrids with hybrid energy storage system using model predictive control. *Applied Energy*, 306:118092.
- Tsikalakis, A. G. and Hatziargyriou, N. D. (2011). Centralized control for optimizing microgrids operation. In *2011 IEEE power and energy society general meeting*, pages 1–8. IEEE.
- Ulutas, A., Altas, I. H., Onen, A., and Ustun, T. S. (2020). Neuro-fuzzy-based model predictive energy management for grid connected microgrids. *Electronics*, 9(6):900.
- Urias, M. E. G., Sanchez, E. N., and Ricalde, L. J. (2014). Electrical microgrid optimization via a new recurrent neural network. *IEEE Systems Journal*, 9(3):945–953.
- Van, N. D., Sualeh, M., Kim, D., and Kim, G.-W. (2020). A hierarchical control system for autonomous driving towards urban challenges. *Applied Sciences*, 10(10):3543.
- Vašak, M., Banjac, A., Hure, N., Novak, H., Marušić, D., and Lešić, V. (2021). Modular hierarchical model predictive control for coordinated and holistic energy management of buildings. *IEEE Transactions on Energy Conversion*, 36(4):2670–2682.
- Vazifeh, M. M., Zhang, H., Santi, P., and Ratti, C. (2019). Optimizing the deployment of electric vehicle charging stations using pervasive mobility data. *Transportation Research Part A: Policy and Practice*, 121:75–91.
- Vázquez-Canteli, J. R. and Nagy, Z. (2019). Reinforcement learning for demand response: A review of algorithms and modeling techniques. *Applied energy*, 235:1072–1089.
- Venayagamoorthy, G. K., Sharma, R. K., Gautam, P. K., and Ahmadi, A. (2016). Dynamic energy management system for a smart microgrid. *IEEE transactions on neural networks and learning systems*, 27(8):1643–1656.
- Veneri, O. (2017). *Technologies and applications for smart charging of electric and plug-in hybrid vehicles*. Springer.
- Villalón, A., Rivera, M., Salgueiro, Y., Muñoz, J., Dragičević, T., and Blaabjerg, F. (2020). Predictive control for microgrid applications: A review study. *Energies*, 13(10):2454.

## References

---

- Wang, J., Zhou, N., and Wang, Q. (2020). Data-driven stochastic service restoration in unbalanced active distribution networks with multi-terminal soft open points. *International Journal of Electrical Power & Energy Systems*, 121:106069.
- Wang, L. (2009). *Model predictive control system design and implementation using MATLAB®*. Springer Science & Business Media.
- Wang, T., He, X., and Deng, T. (2019). Neural networks for power management optimal strategy in hybrid microgrid. *Neural Computing and Applications*, 31:2635–2647.
- Wang, X., Hua, Q., Liu, P., and Sun, L. (2022a). Stochastic dynamic programming based optimal energy scheduling for a hybrid fuel cell/pv/battery system under uncertainty. *Process Safety and Environmental Protection*, 165:380–386.
- Wang, Y., Liu, S., Sun, B., and Li, X. (2022b). A distributed proximal primal-dual algorithm for energy management with transmission losses in smart grid. *IEEE Transactions on Industrial Informatics*.
- Wang, Y., Wen, W., Wang, C., Liu, H., Zhan, X., and Xiao, X. (2018). Adaptive voltage droop method of multiterminal vsc-hvdc systems for dc voltage deviation and power sharing. *IEEE Transactions on Power Delivery*, 34(1):169–176.
- Warnier, M., Dulman, S., Koç, Y., and Pauwels, E. (2017). Distributed monitoring for the prevention of cascading failures in operational power grids. *International Journal of Critical Infrastructure Protection*, 17:15–27.
- Wolf, P. J. (2009). *Chemical process dynamics and controls*. Open Textbook Library.
- Wu, C., Gao, S., Song, T. E., and Liu, Y. (2020). A two-layer stochastic model predictive control approach in microgrids for coordination of wind and energy storage system. In *2020 IEEE Power & Energy Society General Meeting (PESGM)*, pages 1–5. IEEE.
- Wu, X., Hu, X., Yin, X., and Moura, S. J. (2016). Stochastic optimal energy management of smart home with pev energy storage. *IEEE Transactions on Smart Grid*, 9(3):2065–2075.
- Xie, M., Ji, X., Hu, X., Cheng, P., Du, Y., and Liu, M. (2018). Autonomous optimized economic dispatch of active distribution system with multi-microgrids. *Energy*, 153:479–489.
- Xu, Q., Zhao, T., Xu, Y., Xu, Z., Wang, P., and Blaabjerg, F. (2019). A distributed and robust energy management system for networked hybrid ac/dc microgrids. *IEEE Transactions on Smart Grid*, 11(4):3496–3508.
- Yamashita, D. Y., Vechiu, I., and Gaubert, J.-P. (2020a). Real-time parameters identification of lithium-ion batteries model to improve the hierarchical model predictive control of building microgrids. In *2020 22nd European Conference on Power Electronics and Applications (EPE'20 ECCE Europe)*, pages 1–10. IEEE.
- Yamashita, D. Y., Vechiu, I., and Gaubert, J.-P. (2020b). A review of hierarchical control for building microgrids. *Renewable and Sustainable Energy Reviews*, 118:109523.
- Yang, H., Pu, Y., Qiu, Y., Li, Q., and Chen, W. (2019). Multi-time scale integration of robust optimization with mpc for islanded hydrogen-based microgrid. In *2019 IEEE Sustainable Power and Energy Conference (iSPEC)*, pages 1163–1168. IEEE.
- Yazdani, M. and Mehrizi-Sani, A. (2014). Distributed control techniques in microgrids. *IEEE Transactions on Smart Grid*, 5(6):2901–2909.
- Yoldas, Y., Goren, S., Onen, A., and Ustun, T. S. (2022). Dynamic rolling horizon control approach for a university campus. *Energy Reports*, 8:1154–1162.

- Yoldaş, Y., Önen, A., Muyeen, S., Vasilakos, A. V., and Alan, I. (2017). Enhancing smart grid with microgrids: Challenges and opportunities. *Renewable and Sustainable Energy Reviews*, 72:205–214.
- Zahraoui, Y., Alhamrouni, I., Mekhilef, S., Basir Khan, M. R., Seyedmahmoudian, M., Stojcevski, A., and Horan, B. (2021). Energy management system in microgrids: A comprehensive review. *Sustainability*, 13(19):10492.
- Zhang, M. and Li, Y. (2020). Multi-objective optimal reactive power dispatch of power systems by combining classification-based multi-objective evolutionary algorithm and integrated decision making. *IEEE Access*, 8:38198–38209.
- Zhang, X., Guan, J., and Zhang, B. (2016). A master-slave peer-to-peer integration microgrid control strategy based on communication. In *2016 IEEE PES Asia-Pacific Power and Energy Engineering Conference (APPEEC)*, pages 1106–1110. IEEE.
- Zhang, Z., Babayomi, O., Dragicevic, T., Heydari, R., Garcia, C., Rodriguez, J., and Kennel, R. (2022). Advances and opportunities in the model predictive control of microgrids: Part i—primary layer. *International Journal of Electrical Power & Energy Systems*, 134:107411.
- Zhang, Z., Zhang, J., Wenfang, D., Peng, R., and Xu, C. (2018). Research on economic optimal dispatching strategy of microgrid based on model predictive control. In *MATEC web of conferences*, volume 232, page 01058. EDP Sciences.
- Zhao, H., Lu, H., Li, B., Wang, X., Zhang, S., and Wang, Y. (2020). Stochastic optimization of microgrid participating day-ahead market operation strategy with consideration of energy storage system and demand response. *Energies*, 13(5):1255.
- Zhao, Z., Guo, J., Luo, X., Lai, C. S., Yang, P., Lai, L. L., Li, P., Guerrero, J. M., and Shahidehpour, M. (2022). Distributed robust model predictive control-based energy management strategy for islanded multi-microgrids considering uncertainty. *IEEE Transactions on Smart Grid*, 13(3):2107–2120.
- Zheng, L. and Weiye, D. (2021). A hierarchical control strategy for isolated microgrid with energy storage. In *2021 IEEE 1st International Power Electronics and Application Symposium (PEAS)*, pages 1–4. IEEE.
- Zhu, B., Tazvinga, H., and Xia, X. (2014). Switched model predictive control for energy dispatching of a photovoltaic-diesel-battery hybrid power system. *IEEE Transactions on Control Systems Technology*, 23(3):1229–1236.
- Zhu, J., Chen, J., Zhuo, Y., Mo, X., Guo, Y., Liu, L., and Liu, M. (2021). Stochastic energy management of active distribution network based on improved approximate dynamic programming. *IEEE Transactions on Smart Grid*, 13(1):406–416.
- Zia, M. F., Elbouchikhi, E., and Benbouzid, M. (2018). Microgrids energy management systems: A critical review on methods, solutions, and prospects. *Applied energy*, 222:1033–1055.